

Developmental programming of the
cell stress response and metabolic inflammation
in liver and adipose tissue in an ovine model.

By Vivek Saroha MBBS, MD, MRCPCH

Thesis submitted to the University of Nottingham
for the degree of Doctor of Philosophy

May 2016

Abstract

A state of chronic metabolic inflammation and activation of the cell stress response in organs such as liver and adipose tissue are important pathogenic adaptations with the onset of obesity and the metabolic syndrome. The extent to which these processes are modulated by the early life nutritional experience is not well established, especially in large animal models. The overall aim of this thesis was to identify whether nutritional programming during prenatal and postnatal development enhances metabolic inflammation and cell stress response of obesity. A nutritional model of fetal growth restriction achieved by maternal nutrient restriction (NR) to 60% of requirements during late gestation (110 days to term at 147 days) in twin bearing sheep was used. Combination of prenatal and postnatal nutritional interventions were studied with the following three study protocols:

1. Offspring of twin bearing sheep born to mothers nutrient restricted or fed to appetite were separated after weaning at 3 months of age and then exposed to either restricted physical activity leading to obesity or to unrestricted activity and remained lean.
2. Following maternal NR, both twins or only one twin were reared on their mother's milk during suckling period in order to achieve a relatively faster growth rate in the latter.
3. Twin offspring of sheep randomised to NR or feeding to requirement during late gestation were separated after birth and randomised to either formula feeding or being fed by the mother until weaning followed by obesogenic rearing.

Total body weight of sheep in the obese group was raised by ~30% and was unaffected by any intervention. Obesity led to an increased insulin response to the glucose tolerance test, together with hepatic triglyceride deposition, and adipocyte hypertrophy with macrophage infiltration in omental adipose tissue. NR exacerbated obesity associated hepatic triglyceride deposition and upregulated gene expression of hepatic autophagy and omental unfolded protein response. Formula feeding of sheep offspring following NR was associated with slower weight gain and decreased gene expression for MTOR. Sheep offspring fed by mother as singleton gained weight at faster rate during suckling period as compared to offspring fed by their mothers as twins. Neither postnatal interventions exacerbated the state of obesity associated metabolic inflammation and cell stress response. It is possible that the increased hepatic autophagic gene expression is a reflection of defective autophagy and future work should include study of markers of autophagic function. Possible mechanisms of upregulated omental adipose UPR in offspring of sheep undergoing NR could include a programmed decrease in adipocyte number or selective survival of preadipocytes with effective ER stress response. Such adaptations followed by obesity would predispose the adipocytes to initiate inflammation and cell death pathways.

Acknowledgements

Thank you Professor Michael Symonds and Professor Helen Budge for the supervision and support. Michael, thank you for your resourcefulness and always having a solution for every problem. Helen, thank you for your vision and remarkable ability to plan ahead for outcomes of every scenario. You make a great team.

I would like to gratefully acknowledge colleagues and staff from the Academic Child Health at University of Nottingham, who, during my association, provided excellent support and developed great friendships. A particular mention for Dr Sylvain Sebert for all the animal and lab experimentation work, for training me during the beginning stage of the research and for all the ready support even after our career paths have gone in different directions. I am most grateful to Mrs Vicky Wilson and Mr Mark Pope for their excellent technical support and help. Thanks to Dr Andrew Prayle for helping me with automation of data processing. Thanks to my peers Dr Neele Dellschaft, Dr Hernan Feinberg, Dr Jole Martino, Dr Shalini Ojha, Dr Lyndsey Elvidge for their friendships and associations during the various stages of the process. Thanks to my BMed Sci students Dr Charlotte Burton and Dr Dr Paul Andrzejowski for working diligently with me during their research projects.

I would like to thank Professor Andy Field, author of many statistical books, for personally resolving my statistical questions through use of Facebook messages.

I acknowledge my parents Mrs Sarla Saroha, Mr Mahipal Singh and my parents-in-law, Mrs Iqbal Jit and Mr Tirath Singh for all their wisdom and support. My children Jai and Mehar for their understanding. Finally, I would like to thank my better half Gagan Kooner for her immense patience, hard work and for being always there.

Table of contents

Table of Contents

Abstract.....	i
Acknowledgements	iii
Table of contents	iv
Declaration	x
List of Abbreviations.....	xi
List of figures	xvii
List of tables	xxvi
1. Introduction.....	1
1.1 The metabolic syndrome, insulin and insulin resistance	1
1.2 The multiple modifiable risk factors for development of the MetSyn.....	2
1.3 The concept of cell stress response.....	3
1.4 Adipose tissue in pathogenesis of the MetSyn	5
1.4.1 Obesity and metabolic inflammation in adipose tissue	7
1.4.2 Adipose tissue cell stress response in obesity	18
1.4.3 Interactions between inflammation, cell stress response and insulin action	43
1.4.4 Summary of role of adipose tissue in obesity associated metabolic dysfunction.....	48
1.5 The liver.....	49
1.5.1 Non-alcoholic fatty liver disease.....	49
1.5.2 Relationship between NAFLD and insulin resistance	50
1.5.3 Hepatic inflammation in obesity associated metabolic dysfunction.	54

1.6	Developmental programming of insulin resistance and the MetSyn.....	62
1.6.1	The concept of developmental programming	62
1.6.2	The critical windows of development and nutritional programming	64
1.7	Programming of the hepatic and adipose cell stress and inflammation response	73
1.7.1	Experimental approach	75
1.8	Aims and hypothesis	81
2	Materials and methods	82
2.1	Experimental study design.....	82
2.1.1	Nutritional intervention in twin bearing pregnant ewes during late gestation	83
2.1.2	Modulation of early growth of the offspring during the suckling period	85
2.1.3	Post weaning environment of rearing until early adulthood (age 90 days until 17 months).....	86
2.1.4	Overview of the factorial experimental designs	88
2.2	Blood sampling	90
2.3	Tests for glucose tolerance and insulin resistance	90
2.3.1	Glucose tolerance test procedure and analysis.....	92
2.4	Plasma analyses.....	92
2.4.1	Plasma glucose analysis.....	92
2.4.2	Insulin assay	92
2.4.3	Plasma lipid analysis	94
2.4.4	Cortisol Assay.....	96
2.4.5	Plasma leptin.....	96
2.5	Physical activity measurement	97

2.6	Postnatal growth and adipose depots analysis	99
2.7	Euthanasia and tissue sampling.....	100
2.8	Tissue analysis	100
2.8.1	Triglyceride analysis	101
2.8.2	Thiobarbituric acid reactive substances (TBARS)	103
2.9	Gene expression analysis	107
2.9.1	Ribonucleic acid (RNA) extraction.....	107
2.9.2	RNA quantitation and quality control	109
2.9.3	Reverse transcription	115
2.9.4	Oligonucleotide primers for PCR.....	116
2.9.5	Polymerase Chain Reaction (PCR)	120
2.9.6	Quantitative real time polymerase chain reaction (qPCR) .	127
2.10	Histology	134
2.10.1	Tissue processing and microtomy.....	134
2.10.2	Histochemistry	138
2.10.3	Histochemical analysis of hepatic tissue	140
2.10.4	Immunohistochemistry	142
2.10.5	Quantification of adipocyte size.....	148
2.10.6	Quantitative assessment of DAB staining	152
2.11	Statistical analyses	158
2.11.1	Statistical power and sample size.....	158
2.11.2	Choice of statistical tests	162
3	The effect of prenatal nutrient restriction and obesity on the cell stress response and metabolic inflammation in liver and adipose tissue	168
3.1	Introduction and hypothesis.....	168

3.2	Methods	171
3.3	Results.....	174
3.3.1	Maternal and offspring metabolic profile.....	174
3.3.2	Liver weight and triglyceride deposition	194
3.3.3	Liver histology	199
3.3.4	Hepatic gene expression	202
3.3.5	Histological characteristics of omental adipose tissue.....	206
3.3.6	Omental adipose tissue gene expression analysis.....	213
3.4	Discussion	219
3.4.1	NR-LG in twin bearing sheep leads to a state of energy deficit and growth restriction of the developing offspring	220
3.4.2	Body weight and metabolic parameters of the offspring ...	222
3.4.3	The characteristics of liver fat deposition and cell stress response to obesity with and without prenatal NR-LG.	227
3.4.4	The characteristics of sheep omental adipose tissue in obesity and effect of prenatal NR-LG	234
3.5	Conclusion.....	246
4	Interaction of prenatal nutrient restriction and formula feeding during early life on the cell stress response and metabolic inflammation in liver and adipose tissue.	251
4.1	Introduction and hypothesis.....	251
4.2	Methods	254
4.3	Results.....	257
4.3.1	Maternal and offspring metabolic profile.....	257
4.3.2	Liver weight, triglyceride deposition and oxidative stress.	275
4.3.3	Liver histology	278
4.3.4	Hepatic gene expression	280

4.3.5	Omental adipose tissue histological characteristics	283
4.3.6	Omental adipose tissue gene expression analysis.....	286
4.4	Discussion	290
4.4.1	Maternal and offspring metabolic profiles	291
4.4.2	Hepatic fat deposition and cell stress response in formula feeding with, or without, pre-existing NR-LG.	297
4.4.3	Omental adipose tissue characteristics and cell stress response in formula feeding with or without pre-existing NR-LG...	299
4.5	Conclusion.....	300
5	Effect of prenatal nutrient restriction followed by accelerated postnatal growth on the cell stress response and metabolic inflammation in liver and adipose tissue.	302
5.1	Introduction and hypothesis.....	302
5.2	Methods	305
5.3	Results.....	308
5.3.1	Maternal and offspring metabolic and endocrine profile....	308
5.3.2	Liver weight, triglyceride deposition and oxidative stress.	314
5.3.3	Liver histology	315
5.3.4	Hepatic gene expression	316
5.3.5	Omental adipose tissue histological characteristics	320
5.3.6	Omental adipose tissue gene expression analysis.....	322
5.4	Discussion	325
5.4.1	Accelerated early growth in sheep is not associated with development of adult obesity, insulin resistance or altered cell stress response.....	326
5.5	Conclusion.....	330

6	Conclusions	331
6.1	Aims	331
6.2	Summary of findings.....	332
6.2.1	Effects of obesity in young adult sheep	334
6.2.2	Effects of maternal nutrient restriction followed by obesity in offspring	334
6.2.3	Interaction of prenatal nutrient restriction and formula feeding during the suckling period.....	337
6.2.4	Effects of rate of weight gain during suckling period following nutrient restriction in a twin pregnancy.....	339
6.3	Limitations of the model	341
6.3.1	The sheep as a model of obesity and metabolic syndrome	341
6.3.2	The sheep as a model of IUGR secondary to maternal undernutrition.	342
6.3.3	The sheep as a model for formula feeding.....	344
6.3.4	The sheep model of rapid postnatal growth	344
6.3.5	Effect of gender	345
6.3.6	Technical challenges.....	345
6.4	Future work	346
6.4.1	Elucidation of metabolic inflammation in obesity, its effects on organism and developmental programming.	346
6.5	Final remarks.....	349
	Bibliography.....	350

Declaration

The work in this thesis was performed within the Academic Child Health Division, School of Medicine, University of Nottingham between August 2011 and July 2014.

This thesis illustrates my own work, completed under the supervision of Professor Helen Budge and Professor Michael Symonds. This report is an accurate representation of the work performed and no other study reproducing this work, to my knowledge, has been carried out within the University of Nottingham.

Vivek Saroha

September 2017

List of Abbreviations

°C	degree celsius
µl	microlitre
µmol	micromoles
¹²⁵ I	radioactive isotope of iodine
4AAP	4-aminoantipyrine
A	fed to appetite during late gestation
Ac	accelerated growth experienced by offspring suckling on mother's feed without competition from sibling
Acyl CoA	acyl-coenzyme-A
AFRC	Agricultural and Food Research Council
AIF	apoptosis inducing factor
Akt	another name for protein kinase B (PKB)
ALP	alkaline phosphatase
ALT	alanine transaminase
AMPK	5' adenosine monophosphate-activated protein kinase
AP1	activator protein 1
ATF	activating transcription factor
Atg	autophagy related protein
ATG	autophagy related gene
ATP	adenosine triphosphate
BAK	Bcl-2 homologous antagonist/killer
BAT	brown adipose tissue
BAX	Bcl-2-like protein 4
BCA	bicinchonic acid
Bcl2	Apoptosis regulator B-cell lymphoma 2
BDH	tert-butanol -Triton X-100

BECN	gene encoding autophagy protein Beclin1
BHT	butylated hydrotoluene
BiP	binding immunoglobulin protein
BMI	body mass index
bZIP	basic leucine zipper
CD	cluster of differentiation
cDNA	complementary DNA
CHOP	C/EBP-homologous protein
ChREBP	carbohydrate-responsive element-binding protein
CI	confidence interval
CLS	crown like structures
CoA	coenzyme A
COSHH	Control of Substances Hazardous to Health
cpm	counts per minute
CRP	C-reactive peptide
Ct	cycle threshold
Cyt-c	cytochrome C
d	day
DAG	diacyl-glycerol
dGA	days gestational age
DNA	deoxyribonucleic acid
dNTP	deoxyribonucleotide triphosphate
DOHAD	developmental origin of health and disease
DXA	dual-energy X-ray absorptiometry
EARNEST	Early Nutrition Programming Project
EDEM	ER stress degradation enhancer molecule
EDTA	ethylenediaminetetraacetic acid
eIF2	eukaryotic initiation factor 2
ELISA	enzyme linked immuno-sorbent assay

ER	endoplasmic reticulum
ERAD	ER associated degradation
Fm	offspring reared on formula feed
FOAD	fetal origin of adult diseases
FoxO	forkhead box O
g	gram
g	gravity, standard acceleration due to free fall; 9.80665 m/s ²
GC	glucocorticoid
GCR	glucocorticoid receptor
gDNA	genomic DNA
GGT	gamma glutamyltransferase
GRP	glucose regulated protein
GTT	glucose tolerance test
H&E	haematoxylin and eosin
HFD	high fat diet
HOMA-IR	homeostatic model of insulin resistance (HOMA-IR)
HSD	hydroxysteroid dehydrogenase
Hz	hertz
IAP	inhibitor of apoptosis
IKK β	inhibitor of nuclear factor kappa-B kinase subunit beta
IL	interleukin
iNOS	inducible nitric oxide synthase
IPO8	importin 8
IRE1	inositol requiring enzyme 1
IRS	insulin receptor substrate
IUGR	intrauterine growth restriction
I κ B	inhibitor of kappa B
JNK	c-Jun N-terminal kinase

kg	kilogram
L	lean phenotype of offspring raised in field
L	litres
LC3	microtubule-associated protein light chain 3
LiH	lithium heparin
LPA	lysophosphatidic acid
MAPK	mitogen-activated protein kinase
MDA	malondialdehyde
MetSyn	Metabolic Syndrome
mg	milligrams
MJ	megajoule
ml	millilitres
mmol	millimoles
MRC	Medical Research Council
mRNA	messenger ribonucleic acid
mTOR	mammalian target of rapamycin
mTORC1	mammalian target of rapamycin complex 1
N	nutrient restricted to 60% MR requirement during late gestation
NAD	aldehyde dehydrogenase
NAFLD	non alcoholic fatty liver disease
NASH	non alcoholic steatohepatitis
NEFA	non esterified fatty acid
NF- κ B	nuclear factor kappa-B
nm	nanometer
nM	nanomolar
NR-LG	nutrient restriction during late gestation
O	obese phenotype of offspring raised in restricted barn
ob	obese

ObR	leptin receptor
PAMP	pathogen-associated molecular patterns
PBS	phosphate buffered saline
PCR	polymerase chain reaction
PERK	PKR-like eukaryotic initiation factor 2 α kinase
PI3K	phosphatidylinositol 3-kinase
PKB	protein kinase B
PKC	protein kinase C
PKR	double-stranded RNA-dependent protein kinase
PPAR	peroxisomal proliferation activated receptor
PRR	pattern recognition receptors
qPCR	quantitative real time PCR
R	fed to 100% metabolic requirement all through the pregnancy
RAPTOR	regulatory associated protein of mTOR
RIN	RNA integrity number
RNA	ribonucleic acid
RNAse	ribonuclease
ROS	reactive oxygen species
RPL19	60S ribosomal protein L19
rpm	revolutions per minute
RPO	large ribosomal protein
RR	relative risk
SD	standard deviation
SDS	sodium dodecyl sulphate
SGA	small for gestation age
SIRT1	gene encoding protein Sirtuin1
SOCS	suppressor of cytokine signalling
SREBP	sterol regulatory element-binding protein

St	standard growth experienced by offspring reared as twin during suckling
TAG	triglyceride
TBA	thiobarbituric acid
TBARS	thiobarbituric acid reactive substances
TLR	toll like receptors
TMB	tetramethylbenzidine
TNF α	tumour necrosis factor alpha
TOOS	N-ethyl-N(2hydroxy-3-sulphopropyl)m-toluidine
TSC2	tuberous sclerosis complex 2
UCP1	uncoupling protein 1
UDG	uracil-DNA glycosylase
UGGT	UDP-glucose:glycoprotein glucosyltransferase
ULK	unc-51 like kinase
UPR	unfolded protein response
VFA	volatile fatty acids
VLDL	very low density lipoprotein
WAT	white adipose tissue
WHO	World Health Organisation
XPB1	X-box binding protein 1
yr	year
YWHAZ	tryptophan-3 monooxygenase activation protein

List of figures

Figure 1.1 Schematic diagram illustrating the role of cell stress response in cell survival or cell death.....	5
Figure 1.2 Mutually interacting processes in adipose tissue in response to obesity which contribute to metabolic inflammation.	8
Figure 1.3 Schematic diagram showing pathways of fatty acid induced metabolic inflammation.	14
Figure 1.4 Diagram summarising characteristic features of adipose tissue macrophage infiltration.	15
Figure 1.5 Schematic diagram demonstrating protein folding and quality control processes in the ER.	20
Figure 1.6 Schematic diagram demonstrating the multiple outcomes of activation of the unfolded protein response (UPR).....	23
Figure 1.7 Canonical pathways of the unfolded protein response (UPR)	24
Figure 1.8 Schematic diagram depicting overview of the autophagic process.	31
Figure 1.9 Schematic diagram depicting the key pathways conjugation systems required for autophagosome formation.	33
Figure 1.10 Schematic diagram depicting regulation of autophagy by insulin.....	34
Figure 1.11 Regulation of autophagy by ER stress response activation.	35

Figure 1.12 Schematic diagram depicting regulatory role of energy sensing in autophagy activation.....	37
Figure 1.13 Depiction of the central role of JNK in development of insulin resistance and propagation of inflammation.	44
Figure 1.14 Schematic diagram demonstrating mechanisms of inflammation propagation and proposed mechanism of development of insulin resistance in response to IKK stimulation.....	46
Figure 1.15 Diagram summarising interaction of multiple cell stress pathways activated in adipose tissue during obesity.....	48
Figure 1.16 Schematic diagram depicting regulation of hepatocyte lipid metabolism in response to blood glucose concentrations and insulin ...	51
Figure 1.17 Lipid metabolism in hepatocytes in the state of insulin resistance.....	52
Figure 1.18 Sources of inflammatory processes witnessed in non alcoholic fatty liver disease.	55
Figure 1.19 Schematic diagram illustrating the proposed interaction of nutritionally mediated developmental programming s	74
Figure 2.1Flowchart depicting prenatal nutritional intervention in the studies.	84
Figure 2.2: Schematic representation of experimental intervention during the suckling period.	85
Figure 2.3: Schematic representation of post weaning environment of rearing until 17 months of age.	87

Figure 2.4 Schematic representation of the sequential experimental intervention evolving into the three different experimental studies.	89
Figure 2.5 Schematic diagram demonstrating the steps in sandwich enzyme linked immunosorbent assay (ELISA)	93
Figure 2.6: An actogram demonstrating graphical representation of the physical activity data over a period of 48 hours.	98
Figure 2.7: Mechanism of lipid peroxidation	103
Figure 2.8: Image of non denaturing agarose gel electrophoresis of RNA.	111
Figure 2.9: Graph of absorbance at different wavelengths made using Nanodrop ND1100	112
Figure 2.10: Agilent bioanalyser use for RIN determination.....	114
Figure 2.11 Schematic representation the principle of exponential amplification during first few PCR cycles	122
Figure 2.12: Amplification plot of a PCR reaction demonstrating increasing signal from serial dilution of standards and the samples. ...	127
Figure 2.13: A representative graph of standard curve	129
Figure 2.14: Melting curve graph following a qPCR cycle.....	130
Figure 2.15 Representative images of liver tissue stained with H&E (A) and Masson's Trichrome (B) stain visualised at 20X magnification.	141
Figure 2.16: Schematic demonstrating the principle of diaminobenzidine (DAB) staining in immunohistochemistry.	146

Figure 2.17 Graph demonstrating strong correlation of two different quantification methods of adipocyte size measurement.	151
Figure 2.18 A series of representative images demonstrating the process of background correction.	153
Figure 2.19: Colour deconvolution of DAB and haematoxylin stain using the ImageJ software plugin called ColorDeconvolution [394].	155
Figure 2.20 : Images demonstrating thresholding procedure on a representative negative control and sample.	156
Figure 2.21 Representative graphical examples demonstrating ordinal (A) and disordinal (B) interaction.	164
Figure 2.22 Representative example of Syntax used for simple main effects.....	165
Figure 3.1 Schematic flow chart summarising the study hypothesis and expected outcomes of the investigation.	170
Figure 3.2 Schematic diagram depicting the factorial experimental design.....	172
Figure 3.3 Maternal weight gain during late gestation, expressed as percentage gain over the weight at 110 days of gestation (dGA).	175
Figure 3.4 Fasting plasma insulin (A), glucose (B), non-esterified fatty acids (NEFA, C) and triglyceride (D) concentrations.	176
Figure 3.5 Weight gain during the suckling period.....	178
Figure 3.6 Body weight fold change relative to birth weight	179

Figure 3.7 Effect of the post-weaning environment on body weight in offspring.....	181
Figure 3.8 Relative proportion of visceral and non visceral adipose tissue weight at age 17 months.....	184
Figure 3.9 Plasma glucose (A) and insulin (B) concentrations during a glucose tolerance test performed at the age of 7 months.....	187
Figure 3.10 Plasma glucose (A) and insulin (B) concentrations during a glucose tolerance test performed at the age of 16 months.	191
Figure 3.11 Organ weight of the offspring liver in grams (A) and relative (B) to the body weight in grams/kg.	194
Figure 3.12 Correlation analysis of weight of liver at 17 months of age against measured liver triglyceride concentrations (A) and calculated total liver triglyceride content (B) respectively.	197
Figure 3.13 Liver tissue stained with H&E (A) and Masson's Trichrome (B) stains visualised at 10x magnification	199
Figure 3.14 Representative histological sections of sheep liver from lean and obese offspring stained with Masson's Trichrome.....	201
Figure 3.15 Normalised gene of hepatic ATG12 and BECN1 expressed as arbitrary units relative to A-L group.	204
Figure 3.16 Representative images of haematoxylin and eosin stained omental adipose tissue sections from Lean (A) and Obese animals (B).....	206
Figure 3.17 Mean adipocyte area in μm^2 calculated from the histological sections of omental adipose tissue of 17 month old offspring.	207

Figure 3.18 Correlation analysis of adipocyte size with adult body weight (A) and weight of the omental adipose tissue at dissection (B).	208
Figure 3.19 Representative images demonstrating distribution of staining for GRP78 in adipose tissue from lean (A) and obese (B)	209
Figure 3.20 Representative images demonstrating pJNK staining visible in the perinuclear areas in the omental adipose tissue	210
Figure 3.21 Representative images of Iba1 staining of adipose tissue of lean (A and B) and obese (C and D) sheep.	212
Figure 3.22 Relative gene expression in omental adipose tissue for unfolded protein response components:	216
Figure 3.23 Relative gene expression in omental adipose tissue for (A) ATG12 and (B) BECN1.....	217
Figure 3.24 Normalised gene expression of AMPK (A) and mTOR (B) in omental adipose tissue.....	218
Figure 3.25 Schematic diagram depicting (A) the role of constitutive autophagy and UPR maintenance of liver homeostasis and (B) obesity induced defective autophagy and ER stress.....	230
Figure 3.26 Schematic diagram depicting the mechanism of increased transcription of autophagy genes in the state of insulin resistance.. ...	231
Figure 3.27 Schematic diagram of canonical pathways of ER stress....	240
Figure 3.28 Schematic diagram depicting the two proposed mechanisms leading to increased vulnerability of adipose tissue	244

Figure 3.29 Schematic flowchart summarising the overall findings of the study described in this chapter.....	249
Figure 4.1 Schematic diagram depicting the experimental study design	255
Figure 4.2 Weight gain during late gestation (110 -145 days), expressed as percentage gain over the weight at 110 days of gestation.	257
Figure 4.3 Fasting plasma insulin (A), glucose (B), NEFA(C) and triglyceride (D) concentration on 130 days of gestation.....	258
Figure 4.4 Weight gain during the suckling period.....	260
Figure 4.5 Relative weight gain during the suckling period in offspring.	261
Figure 4.6 Plasma glucose (A) and insulin (B) concentrations during a glucose tolerance test performed at the age of 7 months.....	264
Figure 4.7 Offspring body weight measurements following weaning from milk feeds at 90 days of age.	267
Figure 4.8 Correlation analysis of mean 24 hour physical activity measurements performed at the age of 45 days and at 15 months. ...	270
Figure 4.9 Plasma glucose concentrations during a glucose tolerance test performed at the age of 16 months.....	271
Figure 4.10 Plasma insulin concentrations during a glucose tolerance test	272
Figure 4.11 Correlation analysis of weight of liver at 17 months of age against measured liver triglyceride relative concentrations.....	276

Figure 4.12 Correlation analysis of relative triglyceride concentration in the liver tissue at 17 months of age	277
Figure 4.13 Representative histological sections of hepatic periportal area.....	279
Figure 4.14 Representative H&E stained histological sections of omental adipose tissue	284
Figure 4.15 Relative gene expression of A, mTOR; B, AMPK; C, ATG12; D, BECN1 in omental adipose tissue.....	289
Figure 5.1 Schematic diagram depicting the overlap between studies described in Chapters 3, 4 and 5.	306
Figure 5.2 Schematic diagram demonstrating the randomisation and timing of blood sampling and DXA scan investigations.....	307
Figure 5.3 Offspring weight gain from birth to age of 90 days	308
Figure 5.4 Plasma glucose and insulin measurements during glucose tolerance test performed at 7 months (A and B respectively) and 16 months (C and D respectively).	312
Figure 5.5 Representative images of histological sections of liver from (A) St and (B) Ac offspring stained with Masson's Trichrome	315
Figure 5.6 Gene expression for liver TLR4 (A) and leptin receptor (B).	316
Figure 5.7 Relative gene expression in liver for mTOR (A) and AMPK (B)	319

Figure 5.8 Representative images demonstrating distribution of staining in omental adipose tissue for GRP in (A) St and (B) Ac offspring and staining for Iba1 in (C) St and (D) Ac offspring..... 321

List of tables

Table 1.1 Adipokines known to have pro- and anti-inflammatory properties.....	11
Table 1.2 Summary of the outcome of activation the IRE1 pathway of unfolded protein response.	25
Table 1.3 Table summarising the outcome of activation of PERK pathway of UPR.....	26
Table 1.4 Table summarising the outcome of activation of ATF6 pathway of UPR.....	27
Table 1.5 Studies of genetically engineered rodent models demonstrating the role of adipose tissue ER stress response in insulin resistance.....	28
Table 1.6 Interaction of molecular pathways with apoptosis activation.	41
Table 1.7 Table listing some of proposed mechanisms for development of hepatic insulin resistance in NAFLD.	53
Table 1.8 Overview of experimental approach for study of hepatic and adipose tissue cell stress and inflammatory response to obesity and nutritional programming.....	79
Table 1.9 Genes involved in regulation of development of insulin resistance by activation of cell stress response and metabolic inflammation.....	80
Table 2.1 Macronutrient content of ewe and formula milk.	86
Table 2.2: Table demonstrating interaction of prenatal and postnatal experimental conditions used in the factorial design of the experiments	88

Table 2.3 Details of the genes, accession numbers and primer sequences for primers for genes used as reference genes for PCR	118
Table 2.4 Details of the genes, accession numbers and primer sequences for PCR primers designed in-house	119
Table 2.5 Details of the genes, accession numbers and primer sequences for primers sourced from PrimerDesign® company	120
Table 2.6 The components and volume used for reaction of classical PCR.	123
Table 2.7 The stages and program conditions for classical PCR. The steps 3-5 are repeated over 45 cycles before moving to step 6.....	124
Table 2.8 The components and volume of the PCR reaction mix for each reaction. The volume of the individual components varied depending on the source of the primer used.	133
Table 2.9 The steps in the QPCR protocol including the melting curve stage	134
Table 2.10: Tissue processing steps performed using a Shandon Escelsior™ tissue processor	136
Table 2.11: Details of the antibodies used for immunohistochemistry using DAB staining.....	144
Table 2.12: Details of the plugins used with ImageJ software for the process of quantification of the DAB staining in digital images.....	149
Table 2.13: Table listing the commands used in ImageJ software for quantification of the DAB staining in digital images..	158

Table 3.1 Physical activity parameters at 45 days of age in offspring of ewes randomised as described	180
Table 3.2 Physical activity parameters at 12 months of age	182
Table 3.3 Weight of omental, pericardial and perirenal adipose tissue depots at age 17 months.....	183
Table 3.4 Body weight and fat content parameters calculated and extrapolated from DXA measurements.	185
Table 3.5 Markers of insulin sensitivity expressed as area under the curve and HOMA-IR calculated from glucose tolerance test performed at age 7 months..	188
Table 3.6 Plasma metabolic profile in the fasted state at the age of 7 months	189
Table 3.7 Markers of insulin sensitivity expressed as area under the curve insulin and HOMA-IR calculated from glucose tolerance test performed at age 16 months.....	192
Table 3.8 Plasma metabolic profiles in the fasted state at the age of 16 months.	193
Table 3.9 Liver triglyceride concentrations and total triglyceride content in different experimental groups.	195
Table 3.10 Correlation of body weight at 17 months of age (kg) against liver weight (kg) at dissection and total liver triglyceride content (g) respectively for all animals (n=35).	198

Table 3.11 Normalised gene expression of genes involved in regulation of metabolic inflammation expressed in arbitrary units relative to the A-L group.....	202
Table 3.12 Normalised gene expression for components of the unfolded protein response: ATF4, ATF6, EDEM1 and GRP78,	203
Table 3.13 Normalised gene expression of hepatic mTOR expressed in arbitrary units relative to the A-L group.....	205
Table 3.14 Quantitative analysis of GRP78 and pJNK stain expressed as area stained in μm^2 / adipocyte.....	210
Table 3.15 GeNorm normalised gene expression for regulators of metabolic inflammation in the omental adipose tissue of 17 month old offspring.....	213
Table 3.16 Correlation analysis between gene expression and plasma concentration of leptin in all animals and subgroup analysis of obese and lean animals.	214
Table 3.17 GeNorm normalised gene expression for components of the unfolded protein response in the omental adipose tissue.	215
Table 4.1 Birth weight measurements in offspring of ewes fed to requirement during pregnancy	259
Table 4.2 Physical activity parameters at 45 days of age in offspring of ewes fed to requirement during pregnancy	262
Table 4.3 Markers of insulin sensitivity expressed as area under the curve and HOMA-IR calculated from glucose tolerance test performed at 7 months of age.....	265

Table 4.4 Plasma metabolic profile in fasted state at the age of 7 months	266
Table 4.5 Body weight and adipose tissue deposit details in offspring.	268
Table 4.6 Physical activity parameters at the age of 15 months	269
Table 4.7 Markers of insulin sensitivity expressed as area under the curve and HOMA-IR.....	273
Table 4.8 Plasma metabolic profile in the fasted state at the age of 16 months	274
Table 4.9 Liver weight, triglyceride concentrations, calculated total liver triglycerides and hepatic TBARS assay	275
Table 4.10 Periportal fibrosis area quantified from Masson's Trichrome stained histological sections	278
Table 4.11 Gene expression for regulatory factors of inflammation and cell stress response (leptin receptor, TLR4, CD95 and CD68) 8.....	280
Table 4.12 Gene expression analysis for components of unfolded protein response.	281
Table 4.13 Gene expression for the components of autophagy in the liver tissue.....	282
Table 4.14 Mean adipocyte area in μm^2 calculated from the histological sections of omental adipose tissue	283
Table 4.15 Quantitative analysis of GRP78 and pJNK stain	285

Table 4.16 Gene expression analysis of leptin, adiponectin, CD68 and TLR4 in omental adipose tissue	286
Table 4.17 Relative gene expression ATF4, ATF6, GRP78 and EDEM1 .	287
Table 4.18 Macronutrient and calorific content in sheep milk and formula milk used in the study.....	292
Table 5.1 Body weight and physical activity parameters at the age of 45 days and 15 months	309
Table 5.2 Body composition and organ weight of the offspring	310
Table 5.3 Plasma metabolic and endocrine profile of offspring at age 7 and 16 months.....	313
Table 5.4 Liver organ weight, triglyceride content and TBARS measurements	314
Table 5.5 Relative gene expression of liver CD68, CD95 and 11 β HSD1 for lambs.....	317
Table 5.6 Relative gene expression for the components of the UPR (ATF4, ATF6, EDEM1 and GRP78).	318
Table 5.7 Mean adipocyte area in μm^2 and quantification of GRP78 and pJNK.....	320
Table 5.8 Gene expression for leptin, adiponectin, CD68, TLR4 and 11 β HSD1 in the omental adipose tissue.....	322
Table 5.9 Expression of genes responsible for UPR in the omental adipose tissue of lambs.....	323

Table 5.10 Gene expression of regulators and components of autophagy in omental adipose tissue	324
Table 6.1 Summary of the findings of studies described in this thesis listed in a tabular format.	333
Table 6.2 Summary of methodology and relevant outcomes of major epidemiological studies investigating association between early postnatal growth with obesity and adiposity.....	340

1. Introduction

1.1 The metabolic syndrome, insulin and insulin resistance

Metabolic syndrome (MetSyn) is a term used to describe a cluster of conditions which occur together and predispose an individual to the development of type 2 diabetes and cardiovascular disease. These conditions are raised blood pressure, dyslipidaemia (raised triglycerides and lowered high-density lipoprotein cholesterol), raised fasting glucose, and central obesity (defined as Body Mass Index (BMI) of $>30\text{kg/m}^2$). The congregation of these conditions is a recognised phenomenon [1] and is known to be independently associated with cardiovascular events and death. This was confirmed in a meta-analysis [2] of 43 cohorts of adults ($n=17573$) which demonstrated the increased relative risk ($RR=1.78$) of cardiovascular events and death in the presence of the MetSyn. The relative risk remained high ($RR=1.54$) even after adjusting for common cardiovascular risk factors. The MetSyn is associated with a five-fold increased risk of type 2 diabetes [3] and predicts diabetes, independently of glucose intolerance.

The worldwide prevalence of the MetSyn is difficult to estimate due to multiple clinical definitions and diagnostic criteria used in such studies [1]. Irrespective of the diagnostic criteria, MetSyn is highly prevalent in developed [4] and developing countries [5]. In the United States and Europe, 20–25% of the adult population and, in South East Asia, approximately 20% of the adult population have been reported to be affected [5]. Such a high prevalence of the MetSyn and its consequent effects on health is now a global public health problem which has been described as a worldwide pandemic [6, 7].

Insulin is a hormone secreted by pancreatic beta cells in a regulated manner and is important for regulation of body's carbohydrate and fat metabolism. The term insulin resistance describes a state when the cells in the body fail to respond to presence of insulin, thereby adversely affecting the control of normal metabolic processes. The body responds by increasing insulin secretion, resulting hyperinsulinemia occurs and this often precedes the development of type 2 diabetes mellitus which is characterised by presence of hyperglycaemia in presence of insulin.

Insulin resistance is a common feature of the MetSyn and contributes to the pathogenesis of its components [8]. Obesity [9, 10] and, more specifically, fat deposition in the body's truncal region [11] (central adiposity) has been long known to be strongly associated with the development of insulin resistance, whilst weight loss has been demonstrated to improve insulin resistance [12]. The establishment of insulin resistance is considered central to pathogenesis of the adverse cardiovascular and metabolic outcomes of the MetSyn [13].

1.2 The multiple modifiable risk factors for development of the MetSyn

Obesity is a major component of the MetSyn and according to the estimates of the World Health Organisation (WHO) in 2008, out of the estimated 6.8 billion world-wide population [14], 1.5 billion (35% of adults) aged 20 years and over were overweight and, of these, at least 200 million men and nearly 300 million women were obese [15]. The high prevalence of obesity is not limited to the developed world or to adulthood as it is increasing in the developing world [16] and the prevalence of childhood obesity has tripled in the past 30 years [17].

Whilst obesity is a major risk factor for development of the MetSyn [18-20], other mutually interacting factors including ethnicity, low birth weight, nutrition during early life, gender and postmenopausal state, smoking and diet also contribute to the development of the MetSyn and its associated morbidities [7]. A state of subacute inflammation is considered to be one such risk factor [21]. This concept is supported by the increased incidence of the MetSyn and type 2 diabetes in individuals with clinical conditions of chronic inflammatory state such as hepatitis C [22], HIV [23] and rheumatoid arthritis [24]. The modifiable risk factors preceding the development of the MetSyn provide a vital opportunity for preventative and therapeutic measures which have the potential to result in major public health benefits [7].

1.3 The concept of cell stress response

All the living cells in a body are regularly exposed to stimuli with the potential of causing cellular damage or cell death. Such stimuli can originate intrinsic to the cell, for example, malformed protein structure, accumulation of toxic metabolites, DNA damage, energy deficit and activation of inflammatory pathways or can be of extrinsic origin such as pathogen infestation, excess metabolites, osmotic load, excess heat or cold. The response mounted by the cell to these stimuli is dependent on several factors including [25]:

- type and level of insult
- type of organ/cell
- the adaptive capacity of the cell

Cell stress response pathways play a significant role in the physiological and pathological processes of development, ageing and disease [26].

Developmentally, the cell stress response pathways are important component of embryogenesis, implantation and organ development. [27].

Innate cellular mechanisms collectively act to correct the insult, limit or reverse the damage to the macromolecules, organelle or cell structure and are collectively called the cell stress response (Figure 1.1). On activation, the cell stress response eventually leads to intact cell survival or cell death [25]. The elaborate pathways that act to try to restore cell's survival ability are still being discovered and updated but are already known to have considerable overlap. The different interlinked primarily pro-survival pathways are:

- unfolded protein response (UPR)
- heat shock response
- antioxidant response
- DNA damage response
- autophagy

If the pro-survival response is unsuccessful, cell death programmes are activated. These are:

- apoptosis
- autophagy
- necrosis

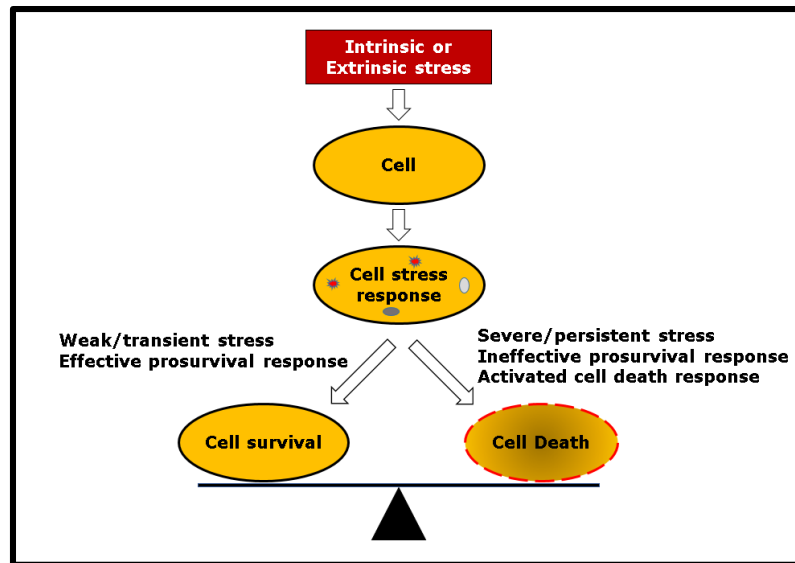


Figure 1.1 Schematic diagram illustrating the role of cell stress response in cell survival or cell death.

Depending upon the type and severity of insult, a cell responds with activation of the cell stress response which either attempts to promote cell survival or directs the cell towards programmed cell death pathways

The DNA damage response is initiated by exposure to chemotherapeutic agents, irradiation and environmental toxins. Known regulators of the heat shock response include environmental factors (heat shock, drugs, oxidative stress, toxic chemicals, heavy metals etc), pathological conditions (fever, inflammation, ischemia and reperfusion) and diseases (such as Alzheimer's Disease and Huntington's Chorea) [28]. These will not be considered in this study. In contrast, the cell stress response pathways, which are known to be activated in nutritional deprivation or obesity include autophagy (Section 1.4.2.2) and unfolded protein response (Section 1.4.2.1), form an important focus of this study.

1.4 Adipose tissue in pathogenesis of the MetSyn

The main storage site for fat in the body, adipose tissues, are distributed in specific locations referred to as adipose tissue depots. In humans, adipose tissue depots are primarily described beneath the skin (subcutaneous fat), around internal organs (visceral fat), in bone marrow (yellow bone marrow) and in breast tissue.

Visceral fat or abdominal fat is packed in between organs such as between stomach, liver, intestines and kidneys, and is composed of several depots including mesenteric, epididymal white adipose tissue (EWAT) and perirenal depots. An excess of visceral fat is known as central obesity. There is a strong correlation between central obesity, insulin resistance and type 2 diabetes [29, 30].

Although adipose tissue exists both as white (WAT) and brown adipose tissue (BAT) in mammals, only WAT increases significantly with obesity whilst BAT decreases [31]. Whilst WAT is mainly storing energy, BAT releases energy from glucose and free fatty acids as heat by activating its unique protein, uncoupling protein 1 (UCP1) [32]. Adult humans still have small depots of brown adipocytes in the supraclavicular region and UCP1-positive cells are also found interspersed in WAT [32]. Whilst the role of BAT is increasingly being characterised, the focus of studies described in this thesis will be on depots of WAT. Unless otherwise stated, the use of term adipose tissue in this thesis represents white adipose tissue.

Adipose tissue consists of several cell types, with the highest percentage of cells being adipocytes which store lipids. Other cell types include fibroblasts, macrophages, and endothelial cells and many small blood vessels.

Adipocytes are derived from multi-potent mesenchymal stem cells that become committed to adipocyte cell lineage in tightly controlled processes [33]. With increasing fat deposition, adipose tissue mass increases by either adipocyte hypertrophy or hyperplasia. The dynamics of fat cell turnover have been under considerable scrutiny. It has been proposed that the number of fat cells in an individual are set during early life and, whilst 10% of the fat cells are renewed annually, the total number of adipocytes in adulthood remains largely constant [34]. In obesity, such restrictions on the total number of adipocytes means that excess fat storage would be dependent on adipocyte hypertrophy. Adipocyte hypertrophy is known to lead to

inflammatory cytokine expression [35] and may potentially put the cell's metabolic pathways under a state of stress and cellular dysfunction [36]. The role of inflammation in adipose tissue in the pathogenesis of metabolic derangements and insulin resistance seen in the MetSyn is described in detail in the sections that follow.

1.4.1 Obesity and metabolic inflammation in adipose tissue

The presence of low grade chronic inflammation in obese individuals has been demonstrated in several animal and human studies [37]. Biomarkers of inflammation (such as C-reactive proteins, interleukin-6 and soluble intracellular adhesion molecules) are present at increased concentrations in individuals who are insulin resistant and obese [38].

This obesity-associated inflammation is distinct from the well described acute phase response inflammation to trauma or infection. This moderate, chronic process is orchestrated by metabolic cells [39], has a largely local action and leads to modification of the tissue environment as reflected in immune cell infiltration and tissue remodelling in adipose tissue. The term metaflammation [39] has been proposed for this type of inflammation in a tissue with a primarily metabolic role.

There are several proposed mechanisms that link the state of nutrient excess, limited fat storage capacity of adipocytes, inflammation and the development of insulin resistance. The pathways which interact, promoting a state of cell stress and metabolic inflammation (Figure 1.2), are:

- adipokine-induced inflammation
- free fatty acid and lipid induced inflammatory processes
- macrophage activation
- endoplasmic reticulum (ER) stress and activation of the UPR

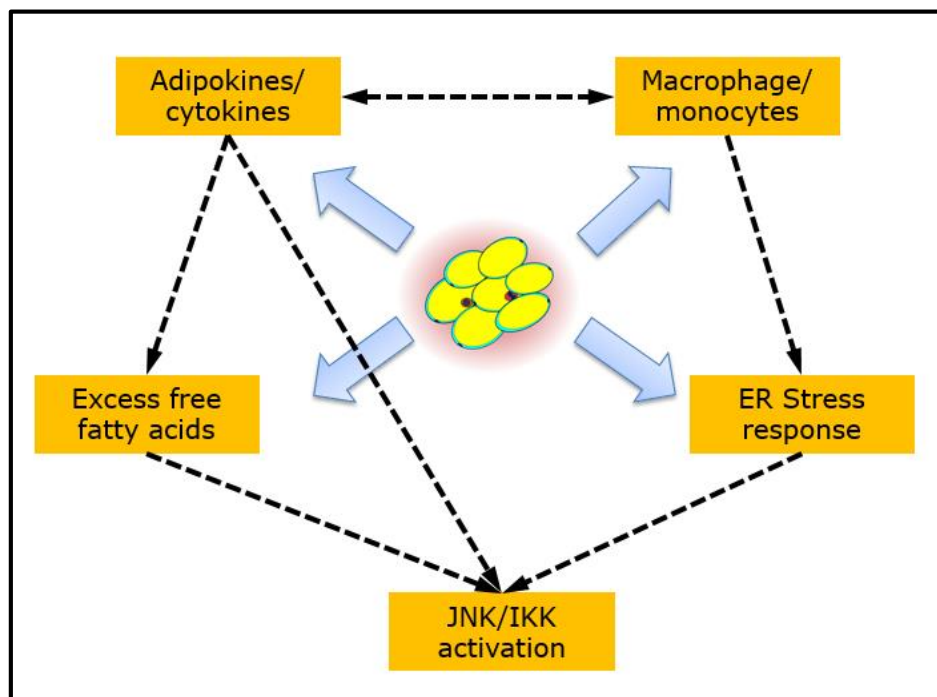


Figure 1.2 Mutually interacting processes in adipose tissue in response to obesity which contribute to metabolic inflammation.

Adipose tissue releases adipokines and cytokines which promote macrophage infiltration, affect metabolism and activate proinflammatory intracellular pathways via c-Jun N-terminal kinase (JNK) and inhibitor of nuclear factor kappa-B kinase (IKK). Excess free fatty acids, activation of endoplasmic reticulum (ER) stress and macrophage mediated inflammation are other mechanisms of this inflammation.

1.4.1.1 Adipokines in metabolic inflammation

As early as 1993, it had been identified that adipose tissue from obese individuals also secrete proinflammatory cytokines (e.g. tumour necrosis factor- α (TNF α)) which were capable of inhibiting insulin signalling [40, 41]. TNF α is a cytokine secreted primarily, but not exclusively, by macrophages and influences host defence and whole body lipid and glucose metabolism. Increased adipose tissue expression of TNF α messenger RNA (mRNA) and protein (local and systemic) has been demonstrated in four different rodent models of obesity and diabetes [40]. In further studies in murine genetic models, lack of TNF α bestows protection from the development of insulin resistance secondary to obesity, demonstrating the definitive role of adipokine-mediated inflammation in the pathogenesis of insulin resistance following obesity [42]. Such substances which have the potential to modify cell signalling and are secreted by adipose tissues are called adipokines.

Leptin, the first adipokine to be described in detail [43], is the product of the obese (ob) gene and is synthesised and secreted by adipose tissue in response to change in body fat and nutritional status. Circulating levels of leptin are increased in obesity in proportion to the body mass index (BMI) [44]. The primary function of leptin is stimulation of anorexigenic pathways through its action on hypothalamus [45]. Leptin's other actions include an insulin sensitising action in myocytes, hepatocytes and pancreatic β -cells where it also reduces the intracellular lipid content [46]. However, elevated leptin concentrations in obesity are, paradoxically, associated with insulin resistance and directly correlate with the severity of metabolic dysfunction [47]. This complex phenomenon has been attributed to leptin resistance and has not yet been fully explained [47].

Leptin has also been demonstrated to affect both innate and adaptive immune responses [48, 49], through a multitude of mechanisms including macrophage cytokine induction, activation of antigen presenting cells,

neutrophils and selective activation of Th1 immune cells. Children with congenital leptin deficiency manifest a reduced number of circulating CD4(+) T cells, impaired T cell proliferation and decreased cytokine release which are all reversed following administration of leptin [46]. Indeed, with increasing evidence of leptin's proinflammatory role a therapeutic role for recombinant leptin is now being proposed [50].

Out of the several isoforms of the leptin receptor (ObR), isoform b (ObRb) has the predominant role in leptin's intracellular action, whereas other isoforms bind, and inactivate, free leptin. The multiple pathways downstream of ObRb activation by leptin include IRS(1/2) phosphorylation, increased transcription of suppressor of cytokine signalling (SOCS) and components of activator protein 1 (AP1) transcription factors [49]. The downstream outcomes of these disparate outcomes include anti- and pro-inflammatory outcomes and also promoting insulin sensitivity and resistance. Whilst the specific pathways establishing leptin's role in obesity related inflammation and adverse metabolic outcomes have not been definitively distinguished [51], there is a consensus that the proinflammatory outcome of excess leptin in obesity contributes to the development of metabolic dysfunction and insulin resistance in obesity [52].

The concept of fat as a producer of important cytokines has evolved with identification of numerous other adipokines with pro and anti-inflammatory properties [53, 54] (Table 1.1).

Adipokines with pro-inflammatory properties
Leptin
Resistin
Retinol binding protein 4
Lipocalin 2
Angiopoietin-like protein 2
Tumour Necrosis Factor
Interleukin-6
Interleukin-18
CC chemokine ligand -2
CXC-chemokine ligand 5
Nicotinamide phosphoribosyltransferase
Adipokines with anti-inflammatory properties
Adiponectin
Secreted frizzled-related protein 5

Table 1.1 Adipokines known to have pro- and anti-inflammatory properties

In adipocyte cell cultures, gene expression of proinflammatory adipokines can occur in response to adipocyte hyperplasia [35]. These adipokines are known to act through proinflammatory pathways including c-Jun N-terminal kinase (JNK) and Inhibitor of nuclear factor kappa-B (IKK) (NF- κ B) (as described in Section 1.4.3), macrophage chemotaxis and activation and modulation of the unfolded protein response [53].

1.4.1.2 Free fatty acid and lipid induced inflammatory processes

Plasma free fatty acids are elevated in obesity [55] and can contribute to development of inflammation and insulin resistance through activation of pathogen sensing receptors [56] known as pattern recognition receptors (PRR) which recognise pathogen-associated molecular patterns (PAMP). PAMP are molecules that are broadly shared by pathogens but distinguishable from host molecules such as bacterial lipopolysaccharides. Primarily part of the innate immune response, PRR are also present on the metabolic cells (liver, adipose tissue and myocytes) of the body and are capable of initiating inflammation and cell stress response. Toll-like receptors (TLR) are membrane bound PRR known to be present in adipose tissue and liver and are a key element of innate and adaptive immunity capable of activating intracellular inflammatory pathways (JNK) and stimulating release of cytokines [57]. Adipose tissue expresses the subtypes TLR4 and TLR2.

Fatty acids of nutritional origin have been demonstrated to activate adipocyte and macrophage TLR4 and this activation contributes to the resulting insulin resistance [58] in mice. In the same experimental study of fatty acid infusion in TLR4 knockout mice, insulin signalling was not suppressed and insulin resistance did not occur. In mice, high fat diet (HFD) feeding also caused an increase in TLR4 expression along with increased expression of mediators of inflammation, IKK complex and c-JNK activity [59]. All these features were blunted in mouse model of genetic loss of TLR4 function [59] and cell specific deletion model of TLR4 [60]. This demonstrated that TLR4 function is essential for activation of inflammatory response and insulin resistance in response to abundant fatty acids and in the high fat diet mouse model.

Activation of TLR also has been demonstrated to be linked with activation of responses in the ER. Activation of mouse macrophages with TLR4 agonists including lipopolysaccharide or tunicamycin leads to upregulation of components of the ER stress response [61] and cytokine release from the macrophages. PAMP activation in presence of excess fatty acids, therefore, can lead to upregulation of metabolic inflammation via direct activation of inflammatory pathways and indirectly via activation of the ER stress response.

Another pathogen sensing receptor, double-stranded RNA-dependent protein kinase (PKR) is also significantly activated (by phosphorylation [62]) in the liver of the classic mouse model of severe insulin resistance resulting from leptin deficiency (ob/ob mice) and in the white adipose tissue and liver of mice on high fat diets as compared to their controls [63]. This was also replicated in a mice model of lipid infusion [63] while inhibitors of PKR lead to improve insulin sensitivity in obese diabetic mice [64]. PKR's primary function is considered to be as sensor for double stranded RNA, an indicator of viral invasion of the cell. PKR acts to regulate the activity of inflammatory kinases like JNK to regulate insulin action [39]. PKR has also been proposed to act in a way similar to the TLR molecules in regulation of inflammation in response to fatty acids [63]. PRRs, including TLR4 and PKR, therefore, play a key role in activation of metabolic inflammation in response to activation by free fatty acids (Figure 1.3).

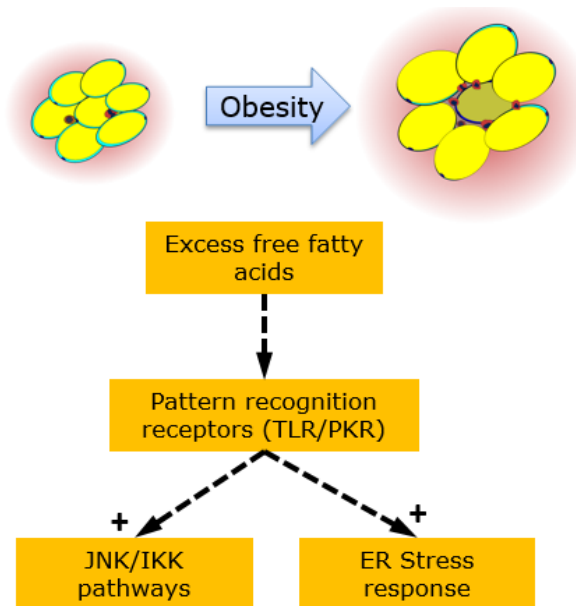


Figure 1.3 Schematic diagram showing pathways of fatty acid induced metabolic inflammation.

Free fatty acids, activate pattern recognition receptors such as toll-like receptors (TLR) and double-stranded RNA-dependent protein kinase (PKR) which stimulate intracellular proinflammatory pathways and ER stress response contributing to metabolic inflammation in obesity.

1.4.1.3 Adipose tissue macrophages

Weisberg *et. al.* [65] identified increased accumulation of macrophages in adipose tissue from obese, as compared to non-obese, mice. They also demonstrated that adipose tissue macrophages are of bone marrow origin and are responsible for almost all adipose tissue TNF- α expression and significant amounts of inducible nitric oxide synthase (iNOS) and interleukin (IL)-6 expression, a finding that has been confirmed in mice models and in humans [65]. The adipose tissue macrophage accumulation in obesity tends to occur in clusters surrounding necrotic adipocytes. Such appearances of macrophage accumulation have been called "crown-like structures" (CLS, Figure 1.4) and have been reported in mouse, sheep and human obese subjects [66-68]. Another pattern of macrophage accumulation, unique to omental adipose tissues, is as milky spots [69-71]. Milky spots, considered to be a lymphoid tissue of the omentum, develops during the late pregnancy in humans and sheep, is developmentally different from other lymphoid

tissue which can be identified as early as 13 weeks gestation in humans [72]. These milky spots are considered to be an important source of macrophages in peritoneal immune responses [71].

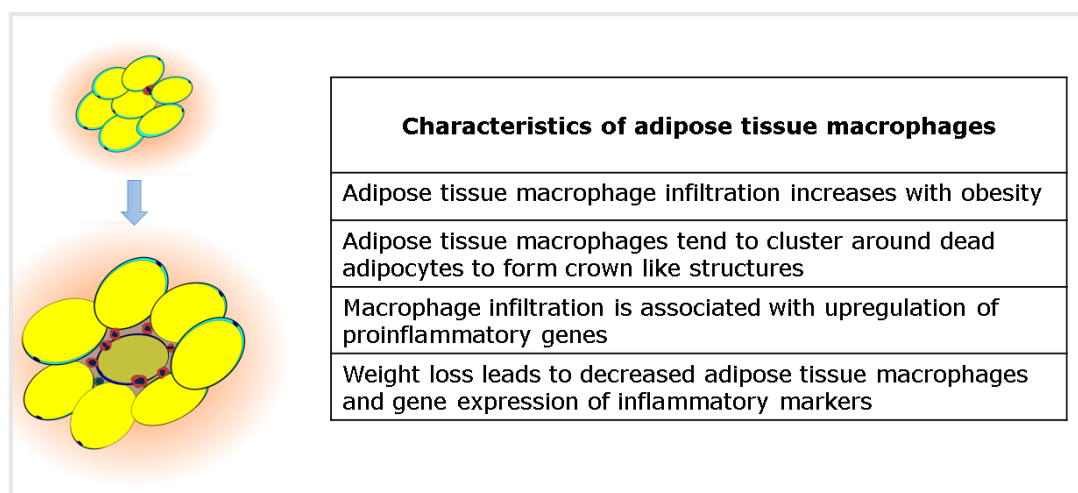


Figure 1.4 Diagram summarising characteristic features of adipose tissue macrophage infiltration.

Macrophages present in adipose tissue increase in number and activation state in response to obesity and are associated with upregulated inflammatory gene expression. Obesity also leads to increased numbers of crown-like structures characterised by necrotic adipocytes surrounded by macrophages.

Adipose tissue macrophages are key to obesity-associated metabolic inflammation. In microarray gene expression analysis of mouse white adipose tissue, Xu et. al. [21] identified highly specific upregulation of macrophage-associated inflammatory genes in adipose tissue of mouse models of genetic and high-fat diet-induced obesity as compared to lean mice. In this experimental study, 59% of the upregulated (more than 2 fold change) genes were inflammatory genes. These findings were confirmed in specific genes of interest by real-time PCR. Furthermore, with increasing obesity, gene expression of inflammatory genes was upregulated and preceded an increase in circulating insulin concentrations.

An association between macrophage activation and obesity has been demonstrated in human subjects. In a study of obese subjects undergoing gastric bypass surgery [67], adipose tissue samples from before, and 3

months after, surgery were investigated and compared with adipose tissue from lean subjects. The adipose tissue of obese subjects had more crown-like structures, stained positive for cluster of differentiation 68 (CD68, a marker of phagocyte activity) and HAM56 (human macrophage 56, a mature macrophage marker) and had increased expression of genes involved in inflammatory or immune processes (as assessed by microarray gene expression). Weight loss following bariatric surgery lead to a decrease in macrophage number with remaining macrophages staining positive for the anti-inflammatory protein, IL-10. A significant decrease in plasma concentrations of leptin, insulin, and C-reactive peptide (CRP), as well as two acute-phase proteins, serum amyloid A and orosomucoid, were observed to be associated with weight loss after gastric bypass surgery.

Macrophages in adipose tissue can exist in one of two activation states [73]. The classically activated, M1 activation, pattern is induced by proinflammatory factors and such macrophages display increased inflammatory gene expression with enhanced reactivity to fatty acids and lipopolysaccharides (LPS). The alternatively activated, M2 macrophages display low levels of inflammatory gene expression, secrete high levels of antiinflammatory factors, such as IL-10 and IL-4, and are poorly activated by fatty acids.

In a human study [74] of subcutaneous adipose tissue from non-diabetic patients undergoing plastic surgery and of omental adipose tissue from organ donors [74], macrophage activation state were characterised. The surface markers on adipose tissue macrophages were compared with peripheral blood monocytes which had been differentiated in vitro to M1 and M2 lineages. Adipose tissue macrophages expressed a surface marker phenotype similar to the M2 lineage and, accordingly, secreted high amounts of IL-10 and IL-1 receptor antagonists. Upon activation, the macrophages were capable of secreting a large amount of proinflammatory cytokines

(TNF- α , IL-6, IL-1, MCP-1 and MIP-1 α) at levels significantly higher than the comparative M1 macrophages. However, this adipocyte macrophage M2 activation is in contrast to findings of another study comparing omental and subcutaneous adipose tissue [75] where macrophages with M1 surface markers were significantly increased in omental as compared to subcutaneous tissue in obese women and also in subcutaneous adipose tissue of obese women as compared to lean women. After weight loss, M2 surface markers were significantly increased in subcutaneous tissues as compared to the pre weight loss.

In conclusion, obesity leads to macrophage accumulation in the adipose tissue and this response is more pronounced in visceral than subcutaneous adipose tissue. Rodent models demonstrate M1 activation pattern in adipose tissue macrophages. However, the evidence regarding activation states of the adipose tissue (M1 or M2 activation states) in humans and large mammals is not yet clear.

1.4.1.4 Role of glucocorticoids in adipose inflammation

Glucocorticoids (GC) are known to regulate adipokines secretion. Leptin expression is known to increase in response to GC[76]. In line with the known anti-inflammatory actions, GCs decrease inflammatory cytokines, namely IL-6, IL-8, and TNF in intact samples of adipose tissues [77, 78]. Accordingly, dexamethasone administration in humans significantly suppresses inflammatory response [79]. Intracellular cortisol levels are regulated by the enzyme hydroxysteroid dehydrogenase (HSD) isoforms 1 and 2. HSD1, a NADPH dependent enzyme, is expressed in many tissues, including liver and adipose tissue, and acts predominantly as a reductase, generating cortisol in vivo [80]. HSD2, highly expressed in kidney and colon, inactivates cortisol to cortisone. A positive correlation has been demonstrated between adipose HSD1 mRNA with both BMI and adipocyte size [80, 81]. In addition, in vitro analyses of HSD1 activity from adipose

tissues demonstrate increased HSD1 activity from tissues from obese individuals [82].

The action of GCs on target cells is thought to be mediated by the type 2 glucocorticoid receptor (GCR), a member of the nuclear receptor superfamily that is expressed in virtually all tissues. Activation of GCR is known to promote macrophage accumulation[83], and differential expression of GCR has been proposed to have role in depot specific differences in macrophage accumulation[80]. In addition, cytokines such as TNF α are known to differentially affect expression of specific isoforms of GCR in adipose tissues [84]. This is particularly important as activation of GCR directly interacts with NF- κ B (discussed in Section 1.4.3) to lead to repression of inflammatory cytokines [85].

1.4.2 Adipose tissue cell stress response in obesity

Cell stress response pathways known to be activated in nutritional deprivation or obesity include autophagy and unfolded protein response which form an important focus of this study.

1.4.2.1 Unfolded protein response

Endoplasmic reticulum (ER) is an organelle inside cellular cytoplasm which appears like a network of flattened sacs composed of membrane in continuation with the nuclear membrane. The organelle broadly consists of two components: smooth endoplasmic reticulum, which is the site for lipid and carbohydrate metabolism and rough endoplasmic reticulum, so called as it is coated with ribosomes and is the main site for cellular protein synthesis. The ER plays a key role in quality control during steps of protein synthesis, which comprise of tightly controlled processes of translation from mRNA as polypeptide chains, folding into secondary structures and post-translational modification.

1.4.2.1.1 Normal protein folding and quality control processes in the ER

Protein synthesis and quality control is a tightly regulated multi step process (Figure 1.5) and the ER is a key organelle responsible for this process.

Following production, a polypeptide chain rapidly folds upon itself into a secondary structure called nascent protein. The conformation of this secondary structure depends upon the thermodynamic and kinetic properties of the polypeptide components and its environment [26]. As a result, the hydrophobic and non-polar aspects of the chain are concentrated in the centre of the protein, whilst the hydrophilic aspects form the exposed surface. Such a conformation protects the hydrophobic sections of protein from damaging interaction with other proteins present in the highly concentrated composition of the ER lumen [86].

Proteins also undergo post-translational modification in the ER. Out of the numerous possible processes, only disulphide bond formation and N-linked glycosylation are linked to the UPR [26]. Both these processes modify the topology and the composition of the protein structure by modifying the hydrophobic (disulphide) and hydrophilic (glycosylated) areas of the polypeptide chain.

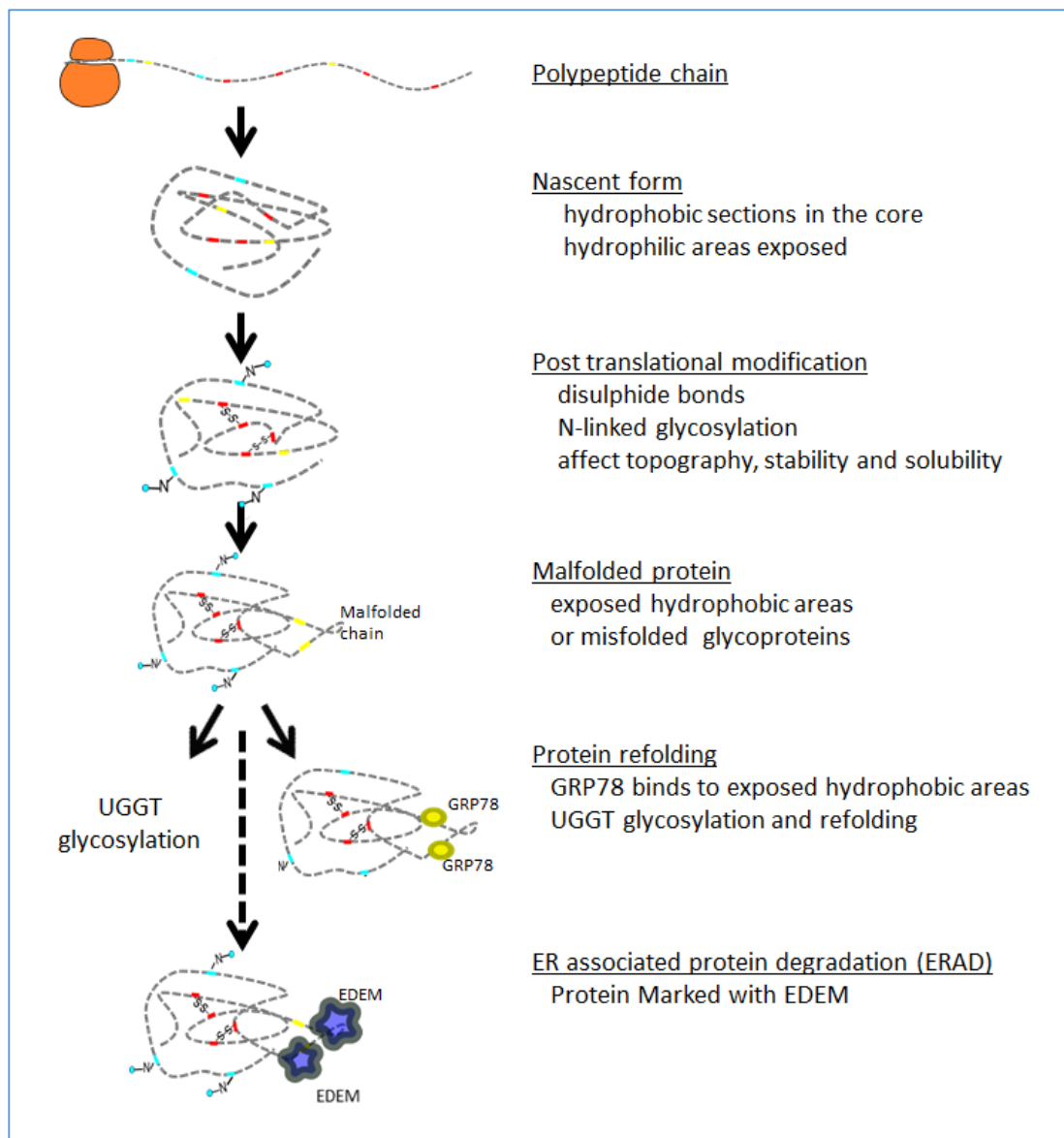


Figure 1.5 Schematic diagram demonstrating protein folding and quality control processes in the ER.

Following translation, polypeptide chains rapidly fold and attain a stable nascent form with hydrophobic core. The exposed hydrophobic areas 78 kDa glucose-regulated protein 78 (GRP78) binds to exposed hydrophobic areas of malformed proteins. In addition, UDP-glucose:glycoprotein glucosyltransferase (UGGT) binds to malformed glycoproteins and attempts to refold such proteins. Remaining malformed proteins are bound to ER stress degradation enhancer molecule (EDEM) and marked for ER-associated protein degradation (ERAD).

During the process of folding and post-translational modification, a proportion of proteins are not able to attain a stable state. Such malformed or unfolded proteins are functionally redundant and structurally unstable due to

their interaction with surrounding protein structures. Two main quality control processes that monitor the ER contents for malformed protein, attempt to correct the malformed protein by unfolding and refolding the protein and, if unsuccessful, direct the protein to cytosolic destruction by labelling with ER stress degradation enhancer molecule (EDEM) [87].

- 78 kDa glucose-regulated protein (GRP78)
- UDP-glucose:glycoprotein glucosyltransferase (UGGT)

GRP78 is also known as binding immunoglobulin protein (BiP) or heat shock 70 kDa protein 5 (HSPA5). As a molecular chaperone, GRP78 binds to exposed hydrophobic areas of malformed proteins, preventing their interaction with other surrounding proteins. Bound and activated GRP78 facilitates disulfide reduction, rearrangement, and reoxidation of the polypeptide chain until the correct protein conformation is achieved [88].

UGGT is another enzyme resident in the ER and monitors misfolded glycoproteins within the ER lumen. Upon identification, UGGT glycosylates such glycoproteins, which are then bound to the resident molecular chaperones, calnexin and calreticulin, and are redirected to process of re-folding [89].

Normally folded proteins are then transferred to Golgi apparatus for further processing or transportation. However, protein chains that remain uncorrected despite the above quality control measures or which quantitatively exceed the ER's ability to monitor and correct are directed to degradation pathways called endoplasmic-reticulum-associated protein degradation (ERAD). In this process, such proteins are labelled with a protein called ER degradation enhancing α -mannosidase-like molecule (EDEM) and directed to cytosolic degradation [87].

1.4.2.1.2 ER stress and the unfolded protein response

If the influx of unfolded polypeptides exceeds the processing capacity of the ER, the physiological milieu of the organelle is unsettled. ER stress is the term used to describe this state of imbalance between protein folding capacity and protein load. The ER actively monitors the load of its unfolded protein cargo and, when this is excessive, a coordinated set of pathways is activated aimed at restoration of the normal ER state. However, if the ER stress stimulus is overwhelming, the same set of pathways lead to activation of cell death processes. The process of activation of such pathways is called the unfolded protein response (UPR) [26]. The cellular processes initiated during the UPR to limit the organelle damage and maintain cellular homeostasis [26] include (Figure 1.6):

- decreased transcription of genes encoding secretory proteins
- decreased translation
- increased folding capacity of the ER by increase in chaperones including GRP78 and C/EBP-homologous protein (CHOP)
- clearance of slowly folding proteins through ERAD
- increased size of the ER

It is believed that, once the ER stress exceeds the pro-survival processing capacity of the UPR, the process of redirection to programmed cell death involves activation of the pathways of apoptosis and autophagy [90-92].

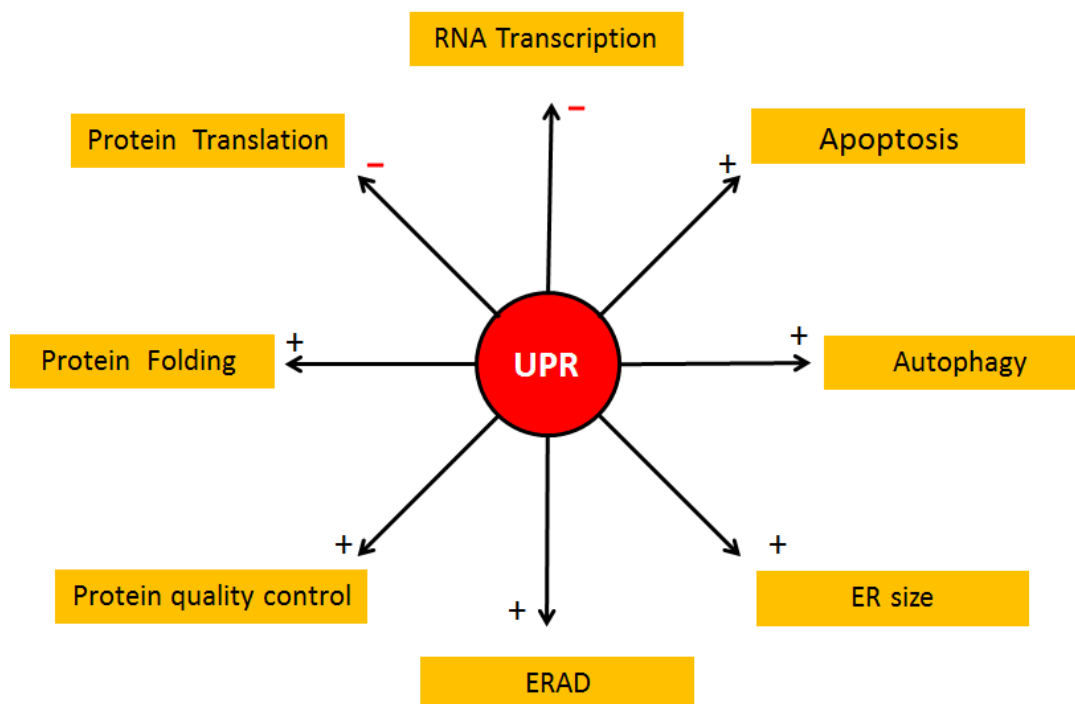


Figure 1.6 Schematic diagram demonstrating the multiple outcomes of activation of the unfolded protein response (UPR) in the endoplasmic reticulum (ER).

UPR activation attempts to decrease ER protein load by decreasing synthesis of ribonucleic acids (RNA) and proteins and increasing synthesis of protein folding and quality control components including increasing the size of the ER. Remaining misfolded protein is directed towards ER-associated-degradation (ERAD). UPR activation is also known to interact with and activate cell death pathways of autophagy and apoptosis.

1.4.2.1.3 The canonical pathways of UPR

The ER membrane bears three distinct transmembrane proteins that monitor the levels of unfolded proteins in the ER lumen and can activate pathways named after them. These proteins are:

- Inositol Requiring Enzyme 1 (IRE1)
- PKR-like eukaryotic initiation factor 2 α kinase (PERK)
- Activating Transcription Factor 6 (ATF6)

In the absence of ER stress, these proteins are maintained in inactivated state bound to protein chaperones like GRP78. On accumulation of unfolded protein within the ER lumen, GRP78 is recruited away from the transmembrane proteins leading to activation of the three well described canonical pathways (Figure 1.7).

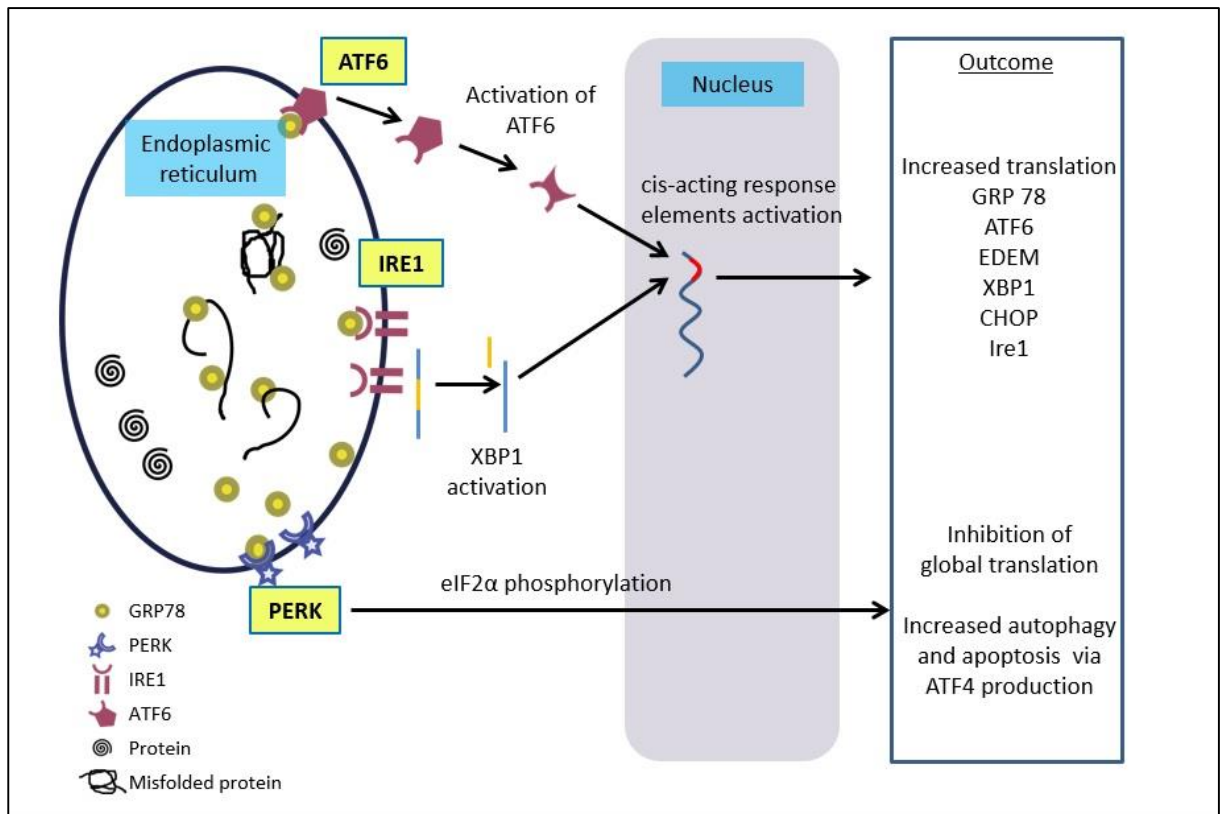


Figure 1.7 Canonical pathways of the unfolded protein response (UPR)

Upon accumulation of excessive amounts of malformed protein inside the ER (ER stress), molecular chaperones like GRP78 get removed from ER membrane proteins ATF6, IRE1 and PERK and preferentially bind to malformed proteins. The unbound ER membrane proteins, ATF6, IRE1 and PERK activate a sequence of downstream steps, called UPR pathways which collectively upregulate genes and proteins aimed at resolution of the ER stress by decreasing generalised transcription and protein translation, increasing UPR components and ER size and if unsuccessful at resolving ER stress, activation of programmed cell death pathways. ER, endoplasmic reticulum; UPR, unfolded protein response; GRP78, glucose regulated protein-78; ATF6, activating transcription factor-6; IRE1, inositol requiring enzyme-1; PERK, PKR-like eukaryotic initiation factor 2α kinase; XBP1, X-box binding protein-1; EDEM1, ER degradation enhancing α-mannosidase-like molecule; CHOP, C/EBP-homologous protein; eIF2α, eukaryotic initiation factor-2α; ATF4, activating transcription factor-4.

1) IRE1 Pathway.

Upon separation of GRP78 from its binding site on IRE1, the latter undergoes oligomerisation and activation of its ribonuclease domain. The substrate for this domain in mammals is X-box binding protein 1 (XBP-1) mRNA. In a unique mechanism, the activated IRE1 catalyses the excision of 26 nucleotide segment (unconventional intron) causing a frame shift mutation in the mRNA [93]. As a result of this splicing, the protein product of the spliced XBP1 (XBP-1s) mRNA is a 371 amino acid isoform instead of the 261 amino acid isoform produced by the unspliced XBP1 (XBP-1u) mRNA.

XBP-1s is a basic leucine zipper (bZIP) domain containing transcription factor and it activates expression of multiple downstream UPR components including ER chaperones, transcriptional increase in EDEM, modulation of inflammation and activation of apoptosis [26](Table 1.2).

Canonical pathway	Process	Outcome	Effect on organ system
IRE 1 pathway	XBP1 splicing	Increased transcription of chaperones like GRP78 and proteins involved in ER biogenesis	Upregulated UPR and ER synthesis
		Transcriptional increase in EDEM [87]	Upregulated ERAD
		Recruitment of TNF alpha receptor associated factor 2 (TRAF2) leading to activation of <ul style="list-style-type: none"> c-Jun N-terminal Kinase (JNK) NF-κB pathway 	Inflammation modulation
		Stimulation of Bcl2 proteins BAX and BAK Recruitment of Apoptosis signalling kinase1 (ASK1)	Apoptosis

Table 1.2 Summary of the outcome of activation the IRE1 pathway of unfolded protein response.

IRE1 pathway activation catalyses splicing of transcription factor XBP1 which upregulates transcription of ER stress response components including chaperones, EDEM. Other outcomes of this pathway activation include activation of proinflammatory JNK and NF-κB pathways and components of apoptosis. IRE1, inositol requiring enzyme 1; XBP1, X-box binding protein 1; GRP78, glucose regulated protein-78; JNK, c-Jun N-terminal kinase; ERAD, ER-associated-degradation; EDEM, ER degradation enhancing α-mannosidase-like molecule; NF-κB, nuclear factor kappa-light-chain-enhancer of activated B cells; Bcl2, apoptosis regulator b cell lymphoma 2; BAX, Bcl-2-like protein 4; BAK, Bcl-2 homologous antagonist/killer.

2) PERK pathway.

Activation of the PERK pathway leads to downstream phosphorylation of the alpha subunit (eIF2A) of protein eukaryotic initiation factor-2 (eIF2). This phosphorylated subunit competitively reduces the function of eIF2B leading to reduced global protein synthesis and reduced workload of the ER. This pathway also interacts with NF-κB (described in Section 1.4.3.2) and modulates inflammation.

Canonical pathway	Process	Outcome	Effect on organ system
PERK pathway	Phosphorylation of eIF2α	Repression of protein translation	Decreased ER load
		Decreased synthesis of IκB leading to activation of NF-κB	Modulation of inflammation and apoptosis
		Preferential translation of ATF4 [94]	Autophagy [95] and apoptotic cell death [90]
		ATF4 mediated inhibition of hepatic Akt/ PKB and increased PPARγ	Hepatic lipid accumulation and decreased insulin sensitivity

Table 1.3 Table summarising the outcome of activation of PERK pathway of UPR.

Inactivating phosphorylation of eIF2α leads to repression of secretory protein synthesis attempting to decrease ER load, proinflammatory pathway NF-κB activation and autophagic and apoptotic cell death pathways mediated by activation of transcription factor, ATF4. PERK pathway also plays a role in hepatic lipid metabolism by promoting insulin resistance and hepatic steatosis via inhibition of Akt and increased PPARγ respectively. PERK, PKR-like eukaryotic initiation factor 2α kinase; ATF4, activating transcription factor 4; eIF2α, eukaryotic initiation factor 2 α subunit; NF-κB, nuclear factor kappa-light-chain-enhancer of activated B cells; IκB, inhibitor of kappa B; Akt/PKB, Protein Kinase B; PPARγ, peroxisomal proliferation activated receptor γ

PERK pathway interacts with cell death pathways at multiple locations through increase in translation of activating transcription factor 4 (ATF4) [94], which in association with C/EBP homologous protein induces cell death [90]. The ATF4 activation through this pathway has been demonstrated to be essential to autophagy activation and cell death [95].

In addition, UPR activation can have direct effects on cellular metabolic functioning. This is particularly relevant for the liver as ATF4 and CHOP affect cellular insulin sensitivity by leading to inhibition of Akt, an insulin sensitising kinase [96, 97] or increasing expression of genes that regulate

lipogenesis (peroxisomal proliferation activated receptor γ , PPAR γ) [98]. The multiple outcomes of PERK pathway activation are summarised in Table 1.3.

3) ATF6 Pathway

Upon release from nuclear membrane, ATF6 translocates to the Golgi complex where through proteolytic steps, the cytosolic bZIP domain is released. The activated ATF6 then translocates into the nucleus and activates transcription. Along with upregulation of the expression for ER chaperones and EDEM, this pathway also decreases cholesterol synthesis through transcriptional repression of low-density lipoprotein receptor [26] (Table 1.4).

Canonical pathway	Process	Outcome	Effect on organ system
ATF6 pathway	Activation by proteolysis and translocation to nucleus; Binding to SREBP2	Increased transcription of chaperone GRP78	Upregulated UPR
		Stimulation of EDEM	Upregulated of ERAD
		Transcriptional repression of LDLR	Decreased cholesterol synthesis

Table 1.4 Table summarising the outcome of activation of ATF6 pathway of UPR.

UPR, unfolded protein response, ATF6, activating transcription factor 6; GRP78, glucose regulated protein-78, ERAD, endoplasmic reticulum associated degradation, EDEM, ER degradation enhancing α -mannosidase-like molecule; NF- κ B, nuclear factor kappa-light-chain-enhancer of activated B cells; LDLR, low-density lipoprotein receptor; SREBP, Sterol regulatory element-binding protein.

1.4.2.1.4 Role of UPR in adipose tissue in obesity

During a state of obesity, adipose tissue homeostasis is affected by factors including energy availability, increased synthetic demand and activation of inflammatory pathways all of which are known to activate the ER stress response [91]. The direct evidence of obesity-related activation of ER stress response in liver and adipose tissue came from studies in HFD mice. In comparison to lean animals, HFD feeding led to activation of PERK and IRE1 α and this was associated with increased JNK activity [99]. This response was

also seen in ob/ob mouse model (genetic obesity resulting from leptin deficiency) in both adipose tissue and liver [99]. In cell culture of mouse embryo fibroblasts (MEFs) derived from XBP-1^{-/-} mice, the cultured cells had impaired ER responses and insulin signalling.

Genetic engineering techniques in rodent models have bolstered the evidence of role of UPR in systemic glucose and lipid homeostasis. Some such experiments have been summarised in Table 1.5.

Target of genetic engineering	Role of target in ER stress	Intervention	Outcome
ER chaperone protein: ORP150 [100]	ORP150 deficiency leads to increased cell susceptibility to ER stress	ORP overexpression in the liver of obese diabetic mice (obese diabetic C57BL/KsJ-db/db mice)	Decreased ER stress markers, improved insulin resistance and glucose tolerance
		Expression of antisense ORP150 in the liver of normal mice (C57BL6)	Impaired glucose tolerance and decreased insulin receptor signalling through phosphorylation of IRS1
ER chaperone GRP78 [101]		ob/ob mice overexpressing GRP78 using an adenoviral vector	Decreased lipogenic gene expression and hepatic steatosis and increased insulin sensitivity.
NCK [102]	Nck1, shown to modulate the UPR	obese Nck1 ^{-/-} and Nck1 ^{+/+} mice and HepG2 cell culture	In vivo improved glucose disposal and in vitro enhanced insulin signalling in NCK ^{-/-} mice and HepG2 cells

Table 1.5 Studies of genetically engineered rodent models demonstrating the role of adipose tissue ER stress response in insulin resistance.

GRP78, glucose regulated protein 78; IRS1, insulin receptor substrate 1; NCK, Noncatalytic region of tyrosine kinase; ORP150, oxygen-regulated protein 150

These have been confirmed in human studies. In a study of abdominal subcutaneous adipocytes from obese and lean individuals, ER stress markers (calnexin, GRP78, IRE1α, PERK), measured using Western blotting, were significantly increased in adipocytes from obese individuals [103].

Furthermore, treatment of cultured human adipocytes with lipopolysaccharide, high glucose and saturated fatty acids increased gene expression of UPR components, a response absent when the treatment was combined in the presence of anti-inflammatory compound salicylate [104]. This finding was confirmed in a study of proteomic, Western blotting and RT-

PCR analyses of subcutaneous adipose tissue biopsies from lean-insulin sensitive and obese-insulin resistant non-diabetic individuals which demonstrated selective upregulation of UPR components [103]. In another human study, subcutaneous adipose tissue of obese subjects was sampled before, and 1 year after, weight-reducing bariatric surgery. Mean weight loss of 39% in the obese subjects led to decreased gene expression for GRP78 and of alternatively spliced XBP-1 associated with decreased adipose tissue protein expression of eIF2 α and cJNK [105]. This has been confirmed in another study of human subcutaneous adipose tissue, demonstrating that the increased gene expression for ER stress markers associated with obesity decreases with weight loss in obese non-diabetic individuals, but not in obese diabetics [106].

These human studies have been performed using subcutaneous adipose tissue. So far, no human or large animal experiments have demonstrated visceral adipose tissue activation of UPR in response to obesity. This study intends to describe the characteristics of the UPR state in a large animal model of obesity in comparison to lean counterparts.

1.4.2.2 Autophagy

Cell death pathways are constitutive to various relevant physiological processes including adipocyte development [107], hepatic development [108], adipose tissue remodelling [109], lipid metabolism [107], formation of crown-like structures, response to ER stress and inflammation [90]. The various pathways of metabolic inflammation in obesity interact with these cell death pathways and, collectively, are part of the cell stress response. Any study of obesity associated cell stress response should, therefore, include exploration of the state of metabolic inflammation and the state of the cell death pathways.

Using morphological criteria, cell death pathways can be classified as either programmed cell death pathways or necrosis [110]. Programmed cell death describes pathways which are intrinsic to the cell and are mediated by a regulated intracellular pathways. In contrast, necrosis is the death of a cell caused by external factors. Out of the two main pathways of programmed cell death, autophagy and apoptosis, the former is particularly important as it is known to contribute not just to cell death but also to lipid metabolism, adipocyte development and metabolic inflammation [107].

The multiple possible pathways of adipose tissue inflammation and cell stress described above have the potential of initiating processes of programmed cell death [25, 111]. The crown-like structures in adipose tissue have a dead adipocyte in the centre surrounded by inflammatory infiltrate [66]. The ER stress pathways interact at multiple levels with autophagy and apoptosis pathways and free fatty acids induced inflammation also has the potential of inducing cell death [112].

1.4.2.2.1 Autophagy: pathway and regulation

The literal translation of the term autophagy in Greek language is “self-eating”. This was initially described as an evolutionary-conserved process wherein, faced with persistent starvation, a cell consumes its own non-essential components to promote survival. However, it is now known that, depending upon the severity and type of the precipitating stress, this tightly-regulated process can progress to the death of the cell [111]. Autophagy is also a constitutive component of several physiological processes including cell and organ development, cell growth and organ adaptive response to stress [113].

The classical process of autophagy (macroautophagy) involves formation of double membrane vesicles called autophagosomes around the cytoplasmic target (organelles, proteins, pathogens) (Figure 1.8). The autophagosome

then fuses with the cellular lysosomes to form autolysosome where the process of enzymatic degradation of the contents begins. The sequestered contents are, thereafter, degraded within the lysosome allowing the cell to either eliminate damaged or harmful constituents or recycle components, thereby contributing to nutrient and energy homeostasis [113].

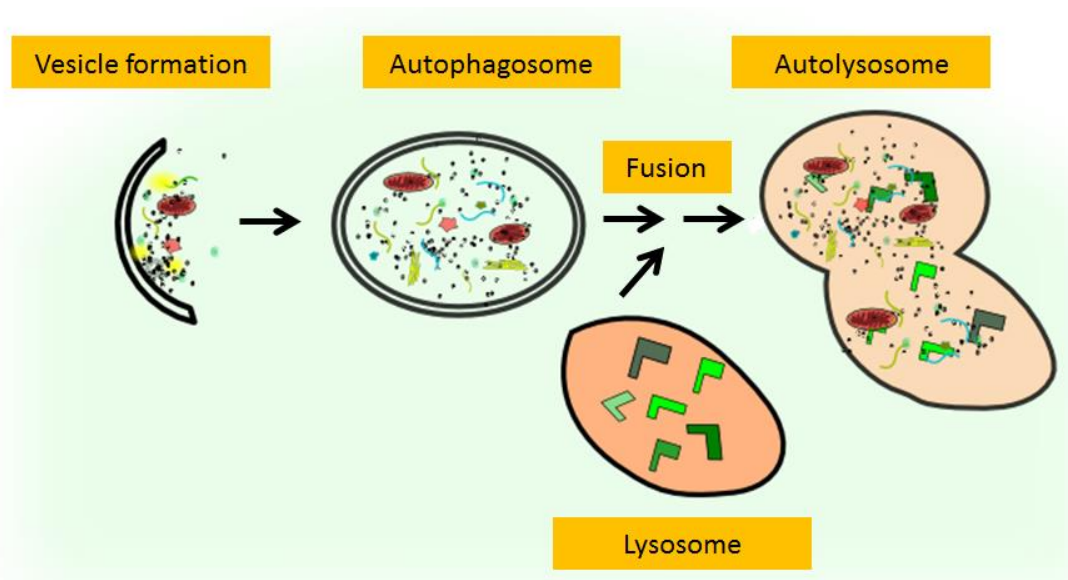


Figure 1.8 Schematic diagram depicting overview of the autophagic process.

Initiation and nucleation steps lead to formation of a phospholipid bilayer which enlarges to engulf cytoplasmic content until the ends of expanding phospholipid membrane close to form an enclosed autophagosome. The autophagosome fuses with lysosome to form autolysosome to enable enzymatic degradation of the contents.

The formation of the phospholipid double membrane autophagosome is the outcome of a highly regulated engagement of pathways involving several autophagy related genes (ATG), eighteen of which have been recognised in eukaryotes. The products of these genes act together, either as complexes, or as the outcome of conjugation pathways, to promote autophagosome formation and functioning [114].

The process begins with initiation and nucleation steps which involve association of two complexes, Unc-51 like kinase (ULK) complex and class III

phosphatidylinositol 3-kinase (PI3K) complex. Beclin 1 is a component of the PI3K complex and is key to the regulation of this initiation. Following the initiation step, forming a phospholipid membrane, two important ubiquitin-like conjugation systems are activated which eventually result in coating of the phospholipid bilayer with specialised ubiquitin like molecules ATG12 and microtubule-associated protein 1A/1B-light chain 3 (LC3). As the expanding phospholipid bilayer engulfs cytoplasmic content and organelles, the proteins like ATG12 and LC3 coat the autophagosome and mark it as a target for lysosomal degradation [114] (Figure 1.9). The process continues until the two ends of the expanding bilayer meet and fuse to form an autophagosome.

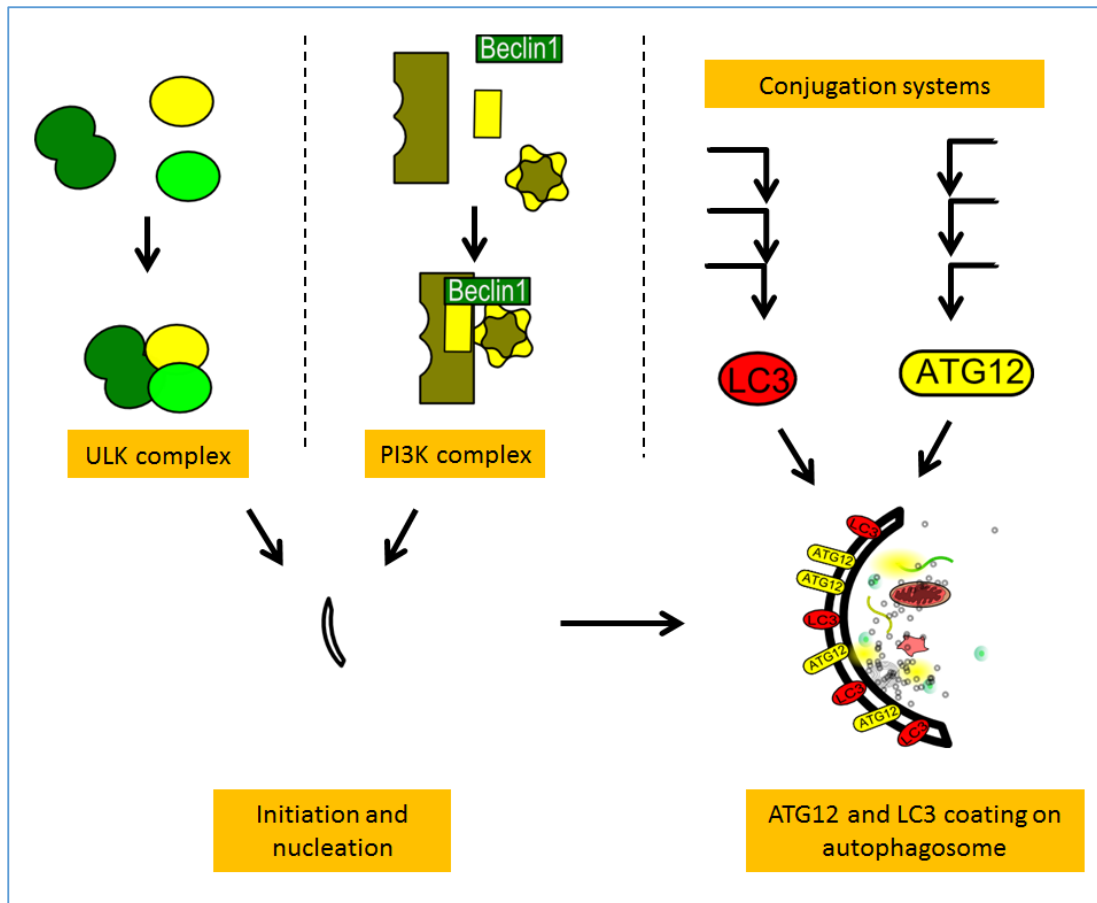


Figure 1.9 Schematic diagram depicting the key pathways conjugation systems required for autophagosome formation.

A phospholipid bilayer is formed following initiation and nucleation steps which require association of two complexes, Unc-51 like kinase (ULK) complex and class III phosphatidylinositol 3-kinase (PI3K) complex. Beclin 1 is a component of the PI3K complex. The expanding bilayer is then coated with specialised ubiquitin like molecules: product of autophagy related gene 12 (ATG12) and microtubule-associated protein 1A/1B-light chain 3 (LC3) which facilitate eventual fusion with lysosomes.

1.4.2.2.2 Regulation of autophagy

Several physiological processes including development, differentiation, cell survival and homeostasis require effective cellular autophagic functioning. Insulin action, ER stress and energy sensing are three known regulators of autophagy in a cell.

Insulin. The protein mammalian target of rapamycin (mTOR) is a nodal component of the processes regulating autophagy. mTOR is part of a

complex mTORC1 which prevents autophagy activation by its binding to the ULK complex and the dissociation of the two leads to activation of autophagy [115]. Insulin receptor activation leads to inhibition of autophagy by activating mTOR (Figure 1.10). This is executed through mediators downstream of insulin receptor. PI3K is a signalling molecule which upon activation of insulin receptor activates Akt/PKB (protein kinase B) pathway [113]. A consequence of this pathway activation is prevention of the Tuberous Sclerosis 1/2 (TSC1/2) complex formation. TSC1/2 normally inhibits mTOR [115, 116]. Therefore, insulin action via its receptor leads to activation of mTOR and inhibition of autophagy in a cell [117].

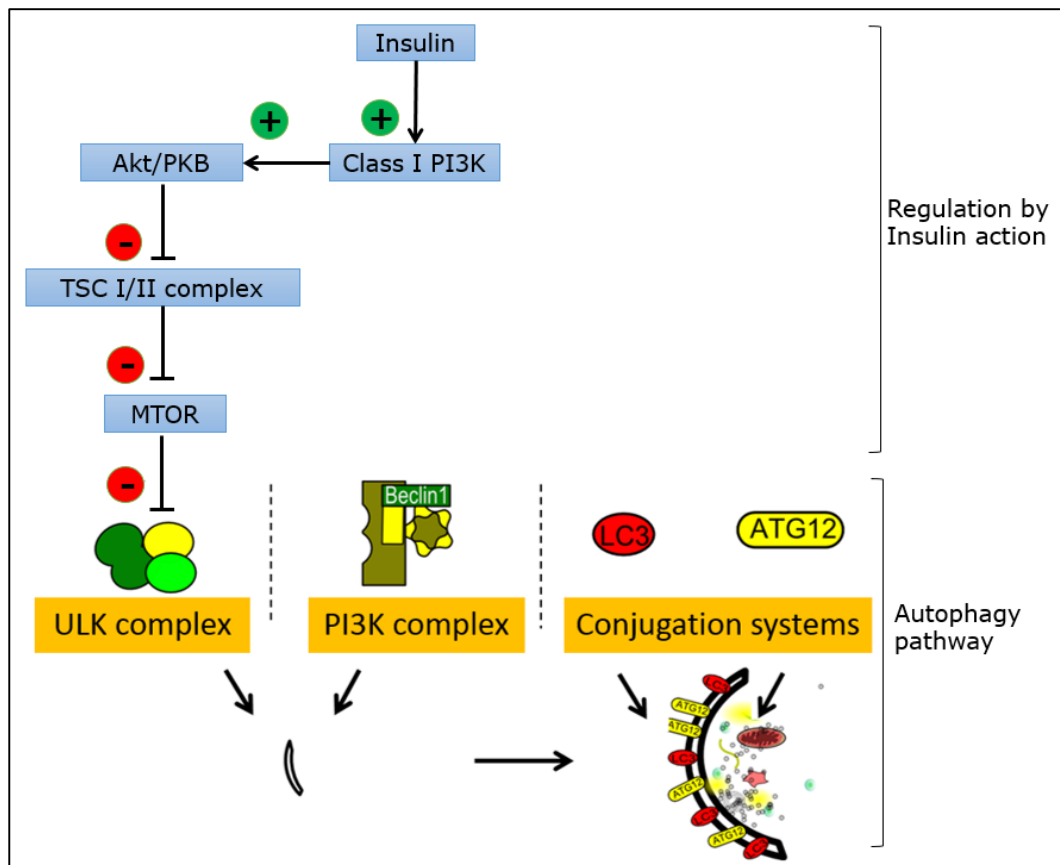


Figure 1.10 Schematic diagram depicting regulation of autophagy by insulin. Insulin receptor activation leads to eventual activation of mTOR leading to inhibition of autophagy.

PI3K, Phosphatidylinositol-4,5-bisphosphate 3-kinase; PKB, protein kinase-B, TSC, tuberous sclerosis complex; mTOR, mammalian target of rapamycin; ULK, Unc-51 like kinase; ATG12, autophagy related gene 12; LC3, microtubule-associated protein 1A/1B-light chain 3

ER stress. Several studies have reported that ER stress can induce autophagy. UPR activation leads to phosphorylation of eIF2 α , which is mediated by PERK (Section 1.4.2.1.3) leading to conversion of LC3-I to LC3-II and to increased ATG12 expression [118]. The transcription factor ATF4 is also known to increase production of ATG8 and ATG5 expression. Other mechanisms that have been proposed include inhibition of PKB-mTOR pathway and increase in intracellular levels of calcium leading to AMPK activation (Figure 1.11).

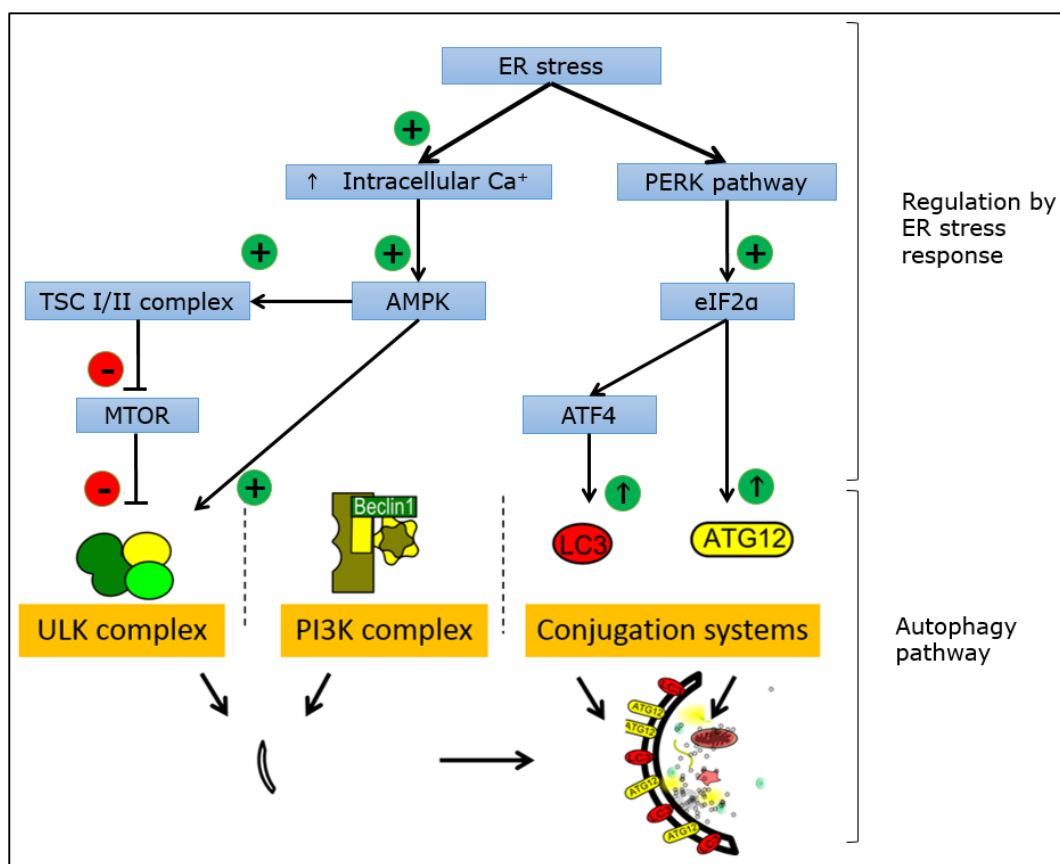


Figure 1.11 Regulation of autophagy by ER stress response activation.

Activation of PERK pathway of ER stress response leads to transcriptional increase in components of autophagic pathway including LC3, ATG proteins. ER stress associated increase in intracellular calcium leads to inhibition of mTOR leading to activation of autophagy. ER, endoplasmic reticulum; PERK PKR-like eukaryotic initiation factor 2 α kinase; ATF4, activating transcription factor 4; eIF2 α , eukaryotic initiation factor 2 α subunit; AMPK, 5' adenosine monophosphate-activated protein kinase; PI3K, Phosphatidylinositol-4,5-bisphosphate 3-kinase; TSC, tuberous sclerosis complex; mTOR, mammalian target of rapamycin; ULK, Unc-51 like kinase; ATG12, autophagy related gene 12; LC3, microtubule-associated protein 1A/1B-light chain 3

Energy sensing. There are two different well described regulators of autophagy in response to nutrient depletion: adenosine monophosphate-activated protein kinase (AMPK) and sirtuin 1 (Figure 1.12).

Nutrient depletion state is conveyed to mTOR through the nutrient sensor AMPK. Decreased ATP production in a state of energy depletion increases AMP:ATP ratio and activates AMPK. AMPK activation leads to inhibition of mTORC1 inhibition by activating phosphorylation of the tuberous sclerosis complex-2 (TSC2) [119] and inactivating phosphorylation of the regulatory associated protein of mTOR (RAPTOR) [120]. AMPK is also known to directly activate ULK1 by phosphorylation [121, 122].

Another important enzyme Sirtuin, product of gene SIRT1, a NAD dependent deacetylase, induces autophagy in response to environmental stress. Cell culture studies of various rat tissues have demonstrated that calorie restriction upregulates SIRT1 expression in brain, kidney, liver, WAT, and skeletal muscle [123]. It has also been demonstrated that SIRT1 is required for autophagy induction by starvation [124]. The components of autophagy pathway ATG5, ATG7 and LC3 are known de-acetylation substrates of Sirtuin1 [124]. Sirtuin1 also activates the transcription factor forkhead box O3a (FOXO3a) [125] which translocates to the nucleus and upregulates multiple autophagy related genes such as ULK2, BECN1, ATG12 and LC3 [126]. Therefore, nutrient depletion states can activate autophagy through various mechanisms including Sirtuin1 and inhibition of mTOR.

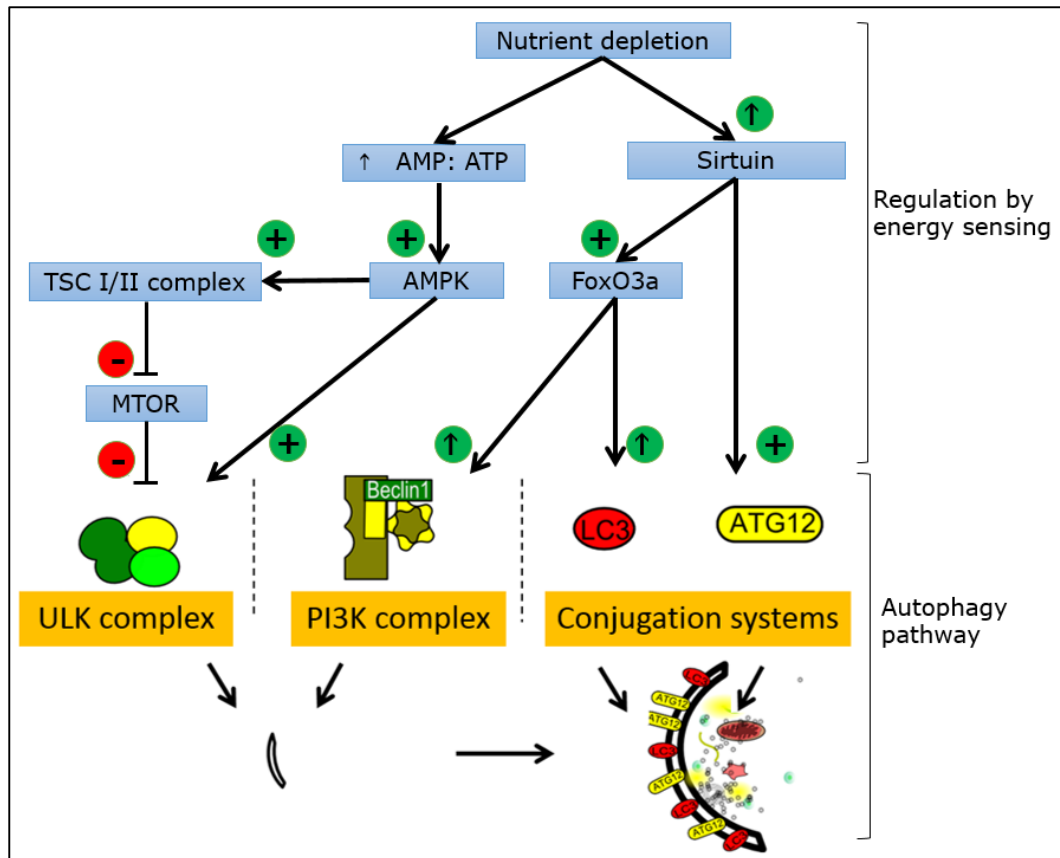


Figure 1.12 Schematic diagram depicting regulatory role of energy sensing in autophagy activation.

Nutrient depletion, via activation of AMPK leads to inhibition of mTOR and direct activation of ULK leading to activation of autophagic pathway. Nutrient depletion also leads to increase in Sirtuin which directly activates components of autophagic pathway and also activates transcription factor FoxO3a leading to upregulation of autophagy. AMP, 5' adenosine monophosphate; ATP, 5' adenosine triphosphate; AMPK, AMP activated protein kinase; PI3K, Phosphatidylinositol-4,5-bisphosphate 3-kinase; TSC, tuberous sclerosis complex; mTOR, mammalian target of rapamycin; ULK, Unc-51 like kinase; ATG12, autophagy related gene 12; LC3, microtubule-associated protein 1A/1B-light chain 3; FoxO3a, forkhead box O3a transcription factor.

1.4.2.2.3 Autophagy in adipose tissues and insulin resistance

In the adipose tissue, autophagy has been identified as a key factor in various physiological functions including lipid metabolism, adipocyte development, modulation of inflammation and insulin sensitivity [127].

Autophagy of lipid droplets (lipophagy) has been identified in hepatocytes [128] as one mechanism contributing to formation [129] and breakdown of intracellular lipid droplets [130]. In contrast, pharmacological inhibition of adipocyte autophagy leads to development of a phenotype resembling brown fat cells characterised by increased mitochondria and small multilocular lipid droplets [131]. Furthermore, adipose tissue-specific disruption of ATG7 in mice reveals that autophagy contributes to regulation of proportion of white and brown fat and determination of the final adipose tissue mass [132]. On a background of the increased autophagy activity that is known to occur during pre-adipocyte adipogenesis [133], autophagy appears to play an important role in adipogenesis.

Autophagy in obesity has been investigated in four main studies of human adipose tissue, consistently demonstrating its upregulation with obesity [106, 134-136]. In a study comparing omental and subcutaneous adipose tissue depots from obese and lean individuals undergoing elective surgery [134], increased autophagy was identified in omental fat as compared to the subcutaneous depot and in obese individuals as compared to lean. This was characterised by increased protein abundance of ATG5, LC3 and ATG12-ATG5 complex, increased mRNA expression for LC3 and ATG5, more autophagosomes identified by immunohistochemistry and increased autophagic flux. Analysis following collagenase digestion demonstrated that increased autophagy gene expression was present in adipocytes as well as the stromal vascular fraction. In addition, a subgroup of individuals exhibiting insulin resistance demonstrated a relatively increased gene expression for autophagy markers. The findings of this study are consistent

with other previous human studies identifying increased autophagy in adipocytes from adipose tissue from patients with type 2 diabetes [135, 137]. In studies of weight loss induced by bariatric surgery, gene expression for BECN and autophagosome formation [106] in adipose tissue were decreased after weight loss as compared to pre-bariatric surgery levels.

Whilst human studies have consistently shown increased adipose tissue autophagy with obesity, high fat diet mice studies have not been consistent with studies reporting obesity-induced decreases [138], or increases, in autophagy [106, 107]. Whilst this highlights the potential limitation of small animal experimental models and the impact of possible variation in experimental conditions, such experimental models are, nevertheless, necessary for experimental studies of pathways and regulation. It has been proposed that obesity itself alters the regulation of autophagy in adipose tissue [106]. This was identified in a study of 40% caloric restriction in a mouse model of HFD as compared to lean mice fed a standard chow diet. In this model, caloric restriction in HFD mice was associated with an increase in markers of autophagy (increased Beclin and p62 protein). However, whilst Beclin and p62 decreased in HFD animals following caloric restriction for 15 days, it led to an increase of the same autophagy markers in the adipose tissue of mice on chow. In the same study, mTOR protein expression decreased following caloric restriction in HFD mice and increased in mice on the standard chow diet.

1.4.2.3 Apoptotic cell death

The term apoptosis was first used to describe a morphologically distinct form of cell death [139] which involves shrinkage and blebbing of cells, nuclear fragmentation with condensation of chromatin and phagocytosis of cell fragments without accompanying inflammatory responses.

Various types of cellular stress stimuli have been shown to trigger apoptosis, including chemotherapeutic agents, irradiation, oxidative stress and ER stress [140]. Apoptosis can be commenced by any of various initiation pathways which all converge onto activation of enzymes called caspases. Synthesised and present constitutively as inactive proenzymes, upon activation caspases cleave various substrates in the cytoplasm and nucleus, eventually leading to the morphological features of apoptosis in the cell [141].

Apoptotic cell death is an outcome of various preceding cellular or extracellular processes including ER stress [140, 142] (Section 1.4.2.1.3), inflammation and autophagy [141, 143]. This is due to modulation of the components of the various apoptosis initiation pathways through increased transcription or activation of pro- or anti-apoptotic constituents of a cell (Table 1.6).

Apoptosis is known to play a major role in embryonic development and ageing. Whilst apoptosis is known to contribute to development of type 1 diabetes by causing cell death of insulin secreting beta cells in pancreas, its role in the pathogenesis of metabolic disease is yet to be explained in detail. Apoptosis has been proposed to be relevant to adipose tissue remodelling [109, 144], fat cell turnover [34] and obesity associated liver disease [145, 146]. Indeed, in parallel to increased ER stress and autophagy, consistently increased apoptosis markers have been found obese animal models. Any

modulation to the constitutive apoptosis mechanisms of body has the potential to programme the susceptibility of an individual to adverse metabolic outcomes.

Mechanism of apoptosis activation	Molecular pathway	Interaction with other cell stress and inflammation pathways
TNF receptor activation (Extrinsic pathway)	TNF receptors: Fas stimulation	Inflammation and TNF release
Mitochondrial pathway (Intrinsic pathway)	Mitochondrial release of Cyt-C, AIF and other factors	<u>Oxidative stress</u> : release of Cyt-C <u>ER stress</u> : upregulation of mitochondrial pathway [142], increase in intracellular Calcium
Ratio of anti-apoptotic and proapoptotic Bcl-2 family proteins [147]	Anti-apoptotic: Bcl-2, Bcl-XL, and Mcl-1 Pro-apoptotic: Bax, Bak, and BH3 domain only molecules	<u>UPR</u> leads to CHOP induction and increase in proapoptotic factors [148]. <u>JNK pathway</u> activates proapoptotic factors [149] <u>NF-κB</u> , regulate inhibitor of apoptosis (IAP) [150]

Table 1.6 Interaction of molecular pathways with apoptosis activation.

Initiation of apoptosis depends upon balance between anti-apoptotic and pro-apoptotic factors which are affected by several extrinsic mechanisms including inflammatory state, ER stress, oxidative stress and cytokines.

TNF, tumour necrosis factor; ER, endoplasmic reticulum, UPR, unfolded protein response; JNK, c-Jun N-terminal kinase; NF-κB, nuclear factor kappa-B; Cyt-C, cytochrome C; AIF, apoptosis inducing factor; Bcl-2, B-cell lymphoma 2

1.4.2.4 Necrosis

The morphological features of necrotic cell death are secondary to the loss of control of ionic balance leading to intracellular uptake of water, swelling of the cell and organelles and plasma membrane rupture leading to cellular lysis [151]. This lysis releases many intracellular constituents, attracting immune cells and provoking an inflammatory response. In the past, this process was considered to be unregulated. However, it is now known that necrosis is also regulated by signalling pathways. Death domain receptors including tumour necrosis factor receptor (TNFR1) and toll-like receptors trigger necrosis, in particular in the presence of caspase inhibitors [152]. Other relevant mediators responsible for necrosis pathway initiation and propagation include reactive oxygen species (ROS) and increases in intracellular calcium.

In obesity, the adipocyte cell death, which is considered to be the primary stimulus leading to macrophage localisation and activation [66] to regions described as crown-like structures (CLS), is considered to be the outcome of necrotic cell death. The precipitating processes that lead to adipocyte necrosis associated with CLS remain the focus of ongoing research [109, 153].

1.4.3 Interactions between inflammation, cell stress response and insulin action

Insulin action is mediated through its transmembrane receptor which belongs to tyrosine kinase family. Amongst the large number of intracellular substrates of insulin receptor, tyrosine phosphorylation of insulin receptor substrate (IRS) proteins is a crucial step in mediation of insulin action. Multiple regulatory mechanisms involve inactivation of these IRS proteins as a means of decreasing the downstream effects of insulin action and thereby generating insulin resistance. Examples of such pathways relevant to metabolic inflammation include c-Jun N-terminal kinase (JNK), IKK (inhibitor of nuclear factor kappa-B (NF- κ B) kinase) [73], PKC, TNF α activation and suppressor of cytokine signalling (SOCS). Both JNK and IKK β can be activated by exposure to cytokines such as TNF α [154], free fatty acids [58] (Section 1.4.3) and ER stress [155]

1.4.3.1 JNK

JNK is a stress activated kinase which belongs to the mitogen-activated protein kinase (MAPK) family. There are ten known isoforms and splice variants of JNK which are all derived from three genes JNK1, JNK2 and JNK3.

Three different downstream outcomes of JNK activation with potential roles in inflammation and insulin resistance have been described (Figure 1.13). Activated JNKs cause inactivation of IRS by serine phosphorylation rendering the cell resistant to downstream action of insulin receptor activation [156]. Obesity in the HFD mice model leads to elevated JNK activity [157] and an absence of JNK1 results in decreased adiposity, significantly improved insulin sensitivity and enhanced insulin receptor signalling capacity. These results were also replicated in the ob/ob mice model [157]. Activation of JNK also transcriptionally controls cytokine release and multiple cellular processes like apoptosis, differentiation and proliferation through transcription factors including activating transcription factor 2 (ATF2) and activator protein 1

(AP1). This release of proinflammatory cytokines in response to JNK activation has been demonstrated in adipose tissue macrophages [158] and hepatic Kupffer cells [159].

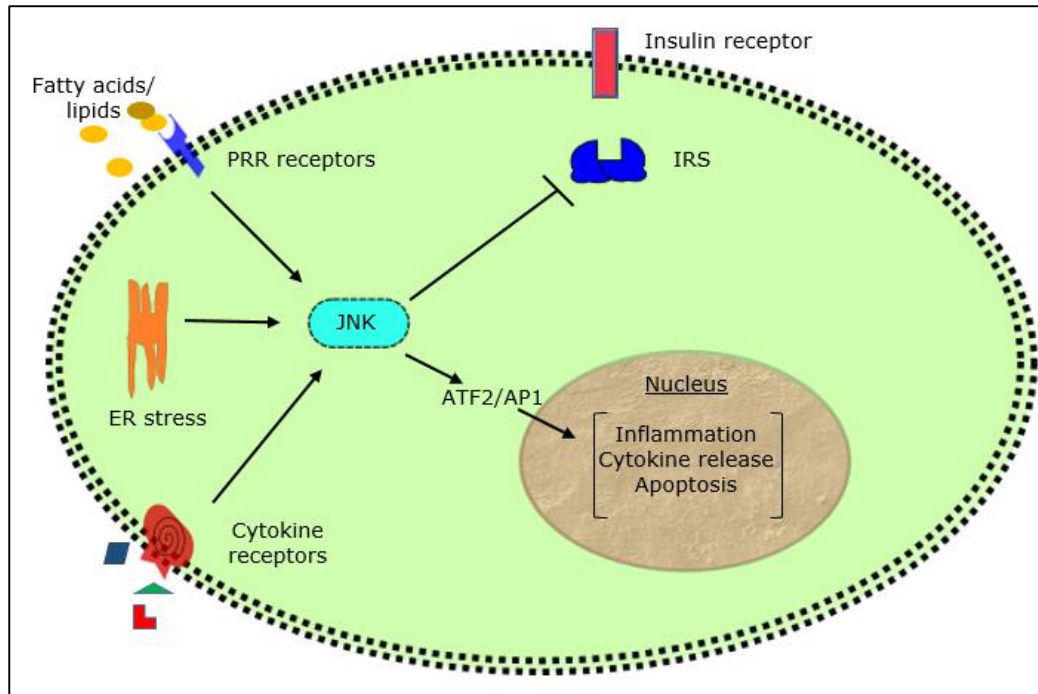


Figure 1.13 Depiction of the central role of JNK in development of insulin resistance and propagation of inflammation.

Upon activation, JNK causes inactivating phosphorylation of IRS and activation of transcription factors ATF2 and AP1 lead to increased gene expression of various proinflammatory and proapoptotic genes. ER, endoplasmic reticulum; PRR, pattern recognition receptors; JNK, c-Jun N-terminal kinase; IRS, insulin receptor substrate; ATF2, activating transcription factor 2; AP1, activator protein 1

1.4.3.2 IKK

In almost all animal cell types, a protein complex called NF- κ B (nuclear factor kappa-light-chain-enhancer of activated B cells) controls transcription of multiple genes propagating cellular inflammation. In an unstimulated cell, NF- κ B is an inactivated dimeric state bound to protein complexes called Inhibitor of κ B (I κ B). The dissociation of this I κ B from NF- κ B is brought about by an enzyme called I κ B kinase (IKK). IKK β is one of two catalytic subunits of the IKK complex.

In cultured cells, activation of IKK β attenuates insulin signalling, whereas IKK β inhibition reverses insulin resistance [160]. As molecular mechanism for the development of this insulin resistance, cell culture experiments have identified that IKK activation leads to inactivating phosphorylation of IRS as a direct substrate [161, 162]. However, in comparison to JNK, the evidence of its in vivo physiological effects through this mechanism is less strong [39].

As molecular mechanism of the development of this insulin resistance, inactivating phosphorylation of IRS as a consequence of direct substrate of IKK has been identified in cell culture experiments

The primary mechanism of insulin resistance following IKK β activation appears to be through induction of proinflammatory cytokines via the upregulation of expression of inflammatory components by NF- κ B. IKK β over-expression in hepatocytes causes local and systemic induction of proinflammatory cytokines and systemic insulin resistance in absence of obesity [163]. Interestingly, IKK β induced insulin resistance was fully reversed with neutralising antibodies against IL6 [163], implying a central role of the cytokine in the development of insulin resistance. Targeted disruption of hepatocyte IKK β genes in mice led to decreased hepatic inflammatory cytokine expression and improved insulin action in liver tissue without improvement in systemic insulin sensitivity [164]. The above studies demonstrate that, whilst IKK β is an important contributor to the development of obesity associated insulin resistance, inflammation modulation is the primary mechanism underlying its role (Figure 1.14).

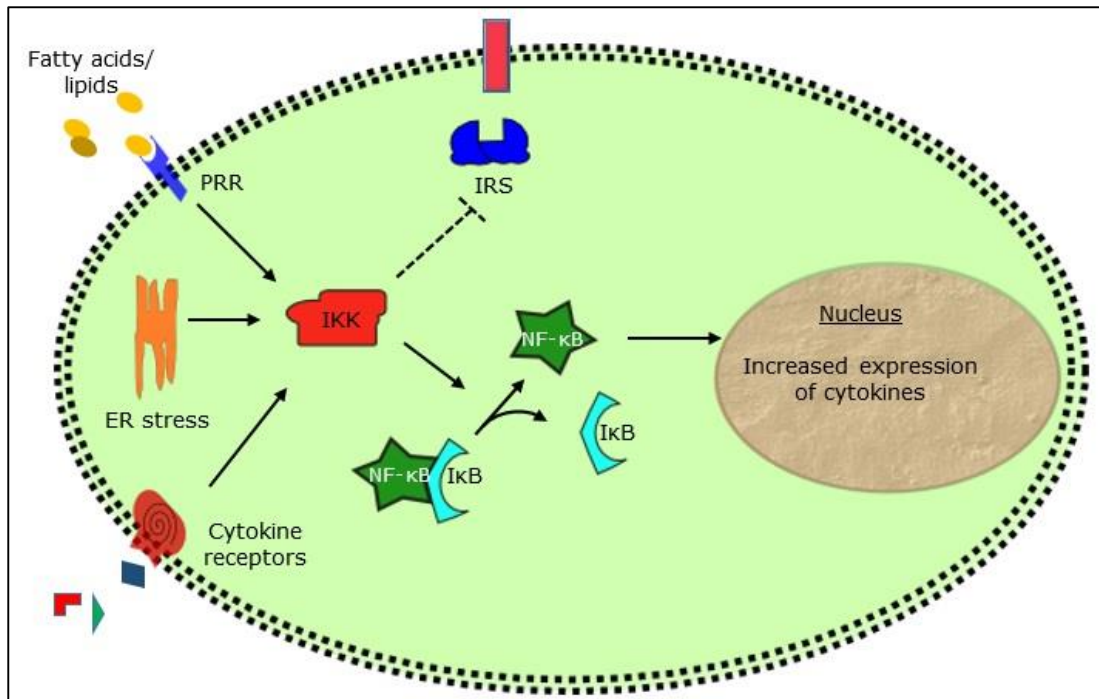


Figure 1.14 Schematic diagram demonstrating mechanisms of inflammation propagation and proposed mechanism of development of insulin resistance in response to IKK stimulation.

Activated IKK catalyses removal of inhibitory IκB from NF-κB and the latter controls transcription of several inflammatory genes. IKK is also proposed to directly inhibit IRS. ER, endoplasmic reticulum; PRR, pattern recognition receptors; IRS, insulin receptor substrate; NF-κB, nuclear factor kappa-light-chain-enhancer of activated B cells; IκB, Inhibitor of κB; IKK, IκB kinase.

JNK and IKK activation, therefore, promote development of insulin resistance in cells exposed to the metabolic and inflammatory stress of obesity by inhibiting intracellular pathways beyond insulin receptor activation and also by further exacerbating the proinflammatory state of the cell and its environment.

1.4.3.3 Cluster of Differentiation 95

Cluster of differentiation (CD95), also known as Fas, is a member of the TNF receptor family. The primary role of this receptor is considered to be the regulation of programmed cell death through apoptosis. However, activation of CD95 receptor can also induce non-apoptotic signalling pathways including those of inflammation [165]. CD95 is known to be expressed in

preadipocytes and adipocytes [166]. Intracellularly, CD95 is predominantly localized in the golgi complex and translocates to cell surface upon stimulation [167]. NF- κ B directly regulates CD95 expression by binding to position 295 to 286 of CD95 gene promoter [168].

CD95 expression is markedly increased in the adipocytes from ob/ob and db/db mice as compared to controls and in the adipose tissue of obese and type 2 diabetic patients [169, 170]. In addition, CD95 deficient and adipocyte-specific CD95 knock out mice have both been shown to be protected from developing insulin resistance secondary to high fat diet feeding [170]. This was associated with reduced adipose tissue expression for inflammatory mediators such as IL6, TNF α , MCP1 and decreased plasma IL6 concentrations.

In addition, adipose tissue CD95 has been shown to affect pathogenesis of hepatic steatosis. High fat diet in mice with adipocyte specific CD-95 knockout demonstrate decreased steatosis, decreased liver ceramides and reduced activation of NF- κ B [170]. In addition to promoting inflammation, the proapoptotic function of CD95 is considered significant in pathogenesis of NASH as a mediator of cytotoxicity in response to excess circulating free fatty acids [171]. CD95, therefore, is considered to be an important nodal point for interaction of cell stress pathways and inflammation with role in development of insulin resistance.

1.4.4 Summary of role of adipose tissue in obesity associated metabolic dysfunction

The evidence presented so far demonstrates that adipose tissue is a dynamic organ and, in addition to its role as a store of excess fat in the body, it is a seat of multiple mutually interacting processes which regulate the state of metabolic inflammation and cell death. In the state of obesity, these pathways both influence the metabolic function of adipose tissue and promote a state of insulin resistance as witnessed in the MetSyn (Figure 1.15). In order to study the developmental mechanisms of obesity associated metabolic dysfunction, it is important to examine the cell stress response pathways in the adipose tissue depots.

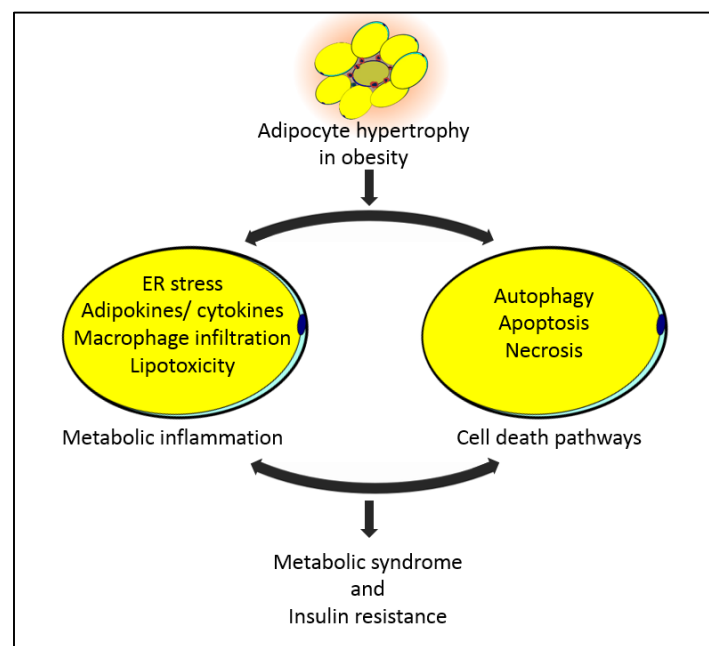


Figure 1.15 Diagram summarising interaction of multiple cell stress pathways activated in adipose tissue during obesity and their collective effect on development of the metabolic syndrome and insulin resistance.

1.5 The liver

The liver, the largest gland in the body, is central to the body's metabolism of major substrates: carbohydrates, proteins, amino acids and lipids.

Following absorption from the intestine, nutrients are delivered to the liver via the portal vein and, depending upon the state of the body's energy levels, these nutrients are allocated to breakdown, storage, processing or distribution. A healthy and well-functioning liver is, therefore, important for maintenance of the entire body's state of metabolic health by maintaining a balance between catabolic and anabolic processes. However, this mechanism is disrupted in disease states such as the MetSyn [172].

The majority of cells (60-80%) in the liver tissue are hepatocytes which perform the metabolic functions of the liver including storage of triglycerides. The other cell types present in the liver tissue include Kupffer cells (resident macrophages), natural killer cells, T cells, sinusoidal cells and stellate cells.

1.5.1 Non-alcoholic fatty liver disease

Non-alcoholic fatty liver disease (NAFLD) is a term used to describe the accumulation of fat within the liver in absence of excessive alcohol use. Whilst there are other rare causes of its occurrence (such as amiodarone, Reye's syndrome and corticosteroids), it is strongly associated with obesity and the MetSyn [173]. First described in 1980 [174], NAFLD covers a spectrum of severity, ranging from asymptomatic accumulation of fat in the liver (hepatic steatosis), hepatic fat accumulation with features of inflammation (non-alcoholic steatohepatitis (NASH)) to the extreme of irreversible hepatic fibrosis and loss of liver function (cirrhosis).

There is a large variation in the reported prevalence of NAFLD primarily owing to its asymptomatic nature and poor sensitivity of the diagnostic radiological tests, especially in mild cases [175]. In Western populations, the incidence has been reported at 20-30% of adults [176, 177]. The

prevalence and severity of the condition also varies with ethnicity, age and gender [177]. This is similar to known ethnic differences in other complications of overnutrition such as insulin resistance, diabetes and the MetSyn and it has been proposed that, like them, NAFLD is an outcome of interaction between a susceptible host and the environment of positive energy balance [178] .

1.5.2 Relationship between NAFLD and insulin resistance

Accumulation of fat in the liver, the hallmark of NAFLD, is strongly associated with all the components of the MetSyn [173]. Indeed, some authors have proposed that the presence of NAFLD should be included in the diagnostic criterion for the MetSyn [179]. NAFLD is present in 50-75% of people with type 2 diabetes and 76% of obese people and has been shown to predict insulin resistance independently from presence of obesity [180].

Insulin resistance has been proposed to promote hepatic triglyceride (TAG) accumulation. The two main sources for hepatic TAG are dietary TAG, transported to the liver via chylomicrons, or as the outcome of intrahepatic synthesis using glycerol and fatty acids (Figure 1.16). The fatty acids required for this synthesis are either sourced from plasma as non-esterified fatty acids (NEFA) or newly synthesised within the hepatocyte by *de novo* lipogenesis (DNL). Whilst the hepatic uptake of NEFA is not regulated and is directly related to plasma NEFA concentrations, *de novo* lipogenesis is a precisely regulated process. Quantification studies in hepatic TAG accumulation in NAFLD have demonstrated that NEFA accounts for 59% of hepatic TAG, 26% from DNL and 15% from dietary sources [181].

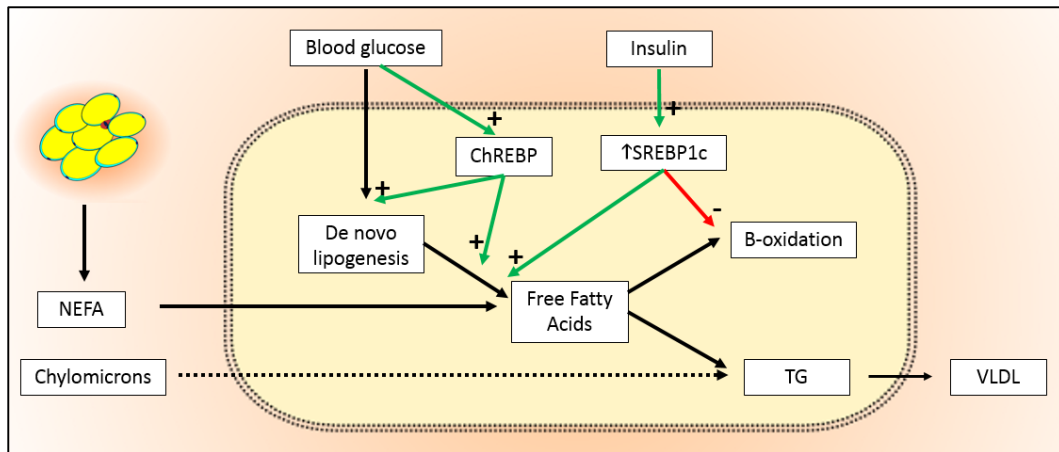


Figure 1.16 Schematic diagram depicting regulation of hepatocyte lipid metabolism in response to blood glucose concentrations and insulin action.

NEFA, non esterified fatty acids; ChREBP, carbohydrate response element-binding protein; SREBP, Sterol regulatory element-binding protein isoform 1c; VLDL, very low density lipoprotein.

Two molecular mediators of lipid metabolism, namely, sterol regulatory element-binding protein isoform 1c (SREBP1c) and carbohydrate response element-binding protein (ChREBP) are important in the regulation of hepatocyte lipogenesis. SREBP1-c, upon activation and transcription upregulation secondary to insulin action [182], transcriptionally upregulates most genes involved in DNL and TAG synthesis and decreases breakdown of fatty acids (β oxidation) [183, 184]. Therefore, through activation of SREBP-1c, normal insulin action in hepatocytes leads to fatty acid build up, providing increased substrate for triglyceride synthesis. ChREBP is activated in hyperglycaemia [185] and, apart from upregulating production of enzymes of DNL, upregulates pathways of glycolysis (the process of glucose metabolism to pyruvate) and, thereby through the Krebs's cycle, provides building blocks for fatty acid synthesis [186]. Hyperglycaemia, therefore, stimulates both glycolysis and lipogenesis by facilitating conversion of glucose to fatty acids in condition of energy excess.

In the state of insulin resistance, the associated hyperglycaemia and the reactive increase in insulin concentrations lead to an unrestricted activation of ChREBP and SREBP respectively (Figure 1.17). This promotes DNL and

inhibits β oxidation within hepatocytes and, hence, promotes the accumulation of triglycerides within the cell [187]. Furthermore, increased plasma concentrations of NEFA, due to absence of insulin mediated suppression of hormone sensitive lipase in adipocytes, also leads to increase FA availability in the hepatocyte. Insulin resistance, therefore, promotes intrahepatic accumulation of triglycerides and development of hepatic steatosis.

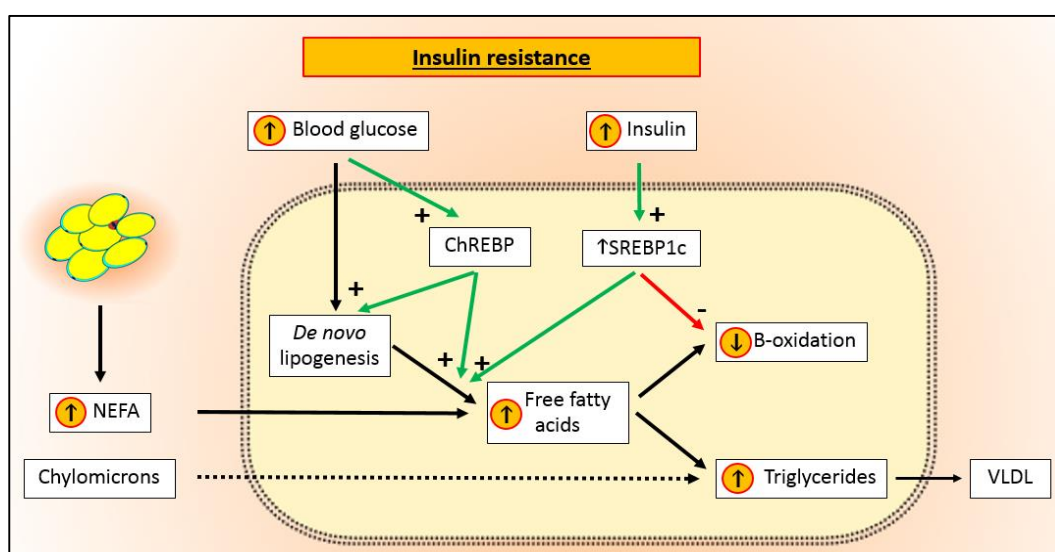


Figure 1.17 Lipid metabolism in hepatocytes in the state of insulin resistance.

Insulin resistance leads to increase in hepatocyte triglyceride synthesis through increased delivery of NEFA and activation of ChREBP and SREBP1c mediators. NEFA, non esterified fatty acids; ChREBP, carbohydrate response element-binding protein; SREBP1c, Sterol regulatory element-binding protein isoform 1c; VLDL, very low density lipoprotein.

Accumulation of lipids within the liver has also been proposed to cause insulin resistance (Table 1.7). Inherited or acquired lipodystrophy [188, 189], a condition characterised by loss or absence of adipose tissue resulting in redistribution of lipids to liver and skeletal muscles, is known to lead to insulin resistance [189]. Hepatic lipidomic analyses of human NAFLD patients have identified selective accumulation of free cholesterol, proinflammatory eicosanoids, diacylglycerides (DAG) and ceramides increasing with NAFLD progression [190]. Hepatic accumulation of DAG, an intermediate of TAG synthesis, strongly correlates with insulin resistance

[191], and has been investigated as a mediator of insulin resistance development [192]. Increased intracellular DAG leads to activation of hepatocyte protein kinase C (PKC) isoform ξ leading to inactivation of serine phosphorylation of IRS [193]. Furthermore, DAG upregulates inflammatory pathways via JNK and IKK (reviewed in [194]). Findings from several genetic studies with transgenic and knockout mice [193, 195-198] support these mechanisms.

Lipid induced insulin resistance- Proposed mechanisms	
Steatosis → ↑ hepatic DAG activated PKC ξ	→ inactivation of IRS
Steatosis → ↑ hepatic DAG	→ activation of JNK and IKK
Steatosis → ↑ hepatic Ceramides	→ inhibition of Akt/PKB
Steatosis → ↑ hepatic Ceramides	→ activation of JNK and IKK
Steatosis → ↑ hepatic cholesterol, LPA, long chain fatty acyl-CoA	

Table 1.7 Table listing some of proposed mechanisms for development of hepatic insulin resistance in NAFLD.

Hepatic DAG, ceramides, cholesterol and long chain fatty acyl-CoA accumulation in NAFLD have all been proposed to cause insulin resistance through inactivation of IRS or activation of inflammation. DAG, diacylglycerides; PKC ξ , protein kinase C isoform ξ ; JNK, c-Jun N-terminal kinase; IKK, Inhibitor of κ B kinase; Akt/PKB, protein kinase B; LPA, lysophosphatidic acid.

Ceramides are a family of lipid molecules composed of sphingosine and a fatty acid. As a component of sphingomyelin, ceramides are found in all cell membranes. Increased accumulation of hepatic ceramides during hepatic steatosis is considered to be secondary to its upregulated *de novo* synthesis and salvage processes secondary to increased saturated fats [199], oxidative stress [200] or inflammatory stress [201]. Increased availability of NEFA to hepatocytes also increases the ceramide load to the cell. Apart from being structural components of the cell membrane, ceramides are also known to take part in lipid signalling. Studies in skeletal muscles have consistently demonstrated Akt/PKB inhibition as the mechanism of promotion on insulin resistance secondary to ceramides [202]. This is supported by in vitro experiments in cultured hepatocytes [203] and by in vivo experiments of inhibition [204] or promotion [205] of hepatic ceramide synthesis.

Furthermore, ceramide accumulation promotes inflammatory cascades activation via JNK and IKK pathways [206].

Other potential mediators of lipid induced hepatic insulin resistance are cholesterol, lysophosphatidic acid (LPA) and long chain fatty acyl-CoA [207].

Experimental and epidemiological evidence, therefore, demonstrate that the presence of insulin resistance and NAFLD foster the development and progression of each other, thereby, advancing the metabolic derangements present in the state of obesity.

1.5.3 Hepatic inflammation in obesity associated metabolic dysfunction.

With advancing NAFLD, the histological features within hepatic tissue progress from lipid accumulation (steatosis) to cellular inflammatory changes, cellular infiltration, fibrosis and associated hepatocellular degenerative changes which have been called non alcoholic steatohepatitis (NASH). There are multiple operational criterion for histological diagnosis of NASH [178]. It is generally accepted that along with presence of inflammatory infiltrate, steatosis and ballooning degeneration of hepatocytes should be histologically demonstrated for a diagnosis of NASH [208].

The inflammation seen in NASH has been demonstrated to be the outcome of multiple pathways extrinsic or intrinsic to the liver (Figure 1.18). Adipose tissues are key source of mediators contributing to hepatic inflammation.

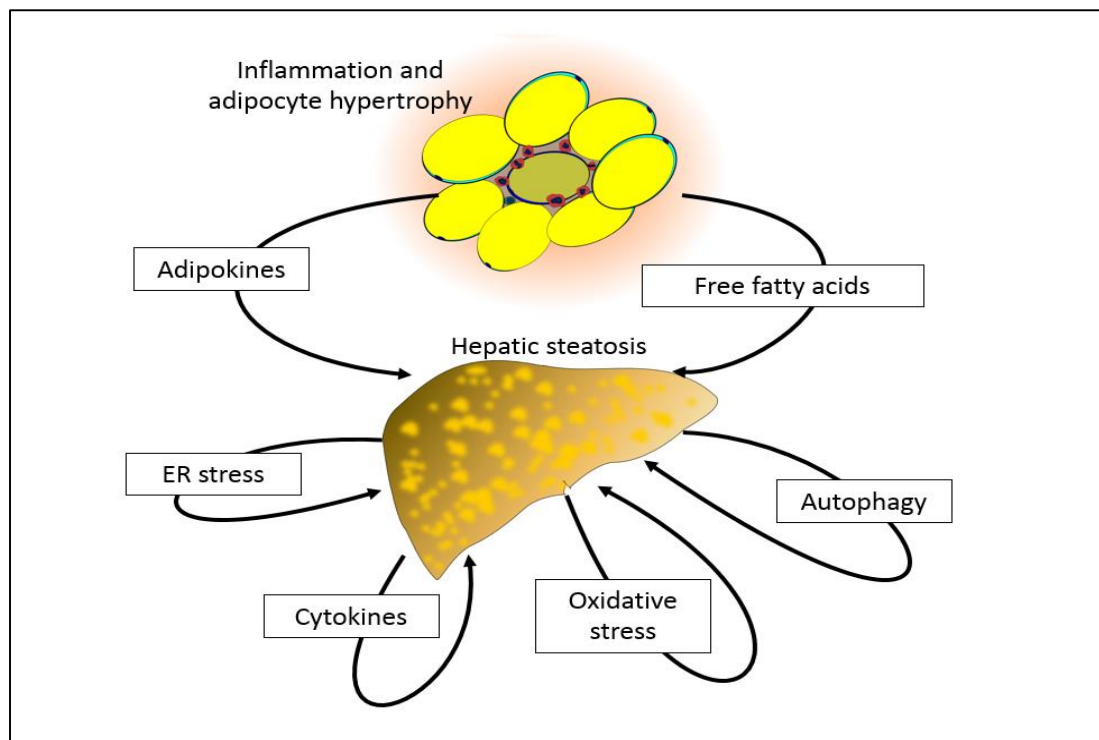


Figure 1.18 Sources of inflammatory processes witnessed in non alcoholic fatty liver disease.

Adipokines and free fatty acids from adipose tissues in obesity are extrinsic sources of inflammation whilst processes intrinsic to liver including ER stress response, cytokines, oxidative stress and autophagy have all been demonstrated to collectively contribute to the activation and progression of hepatic inflammation.

1.5.3.1 Adipose tissue derived factors in hepatic inflammation

Adipose tissue, particularly visceral adipose tissue, has been extensively studied as the source of hepatic inflammation. Intra-abdominal fat is an established risk factor for development of metabolic derangements [209] and NAFLD [210]. Fat transplantation of tissue of subcutaneous origin to an intra-abdominal site in rodents has been shown to improve glucose homeostasis [211]. As described in Section 1.4, adipose tissue is capable of initiating a multifaceted inflammatory response in obesity. A time course study in HFD mice given a cholesterol-enriched diet for 6, 16 and 26 weeks duration demonstrated that macrophage and cytokine transcripts were upregulated in adipose tissue at 6-16 weeks before their appearance in the liver from 16-26 weeks after the start of the HFD and this was associated with macrophage infiltration within the liver at 16 and 26 weeks [212]. In a

study of obese human individuals (BMI>35kg/m²) undergoing gastric surgery, histological analysis from omental adipose tissue and liver demonstrated a significant association between omental macrophage accumulation and hepatic fibroinflammatory lesions.

Adipose tissues are also capable of secreting a variety of substances capable of promoting hepatic inflammation. Dietary [213] and transgenic [214, 215] animal models have consistently confirmed the association of increased plasma free fatty acids with hepatic lipid accumulation. As discussed in Section 1.4.3, free fatty acids activate intracellular inflammatory cascades through activation of pattern recognition receptors including TLR4 and can also promote activation of ER stress. In addition, the effect of adipokines on liver has been extensively investigated. Leptin administration is associated with reversal of NAFLD and abnormal liver function in ob/ob mice [216], db/db mice [217] and humans with lipotrophic diseases [218] following leptin administration [219]. However, studies of correlation of NAFLD with circulating leptin concentrations in humans have produced conflicting results [220-222]. In obese NAFLD patients, increased leptin concentrations have also been shown to correlate with the severity of hepatic steatosis, a phenomenon that has been attributed to leptin resistance [223-225]. The specific role and the mechanism of this adipokine action in hepatic inflammation and insulin resistance is, therefore, not yet fully elucidated [225]. Leptin's role in NAFLD progression has been proposed to be the outcome of its multiple actions including its effects on innate and adaptive immunity [226], profibrogenic role [227] and decreased insulin sensitivity secondary to leptin resistance.

Other adipokines, including adiponectin, resistin, TNF α and IL6, have also been proposed to contribute to the hepatic lipid deposition and inflammation seen in NAFLD (reviewed in [225])

1.5.3.2 Interaction of hepatic inflammation and hepatic cell stress response

1.5.3.2.1 Hepatic ER stress response and inflammation

The hepatocyte ER is the main site for multiple simultaneous metabolic processes including synthesis and secretion of proteins, lipoproteins, very low density lipoprotein (VLDL) and cholesterol [108]. The hepatocyte ER stress response has been extensively studied in the context of NAFLD, its associated inflammation and insulin resistance [99, 228]. The studies investigating the directionality of the cause and effect relationship between NAFLD and ER stress response are summarised below.

HFD and ob/ob mouse models of obesity exhibit upregulation of ER stress markers [99] along with features of insulin resistance and type 2 diabetes. In HFD mice, obesity and the induced ER stress response have been shown to precede JNK activation. Chromium picolinate is used as a dietary supplement by diabetics and acts by decreasing lipid uptake by hepatic cells. Administration of chromium to mice reduced hepatic lipid accumulation and decreased markers of ER stress associated with amelioration of insulin resistance in ob/ob mice. In human studies, hepatic GRP78 and p-eIF2 α are decreased following weight loss after gastric bypass surgery [105].

The above studies suggest ER stress response activation is the outcome of hepatic lipid accumulation.

ER stress activation has also been demonstrated to promote hepatic lipid accumulation through several mechanisms. As discussed in Section 1.5.2, the aggregate liver lipid is the outcome of balance between lipid deposition and secretion from the hepatocytes. Activation of UPR leads to increased lipogenesis due to increased activation of SREBP and can override cholesterol mediated inhibition of SREBP. Decreased protein abundance, a consequence of a decrease in generalised protein translation results in decreased ER

content of inhibitory protein product of insulin-induced gene 1 (Insig1) [229]. Due to its short half-life, the amount of Insig1 within ER decreases rapidly leading to activation of SREBP1 [230]. Hepatic lipogenesis is also increased due to increased PPAR γ with eif2 α activation [98] (PERK pathway), decreased insulin sensitivity due to inhibition of Akt/PKB via the ATF4 (PERK pathway) [97], JNK mediated IRS inhibition (Section 1.4.3.1). Furthermore, attenuated global translation and ERAD also leads to decreased Apolipoprotein B synthesis. This contributes to hepatic steatosis due to decrease in VLDL secretion [231].

The above mechanisms have been tested in experimental models. Overexpression of GRP78 in cultured primary hepatocytes and ob/ob mice led to amelioration of ER stress, inhibition of SREBP1c activation and reduced steatosis [232]. This result is similar to treatment of ob/ob mice with chemical chaperones (4-phenylbutyric acid and taurine-conjugated ursodeoxycholic acid) which presumably improve protein folding which led to decreased ER stress response, improved insulin sensitivity and resolution of fatty liver [233]. Inhibition of eIF2 α arm of UPR also improves steatosis and glucose tolerance [98].

The relationship between NAFLD and ER stress is bidirectional and the reciprocal fostering of each other promotes metabolic inflammation and derangement of cellular function. ER stress response, therefore, plays an important role in NAFLD and associated metabolic dysfunction.

1.5.3.2.2 Autophagy in the liver

The process of autophagy has been identified as key to hepatic metabolism and its role in the development of NAFLD and metabolic diseases of obesity has been extensively investigated [234, 235].

Autophagy contributes to normal hepatocyte lipid metabolism and it has also been proposed that lipid accumulation leads to a defect in the intracellular autophagic processes. Shibata et. al. demonstrated that a normal lipid droplet membrane contains several components of autophagic LC3 conjugation system [129], a finding confirmed in subsequent studies [131] which also identified that starvation leads to transfer of lipid content from lipid droplets to autophagosomes and lysosomes. This autophagy of lipids has been termed lipophagy. Defective lipophagy, secondary to ATG5 knockdown or pharmacological inhibition, leads to excessive lipid accumulation within hepatocytes [236]. The presence of increased autophagic vesicles within a cell does not necessarily imply increased autophagic activity and may reflect a defect in autophagic processing and consensus criterion have been devised to differentiate one from another [237]. It has been proposed that hepatic lipid accumulation in HFD mice, by itself, leads to defective autophagic function contributing to decreased mobilisation of lipids into autophagic compartments in HFD mice facing food withdrawal [130]. Similar defective autophagy has also been demonstrated in other experiments of genetic (ob/ob) and dietary models of murine obesity [234].

Defective autophagy has also been demonstrated in association with increased hepatic lipid and glycogen deposition in the offspring of Wistar rats that underwent gestational nutrient restriction to 35% of metabolic requirements during late gestation (day 14 until birth) [238]. Intra uterine growth restriction (IUGR) secondary to prenatal nutrient restriction in this model was associated with decrease in hepatic autophagic vacuoles and a

decrease in the autophagic protein markers. When fed a high-fat diet until 22 weeks, offspring of control rats showed enhanced autophagic activity in liver, whereas, the IUGR rats maintained lower levels of Atg7 and LC3B II and developed insulin resistance, liver steatosis and ER stress [238].

Normal functioning of cellular autophagic pathways is required for maintenance of cellular insulin sensitivity. In HFD mice, decreased Atg7 expression precedes (16 weeks) the development of insulin resistance (22 weeks) [234]. Suppression of autophagy in *atg7^{-/-}* mice model resulted in upregulation of ER stress and insulin resistance, whereas overexpression of *atg7*, achieved with an adenoviral delivery to the liver of *ob/ob* mice, led to improved glucose homeostasis, insulin action and amelioration of ER stress markers [234]. In addition, normal autophagic function, through its modulating role in immune system and apoptotic cell death pathways (Section 1.5.2.2) can affect hepatic functioning and insulin sensitivity.

1.5.3.2.3 Intrinsic hepatic factors: cytokines, inflammation and oxidative stress

Hepatic lipid accumulation by itself can promote inflammation by NF- κ B activation and cytokine production as demonstrated by Cai and colleagues [239] in a HFD mouse model which had hepatic inflammatory cytokine profile similar to a transgenic mouse model of subacute hepatic inflammation produced by low level activation of NF- κ B. Both these mice models had activation of NF- κ B and its transcriptional targets along with increased hepatic insulin resistance as compared to lean and wild type controls. These effects were reversed in both models by repression of hepatic I κ B α demonstrating that liver lipid accumulation leads to subacute hepatic inflammation through NF- κ B activation and downstream cytokine production. The role of specific lipid intermediates such as ceramides and DAG has been discussed in Section 1.5.2.

The presence of oxidative stress in livers of patients with NASH has been identified with presence of oxidised lipids, proteins and DNA [240-242]. There are multiple possible sources of this oxidative stress including release of reactive oxygen species from uncoupled oxidative phosphorylation in mitochondria [243], peroxisomes [240] and inflammatory cells [244]. However, the role of oxidative stress as primary inducer of hepatocellular injury and dysfunction has not been convincingly demonstrated and antioxidants such as Vitamin E have been tried with limited improvement in the progression of established NASH [245]. It is believed that oxidative stress and/or cytokines are not likely to be the initiators of liver inflammation in NASH. However, it may have roles in insulin resistance and perpetuation of inflammation [246].

In conclusion, hepatic inflammation in NAFLD is brought on by mechanisms originating in adipose tissue and by processes intrinsic to liver. Such obesity-induced mechanisms interact with each other to propagate the inflammatory response, cause hepatocellular damage and dysfunction leading to development of the MetSyn and insulin resistance. In turn, insulin resistance also propagates the hepatic lipid accumulation and cellular damage of NAFLD causing a vicious cycle of disease progression. The cellular stress response of liver and adipose tissues is, therefore, central to the pathogenesis of the MetSyn. Modulation of this cell stress response through developmental, dietary or therapeutic means has the potential of altering an individual's susceptibility to the MetSyn and this may be of great public health or clinical significance.

1.6 Developmental programming of insulin resistance and the MetSyn

1.6.1 The concept of developmental programming

Environmental conditions during the development of an organism can modify the evolution of a single genotype to many diverse structures, physical states and behaviours. Some of these environment-induced changes during early life (conception, fetal life, infancy and early childhood) can have a long term impact on later health and disease risk. Often such changes have graded and subtle effects which, by themselves, do not induce disease but can affect the predisposition to disorders including cardiovascular diseases, obesity, type 2 diabetes and osteoporosis [247]. This process by which changes in the genetic, epigenetic or phenotypic make-up of an individual are brought about as a response to environmental influences in early life is called developmental programming.

The developmental origin of health and disease (DOHAD) concept focuses on the contribution of the environment during the earliest stages of human development to the pathogenesis of adult conditions. Following its introduction as the 'fetal origin of adult diseases' (FOAD) hypothesis by Hales and Barker in 1992 [248], this concept has evolved and has been supported by numerous epidemiological and experimental studies [68, 249-252]. Furthermore, it has become increasingly apparent that, along with the severity of the environmental stimulus, the outcome of the extent of this adaptation is dependent upon the timing of the stimulus with reference to the developmental stage, that is, there are critical windows of development of the organism [253].

It has been proposed that a developing organism makes physiologic adaptations in response to the environmental cues prevalent during such

critical windows of development. If the environmental conditions persist in later life, such adaptations, which have been called 'predictive adaptive response', would provide physiologic advantage to the individual. However, in case of a mismatch between adaptations made and the environmental factors existing during later life, such adaptations may prove to be detrimental for the individual and add to the predisposition to pathologic conditions.

Evidence based on epidemiological studies, such as the Dutch famine cohort, has its own limitations. Health outcomes are typically multifactorial and may be influenced by interaction with the prevailing environmental conditions at the time of the study. Furthermore, the cohort also has progressively increasing loss to follow-up from 84% enrolment at initiation [254] to low of 28% at the follow up in studies done in 2005 [255] increasing the risk of survivor bias. In addition, the timing of nutrient restriction during pregnancy was based on date of birth assuming a 40 weeks gestation of all pregnancies. This approach, along with retrospectively maternal undernutrition into trimesters increases the likelihood of improper classification of timing of undernutrition. It is known that IUGR is associated with preterm delivery and it is therefore likely that a proportion of newborns deemed IUGR at 40 weeks gestation were late preterm AGA infants. The statistical power of large epidemiological studies hopes to account for bias such as these. It is therefore important to attempt to replicate findings of epidemiological studies to well designed experimental studies of appropriate animal models.

1.6.2 The critical windows of development and nutritional programming

1.6.2.1 Suboptimal nutrition during pregnancy

Birth weight became the focus of investigations following the demonstration of a strong association between low birth weight and predisposition to the MetSyn and type 2 diabetes in several longitudinal studies [248, 256]. However, there are several factors that interact together to determine birth weight, such as placental efficiency, genetics, environment and maternal nutrition. Of these, the role of maternal nutrition during specific stages of fetal development, its contribution to birth weight [257] and the onset of the MetSyn became apparent from the follow up studies of survivors of the Dutch famine.

During the German occupation of the Netherlands during the Second World War in 1944-45, there was an extreme shortage of food supplies in the western part of the country. This was due to a railway embargo on food supplies and made worse by inability to resume supplies due to frozen waterways during an unusually severe winter. As a consequence, the average food intake for pregnant women during this period was approximately 800-1000 kcal/d [258] in comparison to the recommended energy intake of 2,140 kcal/d [259, 260]. The offspring of these pregnant women were traced in their later life as part of the Dutch Famine cohort studies. The unique nature and period (Nov 1943 to Jan 1945) of the calorie restriction during pregnancy enabled researchers to study the effect of suboptimal nutrition during each of the three trimesters of the pregnancy. The control groups for these studies were Dutch individuals born before the famine and individuals who were conceived after the famine (born between December 1945 and Feb 1947).

In comparison to the control groups, offspring of mothers exposed to famine during their final trimester in utero had a reduced birthweight, whereas the

mean birthweight of the offspring of mothers exposed in their first or second trimester in utero was not reduced [258, 261]. In analyses performed at 50 years of age, children born after exposure to the famine during the first trimester went on to have a higher rate of coronary heart disease and increased plasma lipids [262]. At the same age, offspring of the pregnant women exposed to famine during late gestation had impaired glucose tolerance [258]. This unique epidemiological study, therefore, identified the distinct impact of undernutrition during specific critical windows of gestational development on the offspring health.

Another epidemiological study of developmental programming potential of decreased perinatal nutrition is that of the 1959-1961 Chinese famine. The 'giant leap forward' campaign, initiated by the Chinese government in 1958, was an economic and social campaign aimed to rapidly transform the agrarian economy into a communist society through rapid industrialisation and collectivisation. However, during execution of the widespread changes, there was a sudden and severe fall in food grain production leading to severe famine. Follow up studies of children born during the periods during, and after, the famine identified that surviving adults affected by gestational undernutrition had a 3.1 times higher risk of developing the MetSyn [263] at the mean age of 44 years. This study, however, was unable to delineate the effects of exposure during specific gestational periods/ critical windows.

The role of gestational undernutrition in developmental programming has been further explored in experimental studies. Offspring of pregnant sheep receiving 70% of recommended calorie intake during late gestation, and then exposed to a restricted, obesogenic environment, demonstrated insulin resistance identified by increased area under the curve during glucose tolerance tests (GTT) along with alteration of plasma lipid and protein profiles [264]. The findings are consistent with results of similar experiments in a small animal model [265]. Late gestation is the period of fetal

development characterised by rapid fetal weight gain and when endocrine functions linked to hypothalamic maturation are established [7]. Late gestational undernutrition in the sheep model has been identified to have a significant impact on the birth weight [266], control of energy metabolism [267] and, more specifically, on the development of adipose tissue in the offspring [268].

Programming of adipose tissues in response to maternal undernutrition has also been investigated. In rats, moderate (50%) and severe (70%) prenatal caloric restriction programmes the offspring to greater fat deposition when presented with hypercaloric diet [269]. There is also evidence that a protein-restricted diet during gestation also programmes susceptibility to obesity and alterations to glucose metabolism in adult rats and mice [270, 271]. In sheep, maternal nutrient restriction during the early period of gestation (28-80 days gestation) increases adiposity and mRNA expression of UCP1 and peroxisome proliferator-activated receptor α (PPAR α) in the offspring at term [272]. In contrast, nutrient restriction during late gestation (115 days gestation until term, ~145 days) led to reduced fetal fat deposition and UCP1 expression in the offspring sampled near term (143 days gestation) [273]. By one year of age, however, the offspring had increased fat mass and were more likely to become glucose intolerant [274]. The variation in adipose depot size in response to nutrition during fetal and early postnatal growth demonstrates the susceptibility of adipose tissue to development programming during this period. Further experimental studies in offspring of sheep exposed to late gestational nutrient restriction have demonstrated altered adipose tissue inflammatory profiles [275].

The liver is also known to be vulnerable to developmental programming during early life. Among 50 human infants matched for gestational age, those born small-for-gestational-age (SGA) were found to have reduced liver and kidney (but not spleen) dimensions, as measured by ultrasonography at

birth [276]. The British Women's Heart and Health study reported a small but consistent linear association between decreasing birthweight and adult age adjusted levels of markers of liver damage (alanine aminotransferase (ALT), gamma glutamyltransferase (GGT) and alkaline phosphatase (ALP)) [277].

Animal experiments of nutritional manipulation with a low protein, isocaloric diet during late gestation in rats have shown that this induces structural and functional changes in the liver [278]. Maternal macronutrient restriction during mid-gestation followed by a postnatal obesogenic environment has also been demonstrated to promote hepatic lipid deposition and increased gene expression for hepatic PPAR γ in sheep as early as one year of age [279].

Existing human and animal studies, therefore, indicate that developmental programming during gestation, and more specifically during late gestation, could play a significant role in the long term metabolic health of an individual. Adipose tissue and liver have both been demonstrated to be susceptible to such programming through nutrient availability during this critical window of development.

1.6.2.2 Early postnatal growth

The association between the rate of infant growth with eventual glucose tolerance and obesity has long been recognised [280]. The growth acceleration hypothesis [281], formulated in 2004, proposed that the increased risk of adult metabolic and cardiovascular morbidity associated with being born small for gestational age (SGA) is a consequence of accelerated early growth.

Early infant growth is determined by several factors including genetic, environmental and nutritional influences [282, 283]. However, during the first 30 days of infancy, the genetic contribution to growth is considered to

be minimal [283] whilst nutrition and the postnatal environment are more important. As a target of public health and clinical interventions for the prevention of long term adverse metabolic and cardiovascular consequences, nutritional interventions could, therefore, be used to modulate early growth.

1.6.2.2.1 Epidemiological evidence

The epidemiological studies describing the association between early growth rate and long term outcome are heterogeneous in their study subjects (preterm, growth restricted or term appropriate for gestational age (AGA) babies) and also in the duration of growth measurements [284-288]. A recent meta-analysis [289] of cohort studies (n=47661) addressed this by performing individual level analysis adjusting for sex, age and birth weight. For each 1 unit increase in weight standard deviation (SD) scores of the infant between 0 and 1 year age, the adjusted risk of childhood obesity was increased nearly twofold (odds ratio=1.97 [95% confidence interval (CI) 1.83, 2.12]). The increase in adjusted risk for adult obesity for the same 1 unit increase in infant weight SD scores was 23% (odds ratio=1.23 [1.16, 1.30]). However, this is in conflict with more recently published Medical Research Council (MRC) retrospective cohort study of 64 year old surviving adults which concluded that greater weight gain in infancy and early childhood (birth to 2 years age) was associated with higher lean mass whereas greater weight gain in late childhood was associated with higher fat mass [290].

A prospective birth cohort study [285] of 851 children measured fasting insulin sensitivity (homeostatic model, HOMA) and insulin secretion post oral glucose tolerance test at age 8 years. In this study, greater weight gain between birth to 3 years of age predicted lower insulin sensitivity and higher BMI and waist circumference.

Epidemiological studies, which can only demonstrate associations, are prone to bias and cannot exclude reverse causality. For example, reverse causality would mean that an obese individual was always predetermined to have higher weight gain and as a result have a larger appetite and more rapid weight gain even from birth. In order to address factors such as these, experimental studies are required.

1.6.2.2.2 Experimental evidence

Exclusive breast feeding and late weaning are both known to lead to slower weight gain as compared to formula fed infants or infants weaned earlier [291]. Identification of such different growth trajectories between breast and formula fed infants has led to development of new growth charts by the World Health Organization (WHO) to reflect their very different growth patterns [292].

In this setting, the relative contribution of the type of feed offered and the early growth rate achieved was studied in a randomised controlled trials of preterm children [286] exploring the impact of type of feeding and early growth on insulin resistance in adolescence. The study was divided into two trial arms. In the first, high energy preterm formula was compared with breast milk (banked breast milk donated by lactating women) and in the second, the milk feeds or supplements were randomised to high energy containing preterm formula or relatively low energy term formula. Fasting 32-33 split proinsulin was used as a marker of insulin resistance and measured at adolescence. These trials demonstrated that the concentration of the fasting split proinsulin was lower in adolescence in those children receiving lower nutrition as compared to those children receiving a nutrient enriched diet. This indicates that the relative growth rate in early life was a risk factor for later insulin resistance in both breast milk and formula milk fed infants. In another prospective randomised controlled trial of infants born

SGA, faster weight gain in infancy was associated with greater fat mass in childhood [293].

Animal experiments using rodent models have used different approaches to alter the energy consumption during the early growth period. These interventions have included the use of maternal diet rich in lard through the suckling period [294] or by decreasing litter size soon after birth (typically to 4-6 pups from 10-14 pups) leading to increased milk availability per pup for the offspring and thus faster early growth [295, 296]. These studies demonstrated predisposition in adult offspring to worse cardio metabolic outcomes such as raised systolic blood pressure associated with hyperinsulinaemia [294] and increased adiposity [296]. In another experimental study, manipulation of rat litter size to produce faster weight gain resulted in decreased insulin stimulated glucose uptake in adipose tissue accompanied by reduced intracellular insulin signalling (reduced GLUT-4, IRS-1 and PI3K expression, and Akt activity) [136]. These studies show that, in rats, early postnatal growth can modulate aspects of insulin sensitivity predisposing an individual to insulin resistance.

It is, however, unclear whether this mechanism is an effect of developmental programming on insulin sensitivity or an indirect effect of increased predisposition to obesity.

Rodent development is also significantly different from humans and other large mammals. The main differences between rodents and large mammals is the former have large litter sizes and differ in fetal organ growth rate and metabolic rate [297]. Importantly, the hypothalamic pituitary adrenal axis is immature at birth in rodents [298]. There have been very few large animal model experiments demonstrating the presence of metabolic consequences of nutritionally altered early growth and its impact on metabolic outcome in the adult.

1.6.2.3 Formula feeding and developmental programming

A number of epidemiological cohort studies have explored associations between type of feed consumed by an infant and its long term programming impact on obesity, the MetSyn and type 2 diabetes. However, such population based studies comparing breast and formula feeding are difficult to interpret due to the inevitable presence of confounding factors of differing socio-economic background. There is also a likelihood of publication bias with studies showing no beneficial effect being less likely to be published.

Formula feeding has been proposed to programme the development of obesity. A recent systematic review [299] analysed 61 studies comparing breast feeding to formula feeding and risk of later obesity. Of these, 28 studies provided unadjusted odds ratio and 6 studies provided odds ratio adjusted for parental obesity, maternal smoking, and social class. The analysis reported that breastfed subjects were less likely to be defined as obese as compared to formula fed subjects (odds ratio: 0.87; 95% confidence interval [CI]: 0.85–0.89). The results remained significant in sub analysis of 6 studies with adjustment for confounding factors. These findings were similar to other published meta-analyses from different authors [300, 301]. Another meta analysis which demonstrated a linear inverse relationship between the duration of breastfeeding and later offspring risk of overweight, that is, the longer an infant was breastfed, the lower was his/her risk of overweight status during childhood and adult [302], also suggests a protective role of breastfeeding against later obesity.

There are no published studies investigating the association between formula feeding and MetSyn as a clinical definition. However, some studies have been published on the long term effects of breastfeeding on single components of the MetSyn. These studies differ in not just the inclusion criteria, but also in their methodologies. The WHO publication in 2007 [303] chose not to correct for current body weight as it considered that a modest

decrease in adult weight is unlikely to have an impact on the serum cholesterol levels of the individual. In contrast, the previously published meta analysis [304] included current weight along with BMI or ponderal index. Notwithstanding the methodological differences, both studies reported absence of a consistent association between feeding type and components of the MetSyn except a modest decrease in adult mean total cholesterol levels by around 0.18 mmol/L (95% CI: 0.06 to 0.30 mmol/L) in the breast fed group as compared to the formula fed group [304]. This decrease represents 3.2% of the median adult cholesterol reported in the study (5.7 mmol/L).

Few studies have evaluated the relationship between breastfeeding duration and later onset of type 2 diabetes [301]. Although breastfed subjects may be less likely to present with type 2 diabetes (pooled odds ratio: 0.63; 95% CI: 0.45–0.89)[305], other studies have reported no association between a surrogate marker of insulin resistance the homeostatic model (HOMA) index and breastfeeding duration [306].

Differences in composition of breast milk and commercial formula milk have also been proposed to affect the later metabolic outcome of the infant. Factors such as milk cholesterol content, reduced milk protein concentrations, increased long-chain polyunsaturated fatty acids [307] and presence of hormones such as leptin, adiponectin and ghrelin [308] in breast milk have been investigated for their effect on long term appetite signalling and body composition of the adult individual.

Nobili et. al. performed a retrospective analysis in 191 biopsy proven cases of children (3-18 years old) with NAFLD and demonstrated that, following correction for age, waist circumference, gestational age and neonatal weight, the odds of non-alcoholic steatohepatitis (OR: 0.04, 95% CI 0.01 to 0.10) and fibrosis (OR: 0.32, 95% CI 0.16 to 0.65) were lower in breastfed versus not breastfed infants [309]. However, another prospective study comparing

intrahepatocellular lipid content quantified through use of using magnetic resonance spectroscopy did not demonstrate any difference in hepatic lipid deposition between breast fed or formula fed infants measured at time points of median age of 13 days and between 6-12 weeks [310]. The same study also demonstrated absence of difference in adiposity between the two groups. However, with a small sample size of 7 subjects across 3 groups, this observational cohort study may not be sufficiently powered to detect the absence of a difference. Whilst various potential mechanisms have been proposed, there have not been any previous published experimental studies in a large animal model investigating the impact of formula feeding on the programming of the cell stress response and metabolic inflammation of the individual.

1.7 Programming of the hepatic and adipose cell stress and inflammation response

Whilst cell stress and inflammation have been widely studied as mechanisms for obesity-induced insulin resistance, the role of developmental programming in modulating cell stress responses has only been recently explored systematically. Sharkey et al. demonstrated in the sheep model, that early gestational nutrient restriction in the sheep model differentially alters ER stress response and inflammation in visceral (perirenal) adipose tissue and kidney [68]. The increased gene expression for ER stress was associated with raised inflammation and presence of CLS in the adipose tissue. This was also associated with increased pJNK in the adipose tissue. In another study [275], late gestation nutrient restriction led to increased CD68 mRNA coupled with increased TLR4 gene expression.

Nutrition during early life and its effect on early growth is a modifiable risk factor with great public health implications. Small animal models investigating programming of inflammation and the immune system have concentrated on maternal obesity [311]. Furthermore, studies investigating

nutritional programming have focussed primarily on brown fat development, hepatic growth factors, insulin sensitivity and ontogeny [312, 313]. Defective autophagy has also been demonstrated in association with increased hepatic lipid and glycogen deposition in the offspring of Wistar rats that underwent, gestational nutrient restriction to 35% of metabolic requirements during late gestation (day 14 until birth) [238]. There have been no other published large animal studies that have explored nutritionally mediated developmental programming of pathways of metabolic inflammation and cell stress response in omental adipose tissue and the liver. The experimental studies performed as part of this thesis explore the nutritional programming of this cell stress response to obesity in omental adipose tissue and the liver (Figure 1.19).

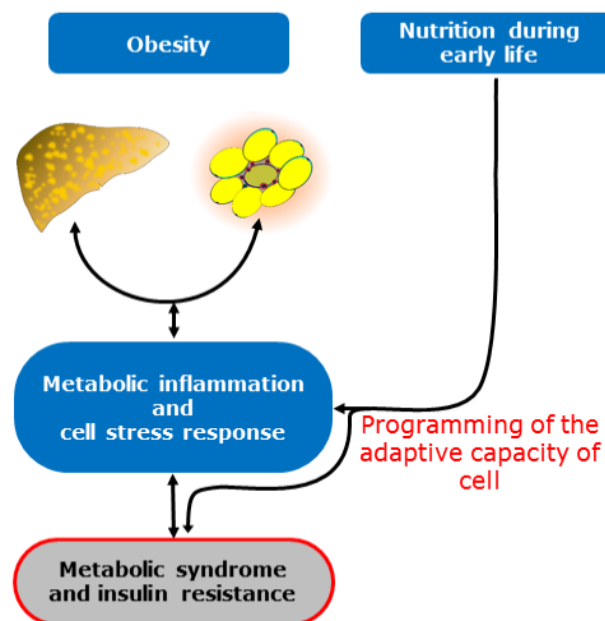


Figure 1.19 Schematic diagram illustrating the proposed interaction of nutritionally mediated developmental programming stimulus in the pathogenesis of obesity induced metabolic syndrome and insulin resistance.

1.7.1 Experimental approach

A robust experimental model, which permits controlled nutritional intervention during pregnancy and early life, allows ongoing monitoring of weight gain and physiological parameters, mimics human organ development and physiology and has precedence of experimental studies in hepatic and adipose tissues is required to optimally study the potential nutritional programming of the obesity-induced cell stress response and inflammation.

1.7.1.1 The sheep as an experimental model for programming

Randomised controlled studies which can control for confounding factors such as genetic predispositions and social status, designed to control for other risk factors such as parity, number of fetuses and gender are best placed to validate findings of epidemiological studies. However, since it is not possible to subject humans to highly invasive physiological or experimental procedures, it would not also be possible to elucidate the molecular biological mechanisms behind the outcome of the interventions. With use of animal models, it is possible to perform interventions in a targeted and controlled fashion and study the effects of these interventions. The outcome of these experimental studies has the potential to be translated to human applications through a step-wise process.

In order to evaluate the mechanisms behind developmental programming, rodent, pig and sheep models have been extensively used. The sheep has many advantages as an experimental model. At birth, the size of the offspring and the relative weight of the fetus to the mother are comparable in sheep. The ovine pregnancy is of longer gestation as compared to rodent models and the organogenesis and maturation stages of the fetus have largely been characterised [314]. The relatively longer gestation of sheep

pregnancy allows researchers to target specific stages of organ growth and development for nutrient manipulation. Furthermore, the gestational stages in sheep are comparable to humans and the late gestational period (110 days to 148 days gestation) is similar to human third trimester of pregnancy and coincident with maximal fetal growth. The specific organ growth rate and fetal metabolic rate are very similar in sheep and humans and very different to rodents [297]. Importantly, the hypothalamic pituitary adrenal axis maturity is similar in sheep and humans through the late gestation and at the time of birth [298] which is not the case with rodent models. Experimental studies of maternal undernutrition during pregnancy performed in the sheep model have demonstrated effects on the fetus comparable to human IUGR with identifiable programming effects on insulin sensitivity [315] and cardiovascular system [316] in later life.

The ovine model also has some disadvantages. Unlike the rodent model, which has shorter gestation (21 days) and large litter size enabling a high turnover and generational studies, performance of such generational studies in sheep models would require extensive logistical and financial resources. Sheep have a cotyledonary placenta as compared to the discoid placenta in humans. Being a ruminant animal, the sheep uses volatile fatty acids (VFA) as main energy source as compared to glucose in humans. The VFAs (acetic acid, propionic acid and butyric acid) are metabolised differently in the liver. Propionic acid is the major source of hepatic gluconeogenesis, whilst acetic acid and butyric acid are utilised throughout the body as energy sources. Despite these differences, credible models of ovine obesity have been developed using programmes of manipulation in maternal diet, postnatal feeding and post-weaning activity [68, 267, 279]. The development of obesity observed in these models shows increased visceral adiposity which is believed to contribute to the development of a low grade chronic inflammatory state and obesity mediated metabolic comorbidities.

1.7.1.2 Omental adipose tissue characteristics

An excess of visceral adipose tissue deposition is known to be associated with central obesity, insulin resistance and type 2 diabetes [29, 30]. Ovine omental adipose tissue is a major proportion of the visceral adipose tissue depot and is known to rapidly expand soon after birth, a characteristic, which could increase its susceptibility to nutritional programming influences. Macrophage cells have been identified in ovine fetal omentum as early as 72 days of gestation whereas T cells have been identified at 140 days of gestation spots' [69]. Adipocyte hypertrophy in omental, but not subcutaneous depot, in obese women was independently associated with dyslipidemia [317]. The numbers of CLS in omentum correlate with the severity of hepatic fibroinflammatory lesions [318] and liver fat content [319] as well as insulin sensitivity [320]). Several chemotactic cytokines are expressed at higher levels in omentum [321]. Omental adipose tissue possess distinct characteristics that make it an important subject for investigations into developmental programming of adult disease.

1.7.1.3 Development of sheep omentum and liver

Like humans, the sheep omentum is derived from cells of mesodermal origin (dorsal mesogastrium) in the early fetal period. During this period, it consists of a gelatinous membrane with evolving blood vessels and no differentiated adipose tissue [322]. However, the cells of immune origin can be identified as early as 72 days of gestation and these rapidly evolve into aggregates known as 'milky spots' [69]. These cells have been identified as macrophages. Adipocytes and T cells start appearing at around 125 days of gestation. At birth, the omentum measures approximately 230 x 90mm [69] and, following birth, the weight of the omental adipose tissue depot rapidly expands to 3 g/kg body weight by the age of 7 days and 10 g/kg body weight by the age of 28 days [323].

The earliest identifiable embryonic hepatic structure originates as a ventral outgrowth from the gut endoderm around the seventeenth day of ovine gestation and is called the hepatic diverticulum [324]. Hepatocytes, the principal cell type in the liver, and biliary epithelial cells are derived from the embryonic endoderm, whilst stromal cells, stellate cells, Kupffer cells and blood vessels, are of mesodermal origin and are incorporated as the diverticulum expands into the surrounding mesoderm. With rapid proliferation and differentiation, hepatic lobes are evident by the twenty first day and hepatic lobules with identifiable structures and endothelial cells are present by the thirtieth day. During fetal development, the liver assumes haematopoietic function until the last 2 months of gestation. The increase in liver size during the pregnancy follows a linear pattern all through the gestation until birth [325].

1.7.1.4 Experimental approach

The sheep model of obesity and nutritional intervention in early life permits measurement of maternal and offspring physical and constitutional characteristics, measurement of physical activity, assay of plasma metabolites and hormones, post-mortem adipose tissue depot size through Dual-energy X-ray absorptiometry (DXA) scan and direct weighing respectively, and genetic and molecular analysis of hepatic and adipose tissue. Such a comprehensive approach permits scrutiny of the physiological response to experimental intervention throughout the experimental study. The role of each study in the establishment of the experimental model is summarised in Table 1.8.

Process under investigation	Physiological parameter
Establishment of model of maternal undernutrition during late gestation, offspring nutrition during suckling period and post weaning obesity	Maternal weight gain Mid intervention maternal paired plasma glucose, insulin, triglycerides and NEFA Offspring weight Relative weight gain during early infancy Physical activity measurement Offspring postweaning weight gain Absolute and relative organ weight
Offspring metabolic outcome of experimental intervention	Glucose tolerance test with timed glucose and insulin assay Plasma triglycerides, NEFA, cortisol and leptin assay
State of adipose tissue metabolism and distribution	Plasma leptin, triglyceride and NEFA measurement Dual-energy X-ray absorptiometry of adipose depots Adipose tissue depot weight
Adipose tissue inflammatory response	Plasma leptin assay Histological analysis for adipocyte hypertrophy, crown-like structure abundance, macrophage infiltration Immunohistological analysis for GRP78 (ER stress), IBA1 (macrophage markers) and phosphorylated JNK staining Gene expression studies
Hepatic structural and metabolic outcome of experimental intervention	Absolute and relative organ weight Hepatic triglyceride assay Hepatic thiobarbituric acid reactive substances assay for oxidative stress Histological analysis for features of steatosis and NAFLD
Hepatic inflammatory response	Histological analysis for features of NASH Gene expression analysis

Table 1.8 Overview of experimental approach for study of hepatic and adipose tissue cell stress and inflammatory response to obesity and nutritional programming.

NEFA, non esterified fatty acids; **NAFLD**, non alcoholic fatty liver disease; **NASH**, non alcoholic steatohepatitis; **GRP78**, 78kDA glucose regulated protein; **JNK**, c-Jun N-terminal kinase.

1.7.1.4.1 Gene expression

In selecting the genes of interest for exploration of the cell stress response and metabolic inflammation, transcriptionally regulated genes relevant to the pathway were identified and experiments were performed only when the primers and the experimental products confirmed to the strict quality control criterion described in Chapter 2. Given above constraints, the following gene expression experiments were performed to investigate the effect of obesity and nutritionally mediated developmental programming in sheep liver and omental adipose tissues (Table 1.9):

Process under investigation		Gene of interest
Modulators and effectors of metabolic inflammation		CD95 TLR4 Leptin receptor (liver) Leptin (adipose) Adiponectin (adipose)
Cell stress response	Autophagy: components and regulators	BECN1 ATG12 AMPK mTOR
	ER stress and UPR	GRP78 EDE1 ATF4 ATF6

Table 1.9 Genes involved in regulation of development of insulin resistance by activation of cell stress response and metabolic inflammation

CD95, cluster of differentiation 95; **TLR4**, toll-like receptor 4; **BECN1**, gene encoding Beclin1; **ATG12**, autophagy related gene 12; **AMPK**, 5' adenosine monophosphate activated protein kinase; **mTOR**, mammalian target of rapamycin; **ATF4**, activating transcription factor-4; **ATF6**, activating transcription factor-6; **EDEM1**- ER stress degradation enhancer molecule-1; **GRP78**, glucose-regulated protein 78.

1.8 Aims and hypothesis

Experimental evidence from current research has demonstrated that the hepatic and adipose cell stress response and metabolic inflammation are important mechanisms in pathogenesis of obesity associated insulin resistance and the MetSyn. Research involving a large animal model describing the state of omental adipose and hepatic cell stress response in obesity related insulin resistance is lacking.

Recent evidence also shows that the cell stress response and metabolic inflammation are susceptible to developmental programming. The potential roles of cell stress response and metabolic inflammation as mechanisms of developmental programming secondary to nutritional interventions in early life have also not previously been investigated. The studies described in the thesis aim to demonstrate the presence of activation of cell stress response in association with metabolic inflammation in important metabolic organs (liver and adipose tissue) and also to identify modulation of the cell stress response and metabolic inflammation in the presence of programming stimuli during critical periods of development.

This thesis will investigate the following hypotheses:

1. that the development of obesity in an ovine model will lead to activation of the cell stress response and metabolic inflammation in the liver and adipose tissue.
2. that early life nutritional interventions during late gestation and the suckling period of infancy will independently programme the adaptive capacity of hepatic and omental adipose tissue cells making them susceptible to the cell stress response and metabolic inflammation, predisposing the individual to insulin resistance.

2 Materials and methods

2.1 Experimental study design

The Early Nutrition Programming Project (EARNEST, FP62007, #FOOD-CT-2005-007036) is a large multidisciplinary investigation into long-term consequences of early nutrition on the metabolic health of an individual [326]. The experiments described in this thesis were performed on sheep as a component of the overall EARNEST programme. The animal experiments were done at the joint animal breeding unit, Sutton Bonington campus of the University of Nottingham (Nottingham, UK), by Dr S. Sebert under supervision of Professor M.E. Symonds and Dr D Gardner. All experiments were performed in accordance with the UK Home Office and the UK Animals (Scientific Procedures) Act (1986) and under licence and ethical approval from the University of Nottingham (Nottingham, UK).

The nutritional intervention in sheep was performed across two generations: pregnant ewes and the offspring and the outcome variables were studied in the latter. The experimental treatments were undertaken in three stages:

Fetal growth	Nutritional intervention in twin bearing pregnant ewes during late gestation (110 days until the birth of twin offspring at term)
Early growth	Early growth modulation of the offspring during the suckling period (birth to 90 days)
Obesity	Post weaning environment of rearing of the offspring (age 90 days until 17 months).

2.1.1 Nutritional intervention in twin bearing pregnant ewes during late gestation

Following ultrasound confirmation of twin bearing gestation at 75 days of gestation (dGA), 39 Bluefaced Leicester cross Swaledale ewes of similar body weights and age were selected for this study. The energy requirements of the pregnant ewes was calculated as per the guidelines of Agricultural and Food Research Council (AFRC) published in the manual of energy and protein requirements in ruminants [2] which takes into account the body weight, gestational age and the expected energy utilisation for basal metabolism and fetal growth. All ewes were fed 40% concentrated pellets and 60% straw nuts (Manor Farm Feeds, Oakham, UK) and had unrestricted access to a mineral block to ensure adequate micronutrient supply. The ewes were randomised to one of three treatment groups which determined the amount of calories offered to them in the late gestation (110dGA to term; normal ovine term gestation period is 145 ± 2 days) see Figure 2.1

The ewes in the nutrient restricted (N) group received 60% of their calculated metabolic requirements ($0.46 \text{ MJ/kg}^{0.75}$ body weight at 110 dGA and $0.72 \text{ MJ/kg}^{0.75}$ body weight at 140 dGA) for pregnant sheep during this period. The second group of ewes were given 100% of their metabolic requirements (R) and the third group were offered feed amounting to 50% more energy consumption than specified by the AFRC manual of the energy and protein requirements and hence consumed 150% of their metabolic requirements ($1.15 \text{ MJ/kg}^{0.75}$ body weight at 110 dGA and $1.80 \text{ MJ/kg}^{0.75}$ body weight at 140 dGA) which was the amount determined from previous experiments [266] with the same model of sheep allowed to feed to their appetite (A).

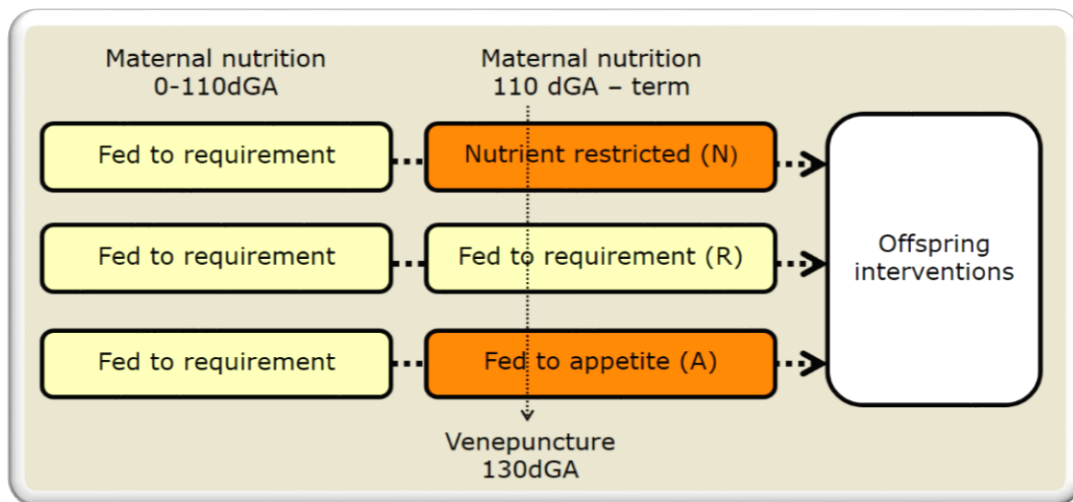


Figure 2.1 Flowchart depicting prenatal nutritional intervention in the studies.

Twin bearing pregnant ewes were fed a diet according to their metabolic requirements until 110 days of gestation following which they were randomly assigned to one of three diets until term (145 days). Nutrient restricted diet (N) meeting 60% of caloric requirements. Sheep fed to requirement (R) were offered 100% metabolic requirements and calorie consumption was measured for sheep fed to appetite (A) who consumed 150% of the metabolic requirements. Blood sample was taken to measure metabolic and physiological indices at 130 days of gestation. After birth the offspring were randomised to experimental conditions described in Section 2.1.3

The feed consumption was monitored by daily weighing the leftover feed and ewes were weighed weekly before feeding and dietary requirements adjusted accordingly. On 130dGA, blood samples were taken from the jugular vein after an overnight fast (≥ 18 h) and collected into 10 ml lithium heparin (LiH) and 10 ml ethylenediaminetetraacetic acid (EDTA) coated tubes. Plasma was separated by immediate centrifugation (10 min, 4000 g, 4°C) of the LiH tubes and all samples were stored in -80°C freezer.

2.1.2 Modulation of early growth of the offspring during the suckling period

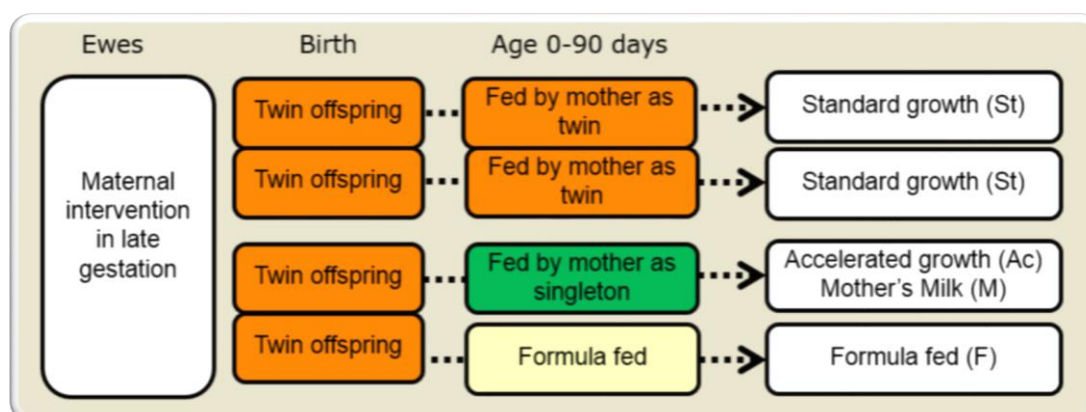


Figure 2.2: Schematic representation of experimental intervention during the suckling period.

Following nutritional interventions to diet of twin bearing pregnant ewes (described in Section 2.1.1), the twin offspring were either both fed by their mothers achieving a standard rate of growth for a twin (St) or separated with only one of the twins reared with the mother with no competition for feed achieving an accelerated rate of early growth (Ac- Accelerated growth/M – mother fed) whilst the other twin randomised to be fed with the standard formula feed (F).

At birth the twin offspring were weighed and randomised to one of three groups (Figure 2.2). The first group consisted of twin offspring, both fed by their mothers thereby achieving a standard (St) growth rate for a twin during the suckling period. The offspring from the remaining ewes were raised separate from each other and were further randomised to one of two groups. One offspring from the twin pair was raised by their mother as a singleton without any competition for the mother's feed from the twin, hence achieving a relatively accelerated (Ac – Accelerated growth; M- mother's milk) rate of early growth whilst the twin of this offspring was fed with the standard formula feed Lamlac™ (Volac international, Royston. UK) giving the phenotype of formula (F) feeding during the early growth period. The constituents of the formula includes whey protein, vegetable oil and is supplemented with Vitamin A (50,000iu/L), Vitamin D3(6,000 iu/L), Vitamin E (100 iu/L), DL-methionine and calcium carbonate. The details of the macronutrient composition of the formula milk are given in Table 2.1. The lambs were kept with their mothers for the first 48h to allow them to receive

colostrum and reduce their risk of death. Once separated from their mothers to a barn, hand feeding with a bottle was initiated 4 times a day until they were able to use the feeder (Volac ewe 2™, Volac international, Royston, UK). The offspring of nutrient restricted and fed to requirement ewes were kept in separate barns. The shared Volac feeding system contained milk calculated for shared maximum intake of 1L/day/lamb. All offspring were weighed twice every week during the first month after birth and then weekly until the end of lactation at 3 months of age.

	Ewe milk*	Formula milk#
Protein (%)	~5	4.8
Fat (%)	~6	4.8
Carbohydrate (%)	~4.8	4.1
Energetic value (MJ/kg)	4.5	4.1

Table 2.1 Macronutrient content of ewe and formula milk.

*****, values as quoted by Park et. al and Dove et. al [327 , 328] ; **#**, as quoted by company analysis (Volac International Ltd, Royston, UK). The formula milk is comprised of whey protein powder (as protein source), vegetable oil (as fat source), wheat gluten and lactose (as carbohydrate source) with added vitamins and minerals.

2.1.3 Post weaning environment of rearing until early adulthood (age 90 days until 17 months)

At 90 days of age, the offspring raised by their mother as twins were randomised to one of the two customised environments of rearing with an aim to alter the amount of physical activity and consequent development of the obesity phenotype. One group of offspring were allocated to an obesogenic (O) environment in a restricted barn with a stocking rate of 6 sheep per 19m². The other group offspring were raised in a field with a stocking rate of 6 sheep per 1125 m² allowing unrestrained physical activity leading to development of a relatively lean (L) phenotype (Figure 2.3). The animals raised in the field for L phenotype were fed by foraging on grass and were given micronutrient supplementation. The animals in the restricted environment were given feed based on a mix of low (3kg/d straw nuts; 8.5 MJ/kg) and high (800 g/d of concentrate pellets; 12.5 MJ/kg) energy dense food. At age 15 months, their physical activity measurements were

performed using a uniaxial accelerometer. Animals were weighed once a month and blood samples taken at 7 and 16 months of age.

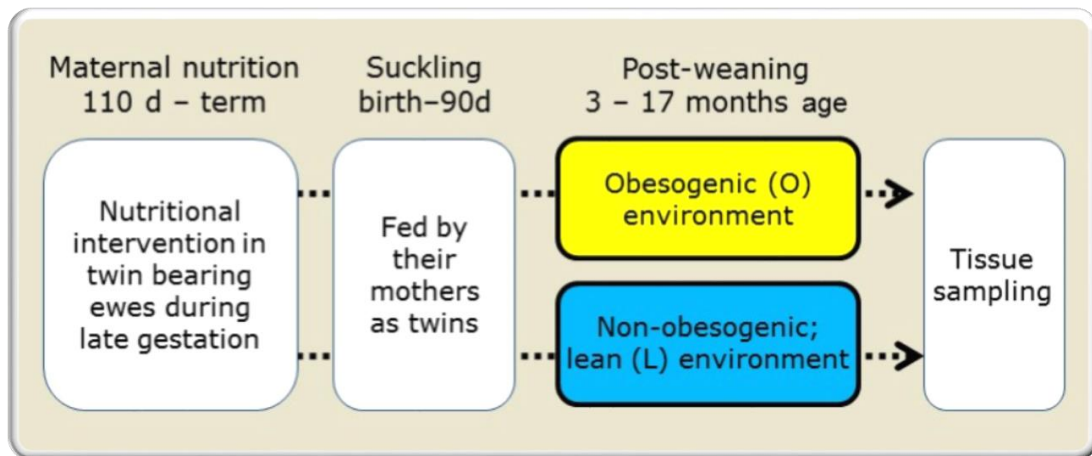


Figure 2.3: Schematic representation of post weaning environment of rearing until 17 months of age.

Following weaning at 90 days of age, the offspring were randomised to one of two experimental groups. Randomisation to a barn with a stocking rate of 6 sheep per 19m² restricted physical activity leading to an obesogenic environment (O) or randomisation to a field with a stocking rate of 6 sheep per 1125 m² allowing unrestrained physical activity leading to development of a relatively lean (L) phenotype.

2.1.4 Overview of the factorial experimental designs

The randomisation of the animals was performed into groups in such a way so as to maintain equity of gender distribution. The experimental animals were exposed to a combination of two of the three experimental treatments described above in order to study the interaction and the relative contribution of interventions in these developmental periods (2X2 factorial design experiment). Notably, out of 77 offspring, 6 offspring died of natural causes. Further details of the specific age and cause of death is not available. The animal deaths were not concentrated to a specific experimental group and is less than overall 10% animal death rate in previous studies [329, 330]. An overview of the factorial design is given in Table 2.2 with a flow chart depiction in Figure 2.4

Maternal nutrition	Early growth	Post weaning environment	Factorial study design
Nutrient restriction/ Fed to appetite		Obesogenic/ Lean	Prenatal nutrient restriction and the post weaning environment of rearing. Control group: fed to appetite and rearing in lean environment (Study 1, Chapter 3)
Nutrient restriction/ Fed to requirement	Suckling as singleton/ Being formula fed		Prenatal nutrient restriction and the effect of formula feeding during early growth. Control group: Fed to requirement and feeding on mother's milk. (Study 3, Chapter 4)
Nutrient restriction	Suckling as twin/ Suckling as singleton		Rate of early growth during suckling following late gestation nutrient restriction. Control group: Suckling as twin. (Study 2, Chapter 5)

Table 2.2: Table demonstrating interaction of prenatal and postnatal experimental conditions used in the factorial design of the experiments

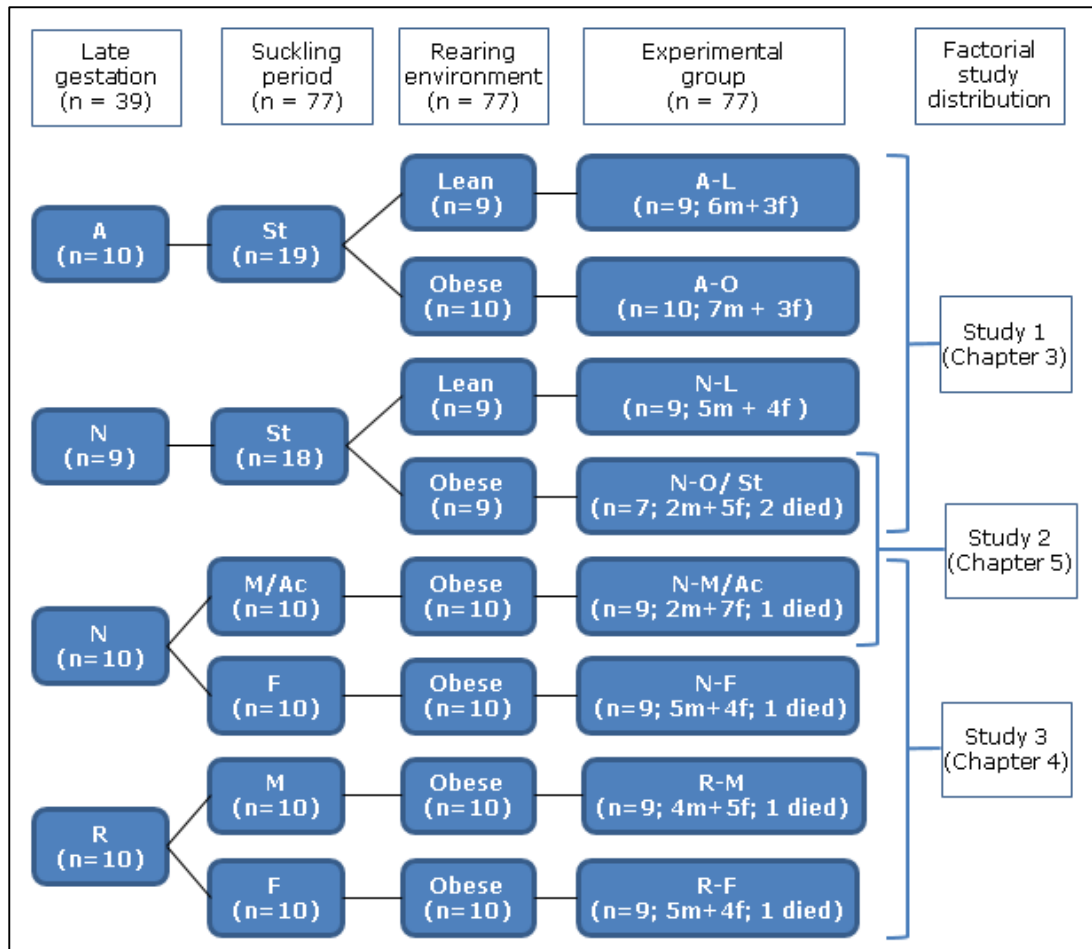


Figure 2.4 Schematic representation of the sequential experimental intervention evolving into the three different experimental studies.

Study 1; During the late gestation (110dGA to term) twin bearing ewes were fed to appetite (A) and following the suckling period (age 90 days) twin offspring were separated to either rearing in an environment restricting physical activity leading to obesity (A-O) or allowing physical activity where they remained lean (A-L). Twin bearing ewes were nutrient restricted to 60% of their caloric requirements during late gestation (N) and after weaning at 90 days age one of the twin offspring twin was reared in an environment restricting physical activity leading to obesity (N-O) or allowing physical activity where they remained lean (N-L). During the suckling period, the offspring were reared together with their mother in all groups.

Study 2; Twin offspring of ewes restricted to 60% nutrient restriction (N) during late gestation were either separated and only one offspring fed to mother's milk without competition achieving an accelerated rate of growth (Ac) or were both fed by the ewes achieving a standard rate of growth for a twin (St). All offspring were raised in obesogenic environment of restricted activity.

Study 3; During the late gestation (110dGA to term) twin bearing ewes were fed a diet meeting 100% caloric requirements (R) and during the suckling period (birth to 90 days) one twin was formula fed (R-F) while the other was fed by the mother (R-M). Twin bearing ewes were nutrient restricted to 60% of their caloric requirements (N) and during the suckling period one twin was formula fed (N-F) while the other was fed by the mother (N-M). Following weaning, all offspring were reared in restricted obesogenic environment.

2.2 Blood sampling

Blood sampling was performed in the pregnant ewes at 130 dGA and in the offspring at age of 7 and 16 months. A jugular intravenous catheter was surgically implanted under local analgesia and glucose tolerance test (GTT) was performed 24 hours after this. The blood samples were transferred to labelled EDTA and LiH tubes. Both heparin and EDTA samples were rapidly centrifuged at 2500g for 10 minutes at 4°C to obtain plasma samples that were then stored at -80°C until analysis. Two days after the glucose tolerance test, another 5ml blood sample was taken and transferred to LiH tubes for determination of plasma leptin and cortisol. The blood sampling and GTT was performed by Dr Sylvain Sebert. The results presented in this thesis were derived from analysis of raw data by the author.

2.3 Tests for glucose tolerance and insulin resistance

The term insulin resistance describes a state of decreased uptake of glucose by skeletal muscles and adipose tissues and also decreased inhibition of hepatic glucose production despite the presence of circulating insulin in the blood at physiological levels. A variety of experimental methods are employed to assess the insulin resistance and glucose tolerance levels in animal and human experiments.

The hyperinsulinaemic euglycaemic glucose clamp test involves continuous infusion of a high dose of insulin (hyperinsulinemia) with an aim to achieve a steady state insulin level by suppressing the body's endogenous insulin response. This is followed by infusion of a variable rate of glucose in order to estimate the amount needed to maintain (clamp) the blood glucose within the normal range (euglycaemia). A direct estimation of glucose disposal ability of the body performed by this method is labour intensive, time consuming and expensive [331] and the analysis performed at a

hyperinsulinaemic state is also not considered to accurately reflect the glucose and insulin dynamics in the physiological state [331].

The second option is performing a glucose tolerance test by administering a glucose load through oral, intravenous or intraperitoneal routes and taking blood samples for plasma glucose and insulin at regular intervals. This test analyses an individual's ability to initiate an insulin production response to a glucose load and the insulin resistant state of the tissues by measuring the rate of decline of the plasma glucose in response to this insulin surge [332, 333]. As a marker of insulin sensitivity, GTT has been demonstrated to correlate well with the hyperinsulinaemic euglycaemic glucose clamp [331, 333].

A commonly used surrogate marker of insulin resistance is the calculation of the homeostatic model of insulin resistance (HOMA-IR) by using the values of fasting plasma glucose and insulin levels[334]:

$$\text{HOMA-IR} = \text{glucose} \left(\frac{\text{mmol}}{\text{L}} \right) \times \text{insulin} \left(\frac{\mu\text{g}}{\text{L}} \right)$$

Equation 2.1: Equation for calculation of homeostatic model of insulin resistance (HOMA-IR)

In human experiments, the outcome of HOMA-IR is normalised with a denominator of 22.5 which represented the expected normal insulin level for a normal fasting plasma glucose thus giving a value of 1 for an individual with normal insulin sensitivity. Both HOMA-IR [334] and GTT [331, 333] have been demonstrated to have a good correlation with the hyperinsulinaemic euglycaemic glucose clamp making the latter labour intensive, time consuming and expensive method superfluous [331] if the desired outcome is determination of relative insulin resistance.

2.3.1 Glucose tolerance test procedure and analysis

This was performed in the offspring at the age of 7 and 16 months, 24 hours after surgical implantation of a jugular intravenous catheter. After overnight fast (≥ 18 hours), a baseline blood sample was taken and transferred to EDTA and LiH tubes. Following this a 0.5g/kg intravenous glucose bolus was administered to the sheep via the catheter and 5ml blood samples were each collected at 10, 20, 30, 60, 90, 120 minutes after the glucose bolus and transferred to labelled LiH and EDTA tubes, centrifuged and stored as described in Section 2.2.

2.4 Plasma analyses

2.4.1 Plasma glucose analysis

Randox RX Imola auto-analyser (Randox laboratories, Crumlin, UK) and reagents were used to perform the plasma glucose quantification. 2 μ l of plasma was mixed with 200 μ l of reagent containing glucose oxidase, 4-aminophenazone, phenol and peroxidase and incubated at room temperature for 25 minutes. The optical density of the coloured complex was measured on a plate reader at 500 nm. Results were compared to a single standard of 5.49 mmol/L in a linear relationship. All the samples and standards were run in duplicate and the samples with a coefficient of variation $<5\%$ between experimental replicates were included. The analysis was performed by Dr Dellschaft and Dr Bloor at the School of Veterinary Medicine and Science, Sutton Bonington Campus, University of Nottingham. The results presented in this thesis were derived from analysis of raw data by the author.

2.4.2 Insulin assay

2.4.2.1 Enzyme Linked Immuno-Sorbent Assay (ELISA)

ELISA is an immunoassay used to determine the quantity of a specific target protein in a plasma sample. A well plate is coated with antibody that specifically binds to the protein of interest. On addition of plasma to the well

plate, this capture antibody binds to the protein and retains the protein when the rest of plasma is washed off using a wash buffer. Non-specific binding to the well plate surface is prevented by its prior coating with another blocking protein which does not bind to the antibody. A second detection antibody, conjugated with biotin and specific to a different sequence present on the same antigen of interest (protein) is added to the well to form an antigen antibody complex with the protein of interest (see Figure 2.5). The biotin bound to the second antibody can form a strong bond with streptavidin-horseradish peroxidase complex. Following subsequent washing off with buffered saline solution, the amount of horseradish peroxidase remaining in the well is proportional to the antigen-antibody complex. The quantity of such residual horseradish peroxidase can be calculated by colorimetric assessment of the blue product when tetramethylbenzidine (TMB) is added to the wells which react with horseradish peroxidase. After a fixed incubation period, the reaction is stopped by addition of sulphuric acid and quantification performed by colorimetry.

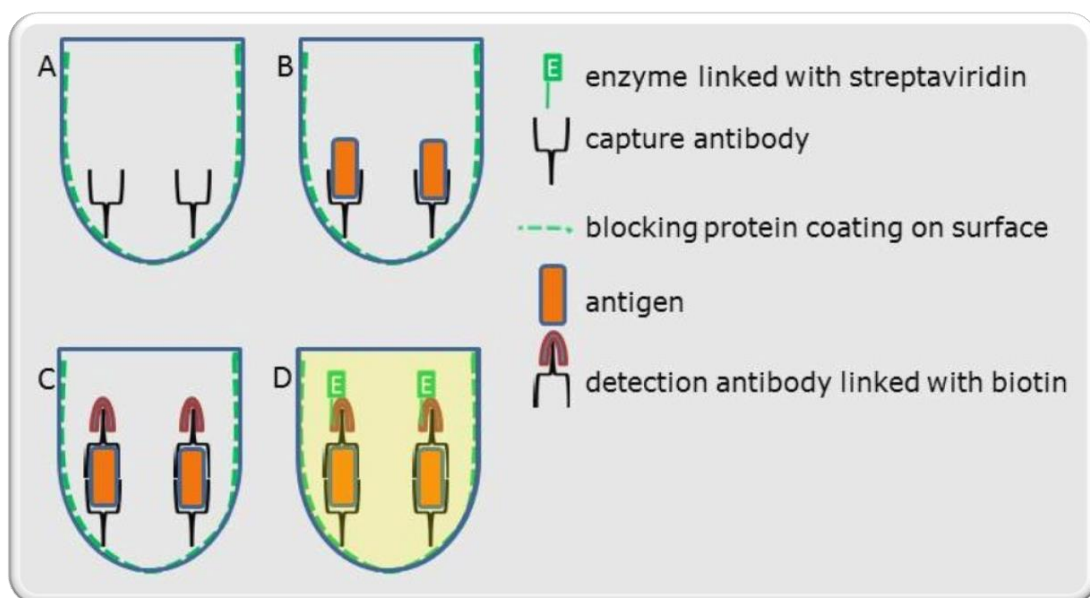


Figure 2.5 Schematic diagram demonstrating the steps in sandwich enzyme linked immunosorbent assay (ELISA)

The Sheep Insulin ELISA kit (Mercodia, Uppsala, Sweden) contains 96-well plates in the kit which are coated with antibodies raised against sheep insulin

(capture antibodies). The reported detection range for the kit is between 0.05 -3 ng/ml as specified in the product information sheet. To each well of the ELISA kit, 25 µl of plasma sample was added followed by addition of 50µl reagent containing detection antibody along with streptavidin-conjugated enzyme and incubated on orbital shaker for 2 hours. The plate was washed thoroughly using buffered saline and this was repeated 6 times following which the excess fluid was removed from the well plate by gently tapping it on absorbent paper. 200ul of TMB solution was added to each well and the reaction was stopped after 15 minute incubation with the addition of 50µl sulphuric acid (0.5mol/L). The optical density was measured on a µQuant plate reader (Bio-tek Instruments Inc., Potton, UK) at 450nm wavelength. The results were corrected in comparison to a blank (all reagents with distilled water as sample) and all samples were performed in duplicate and compared to standard dilution of the standard provided in the kit (0.1 – 2.5 µg/L).

2.4.3 Plasma lipid analysis

The metabolic profile of all the animals was developed by quantifying the levels of plasma triglycerides and non-esterified fatty acids (NEFA).

2.4.3.1 Plasma triglyceride and NEFA quantification procedure

The plasma triglyceride and NEFA quantification procedures were performed on a Randox RX Imola auto-analyser (Randox Laboratories, County Antrim, UK) and using reagents provided by Randox. The plasma samples were thawed gently on ice and loaded into the auto analyser. The auto analyser completed a calibration before measuring each metabolite and all samples were analysed in duplicate. For samples with coefficient of variation higher than 5% between the duplicates, the analyses were repeated. The plasma triglyceride and NEFA quantification was performed by Dr Ian Bloor and Dr

Neele Dellschaft. The results presented in this thesis were derived from analysis of raw data by the author.

2.4.4 Cortisol Assay

2.4.4.1 Competition radioimmunoassay procedure

The reagents which include antibody coated tubes, ^{125}I labelled cortisol solution, standard solution containing 0, 1, 5, 10, 20, 50 nM concentration of cortisol were part of the Coat-A-Count Cortisol In-vitro Diagnostic Test Kit (Diagnostics products corporation, Siemens, Camberley, UK). The reported minimal level of detection of this kit is 5.5 nmol/L (information from product manual). 25 μl of plasma or standards and 1ml of the kit solution containing ^{125}I labelled cortisol were mixed in each coated tube and incubated on a shaker at 37°C for 45 minutes. One extra tube without an antibody coating was also simultaneously treated with the kit solution to determine the background binding of the antibody to the plastic of the tube. All the fluid was then aspirated without disturbing the coated inner surface of the tubes. The radioactive decay in tubes was measured for one minute in a gamma 64 counter (Wizard 1470 automatic gamma counter, Perkin Elmer, Waltham, MA, USA). After correcting for the readings from the background binding tube, the counts per minute were plotted on the standard curve extrapolated from the log-linear graph derived from the standard dilution to determine to cortisol concentration in plasma. The measurement of the standard dilutions was carried out in duplicates and coefficient of variation of <10% was considered acceptable.

2.4.5 Plasma leptin

Plasma leptin concentration quantification was performed by the laboratory of Professor Keisler at the Department of Animal Science of the University of Missouri using the radioimmunoassay method developed by Delavaud [335].

The principle behind this radioimmunoassay procedure is same as the one described in Section 2.4.4. The presence of plasma leptin and ^{125}I isotope labelled leptin in the same solution leads to their competition for binding to

the leptin antibody in a ratio relative to their respective concentration. The heavier antigen antibody complex can be precipitated using polyethylene glycol and after removal of the unbound radiolabelled leptin, the radioactivity in the precipitated complexes in the tube can be measured using the gamma counter. The reported minimum level of detection limit for this assay is 0.3 ng/ml.

100µl of plasma or 50µl of standards (at concentrations of 1.7, 2.5, 5, 8, 15, 40, 50, 80 ng/ml, in triplicates) were mixed with 50 µl primary rabbit anti-ovine leptin antibody (1:1500, raised to establish this assay). The solution was brought to 400 µl with incubation buffer and incubated at 4°C for 24 hours. ¹²⁵I labelled leptin (100µl at 20,000 cpm) was added to this mixture and further incubated for 20 hours at 4°C followed by addition of 100µl ram anti-rabbit secondary antibody and further incubated for 1h. Addition of 2 ml 4.4% polyethylene glycol 6000 (BDH Prolabo, VWR, Radnor, PA, USA) caused precipitation of the antigen-antibody complexes following which the unbound leptin in the solution was removed by aspiration. The radioactivity in the precipitate on the tube was measured using a Cobra II gamma counter (Packard Inc, Downers Grove, Australia) and concentration of leptin calculated by extrapolation from the log-linear graph made from the standard dilution.

2.5 Physical activity measurement

In order to study the impact of the environment of rearing and also of the programming influence of the experimental interventions, an accelerometer was used to measure the spontaneous physical activity of the animals to reflect both the occurrence and intensity of movements [336] and used as a proxy for energy expenditure by bodily movements as previously described [337].

2.5.1.1 Uniaxial accelerometer

Actiwatch (Actiwatch, Linton instrumentation, Diss, UK; now Camntech Ltd., Cambridge, UK) is a piezo-electric accelerometer which records intensity, amount and duration of movement in all directions. The actiwatch accelerometer was attached around the neck of each sheep using a collar and care was taken to avoid causing pain or distress that could otherwise affect their movement. The sheep were returned to their allocated experimental environment to resume their daily routine. The measurements were made in the offspring at age 45 days and again at age 15 months over a continuous period of minimum 48 hours. In order to rule out any potential impact of handling on the physical activity, data from a 24 hour period from the day 2 of the experiment was used (see Figure 2.6).

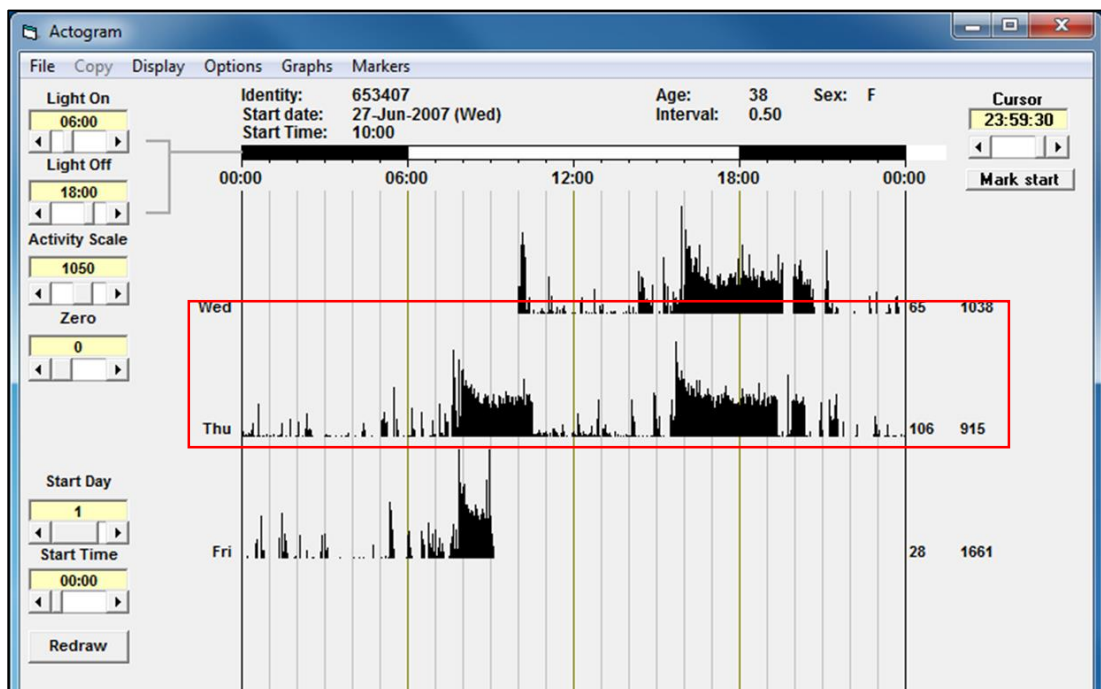


Figure 2.6: An actogram demonstrating graphical representation of the physical activity data over a period of 48 hours. The data from day 2 of the recording (indicated by the red box in the figure) were analysed to rule out any potential impact of handling on the physical activity recordings.

2.5.1.2 Physical activity data analysis

The data analysis was performed by me in collaboration with Dr. Charlotte Burton, a BMed Sci student who worked under my direct supervision. The actiwatch data was downloaded and analysed using the activity and sleep analysis 7 software (CamNtech Ltd, version 7.43). The intensity of activity was measured in a unit called counts and at a sampling frequency of 32 Hz, the actiwatch measured any movement greater than 0.5g and the maximum value was recorded as the count for that second. An epoch is a period defined by the user for purpose of logging the activity data. Three individual counts from every second during that epoch were totalled and gave a value for the activity score. An epoch length of one minute was chosen and data generated for a continuous 24 hour period. The data of physical activity for every minute over the 24 hour period was thus used to calculate three main variables to describe the physical activity phenotype:

- mean activity over 24 hour period
- peak activity over 24 hour period
- duration of mobility over 24 hour period

2.6 Postnatal growth and adipose depots analysis

Body weight measurements were taken using standard weighing scales every 3 days during the first month including birth weight and then every seven days up until 90 days of age and monthly thereafter until the completion of the study.

Dual X-ray absorptiometry (DXA) scan was performed at 16 months of age in sedated sheep (intravenous ketamine and xylazine) and scanned for 15 minutes using Lunar DPX-L bone densitometer (Lunar, Florida, USA). DXA analysis provided the measurements of overall bone densitometry, fat mass and fat free mass in the body. Whole carcass chemical analysis in 14 representative animals was also performed following tissue sampling to validate the DXA findings. Following DXA scanning, half carcasses were

macerated and dried. Nitrogen content and fat percentage analysis was performed on 250g of homogenised tissue from the carcass using a FlashEA1112® nitrogen analyser (Thermo Scientific, Massachusetts, USA) and Gerhardt Soxtherm 406 fat analyser (Wolflabs, York, UK). These experiments and measurements were carried out by Dr Sylvain Sebert. The results presented in this thesis were derived from analysis of raw data by the author.

2.7 Euthanasia and tissue sampling

At 17 months of age, all offspring were fasted overnight and humanely euthanased in the morning by electrical stunning and exsanguination. All major tissues, glands, adipose depots and organs were immediately dissected from the animal, weighed and 'snap' frozen in liquid nitrogen before storage at -80°C. In addition, a sample of the omental adipose tissue was fixed in 10% formalin for histological analysis.

2.8 Tissue analysis

All chemicals, reagents and laboratory procedures were assessed and implemented in compliance with the UK Health and Safety Executive's Control of Substances Hazardous to Health (COSHH, SI No. 1657, 1988) and Risk Assessment guidelines. Unless otherwise specified, all laboratory-based techniques and protocols were conducted within the Department of Academic Child Health, School of Clinical Sciences, Division of Human Development, University of Nottingham and the School of Veterinary Medicine and Science, Sutton Bonington Campus, University of Nottingham.

All samples were kept stored in -80°C freezers to preserve sample integrity and kept on dry ice whenever in transit for sampling or processing. The tissues from all experimental groups were kept in separate doubly labelled bags. The chopped pieces of tissues were allocated random numbers and the experimenter was blinded to the experimental groups whilst performing the

tissue processing to avoid any bias during analysis. In order to eliminate chances of contamination, all the experimental work was performed using autoclaved or sterile equipment, including filter pipette tips, whilst wearing gloves. The work benches and equipment were cleaned with ribonuclease (RNase) Zap® (Ambion, California, USA) and 70% denatured ethanol (Ecolabs, Surrey, UK). Sterile nuclease free water (Ambion, Inc UK) was used for all the gene expression quantification experiments.

2.8.1 Triglyceride analysis

This procedure was performed in two main stages, lipid extraction and then triglyceride analysis. Folch's method of lipid extraction [338] is a commonly used procedure to separate the lipid content of a tissue from the non-lipid cellular component. As the tissues are homogenised in presence of a chloroform-methanol solvent, the lipid component dissolves into the chloroform and can then be separated from the cellular debris by process of filtration. Addition of 0.9% saline to this solvent to give a ratio of 8:4:3 of chloroform: methanol: saline leads to separation of the liquid into 2 phases with the lipids at the bottom phase and non-lipid organic (hydrophilic) molecules in the upper phase. After siphoning off the upper phase, the lipids in the lower phase can be precipitated by evaporating the solvents under air stream.

Triglyceride form 98% of the lipid contents. The Randox triglyceride analysis kit uses colourimetric reaction with a principle similar to the plasma triglyceride analysis described in Section 2.4.3. The enzymatic reactions first use lipases to break down triglycerides to glycerol and fatty acids. The glycerol is then converted to glycerol-3 phosphate using the enzyme glycerol kinase in presence of ATP. Upon oxidation of the glycerol-3-phosphate, hydrogen peroxide is formed which can be used to create quinoneimine, a coloured chromogen.

2.8.1.1 Triglyceride extraction and analysis procedure.

150mg of liver from each animal was kept on ice in a 2ml of 2:1 Chloroform: methanol mixture and quickly homogenised using Dispomix homogeniser (Medic Tools, Zurich, Switzerland) for 40 seconds. This was then centrifuged at 550g for one minute at room temperature followed by gentle agitation for 20 minutes using an orbital shaker at room temperature to ensure adequate exposure of homogenised tissue to the chloroform in the solvent. The cellular debris was removed by passing the homogenate through 24 cm filter paper (Whatman Ltd., Banbury, UK) under gravity and filtrate collected into a 15ml tube. The tubes and the filter paper were washed with 8 ml chloroform to dissolve any remaining lipids. This was followed by centrifugation of the filtrate at 800 g for 10 minutes after adding 2ml 0.9% saline for separation of the lipids into the bottom phase. After removal of the upper aqueous phase by pipetting, 2ml of the bottom lipid phase was transferred to 2ml eppendorf tubes and the liquid evaporated using nitrogen stream from Driblock DB-3 (Techne). The evaporated samples were re-dissolved in 100µl of (60:40 v/v) tert-butanol -Triton X-100 (BDH).

The triglyceride analysis was performed using Randox triglyceride assay kit using a method adapted from the manufacturer's instructions. The analysis was performed in duplicate and results with more than 5% coefficient of variance repeated. In a 96 well plate (Grenier Bio-one, Gloucestershire, UK), 200µl of the enzyme reagent was added to 2µl of sample, standard or negative control and incubated at room temperature for 5 minutes for colour development. The spectrophotometry analysis was performed on µQuant plate reader at 500nm. The results were expressed as triglyceride in micrograms per milligram of the liver tissue.

2.8.2 Thiobarbituric acid reactive substances (TBARS)

Oxidative stress in tissues is difficult to measure directly especially because reactive oxygen species (ROS) have very short half-life [339]. The free radicals (superoxide O_2^- or hydroxylperoxyl HO_2^{\cdot}) combine with a hydrogen atom from the fatty acid chain to make water and a fatty acid radical. These fatty acid radicals react with oxygen and form peroxide radical. The peroxide radical creates more fatty acid radicals and forms lipid peroxide in the process (Figure 2.7) Some of these fatty acids are sourced from cell membranes and hence damage the membrane integrity.

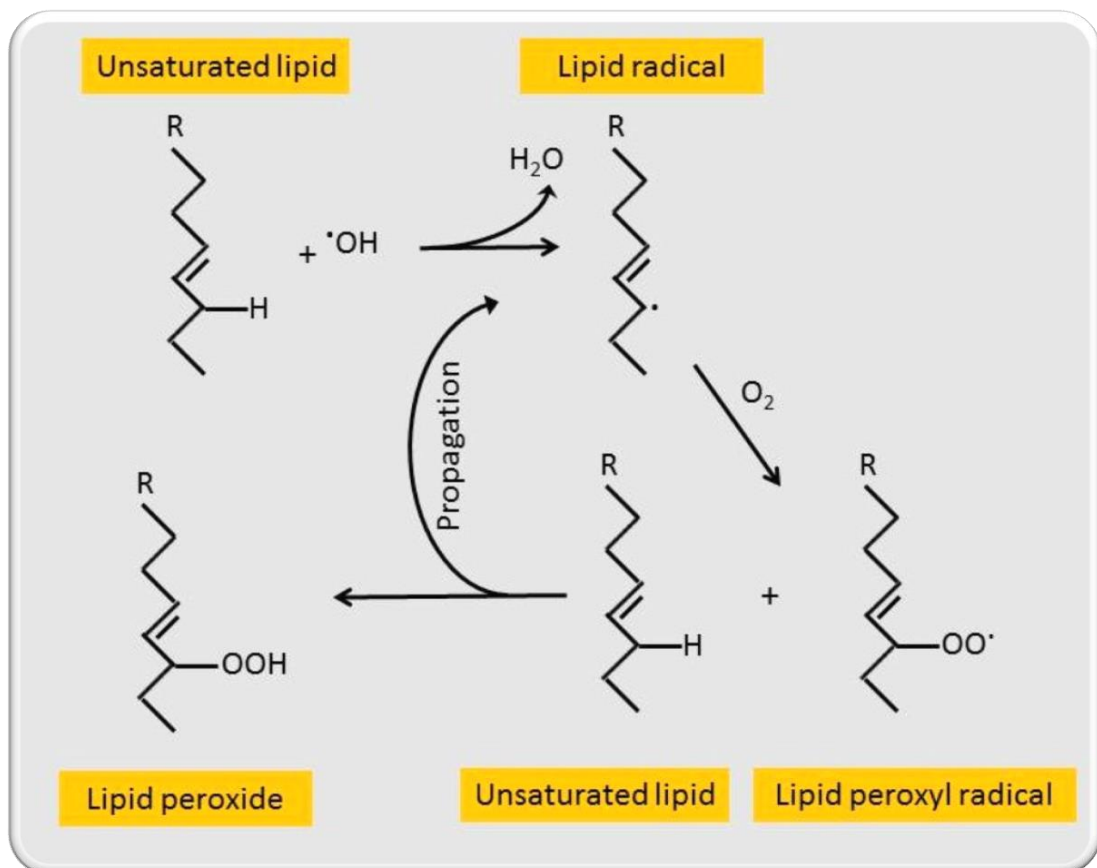


Figure 2.7: Mechanism of lipid peroxidation

Free radicals combine with a hydrogen atom from the fatty acid chain to make water and a lipid radical. These lipid radicals react with oxygen and form peroxide radical. The peroxide radical reacts with another hydrogen atom form a fatty acid and in the process creates more fatty acid radicals and forms lipid peroxide.

TBARS such as malondialdehyde (MDA) are formed as a stable byproduct of this lipid peroxidation which also cause DNA damage. The TBARS react with thiobarbituric acid to give a fluorescent red derivative that can be assayed spectrophotometrically [340]. The method is commonly used as an analysis for lipid peroxidation [341] and has been used as a marker for liver oxidative stress [342] in models of non alcoholic fatty liver disease (NAFLD) [343]. The assay principle is based on an adduct formation after the reaction between MDA and thiobarbituric acid (TBA). The MDA-TBA adduct formed from the reaction of MDA in samples with TBA can be measured colorimetrically [344].

2.8.2.1 TBARS procedure

This was performed using OxiSelect™ TBARS assay kit [344] (Cell Biolabs, California, USA), which included the MDA standards used to prepare dilutions ranging from 0-195 mg/dl . Liver tissue weighing approximately 100mg was sampled from the frozen tissue and care was taken to prevent thawing by keeping on dry ice and transferring to ice before homogenisation in 1ml of 1X butylated hydrotoluene (BHT) kit reagent and phosphate buffered saline (PBS). The samples were centrifuged for 1 minute at 2000g and the supernatant transferred to 1.5ml labelled eppendorf tubes. To ensure complete removal of cell debris, this was followed by repeat centrifugation at 10000g for 5 minutes at 4°C. The supernatant was stored at -20°C until further use for protein quantification or TBARS assay.

For TBARS quantification, 100µl of the supernatant, MDA standards or negative control (distilled water) was added to a fresh 1.5ml eppendorf tube and 100µl of sodium dodecyl sulphate (SDS) lysis solution was added to each tube and incubated at room temperature for 5 minutes. This was followed by addition of 250µl of TBA and the tubes were incubated in a water bath at 95°C for 60 minutes, after which samples were removed and cooled on ice for a further 5 minutes. The tubes were centrifuged at 1200g for 15

minutes and 300µl of supernatant transferred to a fresh eppendorf tube. 300µl of n-butanol was next added to the samples and vortexed for 2 minutes and centrifuged for 5 minutes at 10000g at room temperature to allow for phase separation. The top layer containing n-butanol was pipetted to another eppendorf tube. In a 96 well plate, 200µl of samples and standards were pipetted and spectrophotometric analysis done at wavelength 532nm using µQuant plate reader. The sample concentrations were calculated from the standard curve prepared from MDA standards provided in the kit and normalised against total protein concentration calculated using bicinchonic acid (BCA) method and expressed as TBARS µM /total protein concentration (µg/µl).

2.8.2.2 Bicinchonic acid (BCA) total protein determination

The BCA assay for determination of total protein concentration in a solution [345] involves reaction between proteins, BCA and copper sulphate. In a temperature dependent reaction, the peptide bonds in a protein reduce Cupric (Cu^{2+}) to Cuprous (Cu^+) ions. The amount of Cu^+ ion is proportional to the amount of protein present in the solution which can be quantified by the colour of the product of reaction between BCA and Cu^+ .

2.8.2.3 BCA assay procedure

In distilled water, a w/v solution of 1% bicinchonic acid, 2% sodium carbonate, 0.16% sodium tartrate and 0.4% sodium hydroxide was prepared. The pH was brought to 11.25 with 10% sodium bicarbonate and this was labelled as reagent A. Reagent B consisting of 4% (w/v) copper sulphate solution in distilled water was freshly prepared. Reagent C was prepared by mixing reagents A and B in a ration 50:1 and stored at 4°C until needed.

The reference standards were prepared by making serial dilutions of bovine serum albumin (BSA) in 0.9% saline ranging from 0 to 1.0mg/ml. Aliquots of

the supernatant stored at -20°C during TBARS quantification (Section 2.8.2.2) containing protein was diluted 1:20 in 0.9% saline. In a 96 well plate, 200µl of reagent C was pipetted and to this 10µl of each sample, standards and negative control were added in duplicate. This was incubated on an orbital shaker at 37°C for 30 minutes for colour development and spectrophotometric absorbance was measured at 562nm. Samples were repeated if the coefficient of variance was more than 5%.

2.9 Gene expression analysis

2.9.1 Ribonucleic acid (RNA) extraction

Prior to RNA extraction from biological tissues, steps of tissue lysis and homogenisation were performed in a guanidine-isothiocyanate containing buffer, which ensures intact RNA through immediate inactivation of RNases and also dissolves all proteins in the homogenised tissue. This method is adapted from the published and widely used single step acidified phenol-chloroform homogenisation method [346, 347]. Addition of chloroform to the homogenised tissue in the buffer followed by centrifugation leads to formation of three phase layers. The RNA is dissolved in the top aqueous phase followed by the DNA interphase. The bottom organic phase holds the dissolved proteins. Purified RNA can be extracted from the top aqueous phase after ensuring elimination of genomic DNA (gDNA) by passing the top aqueous phase through a gDNA eliminator spin column.

2.9.1.1 RNA extraction procedure

Tissue samples (weighing between 100 – 150 mg for liver tissue and 450-525 mg for adipose tissue) were added to labelled containers containing 1 ml TRI[®] reagent (Sigma Chemical Co. Poole, UK). The samples were homogenised using a Dispomix homogeniser (Medic Tools, Zurich, Switzerland) at 300rpm for 40 seconds and then centrifuged at 550g for 1 minute to ensure the homogenate settled to the bottom of the tubes.

An additional lipid removal step was incorporated for adipose tissue at this stage. The dispomix tubes containing the homogenised adipose tissue was incubated for 2 minutes in a water bath at 37°C to break down the lipid content and again centrifuged at 1800 g for 1 minute. Following this, the supernatant from the adipose tissue or the complete homogenate from the liver tissue was transferred to 2ml eppendorf tubes. To this tube, 200µl of analytical-grade chloroform (Fisher Scientific, Leicestershire, UK) was added,

mixed by vortexing and then incubated for 15 minutes at room temperature to allow phase separation following which, this was subject to centrifugation at 12000g for 15 minutes at 4°C and the top aqueous phase was used for next steps of RNA purification and extraction.

RNA purification and extraction were performed using RNeasy Plus mini extraction kit (Qiagen, West Sussex, UK). The top aqueous phase was transferred to a gDNA Eliminator spin column from the RNeasy plus kit and centrifuged at 8000g for 30 seconds. An equal volume of 70% ethanol was added to the flow-through liquid to provide appropriate binding conditions to the RNA centrifuge column. All of the mixture was transferred to an RNeasy spin mini column and centrifuged at 8000g for 15 seconds at room temperature. The flow through was discarded and to each column , 700µl of RW1 buffer (containing guanidine isothiocyanate and 70% ethanol) was added and centrifuged for 15 seconds at 8000g followed by addition of buffer RPE (500µl) and another centrifugation for 15 seconds. In order to eliminate any buffer carryover, the column was transferred to another sterile collection tube followed by centrifugation for 1 minute.

To elute RNA from the columns, the column was transferred to a new labelled sterile 1.5ml eppendorf tube. This was followed by pipetting of 50 µl of RNase free water to the centre of the membrane of the column. To elute the RNA, this was then centrifuged at 8000g for 1 minute.

2.9.2 RNA quantitation and quality control

Quality control of isolated RNA is an essential step not just to determine the concentrations of the extracted RNA but also to ensure absence of contamination (by genomic DNA or chemicals used during extraction) or degradation of the RNA. Various methods performing this include, performing gel electrophoresis [348, 349] and the newer methods of spectrophotometry [350] or calculation of RNA integrity number (RIN) [351]. For the RNA extracted from liver tissue, spectrophotometry using Nanodrop ND1100 (NanoDrop, Wilmington, DE, USA) was followed by performing non denaturing agarose gel electrophoresis. The RNA extracted from adipose tissue was also quantified using Nanodrop and the integrity analysis was performed using Agilent 2100 bioanalyser (Agilent Technologies, Danbury, CT, USA). This additional investigation into RNA integrity was performed before performing the PCR as some of the RNA extracted from the adipose tissue had been kept in -80°C storage for about 18 months.

2.9.2.1 RNA gel electrophoresis

The procedure of separating RNA according to its mass (and consequently the chain length) depends upon agarose gel acting as sieve to selectively impede the migration of the negatively charged RNA towards the anode on application of electric current [349]. After electrophoresis, RNA can be visualised using the dye ethidium bromide which intercalates between nucleic acids and fluoresces under ultraviolet light. The RNA identified this way is present in clusters (bands) of RNA organised according to their length which can be identified by comparing with a ladder. Any genomic DNA contamination would appear as a smear of fluorescence next to the well (poor migration owing to the large size). Presence of two distinct bands of 28s and 18s RNA where the 28 band appears approximately twice as intense as the 18s RNA indicates intact RNA whereas a smear instead of these

distinct bands through the far end of the gel would indicate RNA degradation into small fragments.

Non denaturing gel electrophoresis was performed on the RNA extracted from the liver tissue samples. In contrast, the denaturing gel electrophoresis uses one or a combination of heat, urea, formaldehyde or formamide to cause the breakage of hydrogen bonds making the RNA linear (denatured) and hence more uniform in migration rate according to its length. Denaturing gel electrophoresis is more important when the objective is precise measurement of RNA molecular weight which was not the objective of this experiment. The procedure also requires use of either complicated laboratory instrumentation or toxic, carcinogenic, or expensive chemicals [352]. The findings of RNA integrity and purity were confirmed by either spectrophotometry or by calculating the RNA integrity (RIN) number (Section 2.9.2.4).

2.9.2.2 Non denaturing gel electrophoresis of RNA procedure

1% w/v agarose gel was made in TAE buffer (2M Tris (hydroxymethyl amino-methane, 0.2% (w/v) SDS, 1 M glacial acetic acid, 0.5M Na₂EDTA pH8, distilled water up to 1000ml) by heating. After a short cooling period 0.5µl/ml of solution of 0.1% ethidium bromide was added. The solution was allowed to cool in a gel cast with specific combs inserted to form wells inside the gel. Once the gel was set after a period of 30 - 45 minutes, it was then transferred to an electrophoresis chamber. 2µg of RNA, diluted to a volume of 10µl using nuclease free water, was mixed with 5µl gel loading buffer (v/v saturated bromophenol blue, 0.15% (w/v) EDTA, 20% v/v glycerol) and loaded into the wells of the gel. Axygen bioscientific™ 300bb-1Kb DNA ladder (Axygen Inc, CA, USA) was loaded in the wells on the sides. 80 volts of electric current was applied using BioRad power pac (Bio-Rad laboratories, Hemel Hempstead, UK) for 50 minutes - the time the fastest dye had

travelled 2/3 of the gel width. The gel was visualised under a UV trans-illuminator CCD camera (Fuji film luminescent image analyser LAS-1000 v1.01) and a digital image of the gel was saved for records and analysis (see Figure 2.8)

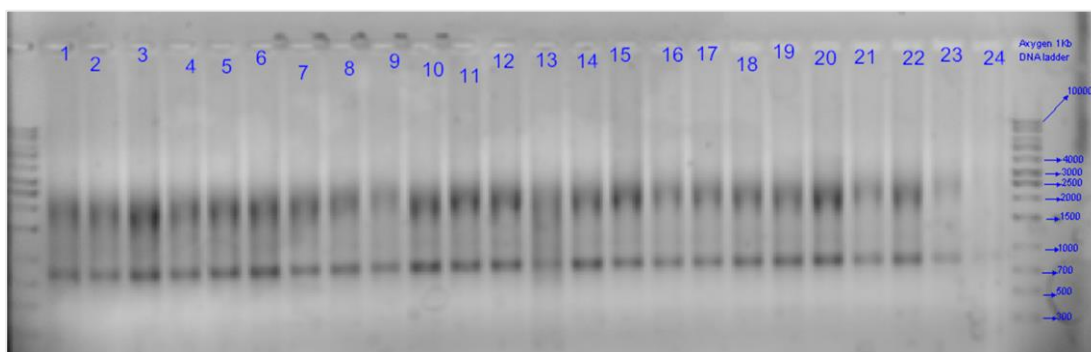


Figure 2.8: Image of non denaturing agarose gel electrophoresis of RNA.

RNA electrophoresis was performed in 1% agarose gel containing ethidium bromide run parallel with 1kB DNA ladder. DNA ladder was used in absence of suitable RNA ladder and equivalent nucleotide size was ascertained by retrospective comparison of DNA and RNA ladder images from published data. Presence of two distinct bands of 28s and 18s RNA where the 28 band appears approximately twice as intense as the 18s RNA indicates intact RNA. A genomic DNA contamination would have demonstrated a smear of large nucleotide size at the top close to the well whereas a denatured RNA shows up as a smear of small nucleotide size at the bottom end of the gel.

2.9.2.3 Spectrophotometry using Nanodrop

RNA concentrations and purity measurements were determined using a Nanodrop® ND-1000 (Nanodrop Technologies, Wilmington, USA) spectrophotometer. The nucleic acid concentration was calculated according to Beer-Lambert equation [353, 354] which uses the absorbance of the Nucleic acids at a set wavelength to calculate their concentration using known constant values of extinction coefficients. For calculation of sample purity, the purity ratio was calculated. Nucleic acids have maximal absorbance at 260nm which declines appreciably as wavelength increases and at a wavelength of 280nm, the absorbance is 1.8 times lower for pure DNA and is halved for pure RNA. A ratio of absorbance at 260nm/280nm of 1.8 – 2.1 indicates suitability of the RNA for downstream application of interest (PCR). Any significant deviation from this ratio of absorbance at 260

and 280nm is an indicator of contamination. The potential contaminants from the RNA extraction steps can be identified according to the shape of the absorbance spectrum of the solution with the nucleic acid (Figure 2.9). If the RNA concentration is higher than the detection range of the spectrophotometer, an aliquot from the RNA extract was diluted using Tris buffer at pH 8 as the pH of the solution can affect the absorbance spectrum of the RNA [355].

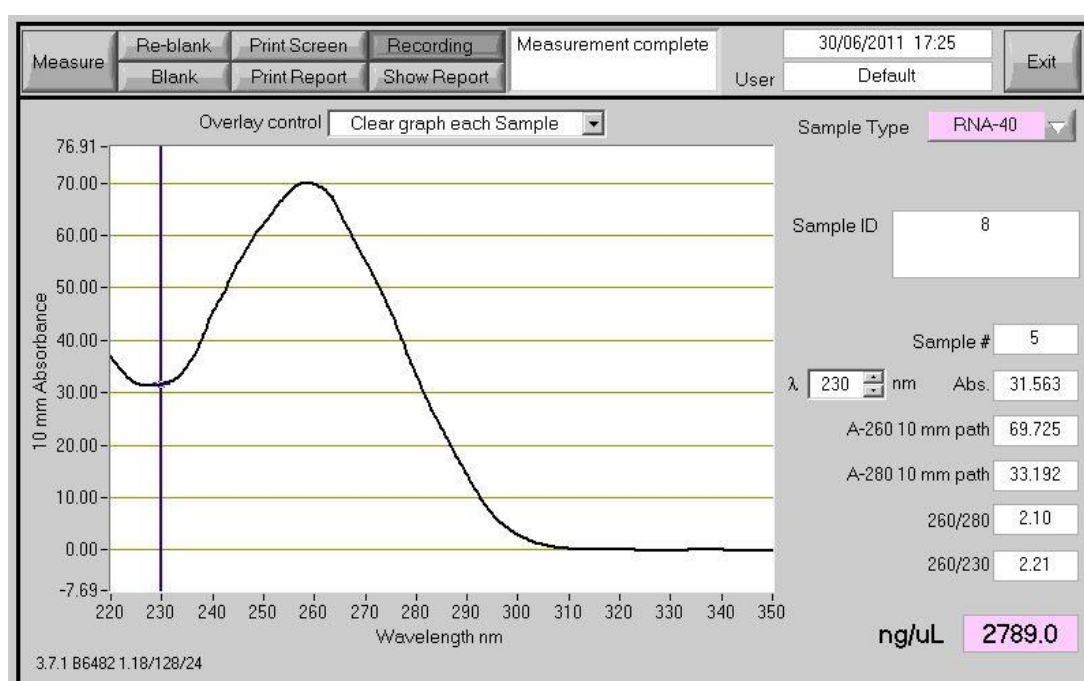


Figure 2.9: Graph of absorbance at different wavelengths made using Nanodrop ND1100 demonstrating evidence of RNA purity, integrity and concentration of a representative sample.

2.9.2.4 RNA integrity number (RIN) determination using Agilent 2100 bioanalyser

The Agilent 2100 bioanalyser uses microfluidics technology to perform electrophoretic migration of RNA through polymer gel in thin glass tubes. This procedure is similar to performing a slab gel electrophoresis described above but is performed on a much smaller scale in a controlled and standardised setting. The glass tubes are part of a standard chip (see Figure

2.10) which is first loaded with the polymer gel mixed with fluorescent dye. The fluorescent dye molecules intercalate into RNA strands which can be detected using laser induced fluorescence. On each chip, 12 RNA samples and one ladder with marker can be loaded in individual wells. The bioanalyser electrodes provide controlled electrical power to each of these wells causing migration of the negatively charged RNA towards the anode and separation of the RNA molecules according to their size where the smaller fragments migrate faster and are identified as they pass a detector in the bioanalyser at different speeds. The data are translated to gel like images (bands) and an electropherogram (peaks). The RNA data can be compared to the RNA ladder which contains six fragments of known concentration and ranging in size from 0.2 to 6 kb.

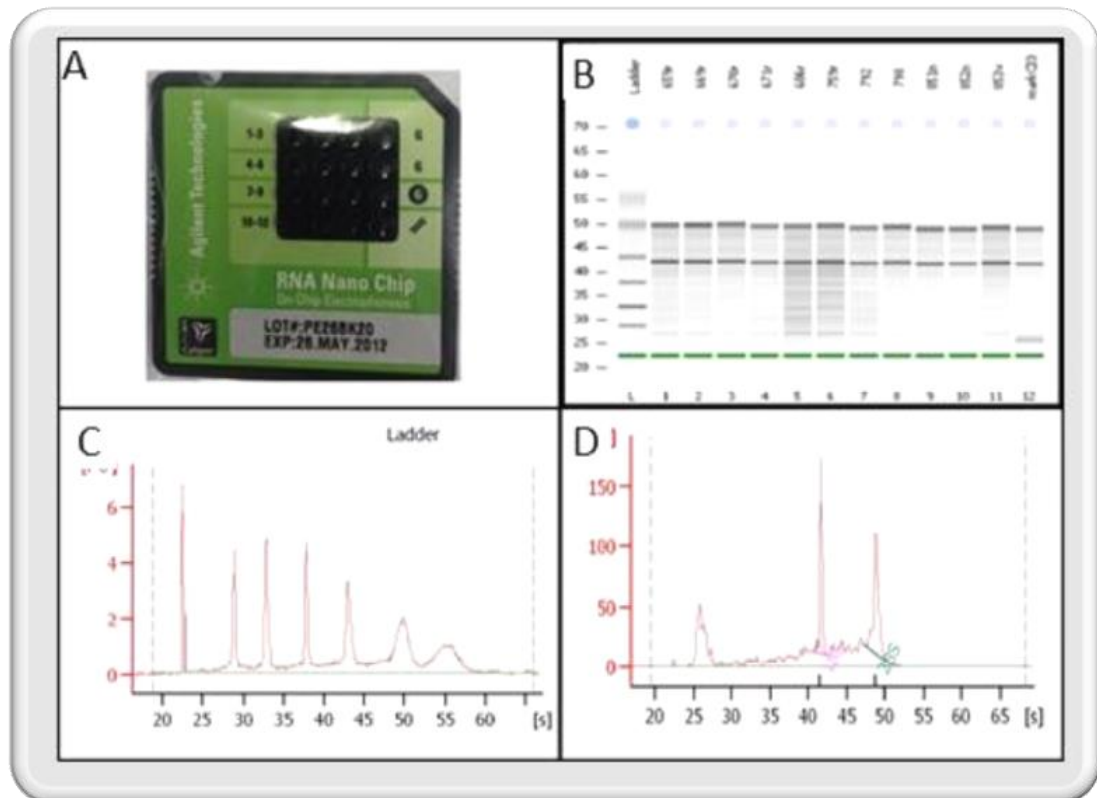


Figure 2.10: Agilent bioanalyser use for RIN determination.

A) RNA Nano chip used to load RNA ladder and RNA into the analyser. The chip is first primed with gel mixed with fluorescent dye. RNA and ladder are loaded into individual wells and electric current applied leading to migration of RNA through the gel. B) A gel like image formed from the data. The extreme left well shows the gel like image of the ladder whilst the remaining bands demonstrate a gel equivalent picture of the RNA. C) An electropherogram of the RNA ladder d) An electropherogram of the RNA gel demonstrating large peaks for the marker, 18s and 28s bands.

For intact RNA, the bioanalyser electropherogram shows two distinct large peaks for 18S and 28S RNA and smaller peaks for other smaller RNA. The software calculates a RNA Integrity Number (RIN) [351] using the electropherogram data based on a numbered scale ranging from 1 to 10 with 1 being the most degraded and 10 being the most intact. A RIN of 5 or above is considered an indicator of suitability of the RNA for the PCR experiments [356]. The RIN is considered as a reliable and informative method and is the current gold standard for analysis of RNA integrity [357, 358] before performing of PCR.

2.9.2.5 RNA handling and storage

To minimise freeze-thawing of the stock RNA which is attributed to RNA degradation, 10µl aliquots of each extracted RNA stock were further diluted (1µg/µl for liver and 0.3 µg/µl for adipose tissue) to normalise samples ready for quantitative RT-PCR. All extracted RNA samples were stored at -80°C until further use.

2.9.3 Reverse transcription

This is the process of transcribing single stranded RNA into double stranded complimentary DNA (cDNA) using a DNA primer and reverse transcriptase enzyme. The expression of any gene of interest can then be quantified from this cDNA using the technique of quantitative PCR (qPCR).

The main components of the reagents used in this technique are the enzyme reverse transcriptase, random hexamer primers, oligo dT primers and deoxyribonucleotide triphosphate (dNTP) mix. Reverse transcriptase is a DNA polymerase enzyme which transcribes single-stranded RNA into single-stranded DNA. dNTP Mix is a premixed solution containing sodium salts of dATP, dCTP, dGTP and dTTP, each at 10mM in water which provide the building blocks for the cDNA production. When incubated with the reverse transcriptase at 37°C, the cDNA strand is synthesised using the deoxyribonucleotides from the dNTP mix.

2.9.3.1 Reverse transcription procedure

This was performed using High Capacity RNA to cDNA Kit™ (Applied Biosystems, Warrington, UK). The kit contains maloney murine leukemia virus reverse transcriptase and buffer mix containing dNTP. The procedure was performed using labelled 0.2ml eppendorf tubes. In a 20µl reaction containing 2µl of diluted mRNA (1µg/µl for liver and 0.3 µg/µl for adipose tissue), 10µl of RT buffer, 1µl of enzyme mix and RNase

free water were added. After brief centrifugation the reaction mix was incubated at 37°C for 60 minutes and the reaction was stopped by heating to 95°C for 5 minutes using the Techne Touchgene Gradient thermal cycler (Techne Incorporated, New Jersey, USA). Simultaneous control experiments containing no reverse transcriptase enzyme were also performed to ensure transcription efficiency. After reverse transcription the cDNA samples were stored at -20°C.

2.9.4 Oligonucleotide primers for PCR

Quantification of a specific gene of interest depends on the ability to make its copies in an efficient and reliable (with high specificity) reaction. Primers are small sequences of nucleic acids (oligonucleotide) which bind to the cDNA and act as markers for starting and finishing points for the process of imprinting of the new DNA sequence (copies). The enzyme DNA polymerase starts replication at the 3' end of the primer, and then copies the opposite strand.

An optimum primer should have several qualities. It should be highly specific and make copies of only the gene of interest on the genome and not to any other unintended genes [359]. The process of ensuring specificity of a primer includes finding the appropriate gene sequence. The open access annotated GenBank gene sequence databases

(<http://www.ncbi.nlm.nih.gov/gene>) of National Center for Biotechnology Information (NCBI) or Ensembl (<http://www.ensembl.org/index.html>) were searched to find the appropriate gene sequence. When the appropriate gene sequence of *Ovis Aries* (sheep) was not available, primers to closely related species (*Bos taurus*) for which the genome has been more widely described were designed and tested for specificity and efficiency against ovine samples. An ideal primer pair would span across an intron on the genomic

sequence to ensure absence of amplification of any possible genomic DNA contaminant in the reaction mix.

An ideal primer would perform efficiently which would mean doubling the number of cDNA copies after every cycle of the polymerase chain reaction (100% efficiency). In order to ensure high efficiency of primers, optimum primer parameters have been designated and published [359]. Both the primers should have a similar melting temperature (T_m). This is important as the annealing to the DNA occurs for both primers at the same time. A significant difference between temperatures may result in an incorrect sequence of DNA or failure to extend at all. In addition, a correct T_m avoids the unintended consequence of the primers annealing with other primers during the reaction, producing primer-dimers. The melting temperature of the primer is dependent on primer length and the percentage of nucleotides guanine (G) and cytosine (C) components of the primer. A primer of around 20 (± 4 base pair length) and 40-60% guanine/cytosine (GC) content is optimum. The sequence in the primer bases should not be complementary to each other (to avoid primer-dimer formation) or to the bases present on itself (to avoid hairpin structure formation). Several open access websites (Primer 3 and NCBI primer blast) and commercially available software packages (Beacon Designer software® Premier Biosoft, Palo Alto, USA) can be used to design optimum primers.

2.9.4.1 Primer design for PCR procedure

The primers used in the experimental protocols were sourced from two different sources. The primers acquired from Sigma Aldrich (Table 2.3 and Table 2.4) were designed in house by myself or by Dr S Sebert, Dr M Hyatt, Dr D Sharkey and Mr M Pope. Some customised primers were also sourced from PrimerDesign Ltd. (Table 2.5). These primers were designed to order by the company in a manner analogous to that above and after supply were tested by myself by agarose gel electrophoresis to ensure the band size matched to the size of the gene of interest and also by matching the primer sequence to the mRNA sequence.

Gene		Primer sequence	Species	NCBI accession number	Source
RPO, Large ribosomal protein	Forward 5' - 3'	CAACCCTGAAGTGCTTGACAT	Bos taurus	NM_001012682	Robinson et al. [360]
	Reverse 5'-3'	AGGCAGATGGATCAGCCA			
YHWAZ, tyrosine 3-monooxygenase / tryptophan 5-monooxygenase activation protein	Forward 5' - 3'	TGTAGGAGCCCGTAGGTCATCT	Ovis aries	NM_174814	Garcia-Crespo et al. [361]
	Reverse 5'-3'	TTCTCTGTATTCTCGAGCCATCT			
RPL19, L19 Ribosomal protein	Forward 5' - 3'	CCGGGAATGGACAGTCACA	Ovis aries	XM_012141899	Garcia-Crespo et al. [361]
	Reverse 5'-3'	CAACTCCCGCCAGCAGAT			

Table 2.3 Details of the genes, accession numbers and primer sequences for primers for genes used as reference genes for PCR

Gene		Primer sequence	Species	NCBI accession number	Source
AMPK, 5' AMP-activated protein kinase	Forward 5'-3'	GCTGGATTTTGAATGGAAGG	Ovis aries	NM_001112816	Sebert et al.[267]
	Reverse 5'-3'	CAGCACCTCATCATCAATGC			
Adiponectin	Forward 5'-3'	ATCAAACCTCTGGAACCTCTATCTAC	Bos taurus	BC140488	Muhlhausler et al.[362]
	Reverse 5'-3'	TTGCATTGCAGGCTCAAG			
ATF4, activating transcription factor-4	Forward 5'-3'	AGATGACCTGGAAACCATGC	Ovis aries	NM_001142518	Sharkey et al. [363]
	Reverse 5'-3'	AGGGGGAAGAGGTTGAAAGA			
ATF6, activating transcription factor-6	Forward 5'-3'	AACCAGTCCTGCTGTTGCT	Ovis aries	AY942654	Sharkey et al.[363]
	Reverse 5'-3'	CTTCTTCTGCGGGACTGAC			
CD68, cluster of differentiation 68	Forward 5'-3'	GTCTGTCTACCACCACAGT	Ovis aries	XM_012122595	Sharkey et al.[363]
	Reverse 5'-3'	GCTGGGAACCATTACTCCAA			
CD95, cluster of differentiation 95	Forward 5'-3'	CGGGATCTGGGTTCACTTGTC	Ovis aries	NM_001123003	
	Reverse 5'-3'	AACAGGTGCTCAGATATAGGC			
GRP78, glucose-regulated protein 78kDa	Forward 5'-3'	TGAAACTGTGGGAGGTGTCA	Bos taurus	NM_001075148	
	Reverse 5'-3'	TCGAAAGTTCCAGAAGGTG			
Leptin	Forward 5'-3'	GGGTCACTGGTTTGACTTCA	Ovis aries	NM_173928.2	Bloor et al. [364]
	Reverse 5'-3'	ACTGGCGAGGATCTGTTGGTA			
mTOR, mammalian target of rapamycin	Forward 5'-3'	GCCTTCCGACCTTCTGCCTTC	Ovis aries	NM_001145455	
	Reverse 5'-3'	CCGCTGTCCGTTCTTCTCC			
ObR, leptin receptor	Forward 5'-3'	TGAAACCACTGCCTCCATCC	Ovis aries	NM_001009763	
	Reverse 5'-3'	TCCACTTAAACCATAGCGAATCTG			
TLR4, Toll like receptor 4	Forward 5'-3'	TGCTGGCTGCAAAAAGTATG	Ovis aries	NM_001135930	Sharkey et al. [275]
	Reverse 5'-3'	CCCTGTAGTGAAGGCAGAGC			
GCR, glucocorticoid receptor	Forward 5'-3'	ACTGCCCAAGTGAAAACAGA	Ovis aries	>NM_001114186	Williams et al. [365]
	Reverse 5'-3'	ATGAACAGAAATGGCAGACATT			

Table 2.4 Details of the genes, accession numbers and primer sequences for PCR primers designed in-house

The design for primers was based on the mRNA sequences published on NCBI online database (<http://www.ncbi.nih.gov>). The primers were first designed using the open access Primer3 software (<http://frodo.wi.mit.edu/primer3/>) specifically for PCR with the above described specifications. The primer sequences were then tested using online software Netprimer (<http://www.premierbiosoft.com>) to rule out presence of hairpin structures and primer dimers. To ensure that the primer sequences would not cross hybridise with other sequences within the genome, the target sequence was tested using the BLAST search engine from the NCBI (<http://www.ncbi.nlm.nih.gov/BLAST>). Once finalised, the primers were ordered from Sigma Aldrich as desalt purification, dry format primers at 0.05µmol format.

Gene		Primer sequence	Species	NCBI accession number
ATG12, autophagy related gene 12	Forward 5' - 3'	CATTCTGCTAAAGGCTGTAGGA	Bos taurus	NM_001076982
	Reverse 5'-3'	GTTCTGAAGCCACAAGTTTAAGG		
BECN1, gene encoding Beclin1	Forward 5' - 3'	CCAGGAGGAAGAGGCTAACT	Bos taurus	NM_001033627
	Reverse 5'-3'	AAGCTGTTGGCACTTTCTGT		
EDEM 1, ER degradation enhancer, mannosidase alpha-like 1	Forward 5' - 3'	GTCTGGAAAAGTACACAAAAGTCA	Bos taurus	NM_001103092
	Reverse 5'-3'	AGCAGATACAGGTATTACAGGTC		

Table 2.5 Details of the genes, accession numbers and primer sequences for primers sourced from PrimerDesign® company

2.9.5 Polymerase Chain Reaction (PCR)

Polymerase chain reaction (PCR) is a method for performing exponential amplification of short DNA sequences within a longer double stranded DNA molecule. PCR entails the use of a pair of primers complementary to a defined sequence on each of the two strands of the DNA. These primers are extended by a DNA polymerase so that a copy is made of the designated sequence. This process can then be repeated over several cycles resulting in

exponential amplification of the sequence. The same primers can be used again, not only to make another copy of the input DNA strand but also of the short copy made in the first round of synthesis. During the reaction, the temperature of the reaction needs to be raised to allow separation of the two strands of the DNA. However, the raised temperature was a hindrance to exponential amplification as it led to denaturation of the enzyme DNA-polymerase. The exponential amplification without the need for adding new polymerase after every round of amplification was made possible by the isolation of enzyme Taq polymerase from the bacteria *Thermus aquaticus* [366] which is stable at high temperatures.

Each cycle of PCR goes through a sequence of steps. The first step is the initiation step. This step consists of heating the reaction to a temperature of 94–96 °C which leads to activation of the DNA polymerase enzyme (hot-start PCR). The next step is the denaturation step involving splitting of the hydrogen bonds between DNA strands leading to formation of single stranded DNA. The reaction temperature is then lowered to 60°C leading to annealing of the primers to the individual strands of the DNA template. Typically the annealing temperature is about 3-5°C below the T_m of the primers used. The primer extension step at temp 72°C leads to new strand synthesis by the enzyme DNA polymerase. This process, over several cycles, leads to exponential amplification of the DNA template (Figure 2.11).

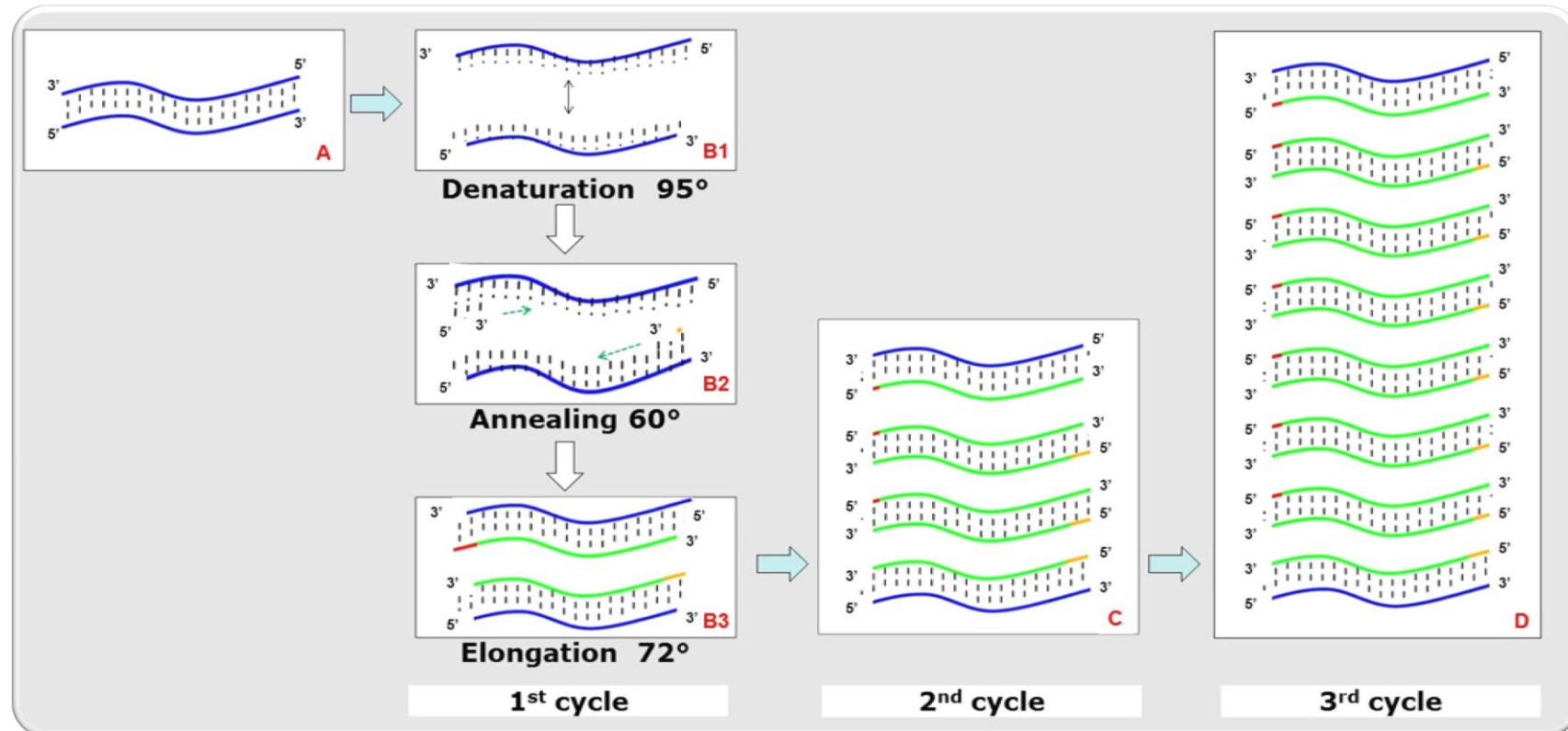


Figure 2.11 Schematic representation the principle of exponential amplification during first few PCR cycles

A) Two parallel long polymer nucleotide chains in a DNA are attached to each other through hydrogen bonds between complementary nucleic acids. B1) Denaturation step: Heating of the PCR reaction to 95°C causes disruption of the hydrogen bonds leading to separation of the DNA strands yielding single stranded DNA. B2) Annealing step upon lowering of the reaction temperature to 60°C, primers form hydrogen bonds to their complementary nucleotides on the single stranded DNA. B3) Elongation step results in formation of complementary strand of DNA resulting in the doubling of the DNA quantity after one cycle. C) Repetition of the Steps B1, B2 and B3 results in 4 times amplification of DNA content after 2 cycles and D) 8 times amplification after 3 cycles. The exponential increase continues and after n cycles 2^n times amplification occurs.

2.9.5.1 Classical PCR procedure

By performing classical PCR, copies of a specific gene can be amplified from the cDNA product of reverse transcription using specific primers. These cDNA copies can then be isolated and extracted by performing agarose gel electrophoresis and visualisation.

The reaction mix varied depending upon the source of the primers and is given in Table 2.6. The reaction was performed in a 20µl reaction in 200µL eppendorf tubes using Thermo start PCR master mix (Abgene Epsom, UK) containing the enzyme Taq polymerase, dNTPs, Mg^{2+} , and buffer. 2µl of cDNA product from the reverse transcription was added to 10µl of the mastermix and specific volumes of primers were added to this reaction mixture (1µl each of forward and reverse primers sourced from Sigma and 0.5µl of combined Primerdesign primers). The total volume was brought to 20µl using nuclease free water.

	Primers from Sigma Aldrich	Primers from PrimerDesign
Thermostart PCR master mix	10µl	10µl
Primer	1µl each of forward and reverse	0.5µl of combined primers
Nuclease free water	6µl	7.5µl
cDNA	2µl	2µl

Table 2.6 The components and volume used for reaction of classical PCR.

The reaction was done in duplicate and negative controls for each gene containing no cDNA were run concurrently to ensure integrity of PCR. The tubes were centrifuged for 1 minute at 3000g and loaded into a Techne thermal cycler (Bibby Scientific Limited, Staffordshire) and run on the PCR program for 45 cycles. The program steps are given in the Table 2.7.

	Process	Temperature (°C)	Duration (mins)
Step 1	Initiation	105	4
Step 2	Enzyme activation	96	15
45 cycles of steps 3-5			
Step 3	Denaturing cDNA strands	94	0.5
Step 4	Annealing	60	0.5
Step 5	Extension	72	1
Single final step			
Step 6	Final Extension	72	7
Final hold	Hold	4	Until moved to storage at -20°C

Table 2.7 The stages and program conditions for classical PCR. The steps 3-5 are repeated over 45 cycles before moving to step 6.

2.9.5.2 Agarose gel electrophoresis and DNA extraction

Negatively charged DNA molecules can be separated with the process of electrophoresis. On application of electric field, DNA fragments migrate towards the positive electrode. The small fragments travel faster and farther in the gel which can then be visualised by staining with ethidium bromide. The dye intercalates between bases of DNA and can then be visualised under ultra violet (UV) light. A positive control DNA fragment "ladder" is used to identify the size of the unknown bands. The DNA band of interest can then be extracted from the gel using commercial gel extraction kits.

2.9.5.3 Agarose gel electrophoresis and DNA extraction procedure

Agarose gel was made by dissolving 3% w/v agarose in hot TAE buffer (described in Section 2.9.2) and after a short cooling period, 0.5µl/ml of 0.1% ethidium bromide was added to this. The solution was allowed to cool in a gel cast with specific combs inserted to make wells inside the gel. Once the gel was set after a period of 30 - 45 minutes, it was then transferred to an electrophoresis chamber which can be connected to electrodes providing customisable electrical field. The 20µl PCR product was mixed with 5µl gel loading buffer (v/v saturated bromophenol blue, 0.15% (w/v) EDTA, 20% v/v glycerol) and loaded into the wells of the gel. For comparison, DNA ladder was added to parallel wells (Generuler™ ultra low range DNA ladder 10-300 bp or Axygen bioscientific™ 300bp-10000 bp DNA ladder). An electric current was applied at 100 volts for 50 minutes using BIORAd power pac 300(Bio-Rad Laboratories Ltd., Hemel Hempstead, UK). The PCR products were visualized under a UV trans-illuminator CCD camera (Fuji film luminescent image analyser LAS-1000 v1.01).

Fluorescent gel bands identified and located at the specific size for the primer product were cut out of the gel, weighed and extraction and purification of the PCR products was performed using the QIAquick® gel extraction kit (Qiagen). In 2ml eppendorf tubes containing the cut gel, 600 µl per 100mg agarose gel of buffer QG (Qiagen), which consists of 5.5 M guanidine thiocyanate and 20 mM Tris hydrochloride, was added and incubated at 50°C for 10 minutes leading to the dissolution of the gel. Addition of 100µl of isopropanol per 100µg of gel to this dissolved solution aids precipitation of the DNA. This solution was then pipetted into a QIAquick spin column and centrifuged at 10000g for 1 minute. The flow-through was discarded and another 500µl of buffer QG added to ensure

elimination of agarose followed by centrifugation and discarding of the flow through. The next step was addition of 700µl of PE buffer containing ethanol to the spin column. This was allowed to stand for 5 minutes and centrifuged at 10000g for 1 minute and the flow through liquid was discarded. The column was transferred to another collection tube (supplied as part of the kit) and centrifuged at 10000g for 1 minute to eliminate any traces of the PE buffer. To elute the cDNA from the column, it was transferred to another sterile 1.5ml eppendorf tube and 50µl elution buffer added to the center of the column. This was allowed to stand for 1 minute and then centrifuged at 10000g for 1 minute leading to elution of the cDNA to the eppendorf tube. The cDNA was quantified using a Nanodrop spectrophotometer as described in Section 2.9.2. For the primers sourced from Sigma Aldrich, the extracted cDNA was sent for sequencing within the University of Nottingham's Centre for Genetics and Genomics and cross referenced with the NCBI online database. The cDNA product of the custom primers from PrimerDesign was not sequenced as the product had been sequenced at the manufacturing site.

2.9.6 Quantitative real time polymerase chain reaction (qPCR)

Quantitative real time polymerase chain reaction (qPCR) also called real time PCR is a technique used to quantify a targeted DNA molecule. This procedure is based on a fluorogenic dye called SYBR green which preferentially binds to the double stranded DNA during the amplification process of PCR and the intensity of its fluorescent signal correlates to the amount of DNA present in the reaction (Figure 2.12).

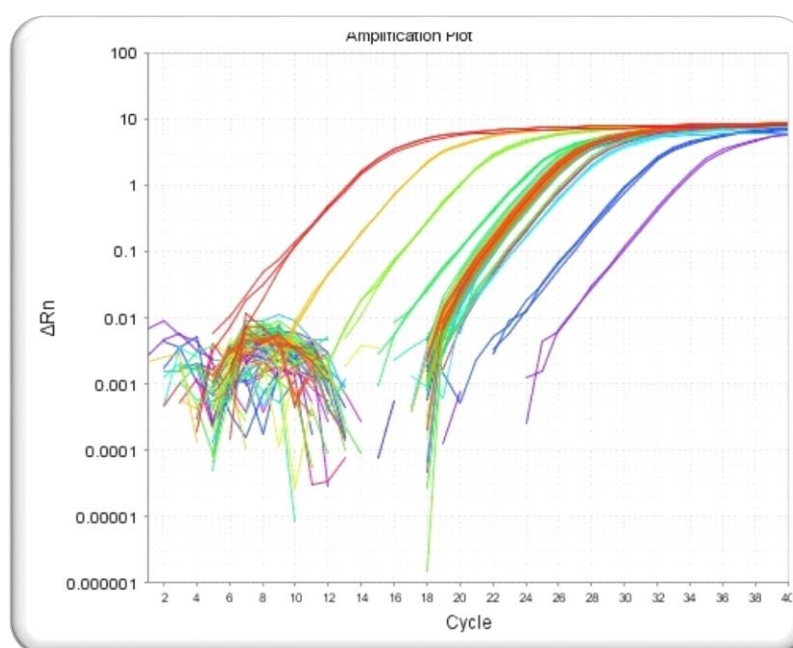


Figure 2.12: Amplification plot of a PCR reaction demonstrating increasing signal from serial dilution of standards and the samples.

The X axis on the plot contains the cycle number and the Y axis demonstrates increasing fluorescent signals.

Along with the dye, the other important components of the reaction mix include Taq DNA polymerase, Uracil-DNA Glycosylase (UDG), a passive reference dye, dNTPs, and buffer components. UDG prevents the reamplification of carryover PCR products by removing any uracil incorporated into single- or double stranded products [367]. In order to adjust for differences in product due to minor pipetting errors, the passive reference dye provides an internal reference to which the product signal can be normalised during data analysis.

The standard method of defining the unit of signal from the exponentially increasing fluorescence data is by identifying the number of cycles taken to reach a fixed value of fluorescence threshold called the cycle threshold (Ct) [368].

To quantify the relative quantity of the gene of interest, a serial dilution is prepared from a fixed amount of cDNA prepared during classical PCR as described in Section 2.9.5. A linear graph (standard curve) is obtained after plotting Ct values of the serial dilution of the cDNA against the log of the concentration (semi-log scale; Figure 2.13). The relative quantities can then be calculated by extrapolating this standard curve.

In an ideal reaction, the amount of cDNA target doubles in each cycle. However, the efficiency of the amplification is often variable among primers and templates. The efficiency of the experiment is calculated by calculating the slope of the standard curve. Therefore, in an efficiency graph where Log (concentration) is plotted on the x-axis and the Ct is on the y axis, the slope of a standard curve with ideal efficiency of 100% with doubling of the PCR product (amplification factor=2) in every cycle would be 3.322.

$$\textbf{Amplification factor} = 10^{(1/\text{slope})}$$

$$\textbf{If slope} = 3.322$$

$$\textbf{Amplification factor} = 10^{(1/3.322)} = 2$$

The correlation coefficient (R^2) of the reaction is also calculated to ensure linearity of the standard curve.

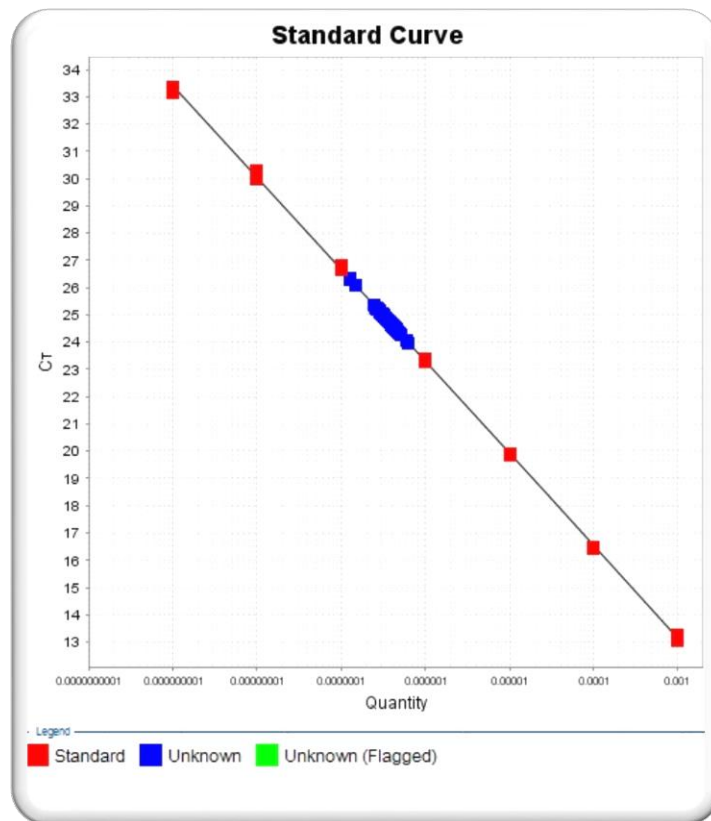


Figure 2.13: A representative graph of standard curve derived by plotting the cycle threshold value (Ct) on the y axis against the serial dilution plotted in semi-logarithmic scale on the X axis.

Another quality control measure in PCR procedure is the melting curve test. This is performed to rule out presence of undesired products of PCR reaction like primer dimers or unintended products of PCR reaction by measuring the fluorescence of the PCR products across a range of temperature following completion of PCR cycles. The temperature of denaturation (splitting of two DNA strands) is dependent on the length and the base composition of the DNA. In a pure solution containing only one cDNA, the fluorescence emitted by the SYBR green suddenly drops after this temperature is reached. The rate of change in fluorescence can be plotted and shows a peak at the temperature of denaturation. If there are unintended products of a different length other than the gene of interest, they will have a separate peak in this melting curve plot. The presence of a single peak of the melting curve plot is therefore used to rule out unintended products in the PCR (Figure 2.14).

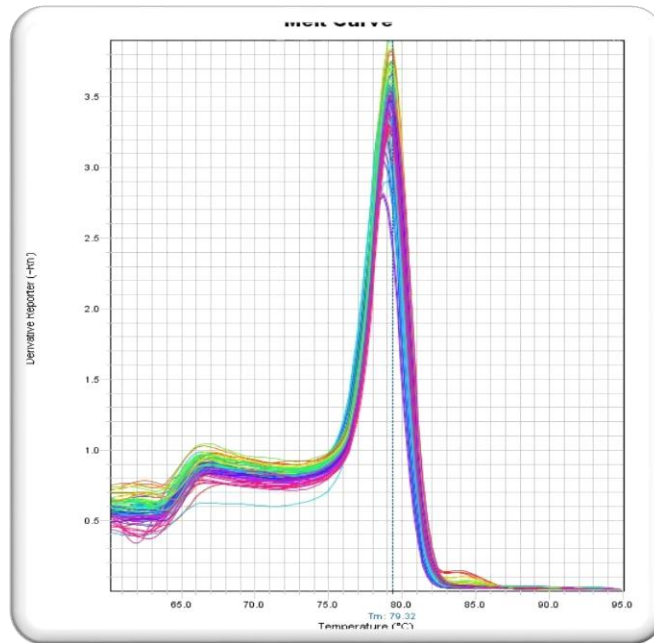


Figure 2.14: Melting curve graph following a qPCR cycle demonstrating presence of a single peak thereby confirming absence of any unintended products at the end of the qPCR

2.9.6.1 Reference gene and relative quantification of the gene of interest

A reference gene (previously known as a housekeeping gene) is a gene expressed constitutively in all the cells at a high level and is not affected by the experimental conditions in question. The expression of this gene can be used to normalise for any variation in RNA abundance at the start of reverse transcription which could be present as a consequence of difference in the amount of tissue used for RNA extraction, variation in enzymatic efficiencies and also difference in overall transcriptional activity in the cell or tissue. The expression of reference gene(s) was measured from all the samples and was used to quantify the expression of the gene of interest.

2.9.6.2 Choosing the most stable reference genes

A good reference gene by definition should have very little variation in expression throughout sample sets and be expressed relatively higher than any genes of interest. The choice of reference gene can be very specific to

the tissue and the experimental protocol. As numerous studies have reported that housekeeping gene expression can vary considerably [369, 370], identification of most stable reference genes followed by using more than one reference genes [371] is becoming standard practice. The GeNorm™ visual basic application incorporated in the Microsoft Excel software developed by Vandesompele et. al [370] uses the premise that expression of good reference genes should be similar in all samples. The calculation of the standard deviation of the log transformed values of the gene expression as a measure of the stability of reference genes can be used to calculate a value which reflects average pairwise variation between a particular gene and all other genes. This value is called M value. Stepwise exclusion of genes with higher M values (reflecting higher pairwise variation) can be performed and a combination of reference genes with least M values selected for data analysis [372].

2.9.6.3 Calculating relative gene expression

The Ct values obtained from the qPCR experiment can be used to calculate the value of gene expression relative to another sample on the same plate. For example, for a twofold change in concentrations between two samples, the difference in the Ct values would be one as the sample with half the concentration would reach the threshold for Ct value during the next cycle, similarly a fourfold change would have a difference of two cycles. This difference in the Ct values between the two samples is called delta Ct (ΔCt) [368]. Relative concentration between any two samples can thus be calculated by the equation.

$$\text{Relative concentration} = \text{Efficiency}^{\Delta Ct}$$

Relative quantification of the unknown sample requires correction for technical sample specific variation (such as differences in total amount of cDNA) and identifying samples with genuine variation in gene expression.

The use of the GeNorm method performs this by calculation of a normalisation factor for all the individual samples (unknowns) in the dataset from the reference genes. This normalization factor is the geometric mean of the calculated relative concentrations of the reference genes. The relative concentration calculated from the PCR run using the formula (Relative concentration= $\text{Efficiency}^{\Delta\text{Ct}}$) was then corrected by dividing this normalisation factor and the corrected values were then used for comparison.

It is well accepted that for calculation of a measure of central tendency, geometric mean is a better value than arithmetic mean especially when the range of values are not on the same scale. For example, in order to calculate the best measure of central tendency from two different results with scales of 1-100 and 1-5, the results from the range 1-100 will get more weightage and any small percentage change in it will make a bigger impact on arithmetic mean. Similarly the geometric mean also controls for outlying values better than the arithmetic mean [370]. Instead of calculating the gene expression relative to all the reference genes and then calculating the geometric mean of the outcomes, GeNorm method determines the normalisation factor by calculating the geometric mean of the reference genes which is then used as a denominator for the relative concentration.

For liver gene expression experiments, previously validated genes [373] for liver large ribosomal protein (RPO), tyrosine-3 monooxygenase/tryptophan-3 monooxygenase activation protein (YWHAZ) and 18S ribosomal RNA were evaluated using the GeNorm™ algorithm [370]. Using the M values as indicator of gene stability, RPO and YHWAZ were identified as the most stable reference genes and used for the normalisation of gene expression. For adipose tissue, in absence of any known published literature of validated ovine or bovine reference genes, a combination of

reference genes studied in human experiments were tested. Importin 8 (IPO8), 60S ribosomal protein L19 (RPL19) and RPO, were evaluated for the gene stability and RPL19 and RPO were identified to be the most stable genes and used for normalisation.

2.9.6.4 qPCR procedure

qPCR was performed using Applied Biosystems Step one plus [™] real time PCR system. This PCR instrument is capable of analysing 96 different samples in individual wells on a PCR plate. The PCR reaction was performed in a 96 well plate (Abgene) to which 3µl of cDNA (1:10 dilution) of samples, serial dilutions (standards), or nuclease free ,5µl SYBR® green Taq polymerase master mix (Thermo Scientific, Leicestershire, UK) and primers (1µl each of 1:40 forward and reverse primers from Sigma or 0.5µl of stock primer mix from PrimerDesign) were added to each well. The volume was brought to 10µl for the reactions containing PrimerDesign primers using nuclease free water (see Table 2.8). All the samples and negative controls were performed in duplicates while the standard dilution was performed in triplicates to obtain a reliable correlation coefficient (R^2) and samples with coefficient of variation > 5% were excluded from the analysis.

	Reaction for primers sourced from Sigma Aldrich	Reaction for primers sourced from PrimerDesign
Fast SYBR® Green Master Mix	5µl	5µl
Primer	1µl each of 1:40 forward and reverse primer	0.5µl of stock primer mix
cDNA	3µl	3µl
Nuclease free water	0µl	1.5µl

Table 2.8 The components and volume of the PCR reaction mix for each reaction. The volume of the individual components varied depending on the source of the primer used.

Once prepared, the well plate was sealed using adhesive seals and centrifuged for 1 minute at 600g and placed in the Step one plus [™] real time PCR system. The qPCR program steps are shown in the Table 2.9

<i>Process</i>	<i>Temperature (°C)</i>	<i>Duration</i>	<i>Number of cycles</i>
Activation of AmpliTaq® Fast DNA polymerase	95	20sec	Hold
Denature	95	3sec	40 cycles
Anneal/extend	60	30sec	
Melting curve	65 to 90 in 1°C increments	15 minutes	Incremental increase

Table 2.9 The steps in the QPCR protocol including the melting curve stage

The qPCR output was measured using the software package StepOne[™] v2.2 (Applied Biosystems). Experiments with R² values > .995 and amplification factor of 2± 0.05 were considered acceptable. The raw gene expression data containing the Ct values was processed and analysed using the GeNorm[™] software package as described in Section 2.9.6.3.

2.10 Histology

Visualisation of the tissue structure and the location of specific protein at a microscopic level requires use of histological techniques. However, specialised tissue processing is required before a tissue can be visualised histologically.

2.10.1 Tissue processing and microtomy

Tissue processing steps ensure maintenance of cell structure and prevents cell damage [374] while the cells are sliced into thin sections. The steps include fixation, dehydration, clearing and embedding. The process of fixation maintains clear and consistent morphology of the cellular and

extracellular structures by minimising loss of enzymatic destruction and also destruction from microorganisms [375]. Formalin is an aqueous solution of formaldehyde which is commonly used for fixation of tissues. Pure formaldehyde is a vapour which when completely dissolved in water forms a solution containing 37% formaldehyde. The commonest used dilution of 10% formalin contains approximately 3.6% (v/v) formaldehyde [374]. Formalin acts by binding to amino acids in tissues to prevent their destruction.

The next tissue processing step of dehydration involves exposing the tissues to increasing concentration hydrophilic reagents like methanol or isopropyl alcohol. This process removes the fixative and water from the tissues. Reagents like xylene, toluene or chloroform are used to clear the tissues of the dehydrating solution and prepare the tissue to receive the infiltrating medium.

The step of infiltration and embedding uses a medium that permeates the tissue and provides it with an internal and external support (embedding) which then solidifies. Paraffin wax is commonly used to infiltrate and embed the tissues. The embedded tissue is then sliced in uniform thickness sections by the process of microtomy and mounted on slides.

2.10.1.1 Tissue processing procedure

A selected amount of the omental adipose tissues was fixed in 10% formal saline (10% v/v formaldehyde on 0.9% (v/v) sodium chloride) at the time of dissection. For the liver, the tissue samples kept in - 80°C freezer following snap freezing in liquid nitrogen as described in Section 2.7 were cut and representative samples of approximate size 1cm diameter and 3-4 mm thickness were taken and kept on dry ice. Care was taken to avoid areas of large blood vessels or portal system vessels during this process. These samples were gradually thawed over 36 hours by first keeping them

in a -20°C freezer for 24 hours and then at -4°C for the next 12 hours as described by Sebert et. al. [267]. The samples were then fixed in 10% formalin for 3 days and then transferred to 70% IMS until further processing was performed.

The tissues were placed in 5mm Histosette II (Simport, Quebec, Canada) plastic cassettes and were processed using a Shandon Escelsior™ tissue processor (Thermo Scientific, Anatomical Instruments Company, Massachusetts, USA). The reagents used included industrial methyated spirit (IMS) (Sigma-Aldrich, Gillingham, UK), xylene (Fisher Scientific) and paraffin wax (Tissue Tek® II, Sakura finetek, Alphen aan den Rijn, Netherlands). The steps of dehydration, clearing and infiltration were performed sequentially as described in Table 2.10.

Step	Reagent	Concentration (% v/v)	Time (minutes)	Temperature (°C)
Dehydration	IMS	75	60	30
	IMS	90	60	30
	IMS	95	60	30
	IMS	100	60	30
	IMS	100	60	30
	IMS	100	60	30
Clearing	Xylene	100	60	30
	Xylene	100	60	30
	Xylene	100	60	30
Infiltration	Paraffin wax	100	80	60
	Paraffin wax	100	80	60
	Paraffin wax	100	80	60

Table 2.10: Tissue processing steps performed using a Shandon Escelsior™ tissue processor

The processed tissues were embedded in paraffin wax using a Tissue Tex blocking machine (Tissue Tek III®, Sakura finetek,).

2.10.1.2 Microtomy procedure

The microtomy for liver tissues was performed using sledge microtome (Anglia Scientific, Cambridge, UK, type 200) and Accu-edge low profile blades (Feather Safety Razor Co, Medical division, Osaka, Japan) and 5 μ m sections were prepared. For adipose tissue, 6 μ m sections were prepared using rotary microtome. The sections were rinsed in 70% ethanol and floated in prewarmed waterbath set at 45°C and mounted on Superfrost® plus electrostatic slides (Thermo Scientific, Massachusetts, USA). The slides were then dried on a heat rack for 15 minutes. These slides were baked in an oven at 37°C for 24 hours.

2.10.2 Histochemistry

During microscopy, the ability to differentiate the structural components of the tissue can be enhanced by performing staining of the tissue with certain dyes. The stains have differential affinity to the components of a tissue or cell and provide a contrast for the section under examination.

2.10.2.1 Haematoxylin and eosin staining.

Haematoxylin is an alkaline stain used to bind to acidic structures in the nucleic acids and demonstrate the nuclei in a slide. Upon oxidation, haematoxylin produces hematein which is a blue coloured dye. Harris's haematoxylin is a commonly used preparation and is used as a regressive dye [376] which reduces in intensity by progressive washing with a weak alkali until the optimum blue stain is produced. Eosin is an acidic dye used to demonstrate the general histological architecture of a tissue.

2.10.2.2 Haematoxylin and Eosin staining procedure

One slide from each sample was placed in slide rack. These were dewaxed by sequential immersion in two xylene troughs for 3 minutes each followed by rehydration through immersion in two troughs containing 100 % IMS for 3 and 2 minutes and then followed by 3 minute immersion in 70% IMS/distilled water. They were finally washed in distilled water trough for 3 minutes before staining. The nuclear staining was performed by immersion in Harris' haematoxylin (VWR International Ltd., Lutterworth, UK) and then rinsed in tap water for 5 minutes to remove excess dye. The slides were then immersed for 5 seconds in acid alcohol solution made by adding 1% hydrochloric acid (Fisher Scientific) made up in 70% IMS, rinsed in tap water and then blued off by immersion for 5 minutes in Scott's tap water (0.2% sodium bicarbonate and 2% magnesium sulphate solution in distilled water). A representative slide was quickly checked under light microscope to ensure adequate staining of the nuclei and the slide rack

was then stained using 0.1% eosin (VWR, as before) for 3 minutes which was then washed off under running tap water for 90 seconds. The sections were then dehydrated by two immersions of 100% ethanol for 2 minutes each and then ethanol cleared during two 3 minute immersions of xylene. Sections were mounted with coverslips (VWR) using DPX mounting medium (Fisher Scientific), and left to dry overnight. The staining was performed by myself and by Dr Paul Andrzejowski, a BMedSci student under my direct supervision.

2.10.2.3 Masson's Trichrome staining

Masson's Trichrome stain is a three colour stain protocol used to identify connective tissue in relation to cells. The nuclei are stained blue or black using haematoxylin, connective tissue can be stained blue or green, muscle fibre and keratin takes up a red colour and cytoplasm appears light pink. The presence of connective tissue highlighted this way can demonstrate the amount and location of fibrosis in pathological processes like advanced non-alcoholic fatty liver disease [208]

2.10.2.4 Masson's Trichrome procedure

One slide each from the liver tissue were placed in a slide rack and dewaxed and rehydrated as described in Section 2.10.1.1. Fresh Weigert's haematoxylin was prepared by mixing equal measures of Weigert's solution A and solution B (Raymond A. Lamb, Eastbourne, UK) and the slides were immersed in the prepared haematoxylin for 10 minutes followed by washing off the excess stain under running tap water for 5 minutes. Similar to Haematoxylin and Eosin (H&E) staining, the slides were immersed in acid alcohol (1% hydrochloric acid in 70% IMS), washed in tap water and blued off in Scott's tap water (0.2% sodium bicarbonate and 2% magnesium sulphate solution in distilled water). After a wash under running tap water, one of the slides was checked for adequate nuclear

staining. The slides were then immersed for 2.5 minutes in Solution A containing 0.5% Acid fuchsin (Nustain – Pathology Dept., University Hospital, Nottingham, UK), 0.5% glacial ethanoic acid (Fisher) in distilled water and excess stain was washed under running tap water. This was followed by a 10 minute immersion in freshly made solution B containing 1% phosphomolybdic acid (Raymond A. Lamb, Eastbourne, UK) and then another 10 minutes in solution C containing 2.5% aniline blue (Nustain), 1% glacial ethanoic acid in distilled water. The sections were then dehydrated by two immersions of 100% ethanol for 2 minutes each and then ethanol cleared during two 3 minute immersions of xylene. As before, sections were mounted with coverslips using DPX mounting medium and left to dry overnight. The staining was performed by myself along with Dr Paul Andrzejowski, a BMedSci student who worked under my direct supervision.

2.10.3 Histochemical analysis of hepatic tissue

The primary purpose of examination of hepatic tissue was to identify and attempt to quantify [208, 377] features of hepatic steatosis and NAFLD in the samples in a blinded fashion. Images were obtained from 10 randomly selected areas of hepatic sections at 10X and 20X magnification using Volocity version 5.2.0 (Perkin Elmer, Washington, USA). The images of histological sections stained with H&E and Masson's Trichrome stain were assessed qualitatively for features of hepatic steatosis represented by presence of large lipid droplets in hepatocytes and of progressive NAFLD constituting inflammatory infiltrate and pericellular and periportal fibrosis (Figure 2.15). Following assessment, the images were deemed non homogeneously stained for reliable quantification of fibrosis severity permitting quantitative assessment of only portal triad size. This was performed using Volocity software by Dr Paul Andrzejowski, a BMedSci student under my supervision.

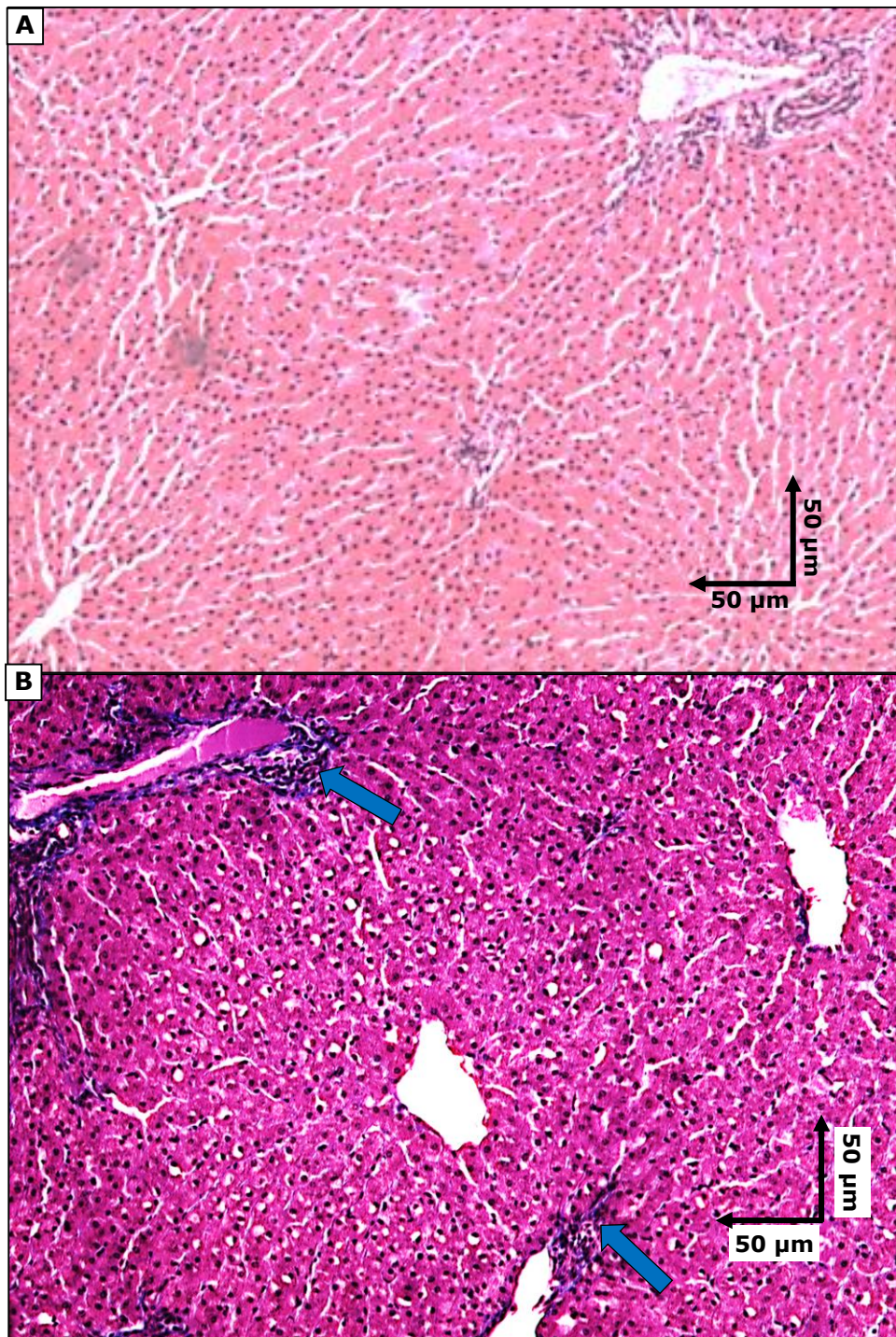


Figure 2.15 Representative images of liver tissue stained with H&E (A) and Masson's Trichrome (B) stain visualised at 20X magnification.

The figures demonstrate differential staining of hepatic lobules. Fibrotic tissue preferentially stains with Masson's Trichrome stain as seen in periportal area in the image B (blue arrows).

2.10.4 Immunohistochemistry

Whilst histochemistry is useful in giving general detail of the structural composition of a tissue, when a detailed examination of specific processes at a microscopic level is required, immunohistochemical techniques can be used. These techniques use the antigenic property of the target protein by using special antibodies generated to the target. Once bound to the antigen in the tissue section, these antibodies called primary antibodies are labelled to a variety of signalling markers which can be made to produce a colour signal (immune staining) or a fluorescent signal (immunofluorescence) by further processing.

2.10.4.1 Primary and secondary antibodies used in immunohistochemistry

The antibodies used to identify the antigen of interest are produced in an animal of species different than the species of experiment (commonly rabbit, goat, pig, horse or guinea pigs). Such antibodies can be either polyclonal or monoclonal. Polyclonal antibodies are produced through immune response stimulation after injecting animals with the whole or a component of the antigen protein. The antibodies thus generated are then isolated from the plasma by affinity chromatography. In polyclonal antibodies, whilst each antibody is able to bind to a specific area of the antigen called as epitope, several types of antibodies produced through this method are able to recognise several epitopes of the same protein.

In contrast, monoclonal antibodies are produced by a different process. After generating an immune response by injecting animals (commonly mice) with the antigen, B lymphocytes are harvested from the spleen or lymph nodes of these animals and are fused with myeloma cells. Such fused cells gain longevity in culture medium and retain their antibody producing ability. These cells are then transplanted to peritoneal cavity of a syngeneic animal and antibodies are harvested from the peritoneal fluid.

Monoclonal antibodies are considered more specific to the target antigen than polyclonal antibodies since they are specific for a single epitope.

In direct immunohistochemistry (IHC) technique, the antibody used to identify the antigen is labelled with a chemical which can be made to generate colour or fluorescence by further processing. The procedure has the advantage of being rapid without the need of additional steps.

However, industrial manufacturing of such specific antibodies make them expensive and due to no further signal amplification, such as with the alternative indirect method, this method is less sensitive.

The indirect immunohistochemistry procedure uses an unlabelled primary antibody that binds to the target antigen and a labelled secondary antibody capable of binding to the primary antibody. The secondary antibodies have been raised against immunoglobulins of the primary antibody species, isolated and then conjugated with the enzyme or the fluorophore. These bind to the antigen-antibody complexes and produce a colour producing reaction (for example in immunoperoxidase staining) or can be detected using a fluorescence microscope (immunofluorescence). The resulting colour change or fluorescence can be used for calculating the differential expression of such protein in the tissues. The primary antibodies used for indirect immunohistochemistry in this study have been listed in Table 2.11.

Antibody	Source	Type	Dilution
Anti glucose-regulated protein 78 (Anti-GRP78)	SPA-826; Stressgen, now Enzo life sciences, Exeter, UK	Rabbit polyclonal against mouse GRP78	1:200
Anti-phosphorylated c-Jun N-terminal kinase (anti-pJNK)	SC6254; Santa Cruz Biotechnology, Santa Cruz, USA	Mouse monoclonal against human pJNK	1:75
Anti ionised calcium binding adapter molecule1 (anti-IBA-1)	019-19741 Wako Chemicals GmbH, Neuss, Germany	Rabbit polyclonal against human Iba1	1:240

Table 2.11: Details of the antibodies used for immunohistochemistry using DAB staining

2.10.4.2 Slide preparation for immunohistochemistry staining

A common enzyme system used for labelling antibodies is horseradish peroxidase (HRP) and its substrate of 3,3 diaminobenzidine (DAB). The enzyme can react with hydrogen peroxide and release atomic oxygen. The free oxygen oxidises DAB and produces an insoluble brown end product which precipitates to leave a stain on the tissue.

However some cells and tissues have endogenous enzymes capable of catalysing the reaction in ways similar to HRP. Such enzymes need to be inactivated prior to the addition of the secondary antibodies by a procedure called quenching which uses the mechanism of enzyme inhibition in presence of excess substrate to form a catalytically inactive product. Hydrogen peroxide is thus used to inactivate the endogenous HRP like activity of tissues.

Another step necessary for effective staining involves the unmasking of the antigen so that it is identified by the antibody (epitope retrieval). This is important for formalin fixed paraffin embedded tissues as during the process of fixation, formalin can cause formation of cross linkages of

unrelated proteins leading to the loss of immunoreactivity [378]. The latter can be restored by one of several epitope retrieval processes [379] which include enzymatic digestion using proteases, microwave heating with citrate buffer, or a combination of both.

Appropriate controls for the reagent and tissues are necessary for the validation of the IHC results. In order to ensure specificity of the staining using the primary antibody, an appropriate negative control is used with all the reagent steps and exclusion of application of the primary antibody. Such a procedure will ensure ruling out of falsely positive results due to inherent peroxidase activity or nonspecific staining due to the binding of the secondary antibody.

2.10.4.3 Staining in immunohistochemistry

In order to visually identify the location and quantity of the target antigen, the antigen antibody complex requires a reporter. The reporters that generate colour are called chromogenic reporters. These are generally enzyme labels attached to the antibody which facilitates reactions between substrates to yield a coloured product visible under light microscopy.

Following appropriate slide preparation with the processes of quenching and epitope retrieval, the antibody attached to the chromogenic reporter, HRP produces a brown precipitate in the presence of DAB. The brown precipitate marks the location of the antibody on the slide which can then be visually identified (Figure 2.16).

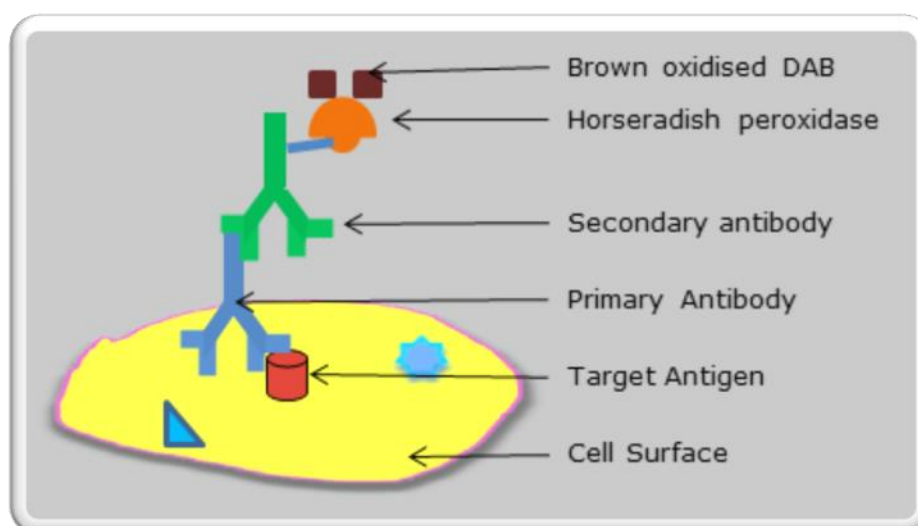


Figure 2.16: Schematic diagram demonstrating the principle of diaminobenzidine (DAB) staining in immunohistochemistry.

Following binding of a primary antibody to the target antigen, a secondary antibody tagged to horseradish peroxidase (HRP) enzyme complex in binds to the primary antibody. On addition of diaminobenzidine (DAB), the HRP enzyme complex converts into a brown precipitate which stains the cell surface at the location of the target antigen.

2.10.4.4 Immunohistochemistry procedure

The Leica BondMax™ automated IHC slide processor (Leica biosystems) which is run with the automated software program Bond version 3.4A (Vision Biosystems) was used for performing the IHC staining using Bond polymer refine detection reagents (Leica). The slides can be stained in batches of 30 after labelling them with a random identifier. This batch processing ensures uniformity of the staining protocol and identical staining on the slides. Optimisation of staining intensity can be performed by configuring the system protocol.

All slides were dewaxed and hydrated using xylene and ethanol washes for one minute each. The slides were incubated in Bond™ epitope retrieval 1 solution containing citric acid, buffer and surfactant and heated to 95°C. The duration of the next step of immersion in 3% hydrogen peroxide for quenching was determined by performing tests in a series of experiments during which 45 minutes quenching was identified to be ideal. This was followed by wash with Bond wash solution™ and distilled water which were

also used for all the subsequent washes mentioned below. All the samples except the negative control were exposed to 150µl of the optimised concentration of the primary antibody dilution as detailed in the Table 2.11 for 15 minutes. The antibody dilutions were prepared in Bond™ primary antibody diluent containing Tris-buffered saline and protein stabiliser. This was washed off and followed by exposure to 150µl of the secondary anti-mouse and anti-rabbit polymer conjugated to HRP. The DAB refine™ reagent was then added for 10 minutes to stain the antigen antibody complexes with brown colour. The background staining was then performed using 0.02% haematoxylin for 5 minutes. The sections were then dehydrated by two immersions of 100% ethanol for 2 minutes each and then ethanol cleared during two 3 minute immersions of xylene. Sections were mounted with coverslips (VWR) using DPX mounting medium (Fisher), and left to dry overnight. The steps of DAB staining and haematoxylin staining were excluded in one slide each to be used as source images for colour vector calculation.

The slides were visualised using Nikon Eclipse 90i microscope equipped with Micropublisher 3.3RTV high-speed colour CCD camera (QImaging, Surrey, BC, Canada). Randomly selected images at 10X and 20X magnification for both liver and adipose tissues were captured and saved using Volocity software version 6. (Improvision Ltd., Coventry, UK). Separate images of the brightfield (no slide in the light path) and darkfield (light path completely occluded with the diaphragm) were also saved for performing background correction.

Serial antibody dilutions were performed for each antibody to determine the appropriate optimum dilution. The recognised method of identifying the optimum antibody dilution [380] as the one that produces good staining whilst the next dilution has a sudden drop in staining intensity.

2.10.5 Quantification of adipocyte size

With increasing evidence indicating the importance of adipocyte size in metabolic inflammation and cell stress response [35, 36], accurate determination of adipocyte size gains importance [381]. Several methods of adipocyte size determination have been described, each with their advantages and disadvantages. The indirect methods include measuring the triglyceride and DNA content and the adipocyte size expressed as the ratio of triglyceride content per unit DNA content. However, the measured DNA content invariably will include the contribution from the stromal vascular fraction of the adipose tissue and hence will not only underestimate the adipocyte size, but also be affected by variation in the stromal vascular component seen in inflammation related to obesity. Another method includes estimation of osmium fixed fat cells derived from a known wet weight of adipose tissue [382, 383]. In this method, osmium fixed adipocytes are counted individually using an electronic counter and this cell number is used to divide the lipid weight measured from a comparable sample. The disadvantages of this method include the possibility of osmium causing the swelling of the cell [384], toxicity of osmium tetroxide and non-availability of an electronic counter. A method of measurement of adipocytes size after collagenase digestion has also been used. However, in this method the free adipocytes are distorted to a uniform circular shape and this method is also known to cause lysis of large adipocytes introducing error [384].

Direct measurement of adipocyte size from microscopic examination has been frequently reported. This can be performed using measured adipocyte diameter [385] or by measuring the adipocyte area [68]. Using the adipocyte diameter to calculate the volume is tedious and also assumes regular-spherical shape of the adipocyte. Using adipocyte area calculated from microscopy provides a better estimate of cell volume and

has been recently used and validated in comparison to other available methods [68, 386]. Automated methods using commercial [386] and public domain [387] software have been published and validated.

ImageJ is a public domain, Java-based image processing program developed at the National Institutes of Health [388, 389] and is widely used for image analysis and quantification of adipocyte size and DAB stain intensity [387, 390-392]. The plugins used in conjunction with the software are listed in Table 2.12 and their use described in individual sections.

Plugin Name	Author	Role
Calculator plus	Wayne Rasband [393] (nih.gov)	Performs calculation on RGB images. Used here to perform background correction of images
Color Deconvolution	Gabriel Landini [394] (bham.ac.uk)	Performs stain separation in a digital images resulting in separate images of individual stain location
Auto Thresholding	Gabriel Landini [395] (bham.ac.uk)	Process of identifying and applying a threshold point of hue in an image. The areas of image below this threshold are excluded as background staining.

Table 2.12: Details of the plugins used with ImageJ software for the process of quantification of the DAB staining in digital images.

2.10.5.1 Adipocyte size quantification procedure

The images were acquired from random areas of the slides and the samples had been given random numbers to keep the acquisition free of bias. Calibration of the images was performed using stage micrometers and constant exposure time and brightness settings were kept for every image for an experiment during the image acquisition and digital storage using the Volocity 6 software (Improvision Ltd, Coventry, UK). Image acquisition was performed at 20X magnification and the calibrated images were then converted to tagged image file format (TIFF) for further analysis using ImageJ software. This format is widely used for scientific imaging and maintains the advanced image data across various software platforms (Volocity, Microsoft paint and ImageJ). ImageJ software is also customisable to perform specific image processing tasks with the use of plugins. The images were manually studied in the Microsoft paint version 6.1 software (Microsoft Corp., USA) and areas of large blood vessels and partially imaged cells at the edge or artefacts were cropped out to exclude them. A minimum of 500 cells per sample were tagged manually using the paintbrush application of Windows paint application and the number counted using the magic-wand tool of the Volocity software. The total area of the image was calculated using the Volocity software and divided by the number of cells counted.

This method was devised in house and permitted an accurate and prompt measurement of mean adipocyte surface area by including a large number of adipocytes in analysis. Previously published methods [68, 396] using Volocity software involve manual measurement of individual adipocyte size making the process tedious leading to inclusion of fewer (approx. 100) adipocytes in the analysis. The in-house method permitted a prompt assessment of a mean 750 cells and demonstrated a high correlation with the previously published methods in 25 randomly selected images (Figure

2.17). Blinded analysis of mean area measured by two individual assessors also demonstrated minimal inter individual variation (Pearson correlation coefficient $r = 0.97$).

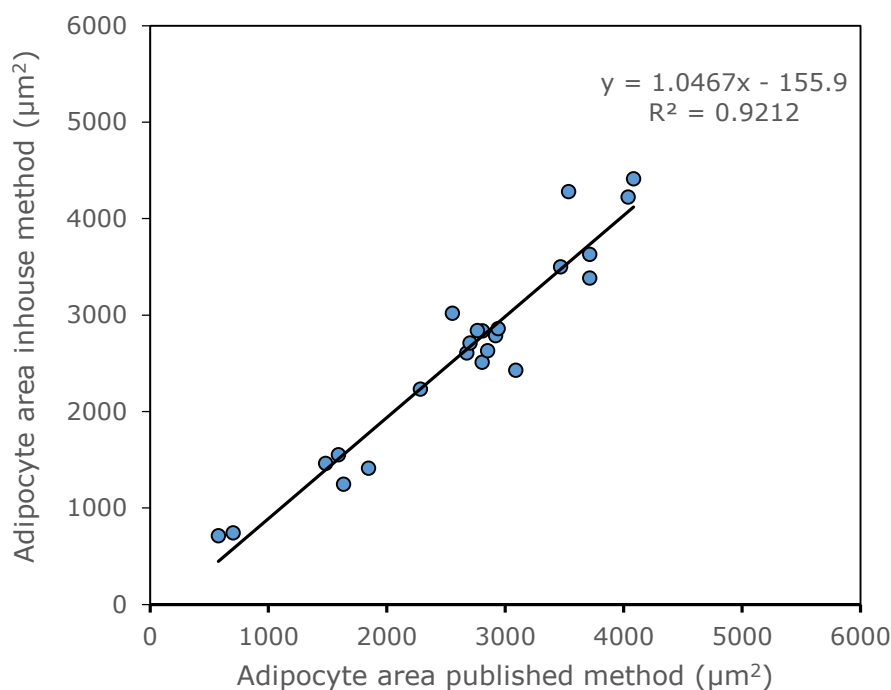


Figure 2.17 Graph demonstrating strong correlation of two different quantification methods of adipocyte size measurement.

The method developed in-house performed adipocyte size measurement as the value obtained by dividing the total surface area visible on a calibrated image from stained adipose tissue section by the total number of adipocytes in the field. The previously used and published method [68] involved manual measurement of individual adipocyte area in the image from stained adipose tissue slide. The correlation was performed in data obtained from 25 randomly selected images.

2.10.6 Quantitative assessment of DAB staining

Immunohistochemical staining is being increasingly used not just as a stain but as a precise, quantifiable immunoassay. A correlation between staining with immunohistochemical stain and protein levels have been demonstrated using Western blotting [397] and enzyme immunoassays [398]. Several automated protocols [390] for quantification of DAB staining are available and standardised computerised image analysis has been shown to be superior to manual methods in several comparative studies [399-401].

Quantification of images using computers involves transforming components of images to quantifiable numbers. A digital image is formed by combination of pixels where each pixel represents the smallest point with individual characteristics. Two of the models used to describe these pixels are intensity with RGB model and colour density with optical density (OD) models.

RGB stands for the initials of the three primary colours red, green and blue. Every colour in the spectrum can be represented by intensity of the red, green and blue components of that colour. In computerised digital images, every pixel of a coloured image has a RGB value and these intensity values often range from 0 to 255, the range that a single byte consisting of 8 bits can offer. For example, pure red pixel in the RGB model can be represented by RGB values of 255, 0, 0 where there is 0 intensity of green and blue colour. Using this colour model, standardised mathematical modifications to all the experimental images can be performed. One such example of a standardised mathematical modification of an image is whilst performing background correction.

A background correction needs to be performed on digital images of microscopic slides to exclude artefacts from the image present due to

variation in background illumination intensity, colour temperature of the light source and also artefacts from the camera (hot pixels) or the light path [402]. A priori correction of the background images uses images of brightfield (with no slide) and darkfield (blocking the light path) captured at the time of image acquisition (Equation 2.2). In the ImageJ software, this process can be done by performing the calculations given in the Equation 2.2 with the use of an open source plugin called Calculator plus published by Rasband [393].

$$\text{Corrected image} = \frac{\text{Specimen} - \text{darkfield}}{\text{Brightfield} - \text{darkfield}}$$

Equation 2.2: Principal equation used in performing background correction using the plugin Calculator plus and the ImageJ software [402].

A brightfield image is taken with the same light source and illumination with no slide and darkfield image is taken with the same settings but an opaque obstruction in the light path. The RGB values of the images are calculated using ImageJ software and following calculation using the equation, the resulting RGB values of each pixel is used to redraw a corrected image.

The corrected image obtained as a result is free from artefacts and variations in image present due to variance in illumination, light path or camera (Figure 2.18).

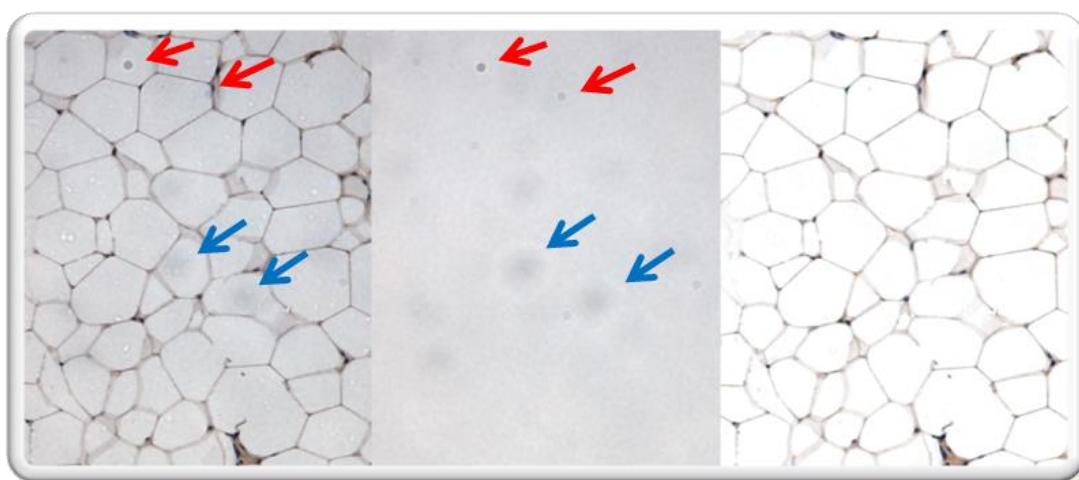


Figure 2.18 A series of representative images demonstrating the process of background correction.

A) Uncorrected images with artefacts (red arrows) and variation in light path (blue arrows) B) Brightfield image with no slide in the light path demonstrating the same artefacts and variance in light path as visible in image A. C) Same image following removal of artefact and variation in illumination after background correction.

Another method of representation of colour intensity is through the OD model where the optical density represents the absorbance of the light by that colour. This model is used for colour differentiation. The process of differentiating one stain from another in an image of a slide has to overcome the challenge of co-localisation of the stains, such as staining of the nucleus by both, haematoxylin and DAB stains. Many techniques of colour separation have been developed with good success reviewed by Bray et. al [390]. The commonly used and validated [403] technique for colour deconvolution [404] was first introduced by Ruifrok et. al. The process requires determining the relative RGB characteristics of the DAB and the haematoxylin stain. For this, samples stained with DAB only and also samples stained with haematoxylin only are first used to determine the RGB and OD values in absence of the other stain. These values can be mathematically normalised after representing them in an orthogonal matrix equation where each row represents the stain and each column represents the optical density values of the RGB components of each stain (Equation 2.3).

$$\begin{array}{ccccccc}
 & \text{R} & \text{G} & \text{B} & & & \\
 \begin{array}{l} \text{r} \\ | \\ \text{L} \end{array} & \begin{array}{l} \text{r1} \\ \text{r2} \\ \text{r2} \end{array} & \begin{array}{l} \text{g1} \\ \text{g2} \\ \text{g2} \end{array} & \begin{array}{l} \text{b1} \\ \text{b2} \\ \text{b2} \end{array} & \begin{array}{l} \text{r} \\ | \\ \text{J} \end{array} & \begin{array}{l} \text{DAB} \\ \text{Eosin} \\ \text{Background} \end{array} &
 \end{array}$$

Equation 2.3: Orthogonal matrix equation. Each row represents a stain and each column represents the optical density of the RGB components of each stain

The normalised optical densities of the counterstain (eosin in the case of immunohistochemistry with DAB) can be subtracted from the DAB OD values and the resultant values used to construct an image with just the outcome of the above calculations (Equation 2.3). The reconstructed

image with just DAB can then be used to quantify the area of DAB staining. The dimensions were not adjusted for shrinkage of tissue.

This software required for this process has been constructed as an open source plugin called Colour Deconvolution[®] Dr G Landini [394]. This free software license plugin can be included into the ImageJ software package and the optical density vectors of the DAB staining particular to the lab can be calculated and used to construct an image with DAB stain only (Figure 2.19)

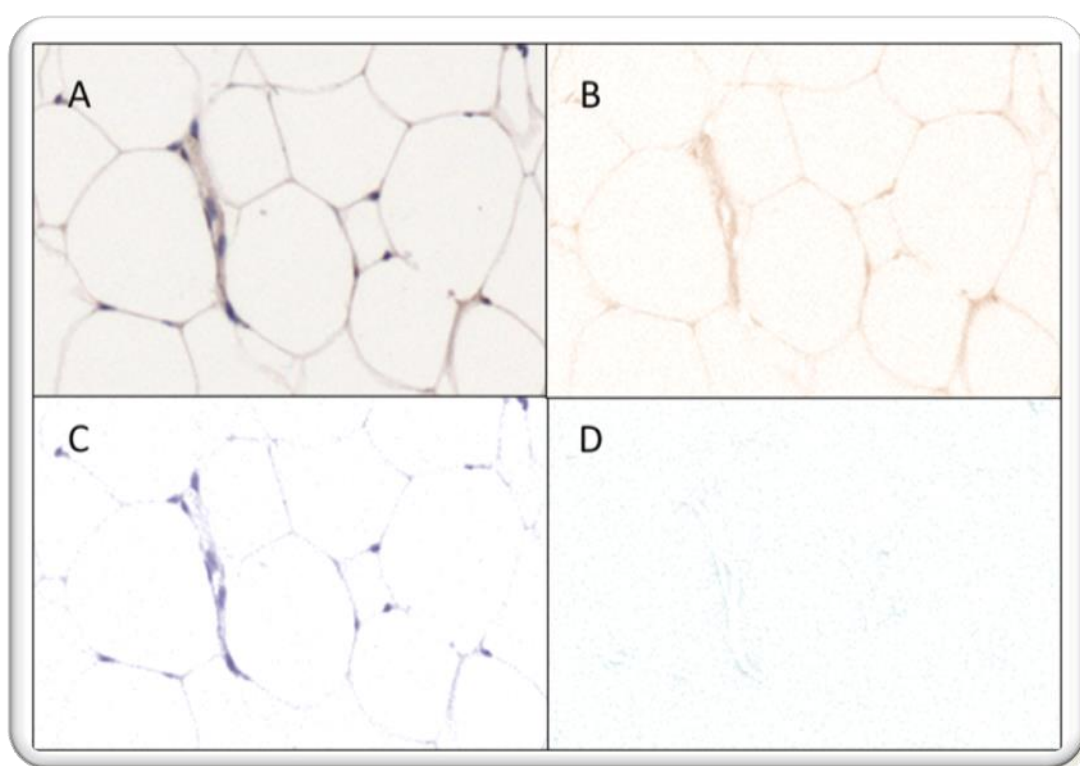


Figure 2.19: Colour deconvolution of DAB and haematoxylin stain using the ImageJ software plugin called ColorDeconvolution [394].

Using custom optical density matrices calculated from slides stained with only haematoxylin and only DAB respectively, a DAB stained digital image (A) can be separated into separate images which pick out the brown stain of the DAB (B), blue stain of the haematoxylin (C) and the background staining (D). The image B can be further processed to quantify the DAB staining.

The next step is quantification of the DAB stain. Before this can be performed, the step of thresholding is performed. This step ensures that nonspecific staining seen in negative control is accounted for. The images are quantifying after removing the background stain by the process of

thresholding [130]. The thresholds were standard for each experiment and were identified from a series of thresholding procedures available in the auto_threshold.jar plugin [395]. The chosen threshold showed minimal staining of the negative control slide (with no antibody; Figure 2.20). The same thresholding procedure was applied to all the sample images and the data obtained in pixels converted to μm^2 using the calibration values obtained by the graticules during the image acquisition.

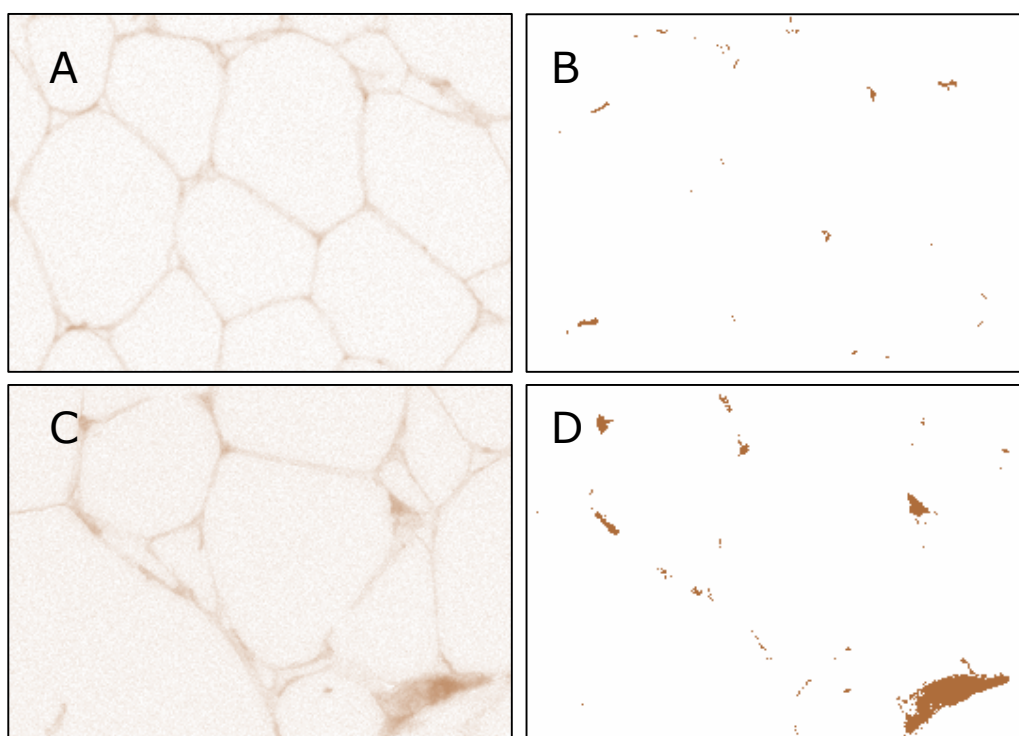


Figure 2.20 : Images demonstrating thresholding procedure on a representative negative control and sample.

A) A 10X image of a negative control tissue slide demonstrating residual background staining similar to DAB B) Same image as B following automatic threshold correction demonstrating minimal false positive uptake of the DAB stain. The amount of false positive uptake was corrected for by using the watershed tool. C) 10X image of a representative sample following colour deconvolution demonstrating DAB staining D) The outcome of thresholding step on image C demonstrating DAB staining isolation.

2.10.6.1 Quantification of DAB staining in adipocytes

The image acquisition using Volocity 6 software (Improvion Ltd, Coventry, UK) for the slides stained with TNF α , pJNK and GRP78 antibodies was performed at 20 X magnification. For slides stained with

Iba1 antibody, 10X magnification was used so as to cover a larger surface permitting analysis of infrequently occurring crown like structures in the tissue. The calibrated images (as described in 2.9.4.1) were then converted to tagged image file format (TIFF) for further analysis using ImageJ software. All the commands described hereafter in this section are summarised in Table 2.13. After performing the background correction using the calculator plus plugin and the tools of the ImageJ software, the images were cropped and surface area of adipocytes was calculated as described above. Images of slides stained without haematoxylin and without DAB were used to calculate vectors for colour deconvolution using the plugin (Commands: Plugins>Colour deconvolution> From ROI, show matrices> save log). The vectors thus generated were used to modify the java plugin and new vectors were saved with customised name UON DAB. The new vectors were then used to perform the colour deconvolution step in all the images. The colour deconvoluted image containing the DAB stain thus generated was processed by automated thresholding to exclude contribution of nonspecific staining. The thresholded images were quantified for the number and area of the stain (Analyse> analyse particles). The data were saved and used for statistical analysis. Notable, in the adipocyte the cytoplasm and the cell organelles were located as a thin rim on the periphery while the lipid formed the majority of the cellular content. As a result the stain in the adipocyte in tissues from obese animals was either spread thinly along the wall or was concentrated in pockets of perinuclear cytoplasmic content. In order to avoid underestimation introduced by increasing lipid fraction of the adipocyte area and in keeping with published methods [68], the immunohistological output was expressed as stained area per adipocyte.

Step	Image J command sequence
Background correction	ImageJ> Process> Image Calculator> Brightfield-Darkfield
	ImageJ> Image> Rename> Divisor
	ImageJ> Process> Image calculator> Image- Darkfield
	ImageJ> Image> Rename> Numerator
	ImageJ> Plugin> Calculator plus; i1= Numerator; i2 = divisor, k1 =255; divide (i1/i2)*k1
	ImageJ> Image> Rename> Background corrected Image
Colour deconvolution	ImageJ> File> Open> Background corrected image> Save
	ImageJ> Plugins> Color Deconvoluton>UON DAB
	ImageJ>Rename>DAB Image> Save
Thresholding	ImageJ> Image>Adjust> Auto threshold>Method-Max entropy; ignore black
	ImageJ> Image> Rename> Thresholded
Quantification	ImageJ>Analyse>Particles

Table 2.13: Table listing the commands used in ImageJ software for quantification of the DAB staining in digital images. The individual steps were automated using the Macro functionality of the ImageJ software. The matrix for the UON DAB command was calculated in-house from images of slides containing no DAB and no haematoxylin respectively.

2.11 Statistical analyses

All animal work presented in this thesis was performed by my colleagues at the University of Nottingham. The intention of this thesis was to investigate the nutritional programming of the cell stress in the omental adipose tissue and liver during different early life developmental periods. Whilst it is important to minimise the number of animals investigated, it is important to ensure that the available number of liver and adipose tissue samples were sufficient to provide adequate sensitivity to statistical result, necessitating the calculation of statistical power.

2.11.1 Statistical power and sample size

The power of a study is defined as the probability of rejecting a null hypothesis when the null is false [405]. An adequately powered study will, therefore obtain a statistically significant result when a difference exists, whereas, an underpowered study may fail to demonstrate a statistical significance when a difference between the experimental groups exists

(type II error). Conventionally the power of a study is kept at 80% which would mean that the maximum probability of a type 2 error is 80% and the value of α , the probability that null hypothesis is rejected when the null is true (the experimental observation occurred by chance) is set at less than 5% (significance criterion of $p < 0.05$).

Ideally, for any experimental study, the sample size calculation is performed prospectively and requires the knowledge of the following variables:

- Standard deviation in the population (s)
- The expected effect size
- The desired values of α (conventionally < 0.05)
- The desired power of the study (conventionally accepted at 80%)

However, there are several factors that preclude *a priori* sample size estimation for studies such as this. Firstly, each of the multiple downstream experiments including physiological parameters, proteomics and gene expression analysis would have their own individual standard deviation and effect size and inclusion of each of these in sample size calculation is not possible. Furthermore, there is absence of a direct relationship between statistical effect size and clinically significant effect. For example, identification of a statistically significant fold change in gene expression, by itself, does not correspond to clinically significant outcome. It is therefore not possible to designate a target effect size of biological studies such as this.

Several approaches have been used to overcome the absence of *a priori* power calculation. These include:

- prospectively calculated sample size for standardised values
- retrospective power calculation
- pattern recognition by analysis of biological pathways through multiple experiments

For calculation of sample size and statistical power, several propriety software packages and online resources are available [406, 407]. However it is important to understand the relationship between observed effect size in an experiment and standardised effect size used to prospectively calculate sample size and power of study. In an experiment involving comparison of continuous variables, the sample size can be calculated using Snedecor and Cochran equation [407] (Equation 2.4 below)

$$n = 1 + 2C\left(\frac{s}{d}\right)^2$$

n = sample size

C = constant based on value of significance criterion and power

s = standard deviation

d = effect size (Cohen's d)

Equation 2.4 Snedecor and Cochran equation used to calculate sample size in randomised experiments involving comparison between two groups of continuous variables.

The value of C is constant for an experiment and can be obtained from statistical resources [407, 408]. For example, in a study design with a statistical power of $\geq 80\%$ and a significant result of $p < 0.05$, the value of C in the equation is 7.5.

The effect size in statistics means the strength of change in a phenomenon. Simplistically it is represented by the difference between the mean values of two experimental groups (mean difference). When the

standard deviation of the two groups is taken to account, it can be standardised to standardised mean difference (Cohen's d). After completion of an experiment or in a pilot study, this can be calculated using the observed means and standard deviations [409, 410]. However, for prospective sample size calculations, in absence of observed effect size, standardised values are used for small, medium, or large effect size and are represented by accepted values of Cohen's d as 0.2 d , 0.5 d and 0.8 d respectively [409].

Therefore, using the Snedecor equation, the recommended sample size for an experiment with 10% standard deviation designed to study a standardised mean difference of 20% would be >4.5 in each group. Even after accounting for losses due to death of offspring, the minimum sample size in the study groups is 7 animals. This study therefore permits experiments to be performed with minimum power of 80% and statistical significance of 0.05 as for experiments where the ratio between the standard deviation and the standardised mean difference is >1.53 .

In absence of prospective power calculation, retrospective power calculations (observed power) can be performed using SPSS. However, the appropriateness of such an approach has been disputed [405, 406, 411]. The opponents of such practice state that whilst the effect size and standard deviations from an experiment can be useful tools for planning a future experiment, in the absence of a non-significant result, a retrospective analysis of observed power is a 1:1 function of the p value [411] and in absence of statistical significance, the calculated power cannot be interpreted. The supporters of retrospective power analysis [405] have argued that identification of high value of observed power in retrospective analysis is helpful as it demonstrates that non significance occurred due to absence of phenomenon. However, a low value of observed power on retrospective analysis is not able to differentiate

whether the non-significance is the outcome of a type II error or a genuine absence of phenomenon.

The third strategy used to minimise error in correlation between statistical result and clinical phenomenon involves investigation of multiple components of same biological pathway through various means including laboratory assays, gene expression and proteomics study. Findings of such descriptive experiments inform further detailed analysis and also provide valuable statistical data for prospective sample size calculation.

2.11.2 Choice of statistical tests

The statistical analysis was performed using IBM SPSS Statistics version 22 software (IBM Corp©). For analysing continuous variables originating from distinct groups such as those in this study, the choice of statistical test depend the distribution of the data around the mean. The data can thus be normally distributed around the mean or have a skewed distribution. During statistical analysis, Shapiro-Wilks test analysis was performed to determine the distribution of data. The relevant parametric test was performed for data found to be normally distributed around the mean. For data demonstrated to have a non-normal distribution, retesting was performed following logarithmic transformation. If the transformed data were also not normally distributed, appropriate non parametric test was performed as described below.

2.11.2.1 Comparison of variables originating from two groups

Data analysis typically involves comparison of means of dependant variables from comparable experimental groups. If the experimental study compares two independent groups (Chapter 4), and data meet the assumptions of homogeneity of variance and normal distribution, the independent t-test was performed. IBM SPSS automatically carries out the Levene's test of homogeneity of variance during such testing and if the

homogeneity of variance was deemed to be unequal (Levene's $p < 0.05$) the outcome of adjusted t statistic was used.

If the data were not normally distributed despite \log_{10} transformation of data, Mann Whitney U test was used for statistical analysis of the continuous data.

2.11.2.2 Data analysis in factorial study design

Continuous data originating from more than two independent groups (as is the case in Chapters 3 and 5) cannot be compared using multiple t testing as such a procedure would increase the probability that any significant finding is a type I error (called familywise error). This is because as more tests are conducted, the likelihood that one or more are significant just due to chance increases. Such data are therefore first analysed using an omnibus test like ANOVA which first attempts to identify overall experimental effect, a finding which is then confirmed by comparison between individual groups.

A factorial study design analyses for interaction between two or more variables. For example the experiment to determine the effect of late gestational nutrient restriction (N) and obesogenic environment (O) on the gene expression for CD68, analyses combinations of two different independent variables (nutrient restriction and obesogenic environment). This experiment is designed not just to study the impact of these independent variables but also their interaction with each other. The output of the omnibus test used in such studies– independent design factorial ANOVA will demonstrate the individual impact of N and O (output described as main effect) on the gene expression of CD68 and also if any interaction is present between N and O (output described as interaction effect) that impact this gene expression. Such an interaction could be ordinal interaction – for example if CD68 gene expression had increased

with obesity but in the nutrient restricted group, the increase was significantly more, exaggerating the value of the outcome variable (Figure 2.21) . In contrast, disordinal interaction would mean that the two variables interact to oppose each other's direction of change. Thus a statistically significant outcome of factorial ANOVA indicates presence of overall difference in the means under comparison and the presence of an interaction. However, it does not provide details of the direction or the extent of the difference between individual groups in the experiment for which further testing is required.

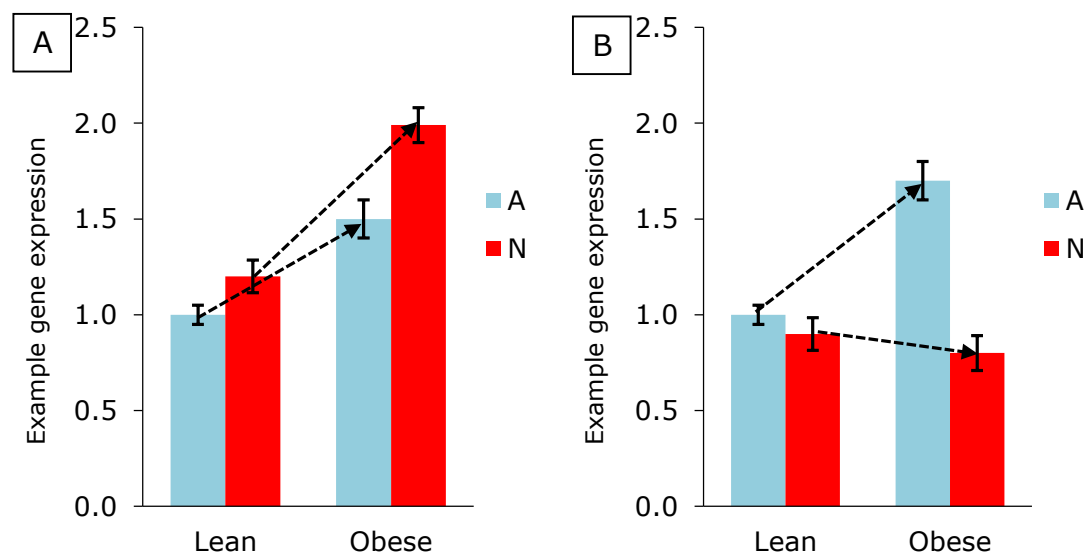


Figure 2.21 Representative graphical examples demonstrating ordinal (A) and disordinal (B) interaction between two variables with dotted arrows denoting the direction of the change.

In Figure A, the direction of change in gene expression in response to the two variables (obesity with groups lean and obese and nutrient restriction with groups fed to appetite (A) and nutrient restricted (N)) is same which would be an ordinal interaction between the two variables. Figure B demonstrates disordinal interaction where the direction of change in gene expression with the two variables is opposite. The gene expression increases with obesity, whereas it is decreasing with nutrient restriction.

In the presence of a significant outcome of factorial ANOVA, indicating either presence of main effects or that of an interaction between the factors under investigation, a hypothesis driven simple main effects analysis can be performed to perform sub group analysis. This pairwise comparison between combinations of the treatment groups ensures that

the familywise error rate is less than the commonly accepted value of 0.05. If the number of sub-groups in a factorial analysis are three or greater, a post hoc test such as Bonferroni needs to be performed. However, in a two by two comparison, such post hoc testing is neither required nor possible [412, 413]. In SPSS, a simple effects sub-group analysis is not available using custom tools. This was performed using Syntax. The syntax for a representative example of simple effects analysis is demonstrated in Figure 2.22.

```
UNIANOVA CD68 BY Factorial_Prenatal Factorial_Obesity
/METHOD=SSTYPE(3)
/INTERCEPT=INCLUDE
/POSTHOC=Factorial_Obesity(TUKEY)
/PLOT=PROFILE(Factorial_Prenatal*Factorial_Obesity)
/EMMEANS=TABLES(Factorial_Prenatal*Factorial_Obesity) COMPARE(Factorial_Prenatal) ADJ(BONFERRONI)
/EMMEANS=TABLES(Factorial_Prenatal*Factorial_Obesity) COMPARE(Factorial_Obesity) ADJ(BONFERRONI)
/PRINT=OPower ETASQ HOMOGENEITY DESCRIPTIVE
/CRITERIA=ALPHA(.05)
/DESIGN=Factorial_Prenatal Factorial_Obesity Factorial_Prenatal*Factorial_Obesity.
```

Figure 2.22 Representative example of Syntax used for simple main effects analysis performed following identification of a significant effect or interaction in two-way ANOVA procedure.

For data which did not confirm to a normal distribution, the 2 way ANOVA is considered a robust test for analyses of data which are of non-normal distribution [414]. However, in keeping with established practise, independent samples Kruskal-Wallis test followed by Mann Whiney was performed to confirm the findings of ANOVA testing and results were reported as significant only when confirmed by the non-parametric tests. However, there is no current method to perform the equivalent of simple effect analysis of subgroups in the event of a statistically significant Kruscall-Wallis test. It was necessary to deduce likely difference by inspection of the medians followed by performance of Mann Whitney U test between the identified sub-groups. For sake of uniformity of presentation and in keeping with standard practice, data were expressed as mean and

standard error of the mean for all the experimental output irrespective of the type of distribution of the data.

2.11.2.3 Analysis of data involving repeated measures

Statistical analysis of a series of data collected over time for the same subject need to account for the repeated measures to prevent occurrence of a type I error. For studies with factorial designs and repeated measures, the purpose of the statistical test is to understand group differences over time where groups are formed by the combination of between-subjects factors. In such a scenario, time is included as an independent factor that is common to the subject (within-subject factor) in addition to the experimental conditions, which differ between the subjects (between-subject factors).

A two-way mixed ANOVA is the choice of statistical test if the design consists of a combination of one within-subject factor and one between-subject factor. For example, a study where animals were fed either formula milk or mother's milk (type of feed is the between-subject factor) have body weight measurements recorded every 2 weeks for 8 weeks (serial body weight measurements are the within subject factors).

If the study design has one within-subject factor in addition to two between-subject factors, the analysis is performed using a three-way mixed ANOVA. For example, three-way mixed ANOVA is used in a study where body weight is measured every 2 weeks for 8 weeks (within-subject factor) in animals that differ in combination of two different variables such as type of feed and mother's nutrition (between-subject factors).

Mixed ANOVA testing identifies interaction amongst the variables as an omnibus test and, by itself, does not specify which specific groups within each factor were significantly different from each other. In the presence of an interaction between experimental factors, additional testing is the

required to identify specifics of differences between groups. When this additional testing explores effect of combinations of experimental factors, it is called simple effects analysis and when this analysis explores the effect of the experimental interventions they are called main effects analysis. For example, the main effect analysis for the three way study design described above would explore the effect of type of feed irrespective of maternal nutrition whereas a simple effect analysis would explore the difference between animals who had same feed type (example formula feeds) but differed in maternal nutrition.

Application of two-way or three-way mixed ANOVA testing method is conditional upon confirmation of data characteristics such as normal distribution, sphericity, homogeneity of variance and absence of large outliers [415]. Appropriate transformations to the data as described in Section 2.11.2 can be attempted to make the data fit the required data characteristics. Post hoc correction for multiple comparisons is required if the number of subgroups in a factorial analysis are three or greater. However, in a two by two comparison, such post hoc testing is neither required nor possible [412, 413]

3 The effect of prenatal nutrient restriction and obesity on the cell stress response and metabolic inflammation in liver and adipose tissue

3.1 Introduction and hypothesis

This chapter describes the outcome of an investigation performed to study the following two questions:

1. does obesity promote cell stress and inflammation in the liver and adipose tissue?
2. does late gestational nutrient restriction (NR-LG) of the mother enhance the effects of cell stress in the liver and adipose tissue in the young adult offspring?

In addition to being important in the body's metabolic functions, adipose tissue and the liver are organs capable of initiating and modulating a cellular stress response and metabolic inflammation in response to a stressful environment [39, 212]. Interventional experiments in small animal models [40] and descriptive studies in humans [41, 387] have demonstrated the role of cell stress responses and metabolic inflammation in both liver [163, 416] and adipose tissue [21] in the development of obesity related insulin resistance. Studies of the Dutch Famine cohort described in Section 1.6.2.1 revealed that, in comparison to a control group of individuals not exposed to *in utero* undernutrition, offspring of women experiencing severe undernutrition in the third trimester had reduced birth weight [258] and impaired glucose tolerance at a mean age of 50 years [261], a finding which was confirmed when the glucose tolerance testing was repeated at the age of 58 years [417]. This cohort also had abnormal lipid profiles [418].

As discussed in Section 1.6.2.1, animal experiments in sheep models of NR-LG have demonstrated compromised glucose and insulin profiles when compared to offspring of sheep fed to requirements [315]. Sharkey *et al.* demonstrated increased gene expression for CD68 and TLR4 in the visceral adipose tissue of juvenile sheep who had experienced NR-LG [275]. In another study, early gestational nutrient restriction led to differential alteration of the ER stress response and inflammation in visceral (perirenal) adipose tissue and kidney associated with increased CLS in adipose tissue following juvenile onset obesity [68]. There have been no large animal interventional studies to characterise the cell stress response to obesity in the liver or other adipose tissue depots or which have examined the potential of developmental programming of this cell stress response pathways as pathogenic mechanisms for the metabolic morbidity of individuals exposed to *in utero* NR-LG.

The experiments described in this chapter investigate the following hypotheses (summarised in Figure 3.1).

1. It is hypothesised that increased fat deposition in liver and features of non-alcoholic fatty liver disease in obesity would be associated with increased gene expression of the regulators and components of the cell stress response.
2. It is hypothesised that obesity would lead to increased adipocyte size in the visceral fat depot located around the omentum, greater abundance of macrophage infiltration and CLS and raised gene expression of components of cell stress response and metabolic inflammatory pathways as compared to non-obese animals.

It is hypothesised that NR-LG would, by the process of developmental programming, promote cell stress within the liver and adipose tissue, thereby exacerbating metabolic inflammation. It is predicted that this would manifest as further augmentation in the gene expression of

pathways of cell stress response and metabolic inflammation. Ultimately, this would further compromise metabolic homeostasis and decreased insulin sensitivity in the offspring born to nutrient restricted mothers.

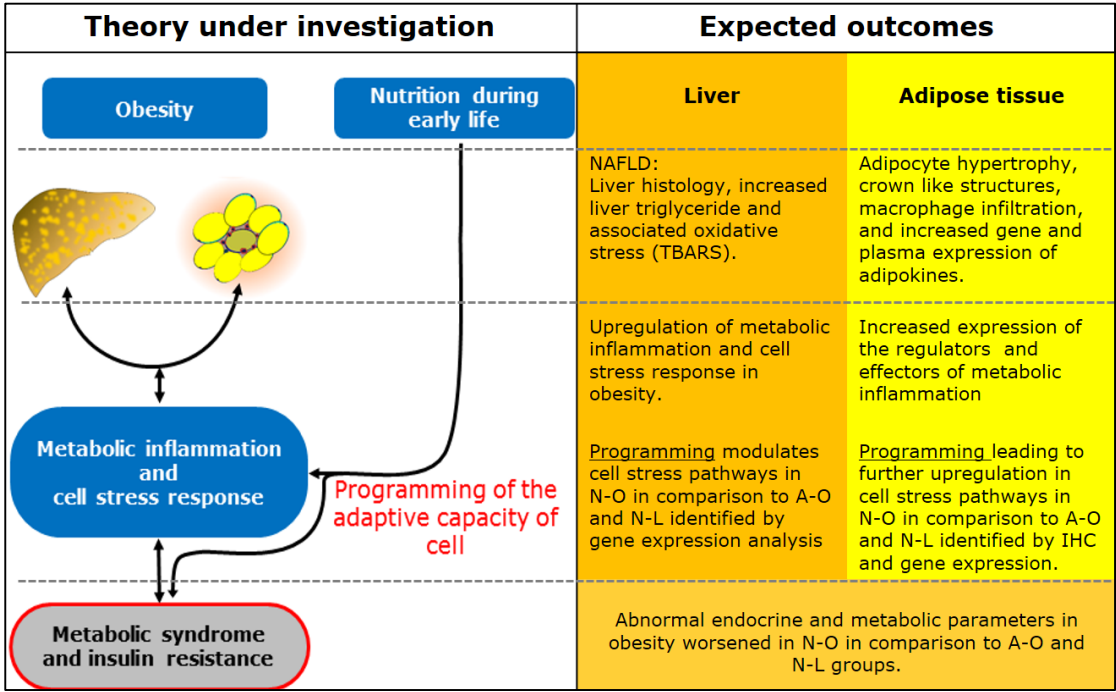


Figure 3.1 Schematic flow chart summarising the study hypothesis and expected outcomes of the investigation.

Offspring of pregnant sheep allowed to feed to appetite during late gestation were either raised in an environment allowing physical activity resulting in a lean phenotype (A-L) or were raised in a restricted obesogenic environment leading to an obese phenotype (A-O). Offspring of ewes nutrient restricted during late gestation were either raised in an environment allowing physical activity resulting in a lean phenotype (N-L) or were raised in a restricted environment resulting in an obese phenotype (N-O). The various experiments performed are marked next to the stage in the proposed pathogenic process in the experimental hypotheses. NAFLD, Non-Alcoholic Fatty Liver Disease; IHC, Immunohistochemistry.

3.2 Methods

The design of the study, animal interventions and all experimental methods used to establish the results described in this chapter are described in detail in the Chapter 2. Briefly, after confirmation of twin gestation by ultrasound scanning, twin bearing ewes were randomised to either nutrient restriction (N) from gestational day 110 until term (145 ± 2 days) or fed to appetite (A) during the same period. After birth, twin offspring were all reared by their mother until weaning at 90 days of age when they were separated to be reared in an environment restricting physical activity leading to obesity (O) or an environment allowing normal physical activity in which they remained lean (L). The combination of prenatal (A and N) and postnatal factors (L and O) develops a factorial experimental design of four groups (A-L, A-O, N-L and N-O) as depicted in Figure 3.2. The control group for the experiments described in this study is the A-L group.

During pregnancy, blood sampling was performed from the ewe at 130 days gestational age and plasma was analysed for concentrations of glucose, insulin, non-esterified fatty acids (NEFA) and triglycerides. Following delivery of the lambs, birth weight was recorded followed by regular body weight measurements; physical activity was measured using accelerometers at age 1.5 months and 15 months; glucose tolerance tests and blood sampling was performed at age 7 months and 16 months respectively; body composition analysis was performed by DXA scanning at 16 months of age. All the animals were humanely euthanased at 17 months of age and, after weighing organs, representative samples from liver and adipose tissue were taken, snap frozen in liquid nitrogen and stored at -80°C until further processing.

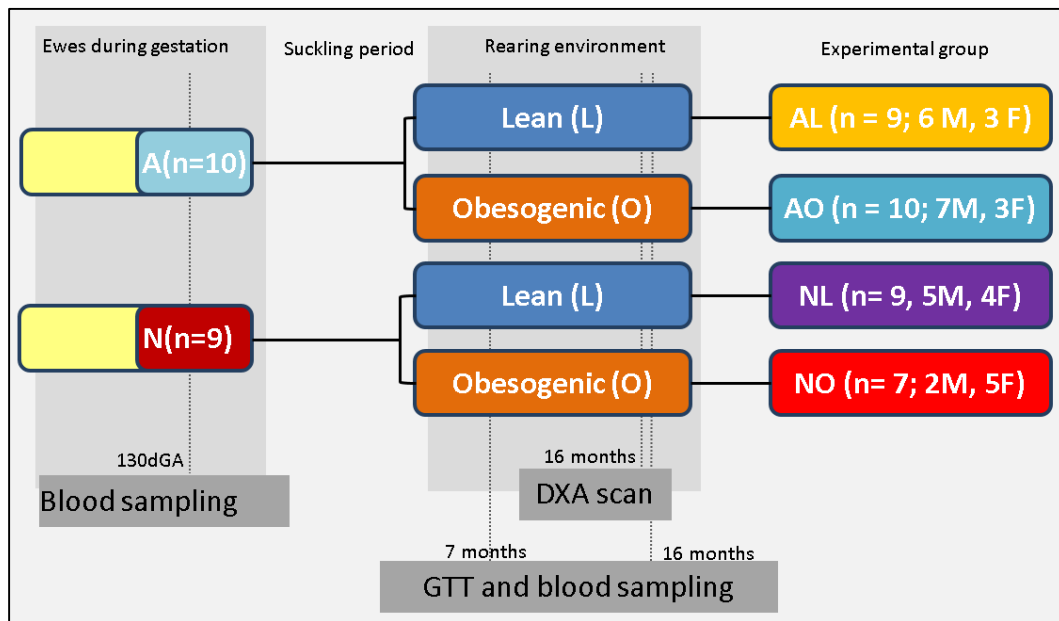


Figure 3.2 Schematic diagram depicting the factorial experimental design for study of interaction of prenatal nutrient restriction and postweaning rearing environment.

From 110 days gestational age (dGA) to term, twin bearing ewes were fed to appetite (A) and, following the suckling period (birth - 90 days), twin offspring were separated either to rearing in an environment restricting physical activity leading to obesity (A-O) or to an environment allowing physical activity where they remained lean (A-L). Twin bearing ewes were nutrient restricted to 60% of their caloric requirements during late gestation (N) and, after weaning, one of the twin offspring was reared either in an environment restricting physical activity leading to obesity (N-O) or in an environment allowing physical activity where they remained lean (N-L). During the suckling period, the offspring were reared together with their mother in all groups. DXA, dual-energy X-ray absorptiometry; GTT, glucose tolerance test; dGA, days gestational age.

The output of laboratory experiments, which were performed in duplicate, was only accepted for analyses if the coefficient of variation between the experimental replicates was less than 5%. The statistical analyses has been described in Chapter 2. Briefly, for the factorial study design, the data were first interrogated with two-way analysis of variance (2-way ANOVA). Upon identification of a significant effect or interaction in the 2-way ANOVA, a hypothesis driven simple main effects analysis was performed for comparison between groups differing in only one factor (prenatal nutrient restriction or environment of rearing). Although the 2-way ANOVA is considered robust for analyses of data which are not

normally distributed [414], non-parametric testing using Kruskal-Wallis test followed by Mann Whitney was performed for any such data for confirmation of the ANOVA findings. Outcome for GTT and body weight measurements produced data with repeated measures in same animal over time. Analyses for such data with repeated measures were performed with two way or three way mixed ANOVA. Time was analysed as within subject factor to assess for interaction between time and experimental conditions (between-subject factors). For sake of uniformity of presentation and in keeping with standard practice, data have been expressed as means and standard error of the means for all the experimental output irrespective of the distribution of the data.

The inequality of numbers in the final experimental groups, as depicted in Figure 3.2 is the result of offspring death at various ages. A total of 4 offspring died or were lost to follow-up. This represents 10% loss in the overall experiment and is in keeping with standard mortality rates in sheep experimental studies [329, 330].

3.3 Results

3.3.1 Maternal and offspring metabolic profile

3.3.1.1 Weight gain and metabolic parameters of pregnant ewes

At the time of randomisation at 110 days of gestation, the body weight of ewes randomised to nutrient restriction (N, n=10, 73.2 \pm 1.8 kg; mean \pm SEM) or to feeding to appetite (A, n=10, 71.9 \pm 1.7 kg) was not statistically different (p=0.87). Two-way mixed ANOVA was performed and time (dGA) was included as a within subject factor to account for repeated measures. There was a statistically significant interaction between the maternal nutrition and time on body weight expressed as percentage of weight at the beginning of intervention (p<0.001). Upon simple effects analysis, the ewes randomised to nutrient restriction were identified to have significantly lower body weight at 120dGA, 130 dGA and at delivery (Figure 3.3).

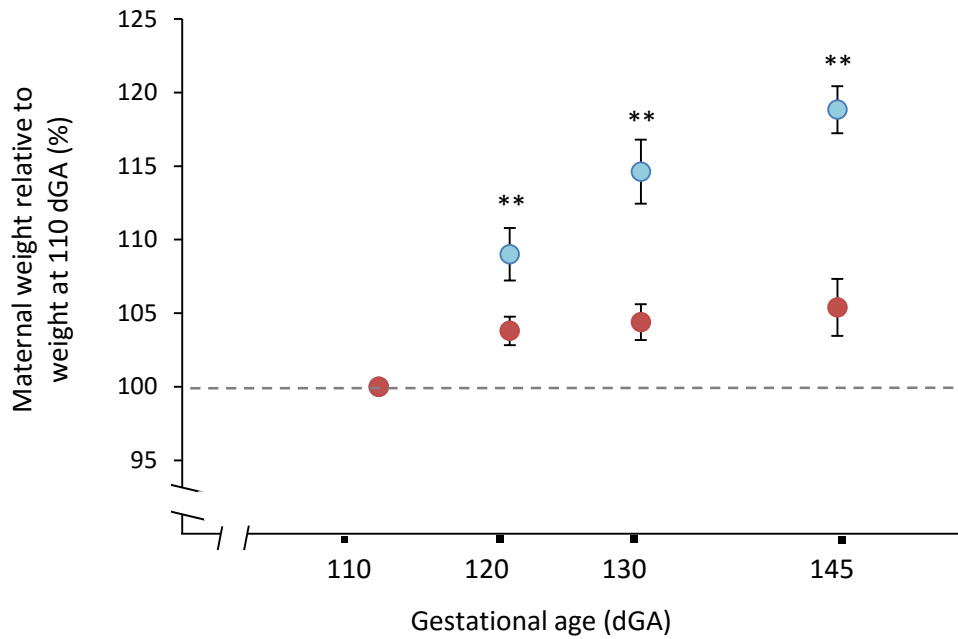


Figure 3.3 Maternal weight gain during late gestation, expressed as percentage gain over the weight at 110 days of gestation (dGA).

Ewes were fed a diet delivering 60% of caloric requirements (N, red, n=10) or were allowed to feed to appetite (A, blue, n=10) between 110 – 145 dGA. Two-way mixed ANOVA was performed with time (dGA) as within subject factor to account for repeated measures. ** $p < 0.001$ for N versus A simple main effect comparison. Data are means with error bars representing SEM.

At 130 dGA, 20 days into the nutritional intervention, the N ewes had lower plasma insulin and glucose concentrations and higher plasma NEFA as compared to A ewes (Figure 3.4 A, B and C). Plasma cortisol concentrations at 130 days gestational age did not differ between N (26.9 ± 5.4 nmol/L) and A (18.0 ± 4.8 nmol/L) ewes.

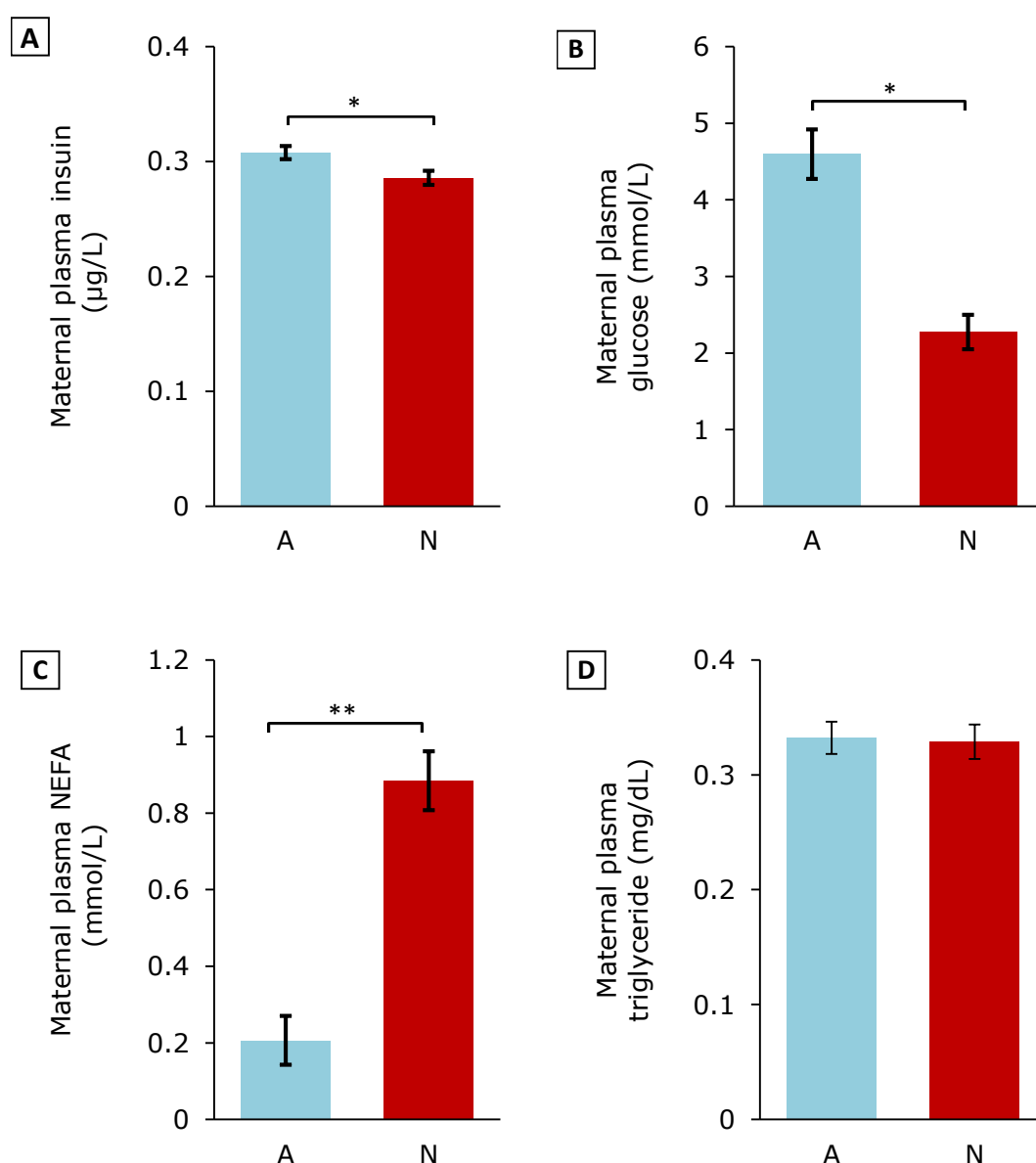


Figure 3.4 Fasting plasma insulin (A), glucose (B), non-esterified fatty acids (NEFA, C) and triglyceride (D) concentration measured from plasma taken at 130 days of gestational age from ewes randomised as described to nutrient restriction (N, red, n=9) or allowed to feed to appetite (A, blue, n=10) between 110 – 145 days gestational age. Data are means with error bars representing SEM * $p < 0.05$ and ** $p < 0.001$ for N versus A comparison. Data analysed by Mann-Whitney U test for plasma insulin and glucose concentrations.

3.3.1.2 Offspring birth weight and weight gain and physical activity phenotype during the suckling period

The birth weight of twin offspring of ewes randomised to restricted nutrition (N) during late gestation was lower as compared to offspring of the A ewes (N: 4.07 ± 0.14 kg; A: 4.63 ± 0.16 kg; $p=0.02$). The mean z-score of the birth weight of N offspring was -3 in comparison to the birth weight of the A group. Two-way mixed ANOVA to account for repeated measures with time (age) as within subject factor analysis did not identify a significant interaction between the experimental groups and time ($p=0.19$). Pairwise comparison demonstrated that the N offspring remained lighter in body weight as compared to the A offspring during for the main effect of prenatal intervention ($p=0.024$, Figure 3.5).

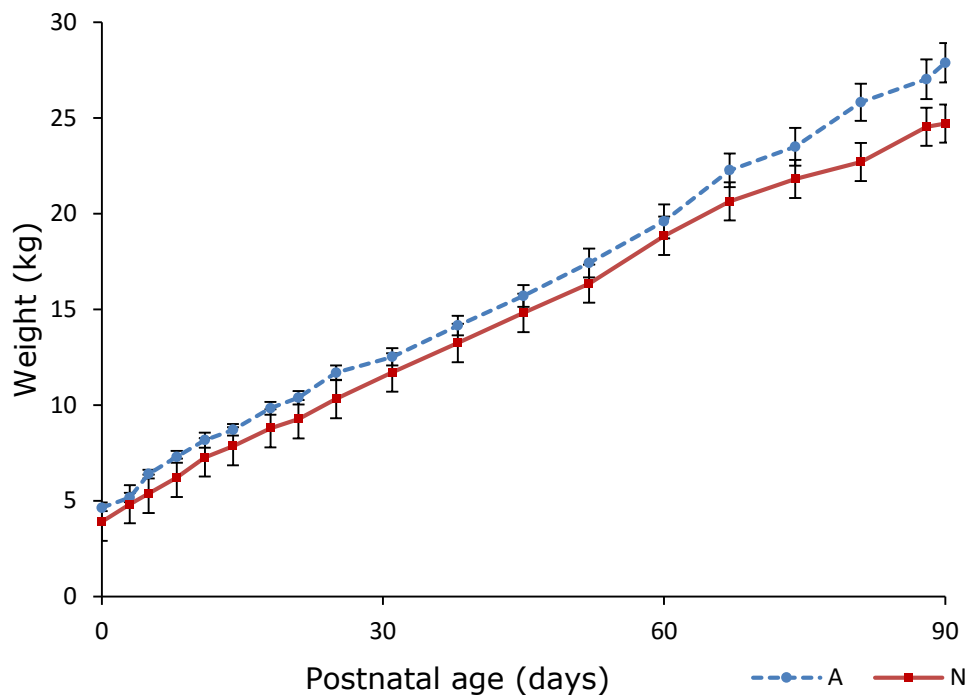


Figure 3.5 Weight gain during the suckling period (birth to 90 days) in offspring of ewes randomised as described to nutrient restriction (N, red, n=16) or allowed to feed to appetite (A, blue, n=19) between 110 – 145 days gestational age. Data are means with error bars representing SEM. Two-way mixed ANOVA was performed with time (age) as within subject factor to account for repeated measures. $p=0.19$ for interaction between prenatal intervention and time. $p=0.024$ for overall main effect of prenatal nutrition.

Body weight gain relative to birth weight (relative weight gain) was not different between the N and R groups (Figure 3.6)

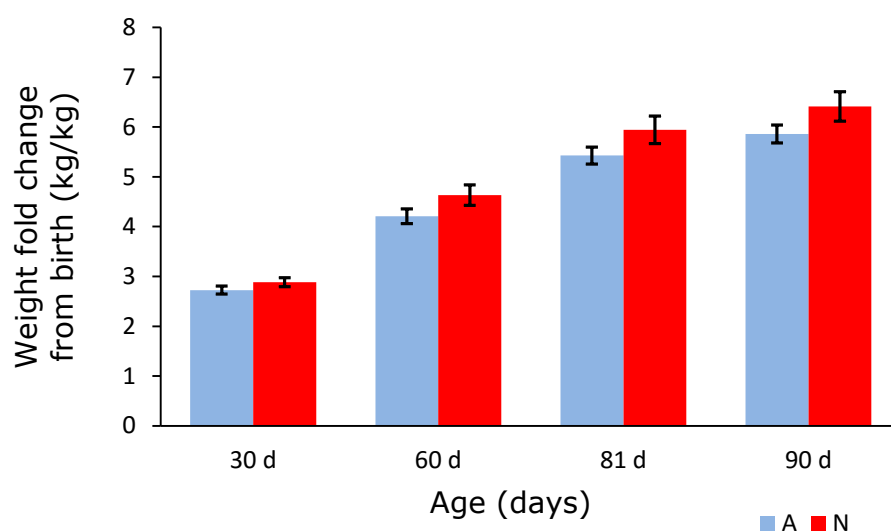


Figure 3.6 Body weight fold change relative to birth weight (i.e. relative weight gain) in offspring of ewes randomised as described to nutrient restriction (N, red, n=16) or allowed to feed to appetite (A, blue, n=19) during late gestation. Data are means with error bars representing SEM.

Physical activity measurements were recorded using accelerometers and expressed as unit counts and analysed as mean activity over a 24 hour period. Mean activity, duration of activity and maximum intensity of activity did not differ in the offspring of N and A ewes at age 45 days (Table 3.1).

Physical activity parameter	A	N
Mean activity (counts)	160 ± 14	173 ± 11
Duration mobile in 24 hours (minutes)	931 ± 64	963 ± 51
Maximum intensity of physical activity (counts)	2972 ± 183	3148 ± 347

Table 3.1 Physical activity parameters at 45 days of age in offspring of ewes randomised as described to nutrient restriction (N, n=18) or allowed to feed to appetite (A, n=19) during late gestation. Data are displayed as means ± SEM.

3.3.1.3 Effect of the environment of rearing on the body weight, physical activity parameters and the adipose tissue depots

Statistical analysis was performed using three-way mixed factorial ANOVA to account for within subject factor of time as a repeated measure. The three-way interaction between age, prenatal nutrition and rearing environment were not statistically significant ($p=0.41$). There was a significant two-way interaction between environment of rearing and age ($p=0.001$). There were statistically significant simple main effects of obesity on weight on measurements after age 12 month ($p=0.001$, Figure 3.7).

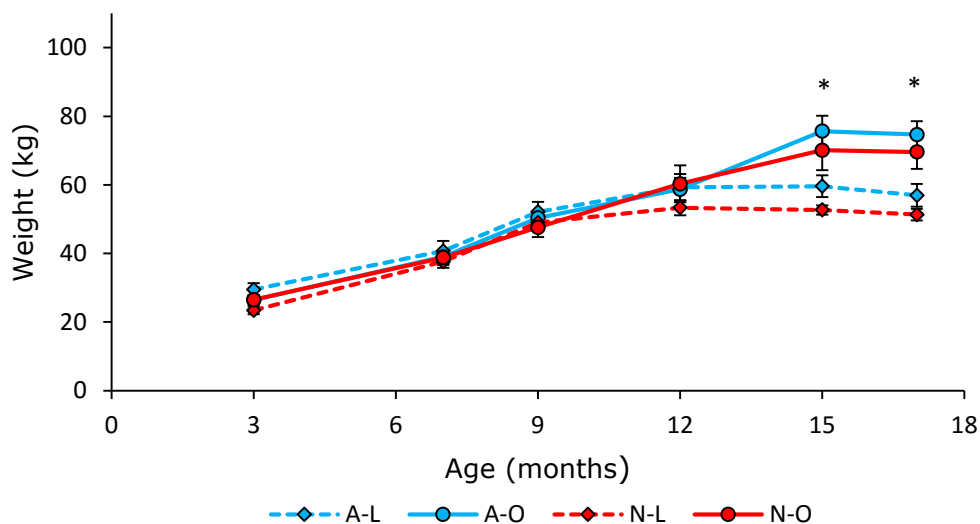


Figure 3.7 Effect of the post-weaning environment on body weight in offspring of sheep fed to appetite during late gestation and reared for a lean phenotype (A-L; $n=9$) or obese phenotype (A-O; $n=10$) and offspring of sheep nutrient restricted during late gestation reared for a lean phenotype (N-L; $n=9$) or obese phenotype (N-O; $n=7$). A three-way ANOVA was performed to account for repeated measurement of weight at different timepoints. * $p<0.05$ for obese versus lean simple main effects following a significant two-way interaction between environment of rearing and time. Data are expressed as means with error bars representing SEM.

Physical activity quantified using accelerometer demonstrated decreased physical activity in both groups raised in obesogenic environment (A-O and N-O) in comparison to their lean comparison groups (A-L and N-L respectively). The duration of mobility was not different in any comparisons and the measurements for the maximum intensity of physical activity were higher in N-L group as compared to the N-O group (Table 3.2).

Physical activity parameter	Maternal nutrition	Phenotype		Prenatal Nutrition <i>p</i> value	Obesity <i>p</i> value	Inter-action <i>p</i> value
		Lean	Obese			
Mean activity (counts)	A	471±67 ^c	150± 13 ^d	0.91	<0.001	0.21
	N	536±69 ^c	74±33 ^d			
Duration mobile in 24 hours (minutes)	A	1018±52	940±68	0.62	0.68	0.87
	N	984±54	541±199			
Maximum intensity of activity (counts)	A	1670±149	1553±131	0.45	<0.01	0.20
	N	1956±168 ^a	1221±77 ^b			

Table 3.2 Physical activity parameters at 12 months of age for offspring of sheep fed to appetite during late gestation and reared for a lean phenotype (A-L; n=9) or obese phenotype (A-O; n=10) and offspring of sheep nutrient restricted during late gestation reared for a lean phenotype (N-L; n=9) or obese phenotype (N-O; n=7). Data are displayed as means ± SEM. Non parametric Kruskal-Wallis tests followed by Mann-Whitney test performed for all comparisons for confirmation of ANOVA outcome. Statistical difference denoted by superscripts a versus b, $p<0.05$; c versus d, $p<0.001$

The weights of visceral adipose tissue depots of omental, pericardial and perirenal adipose tissue sampled following euthanasia at 17 months of age were significantly increased in offspring raised in obesogenic environment as compared to the respective comparative groups. Prenatal nutrient restriction had no impact on the adipose tissue weight (Table 3.3)

Adipose depot (g)	Maternal nutrition	Phenotype		Prenatal nutrition	Obesity	Interaction
		Lean	Obese	p value	p value	p value
Omental	A	313±65 ^c	1526±163 ^d	0.87	<0.001	0.39
	N	224±56 ^c	1655±151 ^d			
Pericardial	A	66±10 ^a	101±9 ^b	0.73	<0.001	0.24
	N	59±16 ^c	116±14 ^d			
Perirenal	A	279±43 ^c	1003±119 ^d	0.84	<0.001	0.62
	N	252±37 ^c	1014±104 ^d			

Table 3.3 Weight of omental, pericardial and perirenal adipose tissue depots at age 17 months for offspring of sheep fed to appetite during late gestation and reared for a lean phenotype (A-L; n=9) or obese phenotype (A-O; n=10) and offspring of sheep nutrient restricted during late gestation reared for a lean phenotype (N-L; n=9) or obese phenotype (N-O; n=7). Data are displayed as means ± SEM. Statistical difference denoted by superscripts a versus b, p<0.05; c versus d, p<0.001 for simple effects analysis following 2-way ANOVA.

The fat free and total fat mass was calculated from DXA scan at 16 months of age and demonstrated an increase in the calculated total body fat content when the offspring were reared in an obesogenic environment as compared to the respective lean groups. Prenatal NR-LG had no impact on the calculated total fat content. To calculate the relative proportion of visceral and non-visceral adipose tissue, the known quantity of visceral fat depots (omental+pericardial+perirenal fat) were used to calculate the relative proportion of visceral and non-visceral fat content of the body (Figure 3.8).

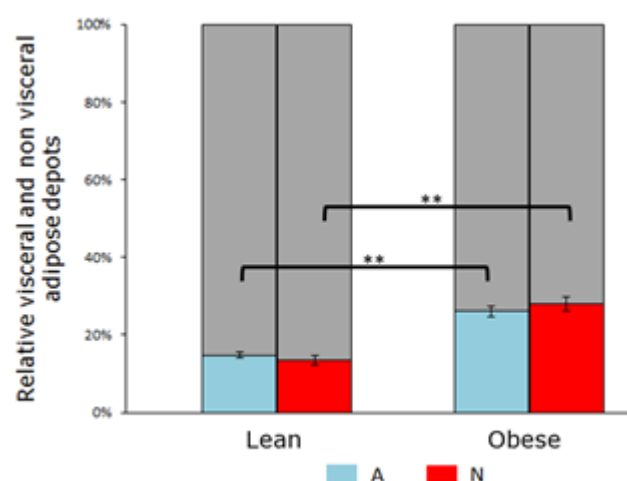


Figure 3.8 Relative proportion of visceral and non visceral adipose tissue weight at age 17 months for offspring of ewes allowed to feed to appetite during late gestation (blue) and reared to a lean phenotype (n=9) or to an obese phenotype (n=10). Offspring of ewes nutrient restricted during late gestation (red) were raised to a lean phenotype (n=9) or to an obese phenotype (n=7). The grey area of the histogram represents proportion of non visceral fat mass. **p<0.001 for simple effects analysis following 2-way ANOVA.

Expressed as a percentage of the total fat content, the proportion of visceral fat was significantly increased in the offspring raised in an obesogenic environment as compared to the respective lean comparison groups, demonstrating a predisposition to increased visceral fat deposition as a response to rearing in an obesogenic environment (Table 3.4).

	Maternal nutrition	Phenotype		Prenatal Nutrition <i>p</i> value	Obesity <i>p</i> value	Interaction <i>p</i> value
		Lean	Obese			
Body weight at DXA (kg)	A N	59.6±3.2 ^a 52.7±1.3 ^a	75.6±4.5 ^b 70.1±5.7 ^b	0.13	<0.001	0.86
Total FAT mass from DXA (kg)	A N	4.4±0.6 ^c 3.9±0.5 ^a	10.3±1.1 ^d 9.9±0.7 ^b	0.60	<0.001	0.97
Relative fat mass from DXA (%)	A N	7.3±0.7 ^c 7.5±0.9 ^c	13.6±1.2 ^d 14.4±1.0 ^d	0.87	<0.001	0.39
Visceral fat as % of total fat (%)	A N	14.8±0.7 ^c 13.4±1.2 ^c	26.1±1.3 ^d 28.1±1.8 ^d	0.82	<0.001	0.60

Table 3.4 Body weight and fat content parameters calculated and extrapolated from DXA measurements for offspring of ewes fed to appetite during late gestation (A) were either reared to a lean phenotype (n=9) or to an obese phenotype (n=10). Lambs born to ewes given nutrient restricted diet during late gestation (N) were either reared to a lean phenotype (n=8) or to obese phenotype (n=7). Data are displayed as means ± SEM. Statistical difference denoted by superscripts a versus b, $p < 0.05$; c versus d, $p < 0.001$ for simple effects analysis following 2-way ANOVA. DXA, dual-energy X-ray absorptiometry.

3.3.1.4 Plasma metabolic profile at the age of 7 months

The glucose measurements were analysed using three-way mixed ANOVA to account for repeated measures of glucose at different timepoints. There was a significant three-way interaction between the prenatal nutrition, environment of rearing and time ($p=0.019$). There was no statistically significant two-way interaction of prenatal nutrition and environment of rearing at any timepoint (Figure 3.9 A). NR-LG had no impact on the glucose measurements taken in offspring at 7 months of age. For the plasma insulin concentrations (Figure 3.9 B), the statistical analyses was not significant for a three-way interaction between experimental conditions and time ($p=0.39$). Further analysis did not identify a two-way interaction between the prenatal nutrition and time ($p=0.32$) or environment of rearing and time ($p=0.52$). Simple main effect test for two-way interaction between prenatal nutrition and environment of rearing was also not significant ($p=0.32$).

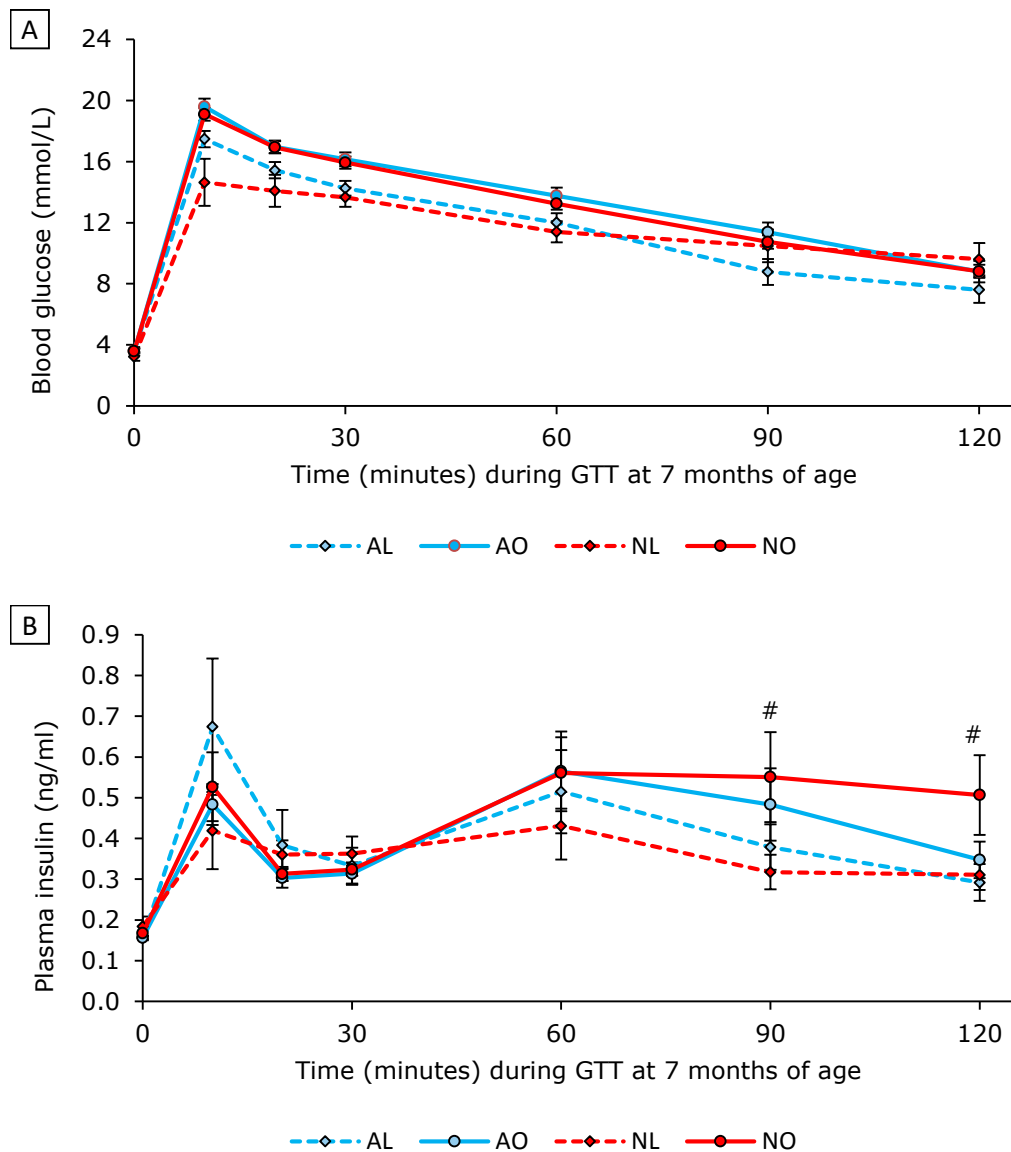


Figure 3.9 Plasma glucose (A) and insulin (B) concentrations during a glucose tolerance test performed at the age of 7 months.

Offspring of ewes allowed to feed to appetite during late gestation were either raised to a lean phenotype (A-L, blue diamond, dashed line, n=7) or to obese phenotype (A-O, blue circle, continuous line, n=9). Offspring of ewes nutrient restricted during late gestation were either raised to a lean phenotype (N-L, purple square, dashed line, n=5 for glucose and 7 for insulin) or to obese phenotype (N-O, red square, continuous line, n=7). *p<0.05 for A-L versus A-O comparison; #p<0.05 for N-L versus N-O comparison. Data are expressed as means with error bars representing SEM.

At 7 months of age, the raised glucose for obese animals during the GTT were reflected in the increased area under the curve (AUC) for glucose (Table 3.5), but the calculation of the surrogate marker for insulin sensitivity measured by homeostatic index-IR (HOMA-IR) was not increased by any experimental intervention.

	Maternal nutrition	Phenotype		Prenatal nutrition <i>p</i> value	Obesity <i>p</i> value	Interaction <i>p</i> value
		Lean	Obese			
Area under the curve glucose (mmol/L)	A	1370±67 ^a	1593±61 ^b	0.90	<0.01	0.69
	N	1377±64 ^a	1549±44 ^b			
Area under the curve insulin (ng/ml)	A	49.1±6.9	51.6±6.1	0.95	0.23	0.40
	N	43.2±5.2	56.7±7.9			
HOMA-IR	A	5.57±0.2	5.54±0.6	0.27	0.61	0.64
	N	6.89±1.8	6.07±0.4			

Table 3.5 Markers of insulin sensitivity expressed as area under the curve and HOMA-IR calculated from glucose tolerance test performed at age 7 months. Lambs born to ewes fed to appetite during late gestation (A) were either reared to a lean phenotype (n=7) or obese phenotype as described (n=9). Lambs born to ewes given nutrient restricted diet during late gestation (N) were either reared to a lean phenotype in (n=7 for area under the curve and 5 for HOMA-IR) or obese phenotype (n=7). Data are displayed as means ± SEM. Statistical difference denoted by superscripts a versus b, $p<0.05$; simple effects analysis following 2-way ANOVA. HOMA-IR, homeostatic index- insulin resistance.

The plasma triglyceride and the plasma non esterified fatty acids (NEFA) concentrations were similar in all groups (Table 3.6). As expected, plasma leptin was increased in obese animals in comparison to their respective lean comparison groups, although the comparison between the N-L and N-O groups did not achieve statistical significance. The morning plasma cortisol samples did not differ between any experimental groups.

	Prenatal nutrition	Phenotype		Prenatal nutrition <i>p</i> value	Obesity <i>p</i> value	Interaction <i>p</i> value
		Lean	Obese			
Plasma triglyceride (mg/dL)	A	0.20±0.02	0.14±0.02	0.84	0.36	0.92
	N	0.20±0.03	0.14±0.02			
Plasma NEFA (mmol/L)	A	1.32±0.11	1.34±0.18	0.79	0.55	0.48
	N	1.39±0.21	1.18±0.13			
Plasma cortisol (nmol/L)	A	48.7±11.7	92.7±24.5	0.27	0.14	0.24
	N	50.1±11.7	55.1±7.8			
Plasma leptin (ng/ml)	A	1.18±0.12 ^c	1.98±0.19 ^d	0.36	<0.01	0.36
	N	1.55±0.26	1.98±0.15			

Table 3.6 Plasma metabolic profile in the fasted state at the age of 7 months

Lambs born to ewes fed to appetite during late gestation (A) were either reared to a lean phenotype (n=7) or obese phenotype as described (n=9). Lambs born to ewes given nutrient restricted diet during late gestation (N) were either reared to a lean phenotype in (n=7) or obese phenotype (n=7). Data are displayed as means ± SEM. Statistical difference denoted by superscripts c versus d, $p < 0.001$; simple effects analysis following 2-way ANOVA. NEFA. Non esterified fatty acids.

3.3.1.5 Plasma metabolic profile at the age of 16 months

During the GTT at 16 months, the plasma glucose and insulin measurements were analysed using three-way mixed ANOVA to account for repeated measurements. The analysis for three-way interaction between prenatal nutrition, environment of rearing and time was not statistically significant ($p=0.765$). Further analyses for two-way interaction did not demonstrate a significant interaction between prenatal nutrition and time ($p=0.74$), environment of rearing and time ($p=0.45$) or between prenatal nutrition and environment of rearing ($p=0.79$). The plasma insulin concentrations did not demonstrate a significant three-way interaction between prenatal nutrition, environment of rearing and time ($p=0.874$). Analysis for 2 way interaction also did not demonstrate between prenatal nutrition and environment of rearing ($p=0.221$) or for environment of rearing and time ($p=0.12$). The interaction between prenatal nutrition and time approached statistical significance ($p=0.058$, Figure 3.10 B).

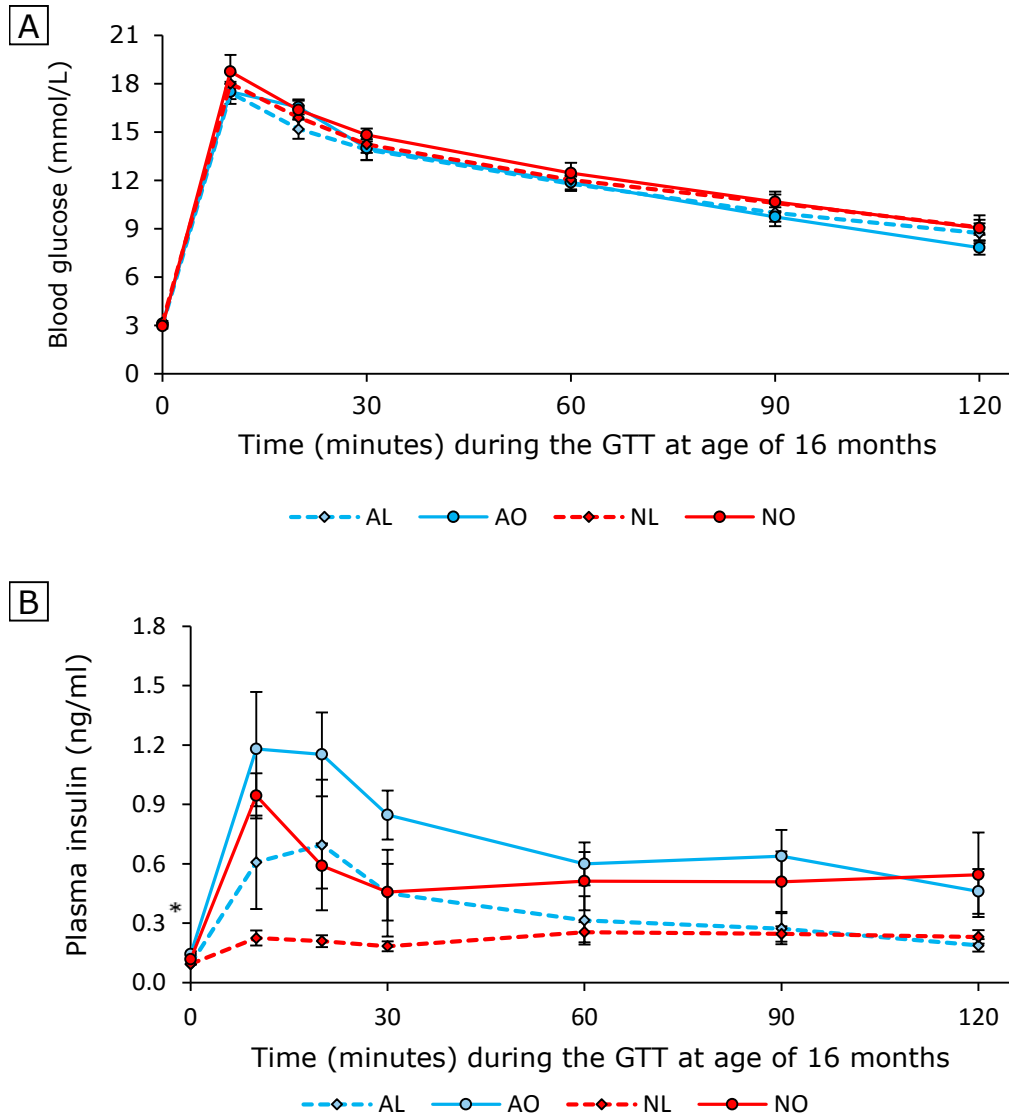


Figure 3.10 Plasma glucose (A) and insulin (B) concentrations during a glucose tolerance test performed at the age of 16 months.

Lambs born to ewes fed to appetite during late gestation were either reared to a lean phenotype (A-L, blue diamond, dashed line, n=7) or obese phenotype as described (A-O, blue circles, continuous line, n=8). Lambs born to ewes given nutrient restricted diet during late gestation were either reared to a lean phenotype (N-L, red diamond, dashed line, n=8) or obese phenotype (N-O, red circles, continuous line, n=6 for glucose and 5 for insulin). Statistical analysis performed using three-way mixed ANOVA to account for repeated measures. Data are expressed as means with error bars representing SEM.

The AUC for insulin response to GTT was significantly increased in obese offspring as compared to their lean counterparts. This finding, suggestive of insulin resistance, is supported by the values of HOMA-IR for sheep at age 16 months where the A-O group had significantly higher values compared to the A-L group (Table 3.7).

	Prenatal nutrition	Phenotype		Prenatal nutrition <i>p</i> value	Obesity <i>p</i> value	Interaction <i>p</i> value
		Lean	Obese			
AUC glucose (mmol/L)	A	1403±52	1402±40	0.17	0.73	0.71
	N	1455±39	1491±69			
AUC insulin (ng/ml)	A	31.7±14.8 ^a	67.7±9.1 ^b	0.60	<0.001	0.60
	N	15.7±3.9 ^a	49.8±14.5 ^b			
HOMA-IR	A	2.8±0.1 ^c	4.3±0.4 ^d	0.31	<0.001	0.90
	N	3.0±0.1	3.6±0.3			

Table 3.7 Markers of insulin sensitivity expressed as area under the curve insulin and HOMA-IR calculated from glucose tolerance test performed at age 16 months.

Lambs born to ewes fed to appetite during late gestation (A) were either reared to a lean phenotype (n=9) or obese phenotype as described (n=8). Lambs born to ewes given nutrient restricted diet during late gestation (N) were either reared to a lean phenotype in (n=8) or obese phenotype (n=5). Data are displayed as means ± SEM. Statistical difference denoted by superscripts a versus b, $p<0.05$; c versus d, $p<0.001$ (simple effects analysis following 2-way ANOVA). HOMA-IR, homeostatic index- insulin resistance.

Plasma leptin concentrations at 16 months of age were higher than the measurements performed at 7 months age in all groups. Furthermore, similar to the findings at 7 months of age, the A-O group had significantly higher plasma leptin concentrations as compared to the A-L group. There was no difference in the concentrations of plasma triglycerides, plasma NEFA or early morning plasma cortisol measurements (Table 3.8)

	Prenatal nutrition	Phenotype		Prenatal nutrition <i>p</i> value	Obesity <i>p</i> value	Interaction <i>p</i> value
		Lean	Obese			
Plasma triglyceride (mg/dL)	A	0.13±0.01	0.14±0.01	0.91	0.48	0.14
	N	0.16±0.01	0.12±0.02			
Plasma NEFA (mmol/L)	A	0.36±0.05	0.42±0.06	0.18	0.23	0.71
	N	0.43±0.07	0.53±0.06			
Plasma Cortisol (nmol/L)	A	26.3±4.7	47.3±15	0.63	0.08	0.70
	N	21.9±3.8	41.9±11.6			
Plasma leptin (ng/mL)	A	2.6±0.3 ^c	4.5±0.4 ^d	0.83	<0.01	0.14
	N	3.1±0.2	3.8±0.5			

Table 3.8 Plasma metabolic profiles in the fasted state at the age of 16 months.

Lambs born to ewes fed to appetite during late gestation (A) were either reared to a lean phenotype (n=9) or obese phenotype as described (n=8). Lambs born to ewes given nutrient restricted diet during late gestation (N) were either reared to a lean phenotype in (n=8) or obese phenotype (n=5). Data are displayed as means ± SEM. Statistical difference denoted by superscripts c versus d, $p < 0.001$ (simple effects analysis following 2-way ANOVA). NEFA, Non esterified fatty acids

3.3.2 Liver weight and triglyceride deposition

The liver weight at dissection was significantly greater in animals reared in obesogenic environment ($p=0.004$) and simple effects analysis reached significance in the N-O offspring in comparison to the N-L group ($p=0.007$). When expressed as proportion of body weight, the lean animals had similar values for the relative liver weight irrespective of prenatal maternal nutrition. However, when expressed as liver weight relative to total body weight, the relative weight of liver in the A-O group was significantly lower in comparison to the N-O group (Figure 3.11).

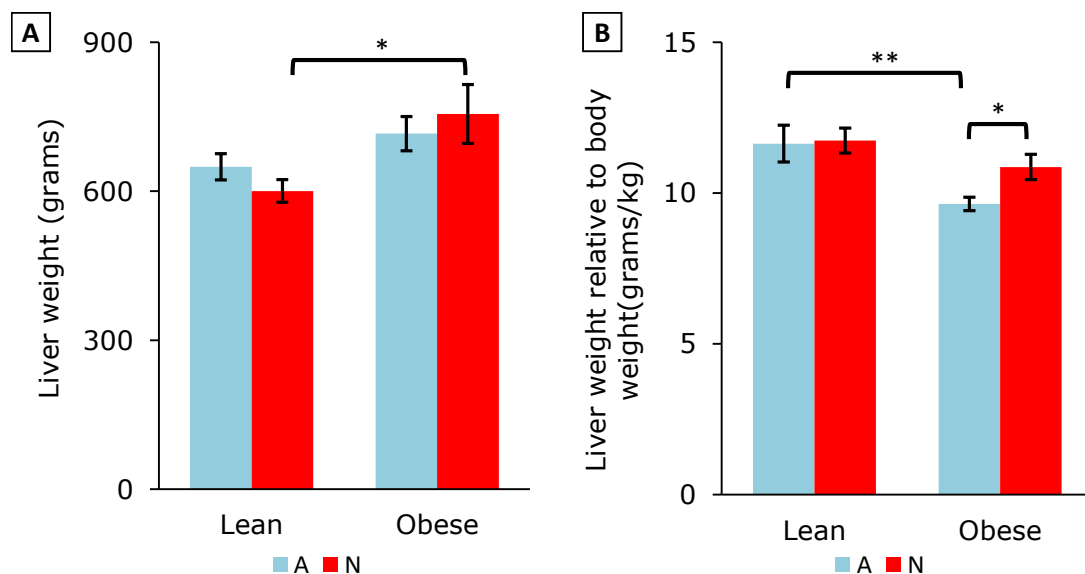


Figure 3.11 Organ weight of the offspring liver in grams (A) and relative (B) to the body weight in grams/kg.

Offspring of ewes allowed to feed to appetite during late gestation (blue) were either raised for a lean phenotype ($n=9$) or for obese phenotype ($n=10$). Offspring of ewes nutrient restricted during late gestation (red) were either raised for a lean phenotype ($n=9$) or for obese phenotype ($n=7$). * $p<0.05$ and ** $p<0.001$ for simple effects analysis following significant two-way ANOVA. Non parametric statistical tests performed to confirm the ANOVA findings for data displayed in the Figure 3.11B

Furthermore, measured liver tissue triglyceride concentrations were significantly increased in N-O offspring as compared to the N-L offspring which was also reflected in the relative total liver triglyceride content, calculated from the known liver weight and the relative concentrations (Table 3.9). This suggests that the increase in liver weight in the N-O group was related to increased triglyceride deposition in the liver.

	Prenatal nutrition	Phenotype		Prenatal Nutrition <i>p</i> value	Obesity <i>p</i> value	Inter-action <i>p</i> value
		Lean	Obese			
Liver weight (g)	A	649±26	716±34	0.89	<0.01	0.23
	N	600±23 ^c	755±59 ^d			
Liver triglyceride (mg/g liver tissue)	A	32.2±6.6	37.0±6.1	0.41	0.04	0.26
	N	28.6±3.78 ^a	48.3±7.8 ^b			
Total liver triglyceride (g)	A	21.2±0.44 ^a	27.0±0.55 ^b	0.55	0.02	0.18
	N	17.0±0.26 ^c	37.8±0.85 ^d			

Table 3.9 Liver triglyceride concentrations and total triglyceride content in different experimental groups.

Lambs born to ewes fed to appetite during late gestation (A) were either reared to a lean phenotype (n=9) or obese phenotype as described (n=8). Lambs born to ewes given nutrient restricted diet during late gestation (N) were either reared to a lean phenotype in (n=8) or obese phenotype (n=5). Data are displayed as means ± SEM. Statistical difference denoted by superscripts a versus b, $p < 0.05$; c versus d, $p < 0.001$ (simple effects analysis following 2-way ANOVA).

Correlation analysis between triglyceride concentration and liver weight demonstrated a stronger relationship between these variables in obese animals as compared to those from the lean groups. This was also reflected in the correlation between liver triglyceride content and the liver weight (Figure 3.12). These findings also support the proposal that the increased in liver weight in obese animals was due, at least in part, to triglyceride deposition within the liver.

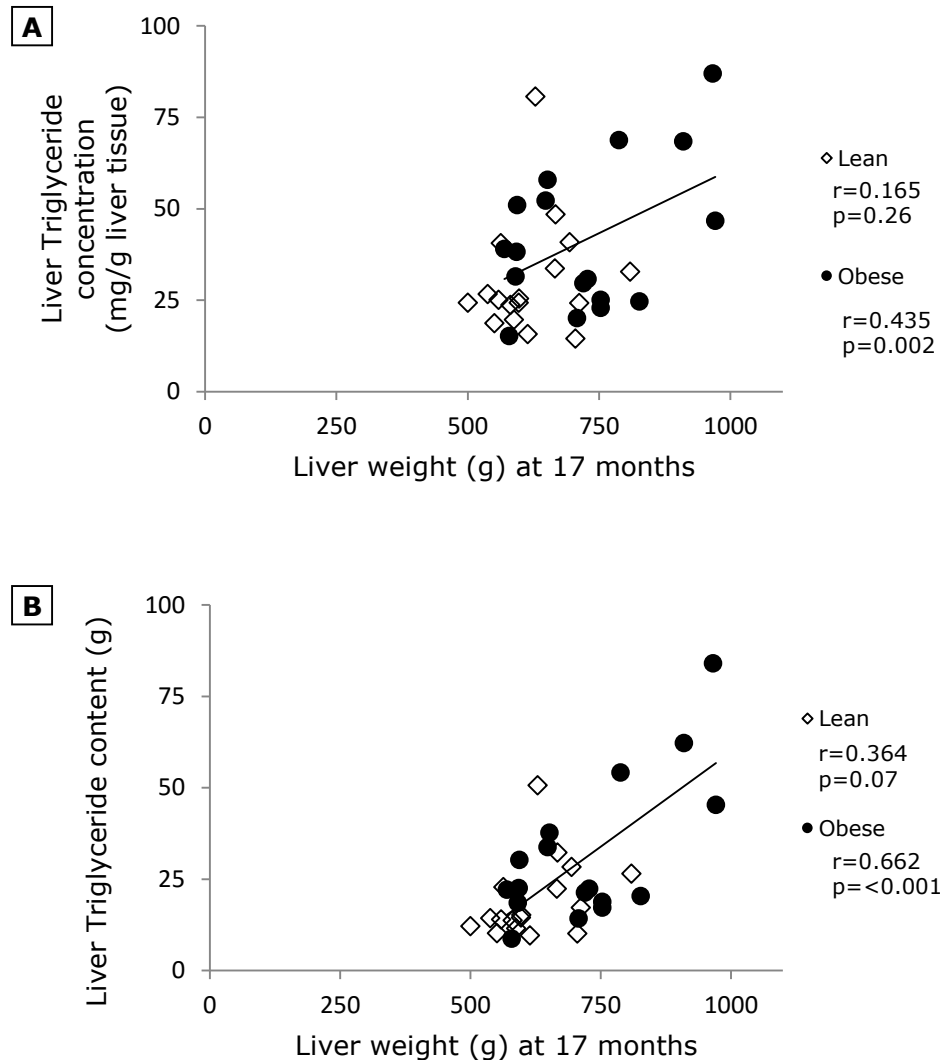


Figure 3.12 Correlation analysis of weight of liver at 17 months of age against measured liver triglyceride concentrations (A) and calculated total liver triglyceride content (B) respectively.

Lambs born to sheep undergoing nutritional interventions as described were reared in environment leading to development of lean phenotype (n=17) or obese phenotype (n=16). Data presented as Pearson's correlation coefficient and two-tailed significance testing. The trendline in both figures depict the statistically significant correlation in values from obese animals

Correlation analysis of total body weight at the age of 17 months performed against total liver weight and against total liver triglyceride content respectively demonstrated a linear relationship (Table 3.10)

Variable 1	Variable 2	Pearson's coefficient (r)	p value (two tailed)
Body weight at 17 months (kg)	Liver weight (g)	0.804	<0.001
Body weight at 17 months (kg)	Liver triglyceride (g)	0.489	0.004

Table 3.10 Correlation of body weight at 17 months of age (kg) against liver weight (kg) at dissection and total liver triglyceride content (g) respectively for all animals (n=35).

3.3.3 Liver histology

Liver samples from representative animals from both obese and lean groups were stained with H&E and with Masson's Trichrome stains to identify features of liver ultrastructure (Figure 3.13).

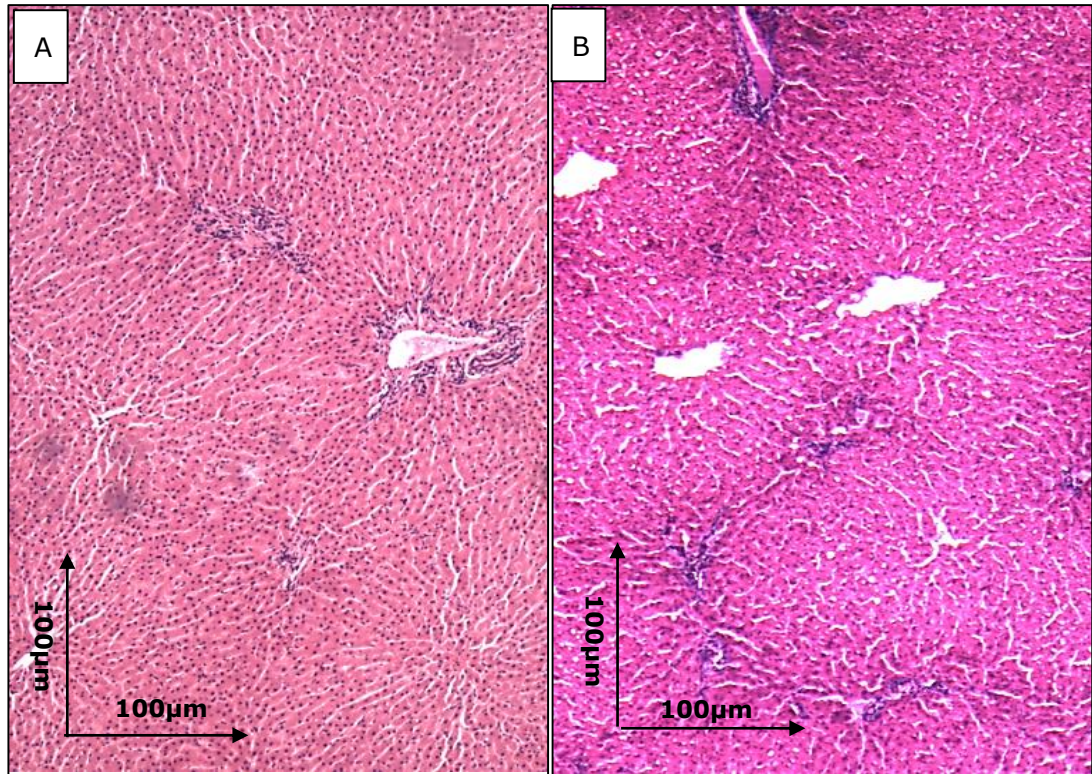


Figure 3.13 Liver tissue stained with H&E (A) and Masson's Trichrome (B) stains visualised at 10x magnification demonstrating the structure of liver lobules.

A liver lobule consists of a central vein surrounded by radially arranged rows of liver cells (hepatocytes). At the perimeter of these lobules are branches of hepatic artery, hepatic portal vein and bile ducts clustered together in a structure called portal triad. The collagenous structures of portal triad are stained blue with Masson's trichrome stain.

Masson's Trichrome stained liver sections were qualitatively analysed to identify features of NAFLD characterised by the presence of inflammatory infiltrate, macrovesicular steatosis and the severity of pericellular and periportal fibrosis. The hepatic tissue from obese animals did not demonstrate any inflammatory infiltrate and, whilst scattered lipid droplets were visible in tissues from both the lean and obese sheep, the distribution and content of the steatosis and fibrosis was not different between the experimental groups (Figure 3.14).

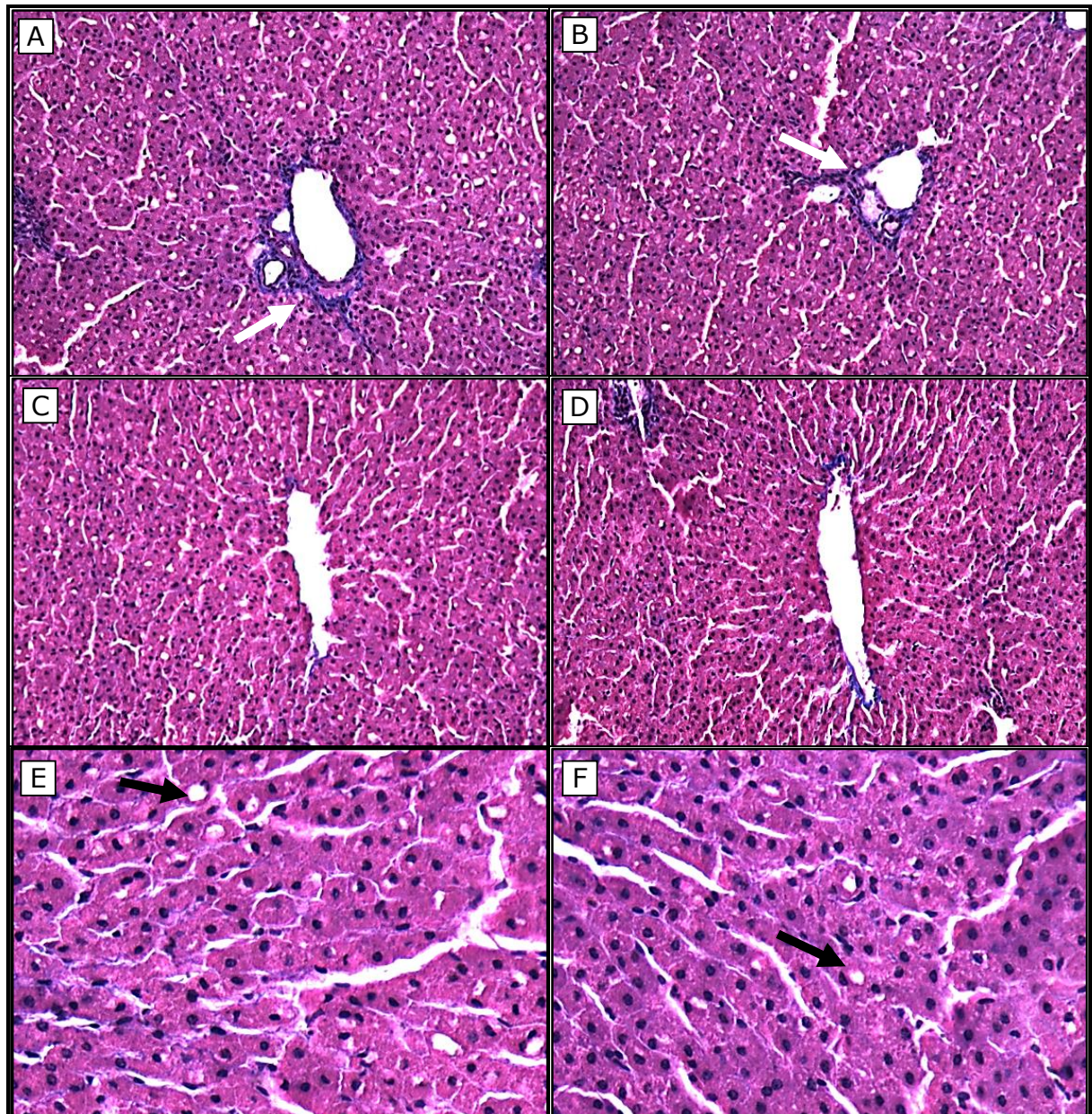


Figure 3.14 Representative histological sections of sheep liver from lean and obese offspring stained with Masson's Trichrome and visualised at 20x magnification.

A, Periportal region from lean offspring (100X); B, periportal region from obese offspring (100X); C, central vein draining zone from lean offspring (100X); D, central vein region from obese offspring (100X); E, sinusoidal area from lean offspring visualised at high magnification (200X); F, sinusoidal area of liver from obese offspring visualised at high magnification (200X). Tissue sections were visualised to identify features of periportal fibrosis identified by blue staining in the periportal area (white arrows) and also faint blue lines in the perisinusoidal region. Steatosis is identified as intracellular lipid droplets large enough to displace the nucleus to the periphery were scattered and infrequent (black arrows).

3.3.4 Hepatic gene expression

3.3.4.1 Gene expression of modulators and effectors of metabolic inflammation in liver

Gene expression studies for 11 β -hydroxysteroid dehydrogenase type 1 (11 β HSD1), cluster of differentiation 95 (CD95), TLR4 showed resilience to change in response to the experimental interventions. Neither obesity nor NR-LG impacted upon the gene expression as shown in Table 3.11.

Gene	Prenatal nutrition	Phenotype		Prenatal Nutrition <i>p</i> value	Obesity <i>p</i> value	Interaction <i>p</i> value
		Lean	Obese			
11βHSD1	A	1.00 \pm 0.06	0.92 \pm 0.03	0.06	0.42	0.99
	N	1.19 \pm 0.18	1.11 \pm 0.10			
Leptin receptor	A	1.00 \pm 0.07	0.91 \pm 0.12	0.29	0.82	0.29
	N	0.98 \pm 0.04	1.11 \pm 0.13			
CD95	A	1.00 \pm 0.18	0.86 \pm 0.16	0.43	0.21	0.59
	N	0.95 \pm 0.27	0.61 \pm 0.13			
TLR4	A	1.00 \pm 0.09	1.05 \pm 0.11	0.84	0.26	0.60
	N	0.93 \pm 0.07	1.09 \pm 0.08			

Table 3.11 Normalised gene expression of genes involved in regulation of metabolic inflammation expressed in arbitrary units relative to the A-L group.

Lambs born to ewes fed to appetite during late gestation (A) were either reared to a lean phenotype (n=9) or obese phenotype as described (n=10). Lambs born to ewes given nutrient restricted diet during late gestation (N) were either reared to a lean phenotype in (n=7) or obese phenotype (n=7). Data are displayed as means \pm SEM. Data were analysed using 2-way ANOVA. 11 β HSD1, 11 β -hydroxysteroid dehydrogenase type 1; CD95, cluster of differentiation 95; TLR4, toll-like receptor-4.

3.3.4.2 Gene expression for the components of the unfolded protein response in the liver

Obesity led to increased gene expression for ER stress degradation enhancer molecule-1 (EDEM1) and glucose-regulated protein 78 (GRP78). However, the subgroup analysis reached statistical significance only for GRP78 in the nutrient restricted animals. The gene expression for activating transcription factor-6 (ATF6) did not change with the experimental interventions (Table 3.12).

	Prenatal nutrition	Phenotype		Prenatal Nutrition <i>p</i> value	Obesity <i>p</i> value	Interaction <i>p</i> value
		Lean	Obese			
ATF4	A	1.00±0.05 ^a	0.86±0.04	0.14	0.86	0.01
	N	0.76±0.03 ^b	0.93±0.10			
EDEM1	A	1.00±0.01	1.03±0.02	0.99	0.02	0.23
	N	0.97±0.00	1.06±0.05			
GRP78	A	1.00±0.08	1.09±0.09	0.88	0.04	0.21
	N	0.86±0.08 ^a	1.21±0.16 ^b			
ATF6	A	1.00±0.09	0.94±0.05	0.14	0.43	0.99
	N	0.88±0.04	0.81±0.13			

Table 3.12 Normalised gene expression for components of the unfolded protein response: ATF4, ATF6, EDEM1 and GRP78, in liver of 17 month old offspring expressed as arbitrary units relative to A-L group.

Lambs born to ewes fed to appetite during late gestation (A) were either reared to a lean phenotype (n=9) or obese phenotype as described (n=10). Lambs born to ewes given nutrient restricted diet during late gestation (N) were either reared to a lean phenotype in (n=7) or obese phenotype (n=7). Data are displayed as means ± SEM. Statistical difference denoted by superscripts a versus b, *p*<0.05 (simple effects analysis following 2-way ANOVA). ATF4, activating transcription factor-4; ATF6, activating transcription factor-6; EDEM1- ER stress degradation enhancer molecule-1; GRP78, glucose-regulated protein 78.

There was a significant interaction between the prenatal intervention and obesogenic environment on the gene expression for activating transcription factor-4 (ATF4). Within the offspring randomised to A treatment, the gene expression tended towards decrease with obesity

($p=0.06$) whereas in the N group, the gene expression was tending to an increase ($p=0.07$) with obesity. The simple main effect for subgroups reached statistical significance only in the A-L versus N-L comparison (Table 3.12).

3.3.4.3 Gene expression for the components of autophagy in the liver

Obesity led to increased hepatic gene expression for both BECN1 and ATG12 (Figure 3.15). Furthermore, the gene expression for BECN1 demonstrated a significant interaction ($p=0.04$) between NR-LG and obesity demonstrating significantly increased BECN1 in obese offspring of NR-LG sheep.

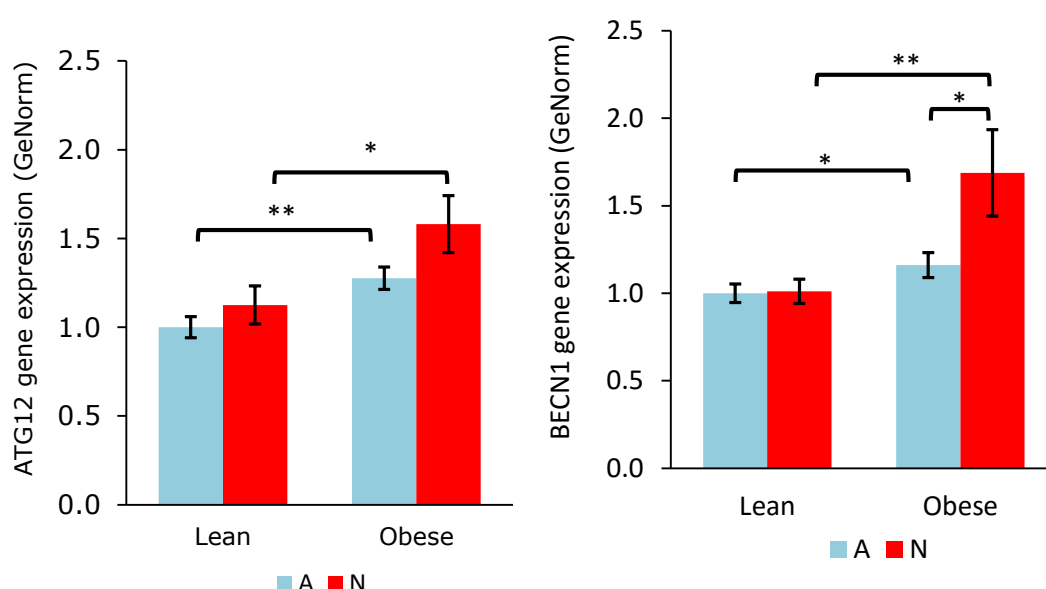


Figure 3.15 Normalised gene of hepatic ATG12 and BECN1 expressed as arbitrary units relative to A-L group.

Offspring of ewes allowed to feed to appetite during late gestation (blue) were either raised for a lean phenotype ($n=9$) or for obese phenotype ($n=10$). Offspring of ewes nutrient restricted during late gestation (red) were either raised for a lean phenotype ($n=9$) or for obese phenotype ($n=7$). Data are expressed as means with error bars representing SEM. * $p < 0.05$ and ** $p < 0.001$ for simple effects analysis following significant two-way ANOVA. Non parametric statistical tests performed for gene expression for BECN1 to confirm the findings of the 2-way ANOVA. ATG12, autophagy related gene 12; BECN1, gene encoding Beclin1.

The gene expression of the mTOR, known to inhibit autophagy, showed no difference with experimental interventions (Table 3.13)

Gene	Prenatal nutrition	<u>Phenotype</u>		Prenatal nutrition	Obesity	Interaction
		Lean	Obese	<i>p</i> value	<i>p</i> value	<i>p</i> value
mTOR	A	1.00±0.09	1.16±0.06	0.54	0.19	0.49
	N	1.01±0.05	1.06±0.11			

Table 3.13 Normalised gene expression of hepatic mTOR expressed in arbitrary units relative to the A-L group.

Lambs born to ewes fed to appetite during late gestation (A) were either reared to a lean phenotype (n=9) or obese phenotype as described (n=10). Lambs born to ewes given nutrient restricted diet during late gestation (N) were either reared to a lean phenotype in (n=7) or obese phenotype (n=7). Data are displayed as means ± SEM. Data were analysed using 2-way ANOVA. mTOR, Mammalian target of rapamycin.

3.3.5 Histological characteristics of omental adipose tissue

3.3.5.1 Adipocyte cell size.

H&E staining of the omental adipose tissue demonstrated adipocytes incorporating unilocular lipid droplets in their centres surrounded by nuclear and cytoplasmic contents (Figure 3.16). The stromal cell content was scant and appeared to be concentrated around fibrous septae traversing through the tissue.

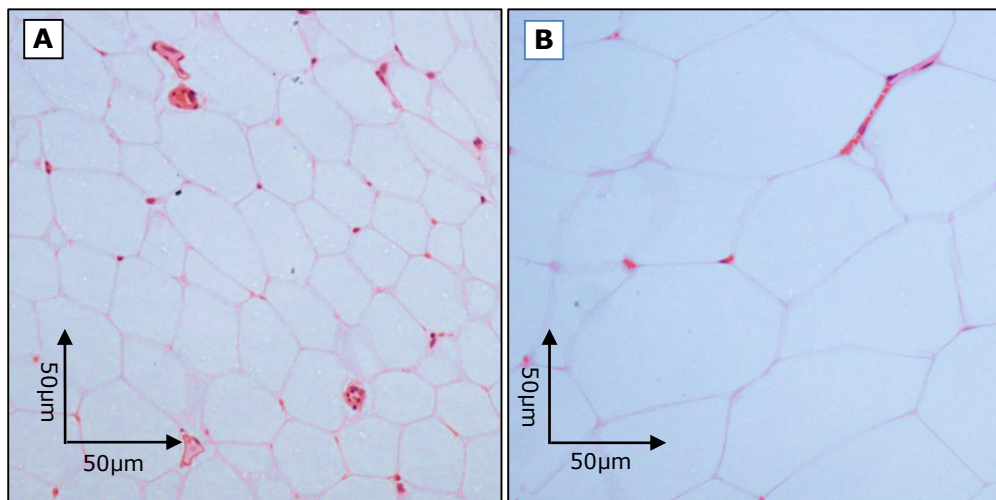


Figure 3.16 Representative images of haematoxylin and eosin stained omental adipose tissue sections from Lean (A) and Obese animals (B) viewed at 20x magnification.

Adipocytes, the predominant cell type in adipose tissue consist of a rim of cytoplasm and cell membrane surrounding empty spaces representing the location of the unilocular lipid droplet. The lipid is not visible in the histological section as it gets removed during histological processing. The other tissue types present in adipose tissues include loose connective tissue, blood vessels and cells of haematogenous origin.

Adipocyte size was significantly increased with obesity. However, there was no effect of NR-LG on the cell size (Figure 3.17).

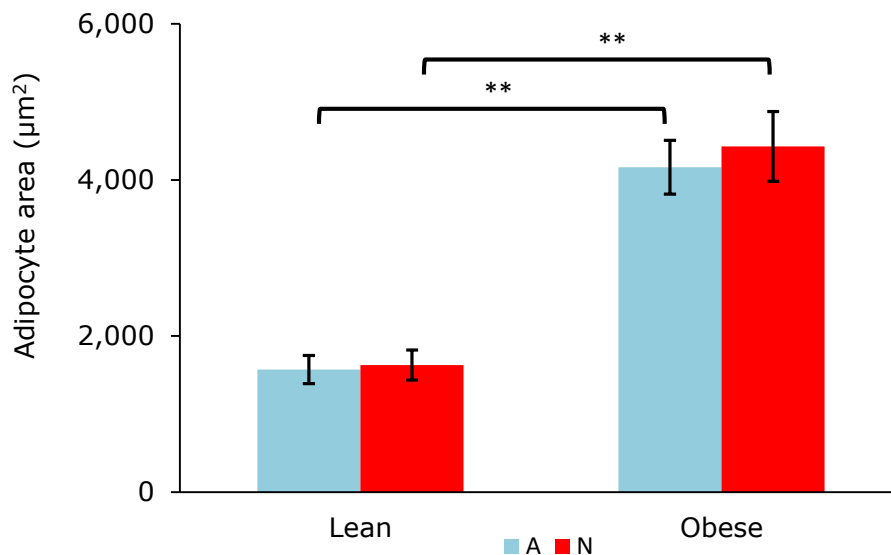


Figure 3.17 Mean adipocyte area in μm^2 calculated from the histological sections of omental adipose tissue of 17 month old offspring.

Offspring of ewes allowed to feed to appetite during late gestation (blue) were either raised for a lean phenotype (n=7) or for obese phenotype (n=10). Offspring of ewes nutrient restricted during late gestation (red) were either raised for a lean phenotype (n=8) or for obese phenotype (n=7). Data are expressed as means with error bars representing SEM. **p<0.001 for simple effects analysis following significant two-way ANOVA.

A significant correlation was identified between the mean adipocyte size with animal bodyweight at 17 months (Figure 3.18 A). The correlation remained significant for subgroup analysis of A offspring ($r=0.489$; $p=0.016$). Correlation of body weight and adipocyte size on N offspring was not statistically significant ($r=0.10$; $p=0.09$). A statistically significant

correlation was present between the mean adipocyte size and weight of the omental adipose tissue (Figure 3.18 B.) The significant correlation was also present on subgroup analysis of the A offspring ($r=0.801$; $p<0.001$) and of N offspring ($r=0.94$; $p<0.001$).

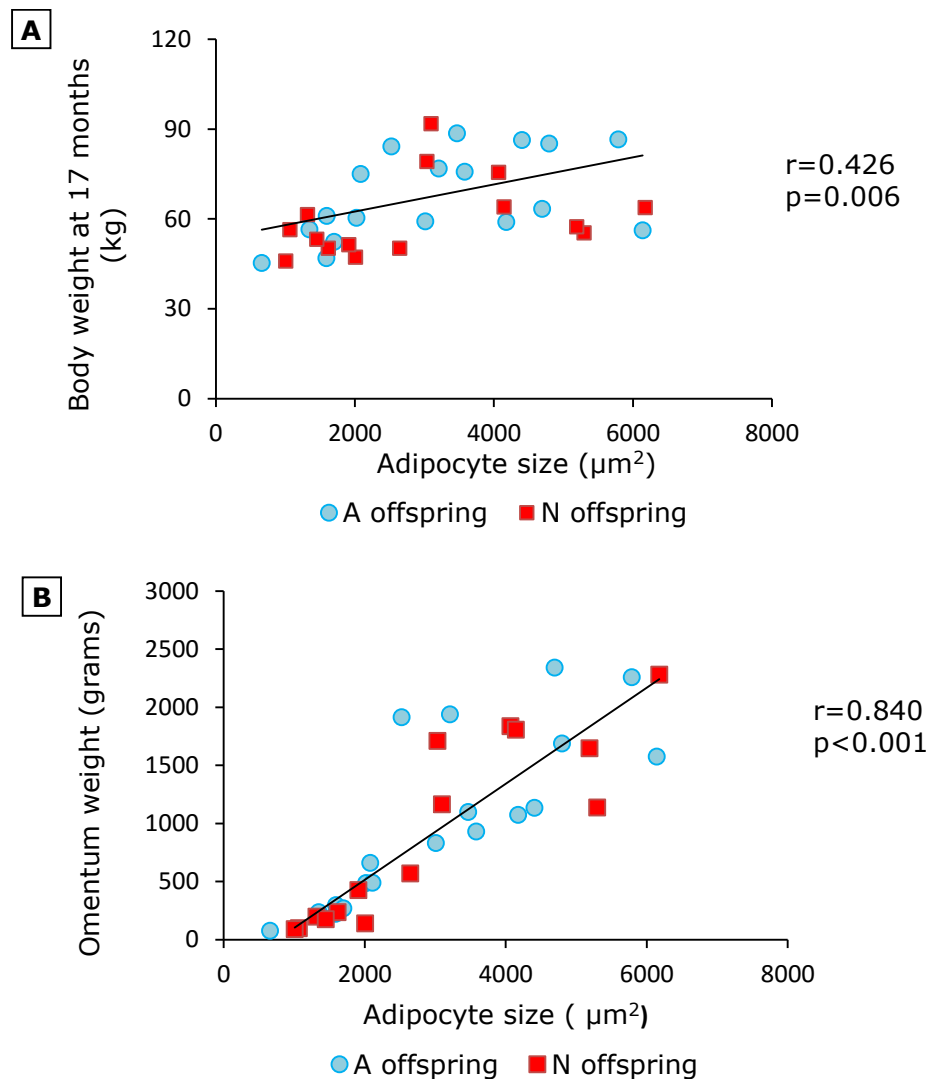


Figure 3.18 Correlation analysis of adipocyte size with adult body weight (A) and weight of the omental adipose tissue at dissection (B) in all offspring.

Offspring born to sheep fed to appetite (A, $n=19$) are demonstrated with blue circles and offspring born to sheep restricted to 60% nutrition (N, $n=17$) during late gestation identified with red squares. Pearson correlation coefficient r and p values of significance as indicated in the figure. The trendline and values of r and p depicts correlation analysis of all animals.

3.3.5.2 GRP78, pJNK and IBA1 staining

GRP78 staining was localised to cytoplasmic content present at the periphery of the adipocytes. In images of adipose tissue of lean animals with relatively small adipocytes, such staining was easily identified all along the adipocyte periphery. In the adipocyte from obese animals, the cytoplasm and the cell organelles were located as a thin rim on the periphery while the lipid form majority of the cellular content. As a result, staining in the adipocyte in tissues from obese animals was either spread thinly along the wall or was concentrated in pockets of perinuclear cytoplasmic content (Figure 3.19).

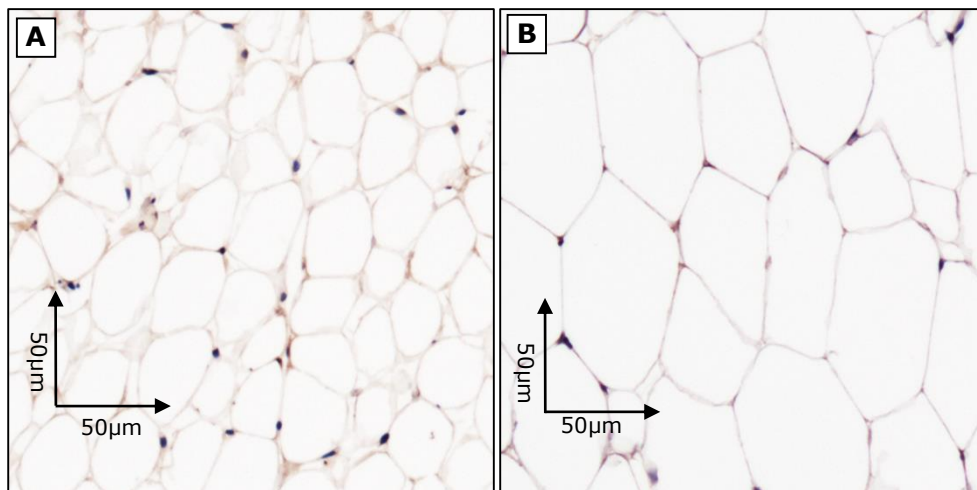


Figure 3.19 Representative images demonstrating distribution of staining for GRP78 in adipose tissue from lean (A) and obese (B) animals at 17 months of age. GRP78 can be identified by brown DAB staining.

Expressed as area stained per adipocyte, the stained area was measured by computerised quantification. Greater GRP78 staining was present in obese animals, with no interaction identified with prenatal intervention Table 3.14.

	Prenatal nutrition	Phenotype		Prenatal nutrition <i>p</i> value	Obesity <i>p</i> value	Interaction <i>p</i> value
		Lean	Obese			
GRP 78 ($\mu\text{m}^2/\text{cell}$)	A	35.9 \pm 21.6	79.8 \pm 24.2	0.51	0.02	0.83
	N	30.4 \pm 11.0	70.9 \pm 21.8			
pJNK ($\mu\text{m}^2/\text{cell}$)	A	29.6 \pm 12.7	53.1 \pm 6.3	0.50	0.36	0.18
	N	55.5 \pm 17.5	44.2 \pm 12.7			

Table 3.14 Quantitative analysis of GRP78 and pJNK stain expressed as area stained in μm^2 / adipocyte.

Lambs born to ewes fed to appetite during late gestation (A) were either reared to a lean phenotype (n=7) or obese phenotype as described (n=7). Lambs born to ewes given nutrient restricted diet during late gestation (N) were either reared to a lean phenotype in (n=6) or obese phenotype (n=7). Data are displayed as means \pm SEM. Data were analysed using 2-way ANOVA. GRP78 Glucose regulated protein-78; pJNK, phosphorylated c-Jun N-terminal kinase.

Staining for the phosphorylated c-Jun N-terminal kinase (pJNK) was mostly restricted to nucleus and the perinuclear areas (Figure 3.20). Obesity or NR-LG did not lead to any difference in the area of pJNK staining per cell (Table 3.14).

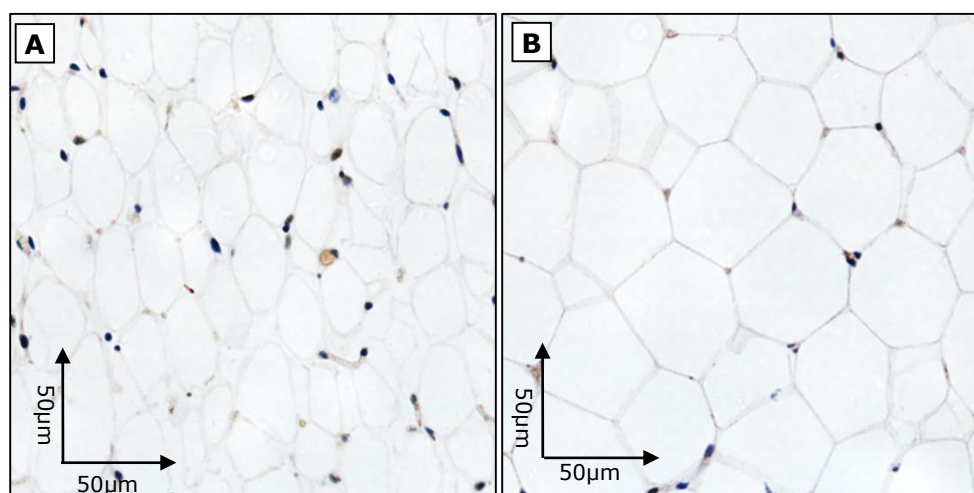


Figure 3.20 Representative images demonstrating pJNK staining visible in the perinuclear areas in the omental adipose tissue from lean (A) and obese (B) sheep.

Iba1 staining for macrophages identified macrophage infiltration in isolation and in clusters consistent with appearance of CLS and milky spots. Macrophage staining in the omental adipose tissue from the lean animals was relatively infrequent, the CLS tended to be present singly and on occasions the adipocytes were not fully surrounded by the macrophages on all sides. In contrast, the staining for adipose tissue macrophages was subjectively more abundant in the obese animals and, along with scattered CLS, remarkable clusters of Iba1 stained cells surrounding necrotic adipocytes were present (Figure 3.21). Some of these clusters of macrophages surrounding dead adipocytes were present in proximity to the blood vessels and connective tissue septae traversing through the adipose tissue. Such clusters were consistent with the described appearance of milky spots. Accurate quantification of Iba1 staining was not possible due to confounding factors including non-homogenous distribution in clusters in obese animals and the unintended uptake of DAB stain by necrotic adipocytes (Figure 3.21 D).

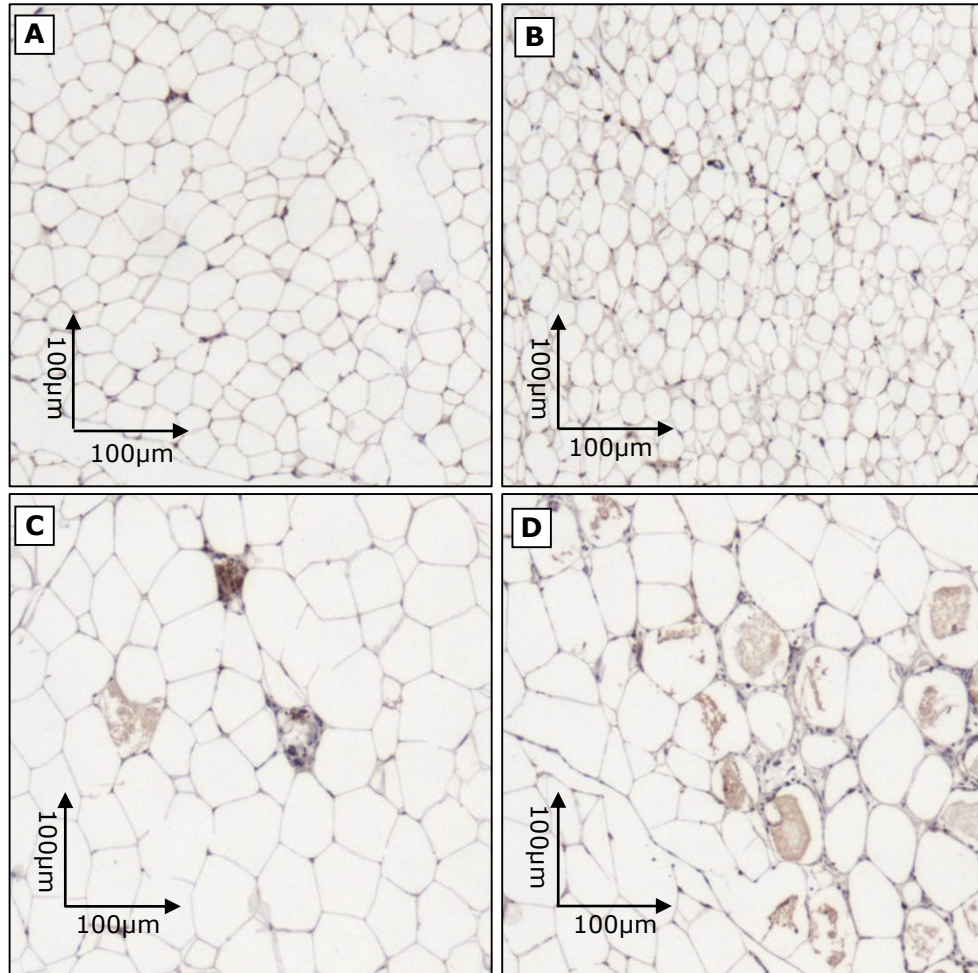


Figure 3.21 Representative images of Iba1 staining of adipose tissue of lean (A and B) and obese (C and D) sheep visualised at 10x magnification.

Iba1 staining identifies macrophages which were present through the tissue in a non-homogenous distribution. The infiltrating macrophage were presented in isolated clusters or around necrotic adipocytes in pattern described as crown like structures in omental adipose tissue visualised at 10x magnification.

3.3.6 Omental adipose tissue gene expression analysis

3.3.6.1 Genes expression of modulators and effectors of metabolic inflammation in the omental adipose tissue.

The experimental factors, obesity and NR-LG, had no impact on the omental adipose tissue gene expression of 11 β HSD1 and GCR (Table 3.15). Gene expression for CD68, leptin and TLR4 was increased with obesity whereas the expression was not affected by NR-LG (Table 3.15).

Gene	Prenatal nutrition	Phenotype		Prenatal nutrition	Obesity	Interaction
		Lean	Obese	<i>p</i> value	<i>p</i> value	<i>p</i> value
11βHSD1	A	1.00 \pm 0.25	0.69 \pm 0.04	0.54	0.51	0.17
	N	0.66 \pm 0.06	0.78 \pm 0.09			
GCR	A	1.00 \pm 0.15	1.11 \pm 0.09	0.60	0.21	0.71
	N	0.89 \pm 0.13	1.10 \pm 0.11			
Leptin	A	1.00 \pm 0.23 ^a	5.42 \pm 1.52 ^b	0.82	<0.001	0.96
	N	0.69 \pm 0.13 ^a	5.51 \pm 1.37 ^b			
TLR4	A	1.00 \pm 0.05	1.33 \pm 0.20	0.51	0.01	0.99
	N	0.92 \pm 0.11 ^a	1.25 \pm 0.07 ^b			
CD68	A	1.00 \pm 0.18 ^a	3.53 \pm 1.03 ^b	0.19	<0.001	0.85
	N	0.65 \pm 0.07 ^a	3.03 \pm 1.56 ^b			

Table 3.15 GeNorm normalised gene expression for regulators of metabolic inflammation in the omental adipose tissue of 17 month old offspring.

Lambs born to ewes fed to appetite during late gestation (A) were either reared to a lean phenotype (n=7) or obese phenotype as described (n=8). Lambs born to ewes given nutrient restricted diet during late gestation (N) were either reared to a lean phenotype in (n=9) or obese phenotype (n=7). Data are displayed as means \pm SEM. Statistical difference denoted by superscripts a versus b, $p < 0.05$ (simple effects analysis following 2-way ANOVA). 11 β HSD1, 11 β -hydroxysteroid dehydrogenase type 1; GCR, glucocorticoid receptor CD95, cluster of differentiation 95; TLR4, toll-like receptor-4e.

Correlations between leptin gene expression and plasma leptin concentrations performed at 16 months of age were statistically significant for all animals and for obese animals. Upon analysis of lean subgroups, there was no correlation between the gene expression for leptin and plasma leptin concentrations (Table 3.16)

Variable 1	Variable 2	Pearson's coefficient (r)	p value (two tailed)
Plasma leptin all animals (ng/ml)	Leptin gene expression all animals	0.478	<0.001
Plasma leptin all obese animals (ng/ml)	Leptin gene expression all obese animals	0.356	0.019
Plasma leptin all lean animals (ng/ml)	Leptin gene expression all lean animals	0.044	0.871

Table 3.16 Correlation analysis between gene expression and plasma concentration of leptin in all animals and subgroup analysis of obese and lean animals.

Sheep were either reared in an unrestricted environment for a lean phenotype (n=17) or were reared in a restricted environment as described to decrease physical activity leading to obese phenotype (n=16). Plasma leptin quantification was performed by the laboratory of Professor Keisler at the Department of Animal Science of the University of Missouri using radioimmunoassay method.

3.3.6.2 Gene expression for the components of the unfolded protein response in the omental adipose tissue

Obesity led to increased gene expression for all the tested components of the UPR (Table 3.17). Subgroup analysis demonstrated increased gene expression for ATF6, GRP78 and EDEM1 in the obese offspring as compared to the lean offspring of sheep experiencing NR-LG. The gene expression of ATF4 was increased in obese offspring irrespective of maternal prenatal nutrition (Figure 3.22).

Gene	Prenatal nutrition	Phenotype		Prenatal nutrition	Obesity	Interaction
		Lean	Obese	p value	p value	p value
ATF4	A	1.00±0.10 ^a	1.53±0.20 ^b	0.12	0.001	0.82
	N	0.82±0.06 ^c	1.32±0.11 ^d			
ATF6	A	1.00±0.09	1.16±0.07	0.12	0.01	0.37
	N	0.81±0.09 ^a	1.13±0.08 ^b			
GRP78	A	1.00±0.16	1.14±0.10	0.04	0.04	0.31
	N	0.69±0.10 ^a	1.05±0.12 ^b			
EDEM1	A	1.00±0.06	1.05±0.08	0.36	0.01	0.23
	N	0.82±0.06 ^a	1.05±0.05 ^b			

Table 3.17 GeNorm normalised gene expression for components of the unfolded protein response in the omental adipose tissue.

Lambs born to ewes fed to appetite during late gestation (A) were either reared to a lean phenotype (n=7) or obese phenotype as described (n=8). Lambs born to ewes given nutrient restricted diet during late gestation (N) were either reared to a lean phenotype in (n=9) or obese phenotype (n=7). Data are displayed as means ± SEM. Superscripts denote statistical difference for simple effects analysis following 2-way ANOVA a versus b, p<0.05; c versus d, p<0.001. ATF4, activating transcription factor-4; ATF6, activating transcription factor-6; GRP78, glucose-regulated protein 78; EDEM1, ER stress degradation enhancer molecule-1

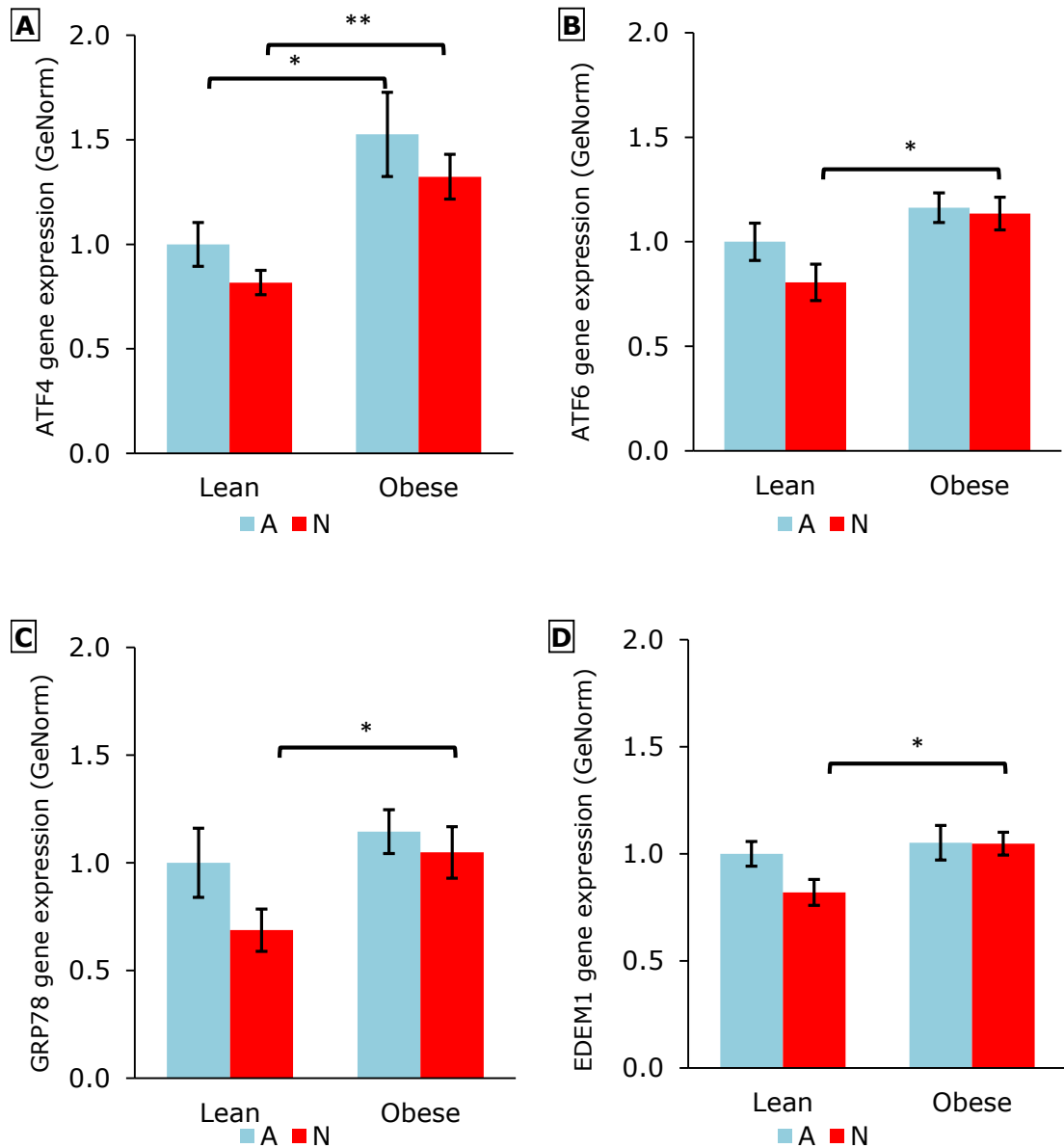


Figure 3.22 Relative gene expression in omental adipose tissue for unfolded protein response components: A, ATF4; B, ATF6; C, GRP78; D, EDEM1.

Offspring of ewes allowed to feed to appetite during late gestation (blue) were either raised for a lean phenotype (n=7) or for obese phenotype (n=8). Offspring of ewes nutrient restricted during late gestation (red) were either raised for a lean phenotype (n=9) or for obese phenotype (n=7). Data are expressed as means with error bars representing SEM. *p<0.05 and **p<0.001 for simple effects analysis following significant two-way ANOVA. ATF4, activating transcription factor-4; ATF6, activating transcription factor-6; GRP78, glucose-regulated protein 78; EDEM1, ER stress degradation enhancer molecule-1.

3.3.6.3 Gene expression for autophagy in the omental adipose tissue

Obesity led to increased gene expression for both the genes, ATG12 and BECN1. This result was significant in subgroup analysis irrespective of the prenatal nutrition (Figure 3.23)

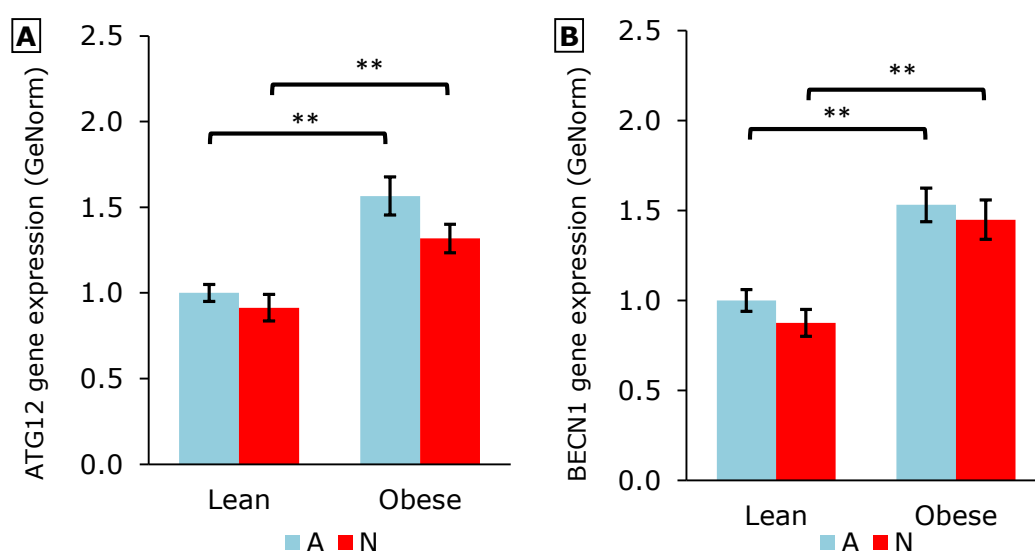


Figure 3.23 Relative gene expression in omental adipose tissue for (A) ATG12 and (B) BECN1. Offspring of ewes allowed to feed to appetite during late gestation (blue) were either raised for a lean phenotype (n=7) or for obese phenotype (n=8). Offspring of ewes nutrient restricted during late gestation (red) were either raised for a lean phenotype (n=9) or for obese phenotype (n=7). Data are expressed as means with error bars representing SEM. **p<0.001 for simple effects analysis following significant two-way ANOVA. ATG12, autophagy related gene 12; BECN1, gene encoding Beclin1.

The gene expression in the omental adipose tissue for both AMPK and mTOR were increased with obesity. This difference achieved statistical significance in comparisons between A-O to A-L group in both genes. In addition, AMPK was also increased in the N-O group as compared to the N-L group (Figure 3.24 A and B).

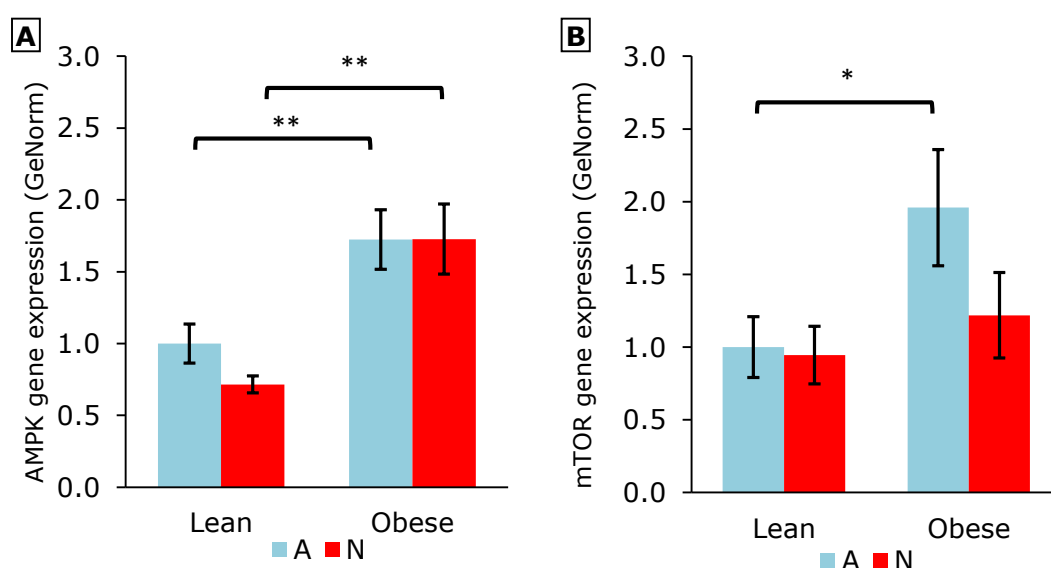


Figure 3.24 Normalised gene expression of AMPK (A) and mTOR (B) in omental adipose tissue of 17 month old offspring expressed in arbitrary units relative to A-L group.

Offspring of ewes allowed to feed to appetite during late gestation (blue) were either raised for a lean phenotype (n=7) or for obese phenotype (n=8). Offspring of ewes nutrient restricted during late gestation (red) were either raised for a lean phenotype (n=9) or for obese phenotype (n=7). Data are expressed as means with error bars representing SEM. *p<0.05 and **p<0.001 for simple effects analysis following significant two-way ANOVA. AMPK, 5' adenosine monophosphate activated protein kinase; mTOR, mammalian target of rapamycin.

3.4 Discussion

The main objectives of the experiments described in this chapter were to:

- establish a study design, in a sheep model, to investigate the interaction between maternal NR-LG during pregnancy and offspring obesity on offspring health.
- describe the characteristics of the cell stress response in liver and omental adipose tissue of obese and lean sheep.
- identify any programming influence of maternal NR-LG on offspring cell stress response to obesity.

Restriction of physical activity in sheep led to development of obesity which was characterised by selective increase in visceral adipose tissue deposition, increased plasma leptin and increased gene expression for leptin from omental adipose tissue. This was associated with features consistent with insulin resistance. The increase in the weight of the omental adipose tissue depot in obese sheep was in direct correlation with omental adipocyte size. In addition, adipose tissue histology identified patterns of distribution of CLS and of Iba1 stained macrophage infiltration in adipose tissue from obese and lean offspring.

Restriction of maternal nutrition to 60% of metabolisable energy during late gestation led to significantly decreased maternal weight gain, lower maternal plasma glucose and higher maternal plasma NEFA concentrations and decreased offspring birth weight as compared to the sheep allowed to feed to appetite during the same period.

In the offspring liver at 17 months of age, obesity led to increased gene expression for UPR genes EDEM1 and GRP78 and autophagy genes BECN1 and ATG12. The obese offspring of sheep who underwent NR-LG, had increased relative liver weight as compared to obese offspring of sheep fed

to appetite. The former also had increased gene expression for BECN1 expression as compared to the latter.

In the omental adipose tissue of offspring, obesity was associated with increased gene expression for leptin, macrophage marker CD68 and autophagy genes. The obese offspring of nutrient restricted mothers had increased UPR genes ATF6, GRP78 and EDEM1 as compared to the lean offspring. The UPR gene ATF4 was increased in all obese sheep irrespective of prenatal nutrition. These results are discussed in detail in the following sections.

3.4.1 NR-LG in twin bearing sheep leads to a state of energy deficit and growth restriction of the developing offspring

Metabolite analysis of plasma samples taken from sheep at 130dGA demonstrated that, in comparison with ewes which fed to appetite, nutrient restriction to 60% of energy requirements led to decreased plasma insulin and glucose along with increased NEFA concentrations. In the state of energy deficit, the initial physiological response of the body involves mobilisation of glucose from hepatic glycogen stores. This is followed by lipolysis of triglycerides in adipose tissue, which results in release of glycerol and NEFA into circulation [419]. NEFA, through the process of beta oxidation, acts as a source of energy and also provides ketone bodies, an important source of fuel for glucose deficient vital organs [419]. In addition, the catabolic state [420] of energy deficit is associated with a decreased plasma insulin and increased glucocorticoid and glucagon concentrations in non-pregnant animals [421]. Plasma biochemistry of the twin bearing N mothers during late gestation was characterised by increased NEFA concentrations and low blood glucose despite decreased insulin and, therefore, conforms to the patterns expected in the state of energy deficit.

Late gestation is a stage of the maximum rate of fetal growth associated with a high requirement of nutrition as indicated by a 14 fold increase in fetal glucose demand [422]. Increased fetal number, by itself, is known to lead to lower birth weight [268, 423]. In a study which had a mixture of singleton and twin bearing ewes, 50% nutrient restriction from gestational day 110 to term in comparison to 100% metabolisable energy consumption did not result in a decreased birth weight [315]. Whereas, twin bearing pregnancies undergoing NR-LG results in lower birth weight of twins in comparison to singletons [268, 423]. The compensatory responses to any decrease in the availability of nutrients at this stage include decreased fetal insulin secretion [424, 425] , increased newborn offspring insulin sensitivity [426] and placental nutritional partitioning [427, 428]. In sheep with twin pregnancies, the placental compensatory mechanisms to decreased nutrition are less effective [429]. Furthermore, growing twin fetuses impose relatively increased nutritional demand in comparison to singletons [430] exacerbating the deficit in nutrient availability for the fetus, leading to the decreased birth weight in the offspring of the twin bearing ewes in the nutrient restricted group. The lower birth weight in N offspring in this study is likely to be the outcome of nutrient deficit during a period of increased nutritional requirements brought about by timing of late gestation and requirements of a twin fetuses.

The sample mean z-score of the birth weight of N offspring was -3 in comparison to the birth weight of the A group. There is no definition of sheep intrauterine growth restriction (IUGR). However, the sample mean birth weight z-score of -3 in N offspring indicates a significant difference from the population mean. Assuming that the mean fetal growth prior to randomisation was the same in both groups, the significant decrease in birth weight is likely to be an outcome of IUGR.

The presence of a plasma metabolic profile consistent with energy deficit, the relatively lower maternal weight gain during the intervention period in the N group and the decreased birth weight of the offspring demonstrate exposure of the mother and the growing fetus to an environment of relative macronutrient deficiency. The animal model described in this study, therefore, is well suited for a study of potential fetal programming in IUGR secondary to relative macronutrient deficiency during the late gestation.

3.4.2 Body weight and metabolic parameters of the offspring

3.4.2.1 Establishment of a model of mild to moderate obesity.

From birth to 90 days postnatal age, all twin offspring fed on their mother's milk. The offspring of sheep in N group, which had been lighter at birth, remained lighter for the first four weeks following which their body weights became similar to the offspring sheep in A group. The absence of rapid postnatal growth over the suckling period in this group is also demonstrated by the similar values for the fold change in body weight. This experimental model, therefore, avoids the significant potential confounding factor of rapid weight gain soon after birth. Such accelerated postnatal growth has been proposed to programme predisposition to adverse metabolic outcomes in later life [286, 431].

When measured at 45 days of age, there was no difference in physical activity parameters between any groups ruling out selective programming of the offspring physical activity with prenatal nutrition. The restricted area of the rearing environment for N-O and A-O offspring led to decreased physical activity measured by accelerometer at 15 months of age in comparison to N-L and A-L groups respectively.

The increased body weight of the offspring randomised to the obesogenic environment as compared to unrestricted environment did not reach

statistical significance for the first 9 months after randomisation to restricted physical activity, differing only after the age of 12 months. Basal metabolic rate, which constitutes the largest component of the energy expenditure, is maximal during the period of body growth [432] and is also increased with raised body mass [433]. As studies of sheep growth curves have identified, the first nine months of age coincide with the period of maximal growth rate [434]. It is plausible that the high basal metabolic rate during the rapid growth period [432, 435] compensated for the excess energy balance during the first half of the intervention and that the difference in body weight of obese and lean sheep became apparent only once the rate of body growth decreased in adulthood with the consequent proportional decrease in basal metabolic rate. Previous studies of sheep reared in a similar restricted environment from the age 15 months until 20 months resulted in a larger difference of 1.5 fold change in absolute weight as compared to lean animals [264]. However, along with restricted physical activity, the animals in that study also experienced increased intake of calories and dietary fat using palm kernel oil.

There is no precise definition of obesity in sheep. In an experiment describing the phases of dietary obesity in sheep, prior to reaching a static phase after 42 weeks of high calorie dietary intake, the weight of animals increased at an accelerated rate until it plateaued at 2.1 fold in comparison to the group fed to metabolic requirements [436]. Existing models of sheep obesity include relative weight increase between 1.5 [264] and more than 2 fold [223, 436]. A model of severe obesity is likely to significantly affect the baseline cellular physiology even at an early age [223], thereby potentially masking any effect of late gestation nutrient restriction in the pathogenesis of obesity related morbidity. For example, if excess obesity led to a substantial adipokine secretion, metabolic inflammation and associated cell stress response in all obese animals, any

modulation of these pathways, of relatively smaller quantity, brought about by the developmental programming would be masked and its demonstration would require a very large sample size. In contrast, the 1.35 fold relative weight gain resulting from this model of physical inactivity-induced obesity can be designated as mild to moderate obesity and such a model is less likely to mask any modulation of obesity associated cell stress response following maternal NR-LG.

3.4.2.2 NR-LG does not predispose offspring to obesity or adiposity.

NR-LG did not lead to any difference in the body weight and adipose deposition in N-L versus A-L and N-O versus A-O comparisons, findings consistent with other sheep studies of NR-LG [264]. This outcome is also in accord with the outcome of the Dutch Famine birth cohort studies which demonstrated that offspring of mothers exposed to famine in the third trimester were of similar body weight at age of 19 years [437] and adiposity at 50 [438] and 58 [418] years as those unexposed.

3.4.2.3 Obesity associated decreased glucose disposal at 7 months and insulin resistance at age of 16 months were not exacerbated with NR-LG.

GTT performed at 7 months showed a significantly higher glucose response in the A-O and N-O groups in comparison with A-L and N-L groups respectively. The values for plasma insulin concentrations in all the groups were similar during the GTT, demonstrating a state of decreased glucose disposal in the animals reared in an obesogenic environment.

Interestingly, the body weights of all the animals at this stage were not different, irrespective of the rearing environment. It is already known that physical activity associated morphological changes in muscles are associated with improved glucose tolerance [439] and this increased insulin-stimulated glucose disposal in physically active individuals is

present irrespective of body weight [440]. It is also plausible that despite there being no change in body weight, changes in tissue composition were already established by this age, a possibility which is supported by the finding of increased plasma leptin concentrations at this age in A-O in comparison to the A-L offspring, whilst the smaller difference in plasma leptin in N-O (2.31 ± 0.44 ng/mL) as compared to N-L (1.54 ± 0.26 ng/mL) offspring did not reach statistical significance.

During the GTT performed at 16 months of age, although there were no differences in the glucose concentrations at any of the standard time points, obesity led to increased plasma insulin with higher values in both obese groups. This finding was also confirmed by the raised area under the curve for insulin and HOMA-IR for obese sheep. NR-LG did not have any impact on glucose and insulin measured in the GTT in the obese and lean offspring.

The obese animals, therefore, demonstrated enhanced insulin secretion in order to achieve a plasma glucose comparable to lean animals. This signifies the presence of peripheral insulin resistance requiring a compensatory increase in insulin secretion in this model of mild to moderate obesity. Human studies have also demonstrated development of obesity related peripheral insulin resistance secondary to obesity as early as the age of 6-12 years [42].

NR-LG did not exacerbate the insulin resistance as determined by the GTT in both lean and obese groups. The follow up cohort of the offspring of mothers exposed to the Dutch famine during late gestation had higher insulin resistance in GTT and also higher fasting plasma proinsulin [261]. The absence of features of insulin resistance in our experiment is inconsistent with the Dutch Cohort findings in humans at age 50 years. The age of 16 months in sheep is considered equivalent to young

adulthood and it is plausible that, by this age, the programming mechanisms of NR-LG may not yet have contributed significantly to the progression of insulin resistance. Previous sheep studies of NR-LG either employed a more severe nutritional challenge (50%) [274] or studied the glucose-insulin axis at older ages as seen in the abnormal glucose-insulin homeostasis apparent in obese offspring at the age of 2 years, but not at 18 months postnatal age [264]. The experiments do not demonstrate any difference in measured markers of insulin resistance between N-O as compared to A-O group at age of 16 months. Any modifications to the biochemical and cellular processes in the N-O as compared to the A-O group would signify programming changes instead of being the outcome of established insulin resistance.

Plasma triglyceride and NEFA did not differ between any of the groups. In the metabolic syndrome, dyslipidaemia, signified by raised plasma triglycerides and decreased high density lipoproteins, is a component of the diagnostic criterion [1]. Such dyslipidaemia is the outcome of insulin resistance which leads to decreased activation of lipoprotein lipase in the endothelial lining of blood vessels [187]. This prevents breakdown of circulating plasma triglycerides and the subsequent uptake of fatty acids by adipocytes, liver or muscle tissue [441]. At the same time, triglycerides continue to be manufactured in the liver, packed up into very low density lipoproteins (VLDL) and released into the circulation. This imbalance between triglyceride released into circulation and disposal by the body leads to raised triglyceride concentrations. In this study, such raised plasma triglyceride concentrations would have indicated a state of insulin resistance and metabolic syndrome.

Lipid metabolism in ruminants is significantly different as compared to humans [442]. In ruminants, the liver contributes little to fatty acid synthesis whilst adipose tissue is the primary site for this [443].

Furthermore, the substrates utilised are mainly glucose and acetate [444] although this does vary between depots [445]. It is plausible that ruminants are more resistant to plasma lipid abnormalities brought about by insulin resistance because of the relatively low contribution of the liver to ovine fatty acid and subsequent triglyceride production. The absence of any differences in plasma triglyceride concentrations in previously published sheep studies, despite the presence of abnormal glucose-insulin homeostasis [264, 274] supports such a proposal. This factor, along with relatively younger age of the animals in the experimental model, may explain the absence of abnormal lipid profile following NR-LG as would have been predicted from the Dutch Famine cohort studies [418] .

3.4.3 The characteristics of liver fat deposition and cell stress response to obesity with and without prenatal NR-LG.

3.4.3.1 Increased hepatic fat deposition in obese sheep is associated with upregulated autophagy and ER stress.

The increased liver weight of obese sheep correlated strongly with the increased hepatic triglyceride content. The values of absolute liver weight at dissection were comparable to previously published literature in ovine model [315, 446] as were hepatic triglyceride content in lean animals (3%) in both sheep [279] and humans [447].

Obesity related ectopic accumulation of fat in the liver can range from asymptomatic steatosis (NAFLD), to more severe non-alcoholic steatohepatitis (NASH) [208], both of which are associated with the presence of the metabolic syndrome [448]. Histological examination of the liver was performed to identify and quantify the features of NASH and steatosis by performing H&E and Masson's Trichrome staining. However, despite multiple attempts at optimising the staining protocol for formalin fixed paraffin embedded histological sections prepared from gradually thawed frozen liver tissue, the staining and quality of histological sections

were unsuitable for reliable analysis. This precluded a confident morphometric confirmation of features of NAFLD or NASH as suggested by the above findings of higher liver weight along with increased triglyceride concentrations in the hepatic tissue.

Oil red O staining of frozen sections of liver has previously been used to identify hepatic steatosis [279]. However, this procedure does not provide any more information regarding hepatic fibrosis, inflammatory infiltrate or other known features of NAFLD-NASH spectrum as described in validated diagnostic methods [377]. Whilst the presence of increased triglyceride with obesity in this model has already been demonstrated, oil red O staining would have only confirmed the increased lipid deposition. In light of the above and time constraints, oil red O staining was not undertaken.

The upregulated ER stress response to obesity as indicated by increased EDEM and GRP78 is in agreement with previous human [105] and animal model studies [99]. The relationship between ER stress and obesity associated NAFLD has been demonstrated to be bidirectional [228]. Furthermore, activated UPR in response to ER stress is capable of promoting other cell stress response pathways such as autophagy. For example, ATF4 activation via the PERK pathway of the ER stress response has been demonstrated to activate autophagy [95].

As previously reported in studies of NAFLD patients and murine models [449, 450], the gene expression of autophagy components was increased with obesity. The accepted role of hepatocyte autophagy is that of lipid disposal preventing the development of hepatic lipid accumulation by promoting lipid metabolism [130], insulin sensitivity [234] and promoting cell survival by maintaining cellular homeostasis (Figure 3.25 A). However, the obese sheep in this study had increased liver tissue triglyceride content despite having similar plasma triglycerides as lean animals. If the

increased gene expression reflected an increase in autophagic function of the hepatocytes, it would predict more efficient lipid disposal by the hepatocytes. It has been demonstrated that this increased gene expression of autophagy in obesity is paradoxically associated with an impaired autophagic flux [234, 450] which correlates with progressive NAFLD [451]. Such a defect in normal functioning of autophagy would promote additional lipid deposition in the liver along with compromising the normal homeostasis of cellular functioning (Figure 3.25 B). The ensuing cell stress, including activation of UPR would activate a state of metabolic inflammation. Increased gene expression for autophagy, in such a scenario, would be a consequence of upregulated cell stress response to obesity (Figure 3.25 B). However, in the absence of additional evidence demonstrating a defect in the autophagic functioning, such explanations for the increased gene expression for autophagy components in this study remain speculative.

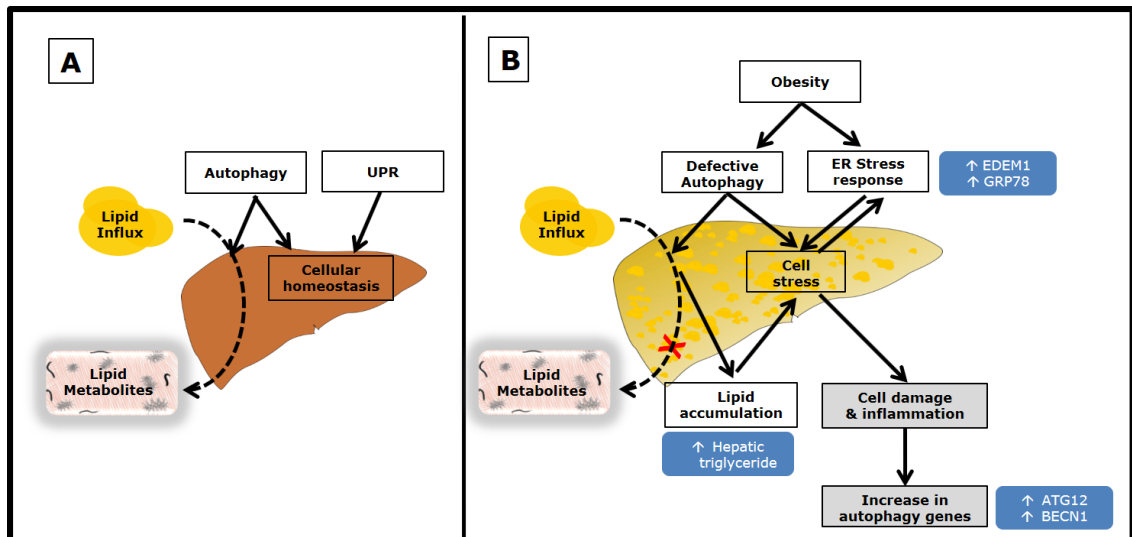


Figure 3.25 Schematic diagram depicting (A) the role of constitutive autophagy and UPR maintenance of liver homeostasis and (B) obesity induced defective autophagy and ER stress response leading to hepatocellular damage and inflammation. Normal functioning of autophagy is important for lipid metabolism and, in conjunction with ER stress response, for cell survival in the hepatocytes. A defect in the functioning of hepatic autophagic processes, as proposed, would promote intrahepatic lipid accumulation and activation of the cell stress response. Along with obesity induced ER stress response, the resultant cell stress response is capable of promoting an increase in gene expression of components of autophagy.

The other known regulators of autophagic pathways include energy sensing and leptin action. Autophagy is known to be activated during a state of energy deficit through activation of AMPK which then inhibits mTOR and also increases autophagic gene expression via activation of the transcriptional factor forkhead boxO1 (FoxO1) [452, 453]. The gene expression of hepatic mTOR was not altered in response to any of the experimental interventions.

Another explanation for increased autophagy in the obese offspring is the possibility of hepatic insulin resistance. Insulin action is known to lead to transcriptional downregulation of autophagy through phosphatidylinositide 3-kinase (Pi3K) - protein kinase B (Akt/PkB) signalling pathway leading to inactivation of transcriptional factor FoxO3 [130]. A state of insulin resistance would lead to activation of FoxO3 transcription factors leading

to increased expression of autophagic genes (Figure 3.26). It is, therefore, plausible that hepatic insulin resistance resulting from obesity associated hepatic steatosis could contribute to the increased autophagy gene expression.

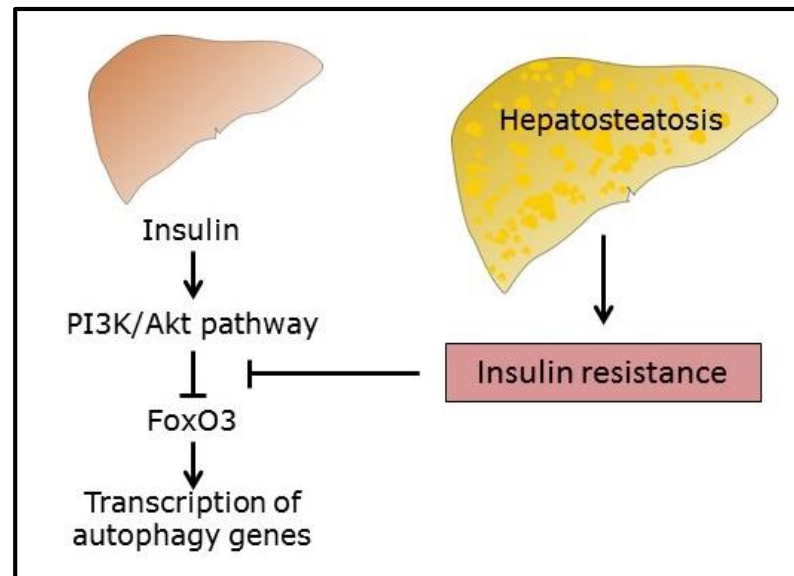


Figure 3.26 Schematic diagram depicting the mechanism of increased transcription of autophagy genes in the state of insulin resistance. The transcriptional factor FoxO3 is maintained in the state of inhibition with normal insulin action. During a state of insulin resistance, as seen secondary to hepatosteatosis, inhibition of FoxO3 transcription factors would be lost, thereby promoting transcription of autophagy genes.

In conclusion, the increased hepatic triglyceride accumulation in sheep secondary to decreased post weaning physical activity is associated with increased gene expression of hepatic autophagy and ER stress indicating a state of increased hepatic cell stress response. This was not associated with changes in gene expression of hepatic energy sensing regulators AMPK, mTOR and hepatic leptin receptors.

3.4.3.2 NR-LG leads to exaggerated hepatic triglyceride deposition in obesity associated and upregulated gene expression of hepatic autophagy.

The hepatic triglyceride concentrations and organ weights at dissection were significantly greater in N-O in comparison to N-L offspring. Furthermore, when expressed relative to body weight, the N-O offspring had higher relative liver weight in comparison to A-O offspring. The findings of increased hepatic triglyceride content along with higher liver weight indicate that exaggerated triglyceride deposition may be the source of the increase in liver weight in N-O offspring.

The association of low birth weight with NAFLD [454] and abnormal liver function [277] has been demonstrated in epidemiological studies. A previous sheep study by Hyatt et al. of 50% nutrient restriction from 30 days to 80 days gestation demonstrated increased hepatic triglyceride deposition in the offspring at 1 year of age, in the absence of any change in birth weight [279]. This was associated with elevated hepatic gene expression for peroxisome proliferator-activated receptor γ (PPARG) and its co-activator PGC1 α , thereby indicating a decrease in hepatic fatty acid oxidation. Such decreased fatty acid oxidation, could be a mechanism of the observed increase in the hepatic triglyceride content. This mechanism is supported by the findings of a study performed in offspring of Wistar rats subject to gestational nutrient restriction to 65% of metabolic requirements during late gestation (day 14 until birth), and then fed a high fat diet [238]. The offspring of nutrient restricted rats developed insulin resistance, liver steatosis and ER stress. In association, high fat diet feeding in offspring of rats fed to appetite during pregnancy showed enhanced autophagic activity in liver whereas, the comparison group of IUGR rats maintained lower levels of Atg7 and LC3B II despite the high fat diet. The defective autophagy in the IUGR offspring was demonstrable as early as 6 hours of age. Developmentally, such an adaptation of defective

hepatic autophagy in a fetus would be consistent with a predictive-adaptive response of the fetal liver towards accumulation of glycogen in the short term and paradoxically, lipids in the long term in response to suboptimal nutrition during late gestation. Indeed, increased hepatic glycogen in IUGR sheep fetuses has been demonstrated [455, 456] and is a subject of mammalian investigation. This type of defective hepatic autophagy, when individuals are exposed to the relative nutrient excess of obesogenic environment, would result in less effective hepatic lipid mobilisation, leading to hepatosteatosis, associated ER stress and eventually, insulin resistance.

In obese humans, defective hepatic autophagy secondary to obesity has been associated with paradoxically increased gene expression of autophagy [450]. In this study, the gene expression of autophagy component BECN1 was maximum in the N-O group and was significantly increased in comparison to A-O and N-L groups. Furthermore, the gene expression of transcription factor ATF4, was increased with obesity in offspring of NR-LG sheep and decreased with obesity in offspring of sheep fed to appetite. ATF4, through its encoded protein also known as cAMP-response element binding protein 2 (CREB-2), promotes autophagy gene expression [95, 457]. Raised gene expression for ATF4, in association with the increased gene expression for BECN1 in the N-O offspring, indicates that, in comparison to obese offspring of sheep fed to appetite, the liver of the obese offspring of NR-LG sheep had activated UPR further enhancing autophagy gene expression. In the absence of any further indicators of autophagic flux, the interpretation of increased gene expression of BECN1 remains speculative. Any further interpretation of the isolated changes in gene expression of autophagy will require study of markers of autophagy function and should form part of any future investigation of this mechanism.

This is the first experimental study performed in a large animal model demonstrating the potential role of autophagy in the pathogenesis of hepatic steatosis in the subgroup of population exposed to *in utero* undernutrition.

3.4.4 The characteristics of sheep omental adipose tissue in obesity and effect of prenatal NR-LG

3.4.4.1 Obesity related changes in adipose tissue depot weight, distribution and adipocyte size are not affected by NR-LG.

As a risk factor for metabolic complications, visceral adiposity is known to be more predictive of adverse outcomes [29]. In this study, DXA scanning of 16 month old offspring demonstrated that fat mass constituted 14% of body weight of obese offspring as compared to 7.5% of body weight in the lean counterparts. These values of percentage fat mass measured by DXA scan are similar to previous experiments in 18 month old sheep raised in obesogenic environment [264]. The visceral depot weight was calculated as the sum of omental, pericardial and perirenal depots. When calculated as proportion of total predicted fat (from DXA scan performed at 16 months age), obese offspring had significantly increased visceral to total fat depot ratio as compared to the lean offspring. Prenatal NR-LG did not affect this preferential deposition of fat in visceral depots.

Obesity lead to a threefold increase in adipocyte size in the omental adipose tissue whereas NR-LG had no effect on the size of adipocytes in either the lean or obese offspring at 17 months of age. A strong correlation was evident between adipocyte size and the weight of the omental adipose tissue depot ($r=0.84$). As mature adipocytes do not divide *in vivo*, adipocyte hypertrophy is considered as the primary mechanism for expansion of white adipose tissue depot in obesity whilst dead cells are replaced by adipocyte precursors present in the stromal vascular fraction [458]. The strong correlation between adipocyte size and the weight of

adipose tissue depot demonstrated in this study supports this proposed mechanism. Spalding and colleagues have previously demonstrated this in experiments using the incorporation of ^{14}C as tracer and calculated that human adipocytes have a half-life of 8.3 years and, upon adipocyte death, new adipocytes replace old dead adipocytes [34]. The adipocyte number in an adult is tightly regulated irrespective of energy balance and in the state of excess energy, the excess lipid deposition is accommodated by increase in cell size.

Apart from storing reserve fuel, this process of adipocyte hypertrophy serves to protect the individual from adverse effects of circulating lipids. However, the metabolic and secretory demands of these hypertrophic adipocytes in obesity puts the cellular functioning under stress [459] leading to activation of the various cell stress response pathways. Exploration of such metabolic inflammation and cell stress response, therefore, is the natural next step in describing the features of obesity associated adipose tissue changes.

3.4.4.2 Obesity is associated with increased macrophage infiltration, the presence of CLS and activated milky spots in omental adipose tissue.

CLS were identified in omental adipose tissue from obese as well as lean animals. This is in contrast to the subcutaneous adipose tissue from the same animals where no CLS were identified from adipose tissue from lean or obese offspring [460]. Furthermore, in the obese animals, two distinct patterns, consistent with previously described CLS [68] and milky spots [461], were evident. In the omental adipose tissue from obese animals, the macrophages tended to be in clusters of CLS or as milky spots surrounding adjacent necrotic cells, whereas in the lean animals the CLS were infrequent and diffuse amongst adipocytes. Milky spots, which are a feature unique to omentum, develop in late gestation and are identifiable

as a large collection of immune cells, predominantly macrophages present in clusters and are considered to be an important source of macrophages for the peritoneal immune response [69]. Such milky spots were more abundantly present in omental adipose tissue from obese animals. However, despite analysing slides containing a minimum of 350 adipocytes per animal, accurate quantification of abundance of macrophage or CLS structures was not possible due to non-homogenous scatter of such structures throughout the adipose tissue sections. Increased abundance of Iba1 stained macrophages with obesity is supported by the finding of a 4-5 fold increase in CD68 gene expression with obesity (Section 3.4.4.3), indicating increased number and activation state with obesity.

3.4.4.3 Obesity associated upregulation of gene expression of adipokines and inflammation in omental adipose tissue is not exacerbated by NR-LG.

As expected, the omental adipose tissue from obese animals had a significantly higher gene expression for leptin which was increased 5 fold in A-O compared to the A-L offspring and increased 8 fold in N-O compared to the N-L offspring. The gene expression for leptin correlated strongly with plasma leptin levels at 16 months of age. Whilst the main function of leptin is in the regulation of appetite, its pro-inflammatory role is well recognised [52]. Elevated plasma leptin has been demonstrated to correlate with severity of metabolic dysfunction [47]. Cytokines of macrophage origin are known to be increased with obesity [462]. Accordingly, the omental adipose tissue from the obese offspring demonstrated significantly greater expression of CD68, indicating an increased number, and activation state, of the macrophages. Gene expression of TLR4, a membrane bound receptor known to be present on adipose tissue cells and capable of activating intracellular inflammatory pathways (JNK) and stimulating release of cytokines [57] was also

increased with obesity. The obesity associated increase in gene expression of leptin, CD68 and TLR4 is in agreement with the study hypothesis.

The lack of a further increase in the gene expression for CD68, TLR4 and leptin in offspring of nutrient restricted sheep fails to support the hypothesised worsened metabolic inflammation in omental adipose tissue. The findings are in contrast to a sheep study of 50% NR-LG (days 110-147) which demonstrated increased gene expression of perirenal adipose tissue CD68 and TLR4 at one year of age [68]. The differences between these findings may reflect the differential mechanisms of development of perirenal and omental adipose tissue. At birth, perirenal adipose tissue is relatively abundant, forming approximately 80% of total adipose tissue of sheep [463] as compared to omental adipose tissue which undergoes all of its lipid deposition after birth [322]. Furthermore, omental adipose tissue is distinctive due to presence of its own immune cell deposits, similar to lymphoid organs known as milky spots. These milky spots develop during the late gestation in humans [69]. The differential developmental processes of the two visceral adipose tissues depots, perirenal and omental, could explain the variance in the gene expression of components of metabolic inflammation CD68 and TLR4 in response to NR-LG. It is also plausible that the severity of nutrient restriction (60% of metabolisable energy) in this study was not severe enough to modify these components of the cell stress response. The age at the time of sampling of tissue may also be an important determinant of the difference in results. It is plausible that, by 17 months of age, the upregulated gene expression for cellular inflammatory pathways masks the relatively subtle impact of the NR-LG on these pathways. However, in the absence of larger studies focusing on depot specific differential gene expression at various stages of development and growth, such explanations are speculative. However, mechanisms of cell stress response intrinsic to the cell, such as autophagy

or ER stress [464], may influence the metabolic inflammation irrespective of lack of further increase in gene expression of extrinsic factors such as macrophage marker CD68 and pattern recognition receptors TLR4. Such intrinsic factors were the focus of further experiments described in this thesis.

3.4.4.4 Obesity associated upregulation of gene expression for autophagy and its energy sensing regulators in omental adipose tissue is not exacerbated by NR-LG.

In line with the study hypothesis, and as previously identified in human descriptive studies of omental adipose tissues of individuals with visceral adiposity [134], obesity led to upregulation of the gene expression for components of the autophagic pathway (ATG12 and BECN1) in omental adipose tissue. Similar to its role in the liver, autophagy contributes to adipose tissue homeostasis by regulating lipid metabolism and adipocyte development. Inhibition, or knockout, of autophagy related proteins ATG5 and ATG7 [131, 132] results in mice with a lean phenotype with decreased white adipose tissue mass and enhanced insulin sensitivity. In addition, autophagy has been closely linked to control of innate and acquired immunity [465]. AMPK, which is activated in a nutrient depleted state, is known to directly upregulate autophagy through phosphorylation. In contrast, mTOR inhibits autophagy. The upregulated gene expression of ATG12, BECN1 and AMPK with obesity, therefore, indicates that obesity enhances autophagy in adipose tissue as has been previously proposed [134].

The direction of relationship and specific role of autophagy in obesity has not been clearly identified. It has been proposed that increased autophagy in obese adipose tissue is a cell survival response to obesity induced metabolic and inflammatory stress and insulin resistance [107]. However, as a process which interacts at multiple nodes with other cell stress

response pathways, activated autophagy has been shown to degrade insulin receptors [466] and promote survival of anti-inflammatory (M2) monocytes. A persistent increase in autophagy also has the potential to promote cell death, a feature of obese adipose tissue microstructure.

NR-LG did not result in the hypothesised accentuation of gene expression for autophagy in omental fat. In conjunction with the previously described findings of increased gene expression of leptin, TLR4 and CD68, these results suggest that whilst autophagy and inflammation are associated with obesity, these pathways may not be a target of nutritional programming during late gestational undernutrition.

3.4.4.5 Omental adipose tissue from obese sheep exposed to NR-LG demonstrates upregulated UPR.

It was predicted in the study hypothesis that obesity would lead to upregulation of gene expression of UPR [99, 103, 105]. In this model of young adult sheep experiencing moderate obesity, upregulation of UPR components ATF6, EDEM1 and GRP78 was limited to obese offspring of NR-LG sheep, in comparison to the lean offspring of the NR-LG sheep. Adipose tissue ATF4 gene expression was uniformly increased in obese offspring in comparison to lean offspring, irrespective of prenatal intervention. Therefore, the tendency for upregulation of UPR in obesity, as evident by increased ATF4, was enhanced by the prenatal undernutrition in the offspring of NR-LG sheep.

The three genes, ATF6, EDEM1 and GRP78, share the same transcriptional regulators (Figure 3.27) called ER Stress Response Element-II (ERSE-II) and UPRE (Unfolded Protein Response Element). Upon activation of UPR, the canonical pathways ATF6 and IRE1 activate these transcription factors leading to increased gene expression of UPR genes [467].

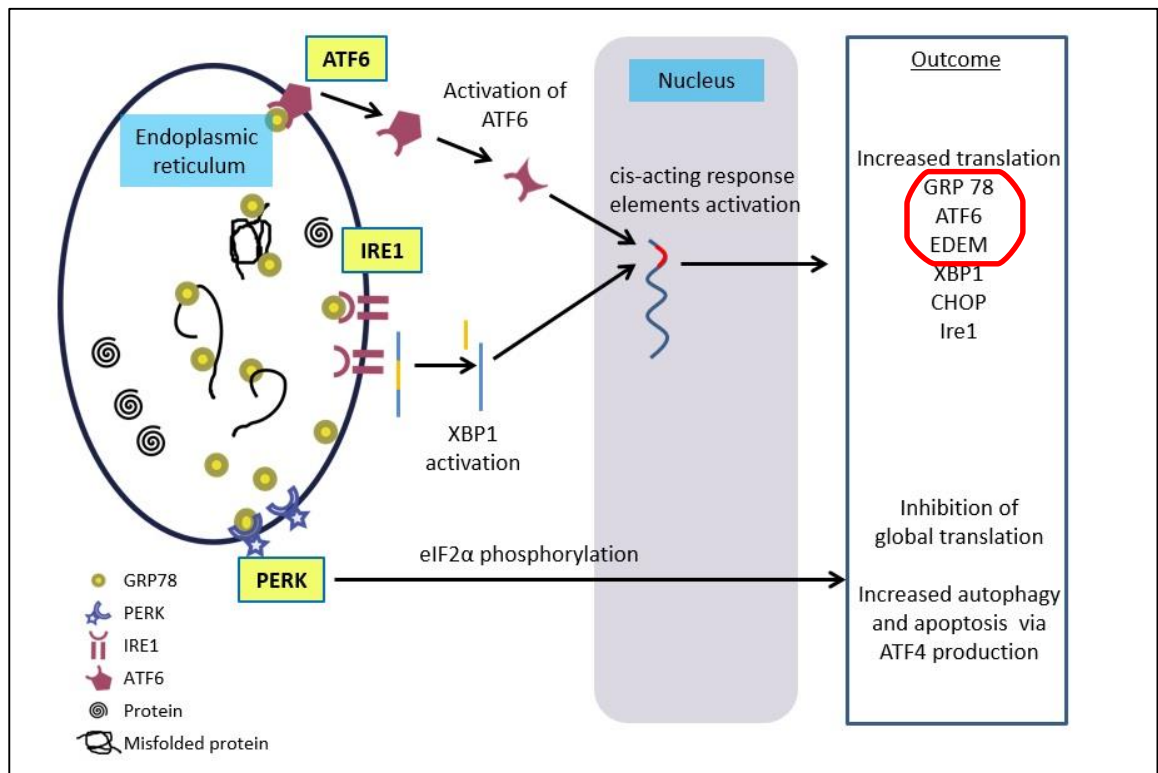


Figure 3.27 Schematic diagram of canonical pathways of ER stress demonstrating the common transcription factor known to upregulate gene expression for GRP78, ATF6 and EDEM (encircled in red).

The adipocyte endoplasmic reticulum plays an important role in maintaining cell homeostasis by contributing to protein folding, secretion of adipokines [112], lipid droplet formation [468] and lipid metabolism [469]. ER stress not only affects the adipocyte protein and lipid metabolism but also leads to upregulation of inflammation and consequent insulin resistance [99].

Upregulated UPR in perirenal adipose tissue of obese sheep has previously been demonstrated in a model of prenatal nutrient restriction to 50% of requirements during early gestation [68]. Sharkey *et al.* then proposed that suboptimal nutrition during adipocyte development programmes a reduced total adipocyte number. When subject to the nutritional abundance of obesity, the fewer adipocytes in the visceral depots would reach their lipid storage capacity sooner. These expanding adipocytes would, therefore, reach the threshold of activation of ER stress response at a lower level of obesity. The activated ER stress response, while initially attempting to restore the cellular homeostasis and survival, can eventually lead to activation of inflammatory pathways, cell death pathways and development of insulin resistance. In such a scenario, the upregulated gene expression of UPR components is the consequence of the expanding adipocyte reaching the threshold of ER stress response sooner.

Omental serosa and omental adipose tissue share the same developmental source of mesodermal stem cells [314]. In humans and sheep, before birth, the omentum is predominantly comprised of serosal tissue and milky spots and there is very little recognisable adipose tissue. During the late gestation, the sheep omentum rapidly increases in size from 90mm² at 50 days gestational age to 21,000mm² by term gestation [69]. Following birth, the omental adipose tissue depot rapidly expands and since mature adipocytes do not divide, this occurs from differentiation of preadipocytes of mesodermal origin present in the omentum [470]. Any suboptimal

nutrition during late gestation could affect the adipocyte precursors making the omentum vulnerable to programming of adipocyte number, and thereafter, to rapid expansion of adipocyte size following birth in a similar fashion as proposed by Sharkey *et al.* for perirenal adipose tissue (Figure 3.28).

Another explanation could be a resetting of such threshold of activation of ER stress response in the offspring of NR-LG sheep. Models of various activation states of the UPR [471] have been proposed. Modulation of UPR activation has been proposed to be mediated by mechanisms such as variation in the concentrations of intra-organelle chaperone proteins [472], alterations in the inactivating binding of such chaperones or turnover rates of the individual components of the UPR[473]. ER is sensitive to nutrient supply as it uses considerable energy for protein processing steps such as protein folding, chaperone functioning and vesicle formation [155]. Furthermore, glucose deficiency by itself has been proposed to cause inefficient protein folding adding to the ER stress load [474, 475]. Indeed, glucose regulated proteins were so named because they were regulated by the glucose concentration in the culture medium [476]. Upregulation of the ER stress response in response to hypoglycaemia has been demonstrated in *in vitro* experiments in tumour cells [477], pancreatic β cells [477], myocytes and adipocyte cell cultures [478]. Apart from the rapid increase in the size of omental serosa containing adipocyte precursors and macrophage collections during late gestation [69], this period also coincides with dynamic nutritional and endocrine changes in other established adipose tissue depots [479] with active protein synthesis in the adipocyte. Any suboptimal nutrient restriction during this period of increased metabolic demand of rapidly growing and developing omental adipocyte precursors would activate an ER stress response. Adipocytes and developing precursors with lower threshold for ER stress response in such

a scenario are more likely to survive and potentially prepare the organ to a poor postnatal environment, as proposed in the predictive adaptive response hypothesis [480]. When this subgroup of animals are further subjected to post-weaning obesity, the ensuing ER stress in the adipocyte, would achieve the threshold of activation of UPR sooner. After the initial pro-survival actions, prolonged UPR in these offspring would initiate inflammation and cell death pathways (Figure 3.28).

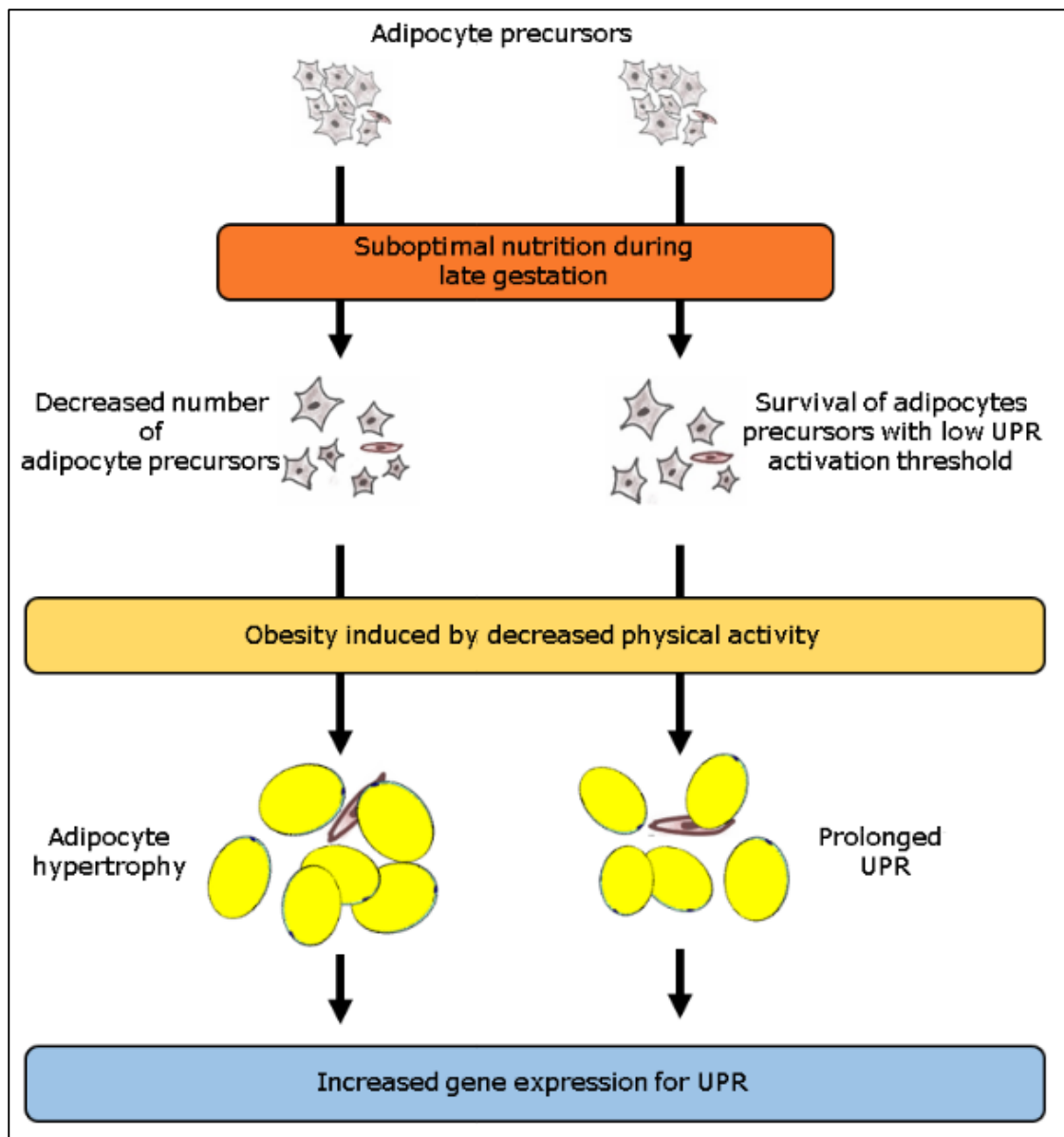


Figure 3.28 Schematic diagram depicting the two proposed mechanisms leading to increased vulnerability of adipose tissue of offspring of nutrient restricted sheep to obesity induced cell stress.

Exposure to undernutrition during late gestation may decrease the number of total adipocytes. When subject to relative nutrient excess of obesity, the adipocytes expand by hypertrophy, thereby predisposing the cells to ER stress and activation of cell stress pathways and inflammation. Alternatively, during the period of prenatal undernutrition, cells capable of instituting UPR at a lower threshold, are selectively able to survive the period of undernutrition. When exposed to hypertrophy and the cell stress of the obesogenic environment, the lower threshold of UPR activation leads to a prolonged UPR which then redirects the cellular response towards inflammation and cell death pathways.

3.4.4.6 Protein abundance of GRP78 was increased with obesity and is not modified by NR-LG.

IHC staining for GRP78 demonstrated localisation of this protein in the cytoplasmic fraction of adipocytes in contrast to pJNK, which was present in the perinuclear area. Adipocyte number was used as a denominator because of the variance in adipocyte size with increasing obesity [68]. Obesity was associated with increased GRP78 staining per adipocyte. NR-LG did not lead to any difference in the quantity of the staining. This fails to confirm the outcome predicted by the gene expression analysis where NR-LG followed by offspring obesity was associated with increased gene expression as compared to the offspring of mothers fed to appetite during late gestation. It is known that the relationship between gene expression and protein expression is not linear as the latter is the outcome of multiple post-transcriptional processes including mRNA processing, postranslational modifications, misfolding and ER associated protein degradation, negative feedback and, most importantly, the sensitivity of the quantifying assay [481]. The increased staining for the protein in obese offspring in comparison to the lean animals suggests that the increase in UPR genes in offspring of NR-LG sheep is in a background of increased ER stress response to obesity as suggested by increased gene expression of ATF4 genes. Increased adipose tissue UPR with obesity is a well-documented phenomenon which is confirmed by this study [112].

3.5 Conclusion

The first objective of this study was to establish a large animal model of obesity and to describe the characteristics of cell stress response to obesity in two metabolically vital organs, liver and omental adipose tissue. Restriction of physical activity, instituted after weaning from mother's feeding at 90 days of age, established a model of obesity with 1.35 fold weight gain in comparison to sheep in an unrestricted environment. In contrast to other sheep studies, such relative weight gain can be designated as mild to moderate obesity. In this study, such a degree of obesity was associated with alterations of glucose homeostasis which were demonstrated by the GTT results of decreased glucose disposal at 7 months of age and insulin resistance at 16 months of age.

The adipose tissue from obese sheep demonstrated preferential lipid deposition in visceral depots as compared to lean animals and omental adipose depot weight was strongly correlated with adipocyte size. A correlation was also demonstrated between plasma leptin concentrations and the gene expression of omental adipose tissue leptin in obese sheep. In omental adipose tissue, obesity was associated with a generalised increased gene expression of components of metabolic inflammation and the cell stress response including autophagy and some components of UPR. Furthermore, obese adipose tissue demonstrated increased abundance structures consistent with activated milky spots and crown like structures as compared to adipose tissue from lean sheep.

In the liver from obese sheep, increased liver weight correlated with hepatic triglyceride content. The study was unable to identify histological features of evolving non-alcoholic fatty liver disease in this sheep model. There was a generalised increase in gene expression for autophagy and ER

stress in association with the increased hepatic lipid deposition demonstrated with obesity in this sheep model in comparison to the lean animals.

The metabolic derangements associated with obesity and the ensuing metabolic syndrome have been proposed to be the outcome of active metabolic inflammation in adipose tissue and liver, leading to cellular dysfunction, death and insulin resistance. This study is unique as it confirms the presence of the activated cell stress response and metabolic inflammation in the adipose tissue and liver and describes their characteristics in a large animal model of physical inactivity induced obesity at young adult age equivalence. This establishes a baseline for investigation of the interactions of obesity with other risk factors such as developmental programming on the cell stress response and metabolic inflammation with the potential to accentuate an individual's risk of worse metabolic outcomes.

Suboptimal maternal nutrition during late gestation is one such risk factor and the second objective of this study was to investigate the developmental programming impact of such poor nutrition on the cell stress response and inflammation at young adult equivalent age. Twin bearing sheep subject to NR-LG to 60% of maternal metabolic requirements had decreased plasma insulin and glucose and increased plasma NEFA in comparison to sheep fed to appetite signifying a state of energy deficit in the environment of the growing fetus. This resulted in lower maternal weight and decreased offspring birth weight in comparison to sheep fed to appetite. NR-LG did not exacerbate markers of obesity induced decreased glucose disposal or insulin resistance as measured during GTT performed at 7 months and 16 months respectively.

Adipose tissue distribution and relative adipose depot weight was not affected by prenatal nutrition. Following NR-LG, obese offspring demonstrated upregulation of all four UPR genes in comparison to lean offspring. The gene expression for UPR component ATF4 was upregulated in all obese offspring irrespective of prenatal nutrition group. Prenatal suboptimal nutrition did not exacerbate obesity induced upregulated omental adipose tissue autophagy and increased gene expression for CD68 and leptin.

Obesity associated increased hepatic weight was exaggerated in offspring of NR-LG sheep in comparison to offspring of sheep fed to appetite, a result similar to a previous study of prenatal nutrient restriction during early gestation [279] which was proposed to be an outcome of decrease in hepatic fatty acid oxidation. Developmentally, such a process would indicate a response of a nutrient deprived fetus leading to a phenotype maladapted to the relative nutrient excess of obesogenic postnatal environment. The obesity associated increased gene expression of hepatic autophagy marker BECN1 was exaggerated with prenatal NR-LG. Obesity is associated with a defective autophagy [234] which can promote hepatic lipid accumulation associated with increased compensatory gene expression. Such defective autophagy has also been identified in offspring of nutrient restricted rats, in association with increased hepatosteatosis [238]. Future studies in this regard should focus of demonstrating the characteristics of the hepatic autophagic function in the obese offspring of NR-LG sheep.

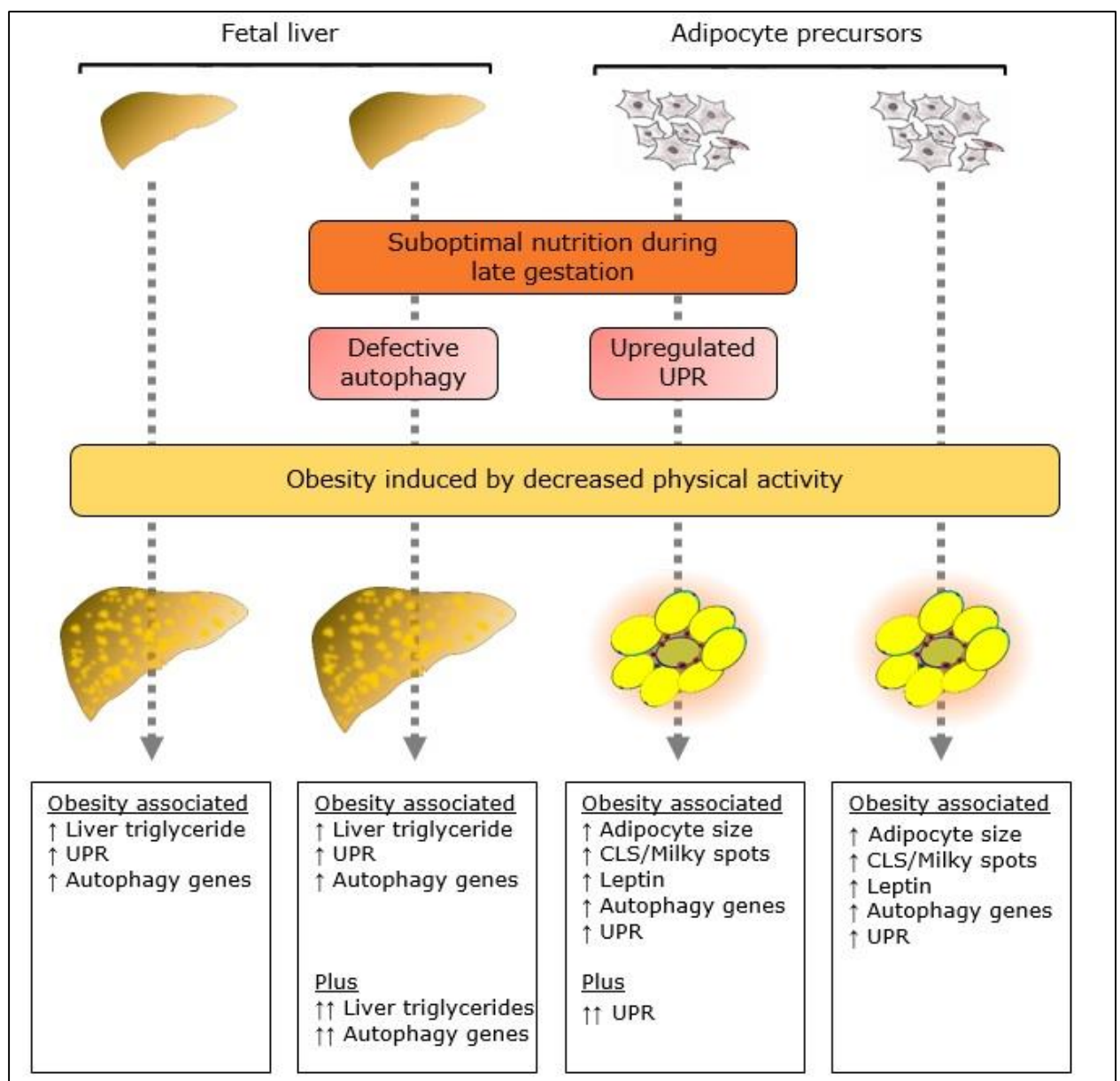


Figure 3.29 Schematic flowchart summarising the overall findings of the study described in this chapter.

Obesity leads to increased liver triglyceride, and increase in UPR and autophagy genes. If obesity is preceded by nutrient restriction during late gestation, the increase in liver triglyceride and BECN1 autophagy gene is further enhanced. In the omental adipose tissue, obesity leads to increased adipocyte size and macrophage infiltration in association to increase in gene expression for UPR and autophagy. If preceded by nutrient restriction during late gestation, the adipose tissue UPR is further enhanced.

In conclusion, the results described in this chapter describe the characteristics of upregulated gene expression of omental adipose tissue UPR and hepatic autophagy in the obese offspring of NR-LG sheep (Figure 3.29). On the background of obesity associated enhanced hepatic and adipose cell stress response and adipose metabolic inflammation in a large animal model described in this chapter, such findings establish a direction for potential future studies.

4 Interaction of prenatal nutrient restriction and formula feeding during early life on the cell stress response and metabolic inflammation in liver and adipose tissue.

4.1 Introduction and hypothesis

Nutrient supply during early infancy has the potential to influence long term health of an individual [281, 344]. Several meta-analyses [299, 300, 482] have demonstrated both a dose response and a categorical relationship between breastfeeding and decreased risk of obesity in later life as compared to feeding with infant formula milk. However, studies investigating the development of metabolic syndrome and its relationship to the type of feeding during infancy are sparse and not conclusive [301]. A recent meta-analysis of breast fed infants (n=76,744) identified a decreased risk of later type 2 diabetes as adults (pooled odds ratio: 0.61; 95% CI: 0.44–0.85; p=0.003) [301, 305]. In contrast, other studies have reported an absence of any association between infant feeding type on the components of metabolic syndrome in adulthood [306].

Experimental studies investigating the mechanisms of the impact of feeding type on development of later obesity and adverse metabolic health have primarily focussed on appetite regulation [307, 308]. However, published literature investigating the effects of the type of infant feeding on the liver and adipose tissue is limited to one observational study demonstrating increased likelihood of developing NAFLD in childhood in formula fed infants [309] and one longitudinal study which demonstrated no difference in hepatic lipid content or adiposity of breast fed in comparison to formula fed infants at 13 and 63 days median age [310]. Both, liver and adipose tissue have a vital role in the pathogenesis of

obesity associated metabolic dysfunction [21, 239]. Therefore, any investigation of mechanisms of increased predisposition to obesity and adverse metabolic outcomes due to formula feeding should focus on describing the hepatic and adipose tissue characteristics and investigate the pathogenic processes in these organs. There are no published experimental studies which investigate the cumulative effect of prenatal undernutrition and formula feeding during early life on the development of obesity and metabolic syndrome.

In the absence of such experimental studies, there is a need for a randomised experimental study performed in a suitable large animal model which compares type of milk used for feeding during early postnatal life and reports the adult outcomes of such groups. The study described in this chapter utilises a sheep model to investigate the impact of formula feeding in comparison to being fed by mother, on the mechanisms influencing long term metabolic health of an individual. In addition, through the use of a 2 by 2 factorial design, this study also investigates if suboptimal maternal nutrition during late gestation interacts with postnatal diet to influence the the long term metabolic health of the offspring. This experimental model aims to reflect individuals who were fed with formula milk after being born growth restricted due to reduced maternal nutrition and then who become obese in later life and compare with individuals fed on the mother's milk.

The results in Chapter 3 describe the characteristics of liver and adipose tissue metabolic inflammation in sheep due to obesity with, or without, a background of prenatal nutrient restriction. The study now described in this Chapter builds on these findings by incorporation of an additional stimulus of formula feeding which has the potential to exacerbate obesity and associated adverse metabolic outcomes [299, 305]. Such outcome measures of adiposity, state of metabolic inflammation in liver and adipose

tissue and overall metabolic health have not been previously described in a large animal model.

In light of findings described in Chapter 3 and the limited evidence summarised above, the experiments described in this chapter investigate the following experimental hypotheses:

1. Formula fed lambs, in comparison to lambs fed by their mother, would experience greater adiposity and visceral fat deposition in young adult age. It is predicted that this will be associated with decreased insulin sensitivity and increased gene expression of components of metabolic inflammation in liver and omental adipose tissue.
2. Formula fed offspring born to mothers exposed to nutrient restriction in late gestation (NR-LG), in comparison to the group not exposed to *in utero* undernutrition, will demonstrate a greater increase in hepatic and adipose tissue metabolic inflammation and an exaggerated cell stress response to obesity. It is predicted that this would manifest as augmented gene expression of pathways of metabolic inflammation and the cell stress response, worsening of metabolic parameters and decreased insulin sensitivity in the formula fed offspring of the nutrient restricted group in comparison to the group not exposed to *in utero* undernutrition.

4.2 Methods

The design of the study, animal interventions and all experimental methods used to establish the results described in this Chapter are described in detail in Chapter 2 and summarised in Figure 4.1. Briefly, after confirmation of twin gestation by ultrasound scanning, twin bearing ewes were randomised to either nutrient restriction (N) to 60% of metabolic requirements from gestational day 110 until term (145 ± 2 days) or fed to 100% of metabolic requirements (R) through the entire gestation. After birth, the twin offspring were separated during the suckling period (birth to 90 days): one twin was formula fed (F) whilst the other was fed by their mother (M). The resulting combination of prenatal (R and N) and postnatal factors (M and F) render a factorial experimental design with four groups (R-M, R-F, N-M and N-F). Post-weaning, the offspring were all raised in a barn with a stocking rate of 6 sheep per 19m².

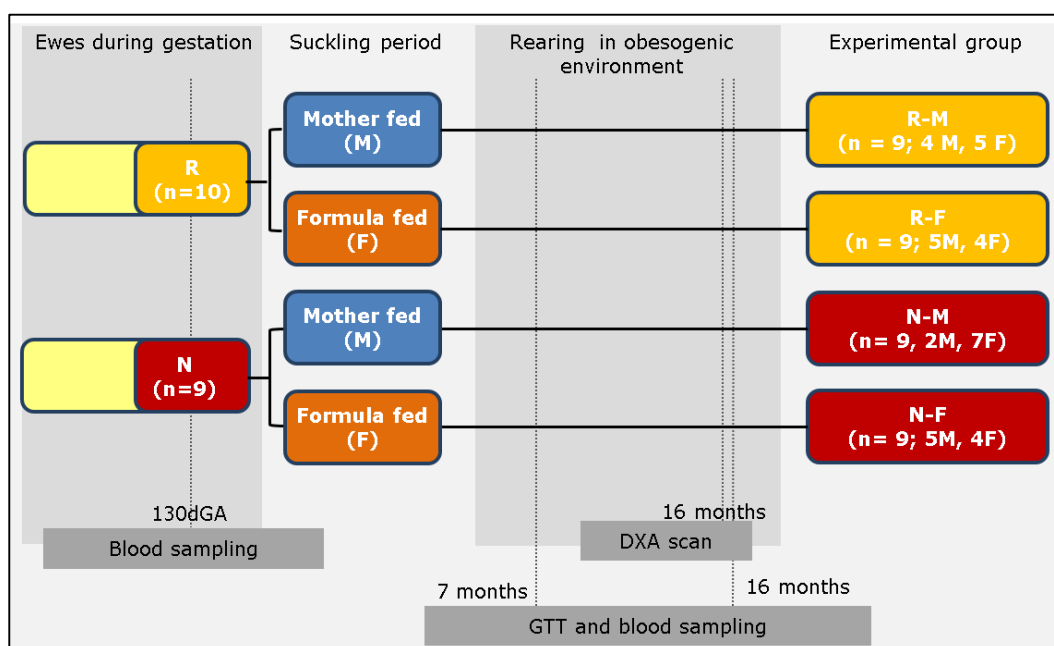


Figure 4.1 Schematic diagram depicting the experimental study design investigating effect of late gestation maternal nutrient restriction and type of feeding during suckling period (birth to 90 days age) on obesity and metabolic health of 17 month old sheep.

From 110 days gestational age (dGA) to term, ewes were fed a diet meeting requirements (R, n=10) or a nutrient restricted diet (N, n=9). During the suckling period, twin offspring were separated where one twin was reared by mother (M) and the sibling was separated from their mother and fed with formula milk. DXA, dual-energy X-ray absorptiometry; GTT, glucose tolerance test; dGA, days gestational age.

All the animals were humanely euthanased at 17 months of age and, after weighing organs, representative samples from liver and adipose tissue were snap frozen in liquid nitrogen and stored at -80°C until further processing for analyses such as gene expression analysis, histological and immunohistochemical analysis and hepatic triglyceride content and thiobarbituric acid reactive substances (TBARS) analyses. The animal experiments were performed at the joint animal breeding unit, Sutton Bonington Campus of the University of Nottingham (Nottingham, UK), by Dr S. Sebert under supervision of Professor M.E. Symonds and Dr D. Gardner. The results presented in this thesis were derived from analysis of raw data by the author.

The statistical analyses are described in detail in Chapter 2. Briefly, for the factorial study design, the data were first interrogated with two-way analysis of variance (2-way ANOVA). Upon identification of a significant effect or interaction on the 2-way ANOVA, a hypothesis driven simple main effects analysis was performed for comparison between groups differing in only one factor (prenatal nutrient restriction or environment of rearing). If required, non-parametric testing was performed using Kruskal-Wallis test followed by Mann Whitney. Outcome for GTT and body weight measurements produced results with repeated measures in same animal over time. Analyses for such data with repeated measures were performed with two way or three way mixed ANOVA and time was included as a within-subject factor to assess for interaction between time and experimental conditions. For sake of uniformity of presentation and in keeping with standard practice, data have been expressed as mean and standard error of the mean for all the experimental output irrespective of the type of distribution of the data.

The final animal numbers in the experimental groups, as depicted in Figure 4.1 excludes the 4 offspring, one in each of the four experimental groups that died unexpectedly prior to the studies' end. The specific causes of animal deaths are not known. The deaths were not concentrated in any specific experimental group and are fewer than 10% reported natural death rate in similar populations [329].

4.3 Results

4.3.1 Maternal and offspring metabolic profile

4.3.1.1 Weight gain and metabolic profile of pregnant ewes.

The body weight of sheep randomised to NRLG (N, n=9, 72 ± 1.9 kg) did not significantly differ ($p=0.78$) from sheep randomised to a diet meeting metabolic requirements (R, n=10, 69.7 ± 1.8 kg). Two-way mixed ANOVA was performed with time (dGA) as within-subject factor to account for repeated measures. There was a statistically significant interaction between the maternal nutrition and time on body weight expressed as percentage of weight at the beginning of intervention ($p=0.008$). Sheep undergoing NR-LG to 60% of ME gained significantly less weight during the late gestation (Figure 4.2).

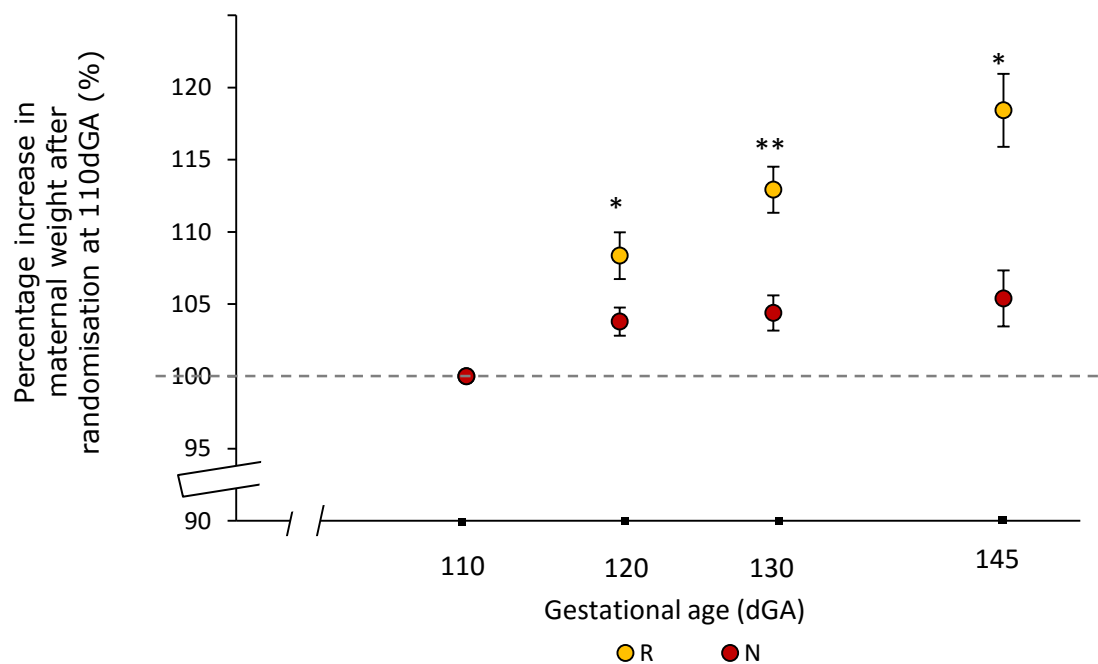


Figure 4.2 Weight gain during late gestation (110 -145 days), expressed as percentage gain over the weight at 110 days of gestation in ewes fed a diet meeting requirements (R, yellow, n=10) or a nutrient restricted diet (N, red, n=9) during late. Data are means with error bars representing SEM. Two-way mixed ANOVA was performed with time (dGA) as within subject factor to account for repeated measures. * $p < 0.05$ and ** $p < 0.001$ for N versus R simple main effects comparison.

At 130dGA, ewes in the nutrient restricted group had a lower plasma glucose and higher plasma NEFA concentrations. There was no difference in plasma insulin and plasma triglyceride levels (Figure 4.3). The fasting early morning plasma cortisol was also not different between the N (mean \pm SEM; 26.8 ± 5.4 nmol/L, n=9) and R (17.7 ± 2.5 nmol/L, n=10) groups.

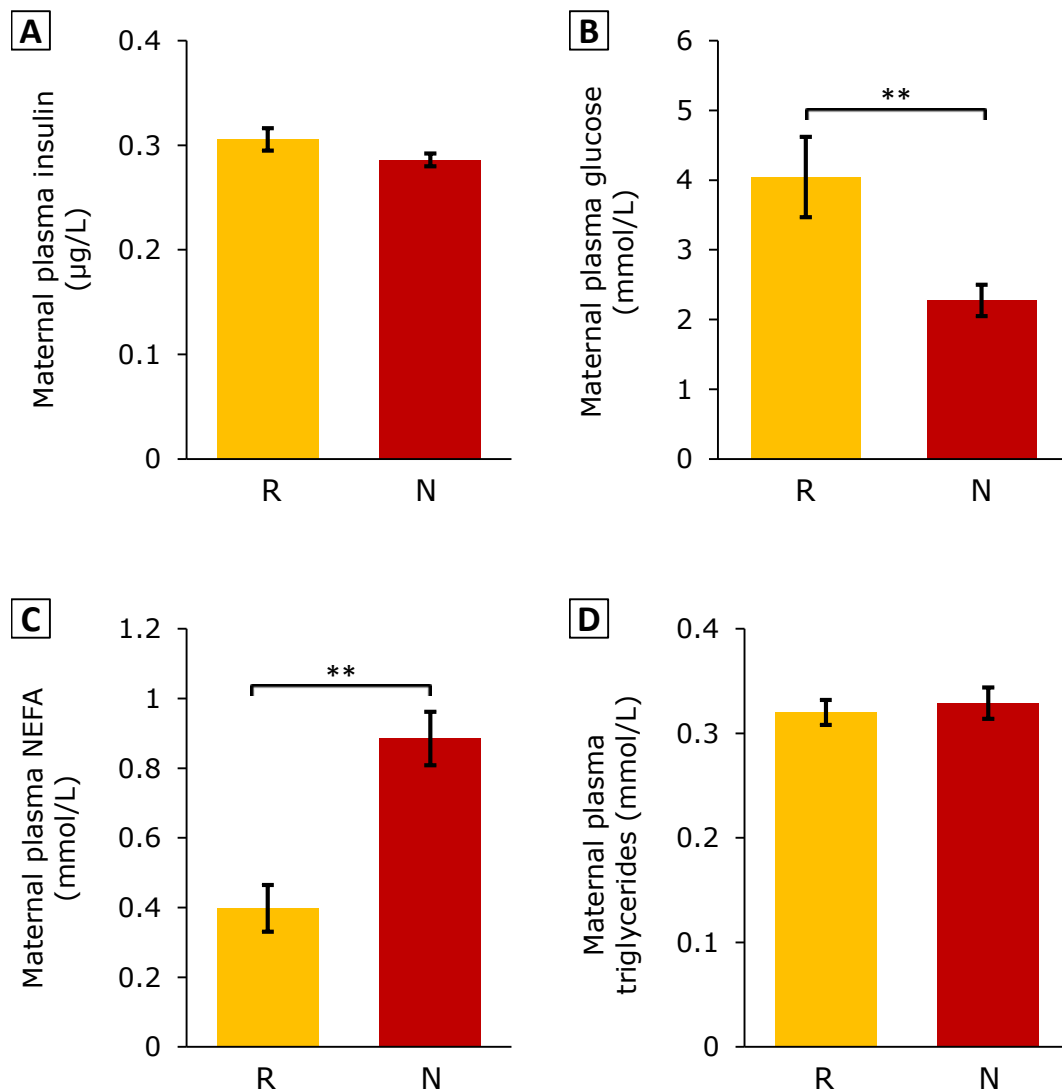


Figure 4.3 Fasting plasma insulin (A), glucose (B), NEFA(C) and triglyceride (D) concentration on 130 days of gestation in ewes fed a diet meeting requirements (R, yellow, n=10) or a nutrient restricted (N, red, n=9) between 110–145 days of gestation. Data are means with error bars representing SEM. **p<0.001 for N versus R comparison identified by independent sample t tests. NEFA, non-esterified fatty acids.

4.3.1.2 Offspring birth weight, weight gain and physical activity phenotype during the suckling period

The birth weight of the twin offspring of ewes in N group (3.75 ± 0.11 kg, $n=18$) was significantly lower than the offspring of the ewes in R group (4.86 ± 0.14 kg, $n=17$; $p < 0.001$).

One of each twin pair of offspring was randomised to being fed by the mother whilst the sibling was randomised to being fed on formula milk. There was no difference in the mean birth weight measurements of the offspring randomised to feeding on formula milk or on their mother's milk as detailed in Table 4.1.

	Prenatal nutrition	Feeding method		Prenatal nutrition	Feeding method	Interaction
		Mother fed	Formula fed	p value	p value	p value
Birth weight (kg)	R	4.96 ± 0.27^c	4.78 ± 0.17^d	<0.001	0.87	N/A
	N	3.69 ± 0.17^c	3.81 ± 0.16^d			

Table 4.1 Birth weight measurements in offspring of ewes fed to requirement during pregnancy randomised to formula feeding (R-F, $n=9$) or being fed by mother (R-M, $n=9$) and offspring of ewes nutrient restricted during late gestation randomised to formula feeding (N-F, $n=9$) or to being fed by mother (N-M, $n=9$). Data presented as means \pm SEM. Statistical significance denoted by superscripts c versus d, $p < 0.001$ for simple effects analysis of 2-way ANOVA

To account for repeated measurement of weight at different timepoints and factorial study design, a three-way mixed ANOVA was performed with weight at different timepoints as the within-subject factor. The analysis was not significant for a three-way interaction. However, a significant ($p=0.003$) two-way interaction was present between feeding method and weight at different timepoints. The simple main effects analysis demonstrated difference between weight of formula fed and mother fed offspring at all measurements during the suckling period (Figure 4.4)

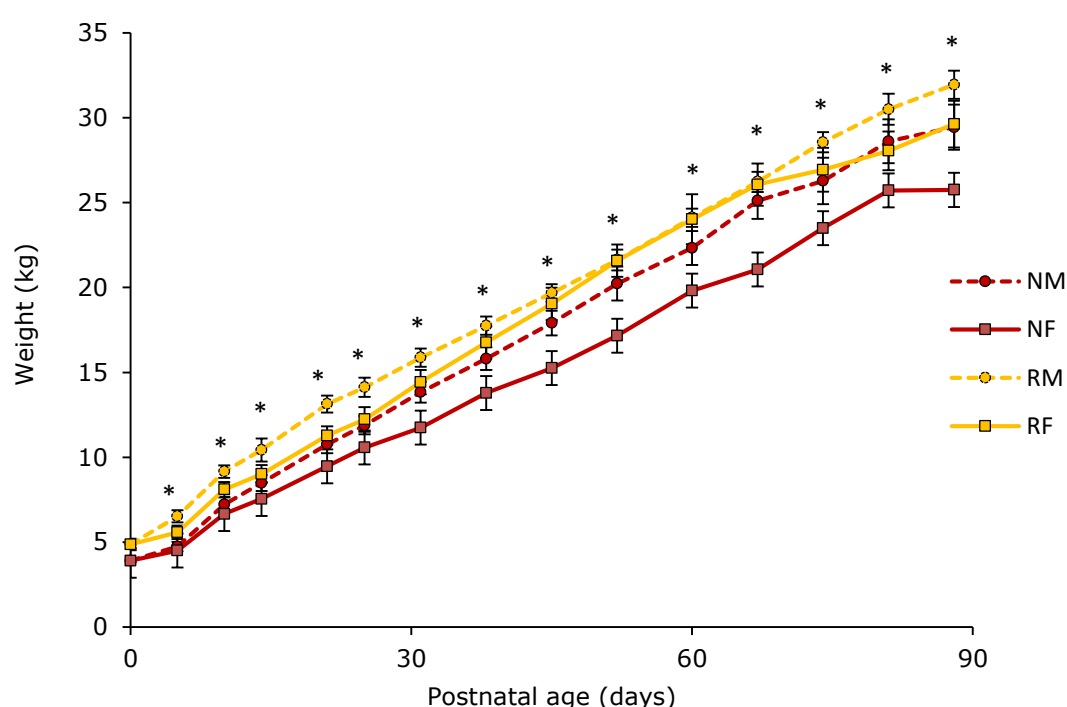


Figure 4.4 Weight gain during the suckling period for the N-F (red squares, continuous red line, $n=9$), R-F (yellow square, continuous line, $n=9$), N-M (red circles, dashed red line, $n=9$) and R-M (yellow circles, dashed line, $n=9$) offspring. Three-way mixed ANOVA accounting for repeated measures across time was performed. ** $p<0.05$ for main effect analysis between formula fed and mother fed offspring. Data presented as means with error bars representing SEM

The relative rate of growth, expressed as fold change from birth to 30, 60 and 90 days of age was greatest in the N-M group in comparison to N-F and R-M offspring respectively (Figure 4.5).

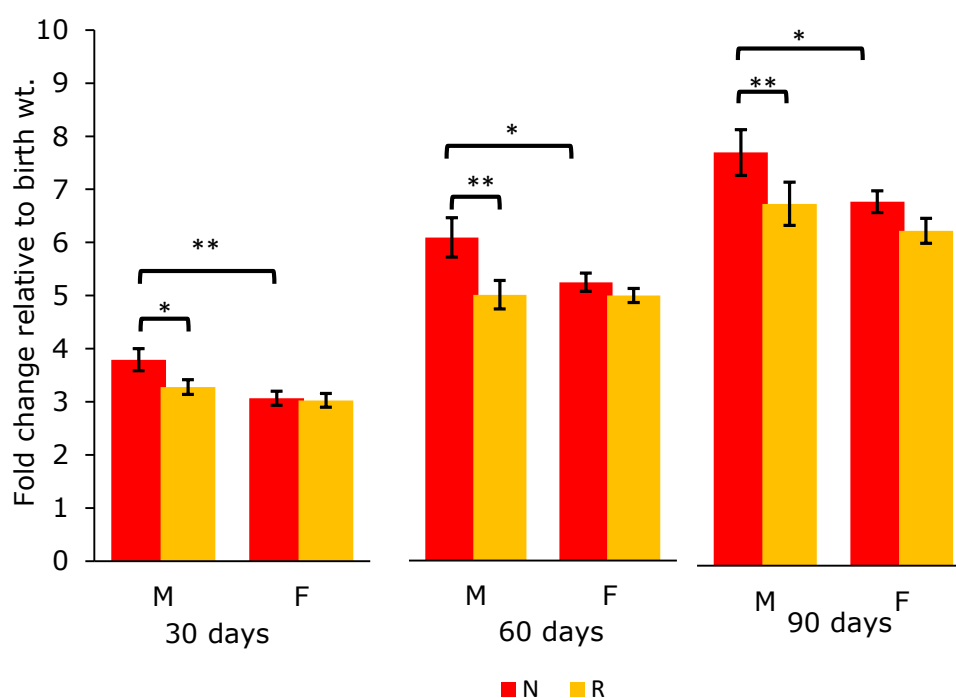


Figure 4.5 Relative weight gain during the suckling period in offspring of ewes fed to requirement during pregnancy randomised to formula feeding (R-F, n=9) or being fed by mother (R-M, n=9) and offspring of ewes nutrient restricted during late gestation randomised to formula feeding (N-F, n=9) or to being fed by mother (N-M, n=9). Data presented as means with error bars representing SEM. * $p < 0.05$, ** $p < 0.001$ for simple effects analysis following 2-way ANOVA.

The recordings of physical activity performed at 45 days of age identified that formula fed offspring were less active in comparison to the offspring fed by their mother. The duration of mobility during a 24 hour period also approached statistical significance with a trend towards decreased activity in formula fed offspring irrespective of the prenatal nutrition (Table 4.2).

	Prenatal nutrition	Feeding method		Prenatal Nutrition p value	Feeding method p value	Interaction p value
		Mother fed	Formula fed			
Mean activity (counts)	R N	155±5 ^a 158±14 ^c	105±10 ^b 99±13 ^d	0.90	<0.001	0.71
Duration mobile in 24 hours (minutes)	R N	972±60 1049±55	944±57 826±88	0.76	0.08	0.16
Maximum intensity of physical activity (counts)	R N	2042±171 2627±449	2188±247 3543±635	0.03	0.22	0.37

Table 4.2 Physical activity parameters at 45 days of age in offspring of ewes fed to requirement during pregnancy randomised to formula feeding (R-F, n=9) or being fed by mother (R-M, n=9) and offspring of ewes nutrient restricted during late gestation randomised to formula feeding (N-F, n=9) or to being fed by mother (N-M, n=9). Data presented as means ± SEM. Statistical significance denoted by superscripts a versus b, p<0.05; c versus d, p<0.001 for simple effects analysis of 2-way ANOVA

4.3.1.3 Plasma metabolic profile at the age of 7 months

Offspring feeding method or maternal nutrient restriction during late gestation had no significant impact on fasting blood glucose or insulin at 7 months of age (Table 4.3). The analysis was performed using three-way mixed ANOVA to account for repeated plasma glucose measurements at different time points. There was no significant three-way interaction between prenatal nutrition, feeding method and time ($p=0.66$, Figure 4.6A). The analysis also demonstrated lack of two-way interaction between prenatal nutrition and time ($p=0.38$) and feeding method and time ($p=0.51$). Simple main effect test for two-way interaction between prenatal nutrition and feeding method was also not significant ($p=0.80$).

The plasma insulin concentrations (Figure 4.6) did not demonstrate a statistically significant three-way interaction between the experimental groups and time ($p=0.62$). Analysis for two-way interactions also did not identify an interaction between prenatal nutrition and time ($p=0.82$) or feeding method and time ($p=0.52$). Simple main effect test for two-way interaction between prenatal nutrition and feeding method was also not significant ($p=0.34$).

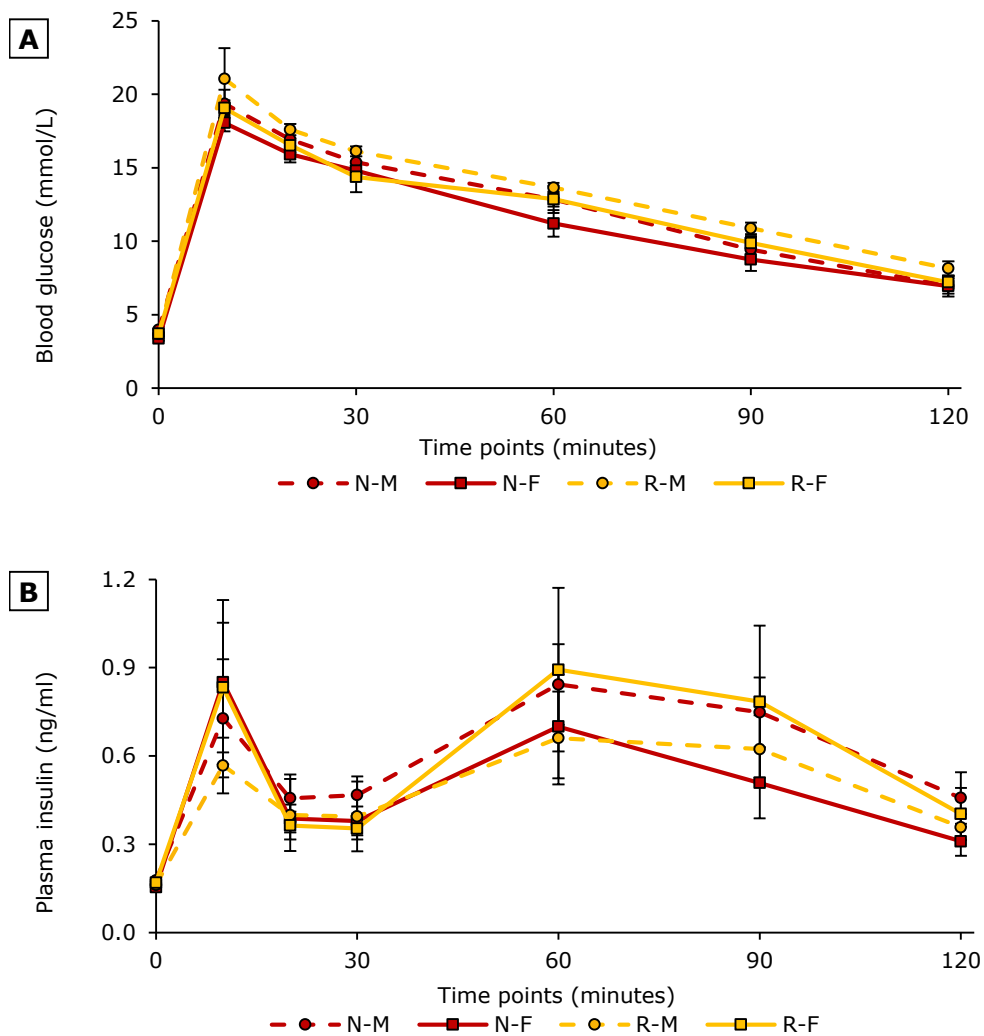


Figure 4.6 Plasma glucose (A) and insulin (B) concentrations during a glucose tolerance test performed at the age of 7 months from lambs randomised as described to formula feeding (R-F, n=8; N-F, n=7) or being fed on their mother's milk (R-M, n=9; N-M, n=9). Data presented as means with error bars representing SEM. Statistical analysis performed with three-way mixed ANOVA.

The area under the curve for glucose and insulin measurements during the GTT was calculated and did not differ between the groups (Table 4.3). Analysis of HOMA-IR index calculated using the baseline glucose and insulin concentrations demonstrated a significant interaction between the experimental measures. However, there was no statistical difference on subgroup analysis for simple effects.

	Prenatal nutrition	Feeding method		Prenatal nutrition	Feeding method	Interaction
		Mother fed	Formula fed	p value	p value	p value
AUC glucose (mmol/L)	R	1585±45	1452±51	0.10	0.07	0.84
	N	1462±90	1355±71			
AUC insulin (ng/ml)	R	42.8±11.3	56.0±17.0	0.97	0.99	0.30
	N	55.5±9.57	40.1±9.49			
HOMA-IR	R	6.0±0.4	6.4±0.7	0.12	0.82	0.03
	N	7.4±0.6	5.2±0.3			

Table 4.3 Markers of insulin sensitivity expressed as area under the curve and HOMA-IR calculated from glucose tolerance test performed at age 7 months of age in offspring of ewes fed to requirement during pregnancy randomised to formula feeding (R-F, n=9) or being fed by mother (R-M, n=9) and offspring of ewes nutrient restricted during late gestation randomised to formula feeding N-F, n=9) or to being fed by mother (N-M, n=9). Data presented as means ± SEM. Data were analysed using 2-way ANOVA

Comparison of the plasma metabolic profile which consisted of plasma triglyceride, plasma NEFA, plasma leptin and plasma cortisol concentrations showed no effect of either formula feeding or maternal nutrient restriction (Table 4.4).

	Prenatal nutrition	Feeding method		Prenatal nutrition	Feeding method	Interaction
		Mother fed	Formula fed	p value	p value	p value
Plasma triglyceride (mg/dl)	R	0.16±0.01	0.18±0.02	0.54	0.53	0.58
	N	0.16±0.01	0.16±0.02			
Plasma NEFA (mmol/L)	R	1.32±0.07	1.12±0.16	0.36	0.36	0.56
	N	1.11±0.08	1.07±0.15			
Plasma cortisol (nmol/L)	R	74.4±19.0	63.3±12.3	0.69	0.30	0.39
	N	60.5±40.2	61.2±9.2			
Plasma leptin (ng/ml)	R	1.80±0.23	2.2±0.38	0.72	0.58	0.68
	N	2.45±0.45	2.29±0.22			

Table 4.4 Plasma metabolic profile in fasted state at the age of 7 months in offspring of ewes fed to requirement during pregnancy randomised to formula feeding (R-F, n=9) or being fed by mother (R-M, n=9) and offspring or ewes nutrient restricted during late gestation randomised to formula feeding N-F, n=9) or to being fed by mother (N-M, n=9). NEFA, Non-esterified fatty acids. Data presented as means with error bars representing SEM. Statistical analysis performed with 2-way ANOVA.

4.3.1.4 Adult weight, adipose tissue depots and physical activity parameters of the offspring.

Analysis of body weight measurements after weaning, performed using a three-way mixed ANOVA using weight measurements at different timepoints as repeated measures, did not demonstrate a three-way interaction between measurements ($p=0.057$). Analysis for main effects of prenatal nutrition ($p=0.76$) and feeding method ($p=0.65$) also did not identify a significant effect of these interventions (Figure 4.7).

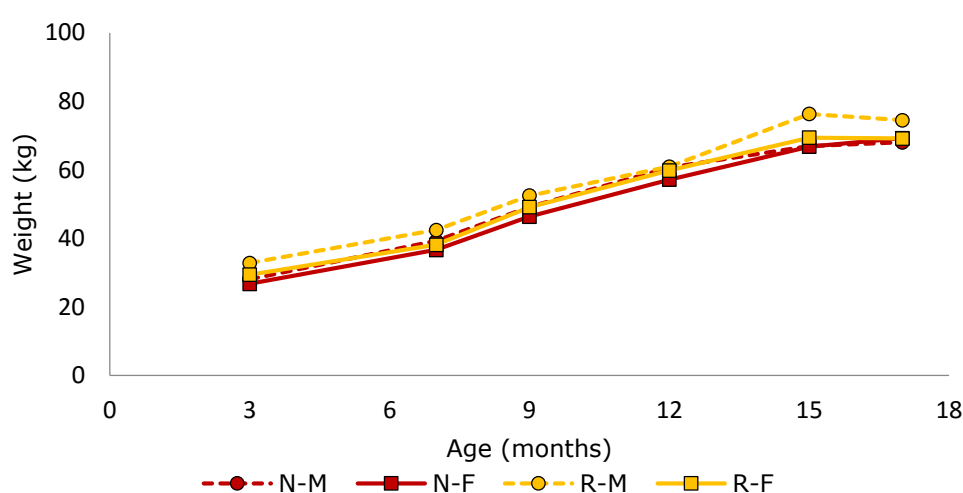


Figure 4.7 Offspring body weight measurements following weaning from milk feeds at 90 days of age until the culmination of experimental intervention at the age of 17 in offspring of ewes fed to requirement during pregnancy randomised to formula feeding (R-F, $n=9$) or being fed by mother (R-M, $n=9$) and offspring of ewes nutrient restricted during late gestation randomised to formula feeding N-F, $n=9$) or to being fed by mother (N-M, $n=9$). Data presented as means with error bars representing SEM. The statistical analysis was performed using a three-way mixed ANOVA to account for repeated measurements of weight over time.

The weight of visceral adipose tissue depots of omental, pericardial and perirenal adipose tissue sampled following euthanasia at 17 months of age did not differ with the experimental interventions. The calculated non-fat and total fat mass extrapolated from DXA scan at 16 months of age demonstrated that the gross adult body fat content and distribution was not affected by maternal nutrient restriction or by feeding method during early life. There was a non-significant trend towards decreased adiposity in N-F offspring as compared to N-M offspring. Similarly, the proportion of visceral fat (calculated as sum of omental, perirenal and pericardial fat) to total fat also did not differ between experimental groups (Table 4.5).

	Prenatal nutrition	Feeding method		Prenatal nutrition	Feeding method	Interaction
		Mother fed	Formula fed	p value	p value	p value
Weight of omental adipose depot (g)	R	1451±174	1173±90	0.33	0.13	0.72
	N	1563±381	1045±203			
Weight of pericardial adipose tissue (g)	R	109±8	100±12	0.95	0.67	0.18
	N	96±8	114±10			
Weight of perirenal adipose tissue (g)	R	1016±149	1130±201	0.44	0.64	0.28
	N	1073±239	787±99			
Relative fat mass (% of body wt.)	R	13.1±2.2	14.8±2.1	0.90	0.43	0.11
	N	17.1±2.8	11.3±1.4			
Visceral fat (% of total body fat)	R	25.6±2.2	25.1±2.1	0.65	0.64	0.52
	N	22.7±2.3	25.5±3.6			

Table 4.5 Body weight and adipose tissue deposit details in offspring of ewes fed to requirement during pregnancy randomised to formula feeding (R-F, n=9) or being fed by mother (R-M, n=9) and offspring of ewes nutrient restricted during late gestation randomised to formula feeding N-F, n=9) or to being fed by mother (N-M, n=9). Data presented as means ± SEM. Statistical analysis performed with 2-way ANOVA.

At 15 months of age, physical activity indices measured for 24 hour period using an accelerometer did not reach statistical significance for difference between experimental conditions. There was a trend towards decreased activity in the mother fed offspring ($p=0.07$) as compared to formula fed offspring (Table 4.6).

	Prenatal nutrition	Feeding method		Prenatal nutrition	Feeding method	Interaction
		Mother fed	Formula fed	p value	p value	p value
Mean activity at 15 months (counts)	R	117±14	128±14	0.05	0.68	0.75
	N	149±22	164±12			
Duration mobile/day at 15 months (minutes)	R	834±94	933±88	0.45	0.07	0.72
	N	892±79	1045±58			
Maximum intensity at 15 months (counts)	R	1781±247	1415±82	0.43	0.75	0.13
	N	1579±131	1727±105			

Table 4.6 Physical activity parameters at the age of 15 months in offspring of ewes fed to requirement during pregnancy randomised to formula feeding (R-F, n=9) or being fed by mother (R-M, n=9) and offspring of ewes nutrient restricted during late gestation randomised to formula feeding (N-F, n=9) or to being fed by mother (N-M, n=9). Data presented as means ± SEM. Statistical analysis performed with 2-way ANOVA.

In order to analyse if the physical activity phenotype of decreased physical activity in formula fed animals persists post-weaning, a correlation analysis was performed between mean 24 hours' physical activity counts measured at age of 45 days and at 15 months. Measurements from lambs from formula fed and mother fed groups demonstrated a significant linear correlation between physical activity measurements at age of 45 days with the measurements at age of 15 months in lambs (Figure 4.8).

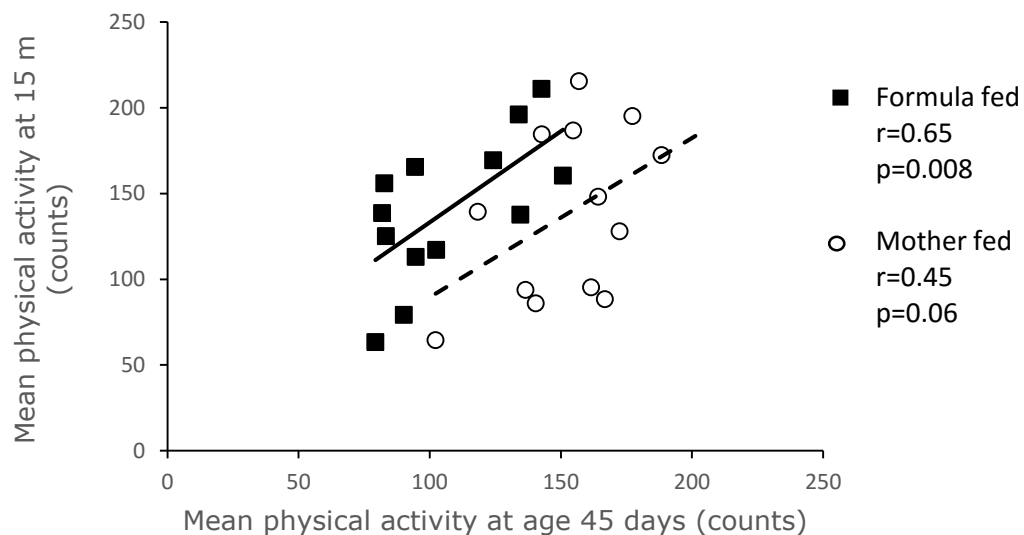


Figure 4.8 Correlation analysis of mean 24 hour physical activity measurements performed at the age of 45 days and at 15 months.

Lambs fed on formula milk during the suckling period are represented by black squares ($n=14$) and lambs fed by their mother are represented as open circle ($n=14$). Data presented as Pearson's correlation coefficient (r) and p value from two tailed significance testing.

4.3.1.5 Plasma metabolic profile at the age of 16 months

The plasma glucose and insulin concentrations during GTT were analysed using three-way mixed ANOVA to account for repeated measurements at different time points. For glucose (Figure 4.9), there was no significant three-way interaction between prenatal nutrition, feeding method and time ($p=0.67$). Analysis of glucose concentrations for two-way interactions also did not identify an interaction between prenatal nutrition and time ($p=0.78$) or feeding method and time ($p=0.10$). Simple main effect test for two-way interaction between prenatal nutrition and feeding method was also not significant ($p=0.67$).

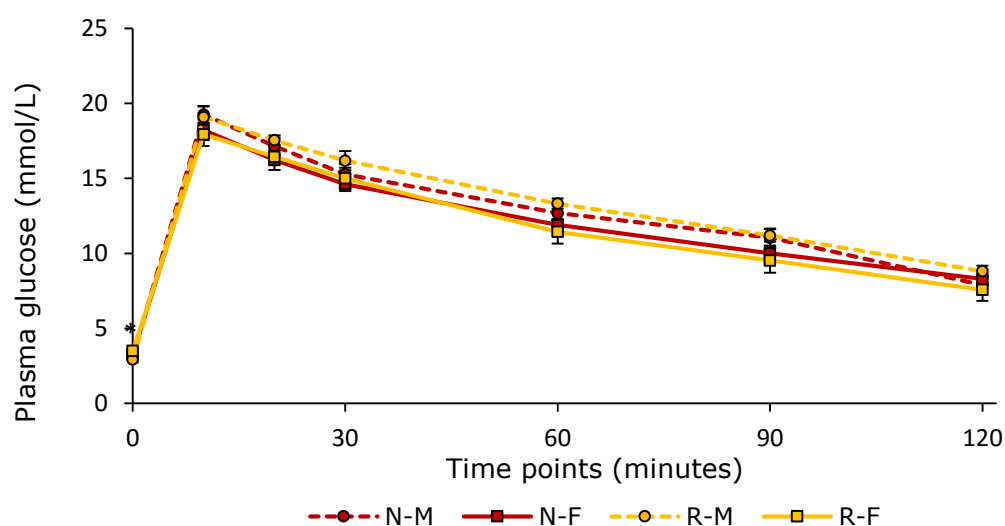


Figure 4.9 Plasma glucose concentrations during a glucose tolerance test performed at the age of 16 months in offspring of ewes fed to requirement during pregnancy randomised to formula feeding (R-F, $n=9$) or being fed by mother (R-M, $n=9$) and offspring of ewes nutrient restricted during late gestation randomised to formula feeding N-F, $n=9$) or to being fed by mother (N-M, $n=9$). Data presented as means with error bars representing SEM. Statistical analysis performed with three-way mixed ANOVA to account for repeated measures over time.

The plasma insulin concentrations (Figure 4.10) also did not demonstrate a three-way interaction between experimental groups and time ($p=0.85$). Analysis for a two-way interaction also did not demonstrate a significant interaction between prenatal nutrition and time ($p=0.36$) or feeding method and time ($p=0.39$). Simple main effect test for two-way interaction between prenatal nutrition and feeding method was also not significant ($p=0.65$)

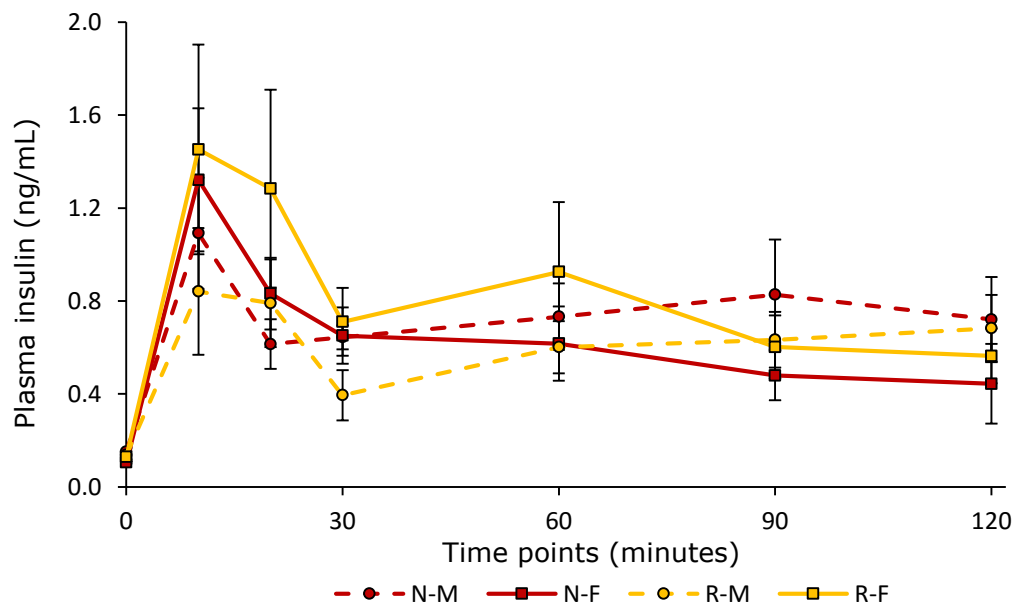


Figure 4.10 Plasma insulin concentrations during a glucose tolerance test performed at the age of 16 months in offspring of ewes fed to requirement during pregnancy randomised to formula feeding (R-F, $n=9$) or being fed by mother (R-M, $n=9$) and offspring of ewes nutrient restricted during late gestation randomised to formula feeding N-F, $n=9$) or to being fed by mother (N-M, $n=9$). Data presented as means with error bars representing SEM. Statistical analysis performed with three-way mixed ANOVA.

Fasting blood glucose concentrations at 16 months in the R-F offspring were higher than those of the R-M group (Table 4.7). The area under the curve for glucose and insulin measurements during the GTT were compared and did not differ between the groups (Table 4.3). Analysis of HOMA-IR index calculated using the baseline glucose and insulin concentrations demonstrated a significant interaction between the experimental measures. However, there was no statistical difference on subgroup analysis for simple effects.

	Prenatal nutrition	Feeding method		Prenatal nutrition	Feeding method	Interaction
		Mother fed	Formula fed	p value	p value	p value
Fasting glucose (mmol/L)	R	2.9±0.2 ^a	3.5±0.2 ^b	0.53	0.02	0.13
	N	3.2±0.1	3.3±0.1			
AUC glucose (mmol/L)	R	1572±32	1434±41	0.45	0.09	0.44
	N	1515±64	1434±42			
AUC insulin (ng/ml)	R	55.7±12.8	64.9±10.3	0.59	0.98	0.44
	N	71.9±11.6	61.9±14.1			
HOMA-IR	R	3.2±0.3	4.6±0.6	0.73	0.15	<0.01
	N	4.6±0.4	3.4±0.1			

Table 4.7 Markers of insulin sensitivity expressed as area under the curve and HOMA-IR calculated from glucose tolerance test performed at the age of 16 months in offspring of ewes fed to requirement during pregnancy randomised to formula feeding (R-F, n=9) or being fed by mother (R-M, n=9) and offspring of ewes nutrient restricted during late gestation randomised to formula feeding N-F, n=9) or to being fed by mother (N-M, n=9). Data presented as means ± SEM. Data were analysed with 2-way ANOVA. superscript a vs b, p<0.05 for simple effects analysis of 2-way ANOVA.

The experimental groups did not differ in the plasma concentrations for NEFA or cortisol. Offspring of sheep undergoing late gestation nutrient restriction had lower plasma triglyceride concentration but was unaffected by formula feeding (Table 4.8). A statistically significant interaction was present between prenatal intervention and feeding type for the plasma leptin concentrations. Subgroup analyses demonstrated lower leptin measurements in N-F offspring in comparison to N-M group.

	Prenatal nutrition	Feeding method		Prenatal nutrition	Feeding method	Interaction
		Mother fed	Formula fed	p value	p value	p value
Plasma triglyceride (mg/dL)	R	0.18±0.02	0.19±0.03	0.03	0.96	0.75
	N	0.13±0.03	0.13±0.01			
Plasma NEFA (mmol/L)	R	0.39±0.06	0.55±0.08	0.74	0.19	0.37
	N	0.43±0.09	0.46±0.04			
Plasma cortisol (nmol/L)	R	40.8±9.3	33.1±13.9	0.36	0.26	0.65
	N	56.1±13.9	38.4±5.0			
Plasma leptin (ng/mL)	R	4.1±0.6	5.2±0.9	0.71	0.36	0.03
	N	6.2±0.7 ^a	3.7±0.5 ^b			

Table 4.8 Plasma metabolic profile in the fasted state at the age of 16 months in offspring of ewes fed to requirement during pregnancy randomised to formula feeding (R-F, n=9) or being fed by mother (R-M, n=9) and offspring of ewes nutrient restricted during late gestation randomised to formula feeding (N-F, n=9) or to being fed by mother (N-M, n=9). Data presented as means ± SEM. Statistical significance denoted by superscripts a versus b, p<0.001 for simple effects analysis of 2-way ANOVA. NEFA, Non-esterified fatty acids

4.3.2 Liver weight, triglyceride deposition and oxidative stress.

Neither liver weight, triglyceride or malondialdehyde (MDA) concentrations (the latter as a marker for thiobarbituric acid reactive substances (TBARS)) differed between experimental groups (Table 4.9). There was a trend towards increased triglyceride concentrations ($p=0.05$) and liver TBARS concentration ($p=0.05$) in formula formula fed offspring as compared to offspring fed by their mother.

	Prenatal nutrition	Feeding method		Prenatal nutrition	Feeding method	Interaction
		Mother fed	Formula fed	p value	p value	p value
Liver weight (g)	R	717±33	695±33	0.21	0.75	0.78
	N	660±39	658±38			
Liver triglyceride (mg/g liver)	R	29.8±1.7	36.8±5.4	0.519	0.05	0.68
	N	30.8±1.5	41.5±7.4			
Total liver triglycerides (g)	R	37.8±8.5	20.3±1.5	0.817	0.10	0.83
	N	20.4±1.6	28.5±6.2			
Liver TBARS (MDA μM/ protein μg/μl)	R	1.02±0.08	0.79±0.06	0.60	0.05	0.37
	N	0.90±0.08	0.82±0.08			

Table 4.9 Liver weight, triglyceride concentrations, calculated total liver triglycerides and hepatic TBARS assay at the age of 17 months in offspring of ewes fed to requirement during pregnancy randomised to formula feeding (R-F, n=9) or being fed by mother (R-M, n=9) and offspring of ewes nutrient restricted during late gestation randomised to formula feeding N-F, n=9) or to being fed by mother (N-M, n=9). Data presented as means \pm SEM. Statistical analyses performed using 2-way ANOVA

Correlation between liver weight and triglyceride content varied depending upon the type of feeding. There was no correlation between the above two variables for offspring fed on their mother's milk, whereas, for formula fed offspring, liver weight was positively correlated with the triglyceride concentrations (Figure 4.11).

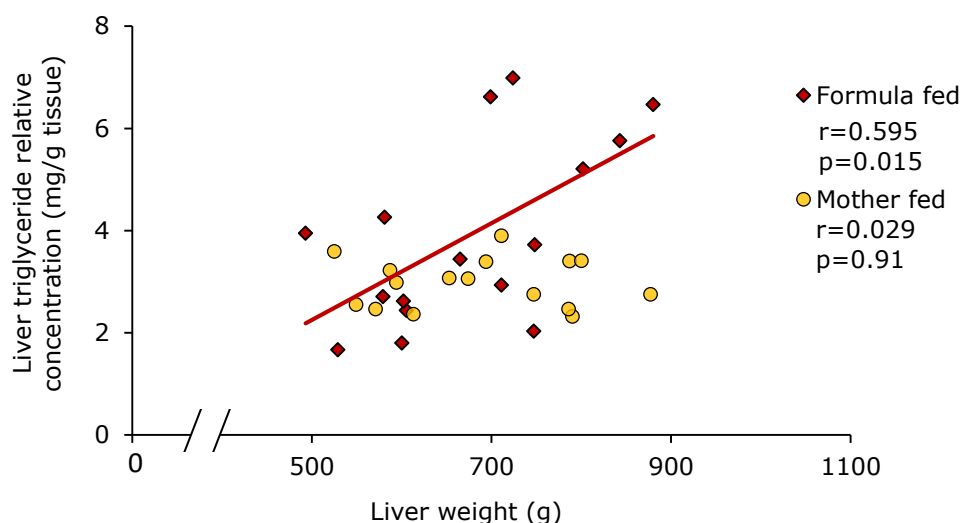


Figure 4.11 Correlation analysis of weight of liver at 17 months of age against measured liver triglyceride relative concentrations for lambs randomised to formula feeding (n=16) or to being fed by their mother (n=16). Data presented as Pearson's correlation coefficient (r) and two tailed significance testing. The trendline depicts the statistically significant linear relationship between the variables of formula fed animals only.

The correlation between liver TBARS and triglyceride concentrations for the offspring fed on formula milk was weakly positive ($r=0.543$) but statistically significant ($p=0.03$), whereas, no such correlation was present in the offspring fed on mother's milk (Figure 4.12). There was no correlation between liver TBARS concentration and liver weight for formula fed ($p=0.81$; $r=0.06$) and mother fed ($p=0.13$; $r=0.418$).

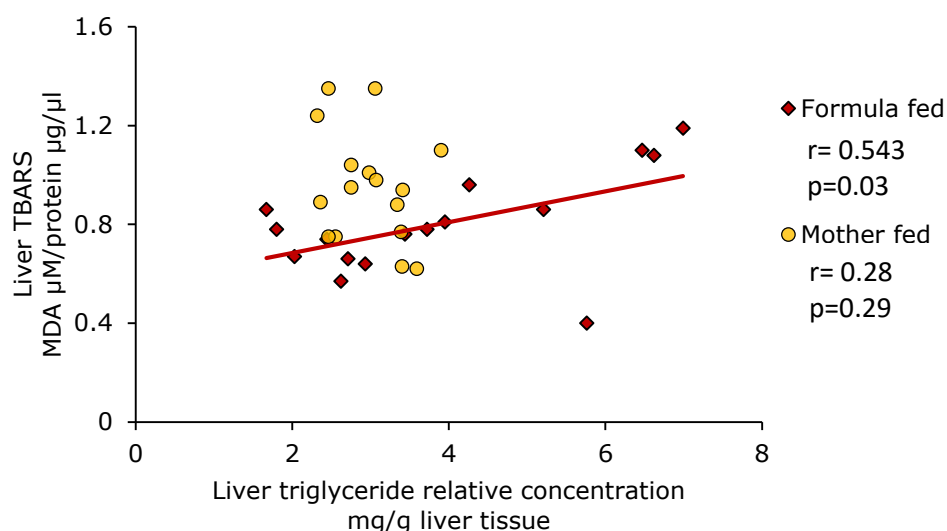


Figure 4.12 Correlation analysis of relative triglyceride concentration in the liver tissue at 17 months of age against measured liver TBARS for lambs randomised to formula feeding (n=12) or to being fed by their mother (n=12). Data presented as Pearson's correlation coefficient (r) and two-tailed significance testing. TBARS, Thiobarbituric acid reactive substances; MDA, malondialdehyde. The trendline depicts the linear relationship between the two variables from formula fed offspring only.

4.3.3 Liver histology

Histological images were analysed for appearance of steatosis and steatohepatitis (Figure 4.13). There was no difference in appearances of macrovesicular steatosis or cellular infiltration with experimental intervention which was similar to findings described in detail in Section 3.3.3. Quantification was performed for periportal fibrosis in Masson's Trichrome stained areas of liver tissue using volocity software which did not show any difference in fibrosis with experimental interventions (Table 4.10).

	Prenatal nutrition	Feeding method		Prenatal nutrition	Feeding method	Interaction
		Mother fed	Formula fed	p value	p value	p value
Periportal fibrosis area (X100µm²)	R	56±08	67±05	0.22	0.65	0.18
	N	78±13	79±14			

Table 4.10 Periportal fibrosis area quantified from Masson's Trichrome stained histological sections and standardised by dividing by portal vein perimeter in offspring of ewes fed to requirement during pregnancy randomised to formula feeding (R-F, n=9) or being fed by mother (R-M, n=9) and offspring of ewes nutrient restricted during late gestation randomised to formula feeding N-F, n=9) or to being fed by mother (N-M, n=9). Data presented as means ± SEM. Statistical analyses performed using 2-way ANOVA.

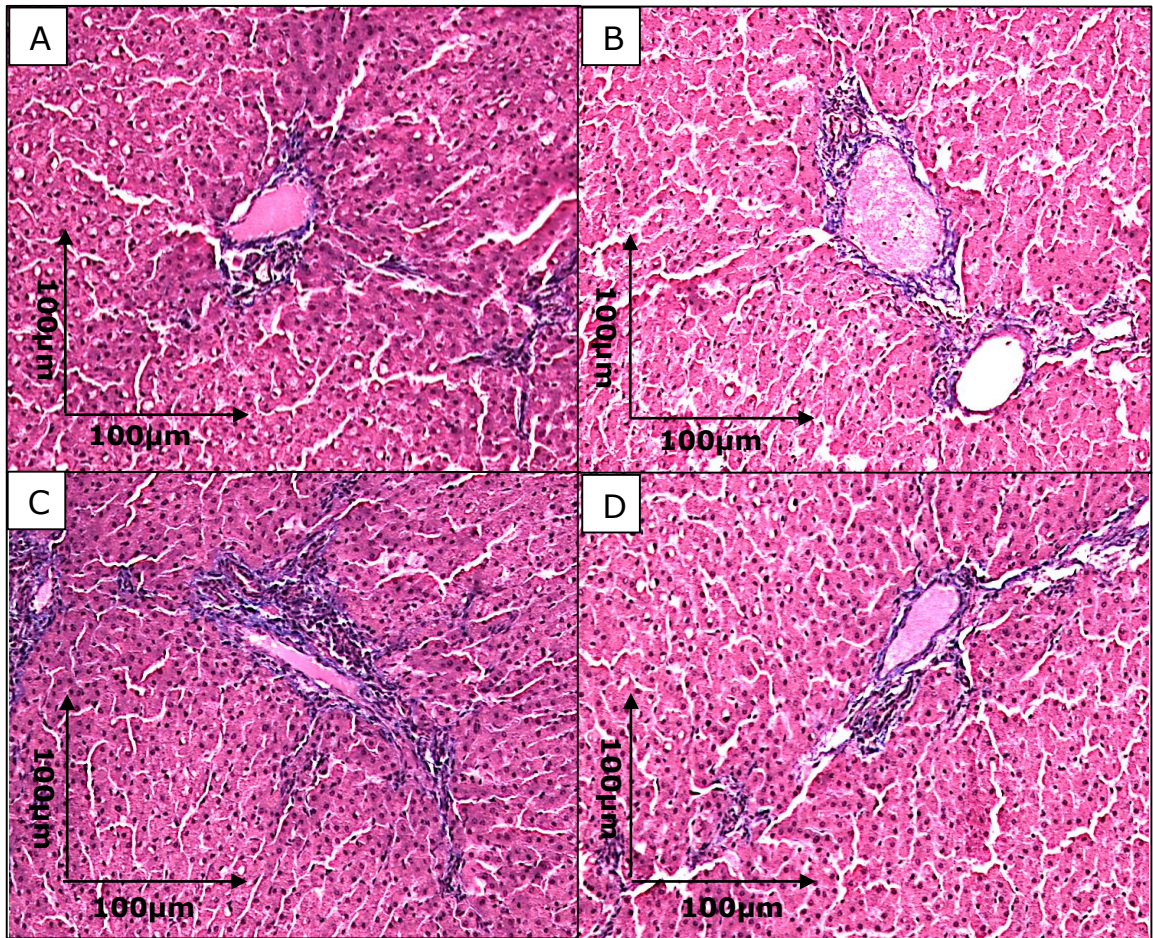


Figure 4.13 Representative histological sections of hepatic periportal area from sheep from (A) R-M offspring, (B) R-F offspring, (C) N-M offspring and (D) N-F offspring demonstrating staining of periportal area with Masson's Trichrome and visualised at 20x magnification.

4.3.4 Hepatic gene expression

4.3.4.1 Gene expression for modulators and effectors of metabolic inflammation in liver

The gene expression for leptin receptor, toll-like receptor-4 (TLR4), cluster of differentiation-95 (CD95), and cluster of differentiation-68 (CD68) did not differ with experimental interventions (Table 4.11). There was a trend towards decreased CD95 expression with prenatal nutrient restriction ($p=0.06$) as compared to offspring of sheep fed to requirement.

Gene expression	Prenatal nutrition	Feeding method		Prenatal Feeding Nutrition method		Interaction p value
		Mother fed	Formula fed	p value	p value	
Leptin receptor	R	1.00±0.17	0.98±0.17	0.22	0.93	0.95
	N	1.20±0.16	1.19±0.17			
TLR4	R	1.00±0.23	1.26±0.34	0.10	0.66	0.61
	N	1.59±0.29	1.57±0.23			
CD95	R	1.00±0.03	0.98±0.02	0.06	0.38	0.47
	N	0.93±0.01	0.95±0.03			
CD68	R	1.00±0.11	1.20±0.21	0.26	0.42	0.73
	N	0.89±0.09	0.98±0.13			

Table 4.11 Gene expression for regulatory factors of inflammation and cell stress response (leptin receptor, TLR4, CD95 and CD68) in offspring of ewes fed to requirement during pregnancy randomised to formula feeding (R-F, n=9) or being fed by mother (R-M, n=9) and offspring of ewes nutrient restricted during late gestation randomised to formula feeding N-F, n=9) or to being fed by mother (N-M, n=9). Data presented as means ± SEM. Statistical analyses performed using 2-way ANOVA. TLR4, toll like receptor 4; CD95, cluster of differentiation 95; CD68, cluster of differentiation 68.

4.3.4.2 Gene expression for the components of the unfolded protein response in the liver

The unfolded protein response was investigated by analysing the gene expression for ATF4, ATF6, EDEM1 and GRP78, none of which demonstrated any influence of the experimental intervention (Table 4.12).

	Prenatal nutrition	Feeding method		Prenatal nutrition	Feeding method	Interaction
		Mother fed	Formula fed	p value	p value	p value
ATF4	R	1.00±0.10	0.95±0.05	0.33	0.86	0.61
	N	0.89±0.06	0.91±0.07			
ATF6	R	1.00±0.09	0.88±0.05	0.68	0.26	0.63
	N	0.93±0.08	0.89±0.04			
EDEM1	R	1.00±0.07	0.99±0.07	0.24	0.15	0.40
	N	0.97±0.05	0.83±0.08			
GRP78	R	1.00±0.15	0.91±0.09	0.21	0.45	0.89
	N	0.85±0.10	0.79±0.04			

Table 4.12 Gene expression analysis for components of unfolded protein response in offspring of ewes fed to requirement during pregnancy randomised to formula feeding (R-F, n=9) or being fed by mother (R-M, n=9) and offspring of ewes nutrient restricted during late gestation randomised to formula feeding N-F, n=9) or to being fed by mother (N-M, n=9). Data presented as means ± SEM. Statistical analysis performed with 2-way ANOVA. ATF4, activating transcription factor-4; ATF6, activating transcription factor-6; EDEM1- ER stress degradation enhancer molecule-1; GRP78, glucose-regulated protein 78.

4.3.4.3 Gene expression for the components of the autophagy in the liver

Prenatal nutrient restriction followed by formula feeding was associated with increased gene expression for mTOR in comparison to formula fed offspring of sheep fed to requirements. The experimental interventions, however, did not induce any change on the gene expression of AMPK, ATG12 or for BECN1 (Table 4.13).

	Prenatal nutrition	Feeding method		Prenatal nutrition	Feeding method	Interaction
		Mother fed	Formula fed	p value	p value	p value
mTOR	R	1.00±0.13	1.14±0.12 ^a	0.03	0.10	0.34
	N	1.24±0.16	1.74±0.28 ^b			
AMPK	R	1.00±0.11	1.06±0.07	0.617	0.32	0.88
	N	0.95±0.05	1.00±0.07			
ATG12	R	1.00±0.05	0.98±0.03	0.06	0.38	0.70
	N	0.93±0.03	0.88±0.44			
BECN1	R	1.00±0.10	0.95±0.10	0.22	0.41	0.82
	N	0.83±0.15	0.81±0.09			

Table 4.13 Gene expression for the components of autophagy in the liver tissue from offspring of ewes fed to requirement during pregnancy randomised to formula feeding (R-F, n=9) or being fed by mother (R-M, n=9) and offspring of ewes nutrient restricted during late gestation randomised to formula feeding N-F, n=9) or to being fed by mother (N-M, n=9). Data presented as means ± SEM. Statistical analyses performed using 2-way ANOVA. mTOR, mammalian target of rapamycin; AMPK, 5' adenosine monophosphate-activated protein kinase; ATG12, autophagy related gene 12; BECN1, gene encoding Beclin1. superscripts a versus b denote p<0.05 for simple effects analysis.

4.3.5 Omental adipose tissue histological characteristics

4.3.5.1 Adipocyte cell size and characteristics.

Histological observation (Figure 4.14) of omental adipose tissue demonstrated adipocytes containing unilocular lipid droplets, scant stromal connective tissue and non-homogenously dispersed clusters of IBA1 positive macrophages present within crown like structures and milky spots.

Mean adipocyte area in the omental adipose tissue was not affected by nutrient restriction during late gestation or by feeding method during the suckling period (Table 4.14).

	Prenatal nutrition	Feeding method		Prenatal nutrition	Feeding method	Interaction
		Mother fed	Formula fed	p value	p value	p value
Adipocyte area (μm^2)	R	3762 \pm 545	3825 \pm 273	0.76	0.76	0.67
	N	4116 \pm 546	3767 \pm 373			

Table 4.14 Mean adipocyte area in μm^2 calculated from the histological sections of omental adipose tissue from offspring of ewes fed to requirement during pregnancy randomised to formula feeding (R-F, n=9) or being fed by mother (R-M, n=9) and offspring of ewes nutrient restricted during late gestation randomised to formula feeding N-F, n=9) or to being fed by mother (N-M, n=9). Data presented as means \pm SEM. Statistical analyses performed using 2-way ANOVA

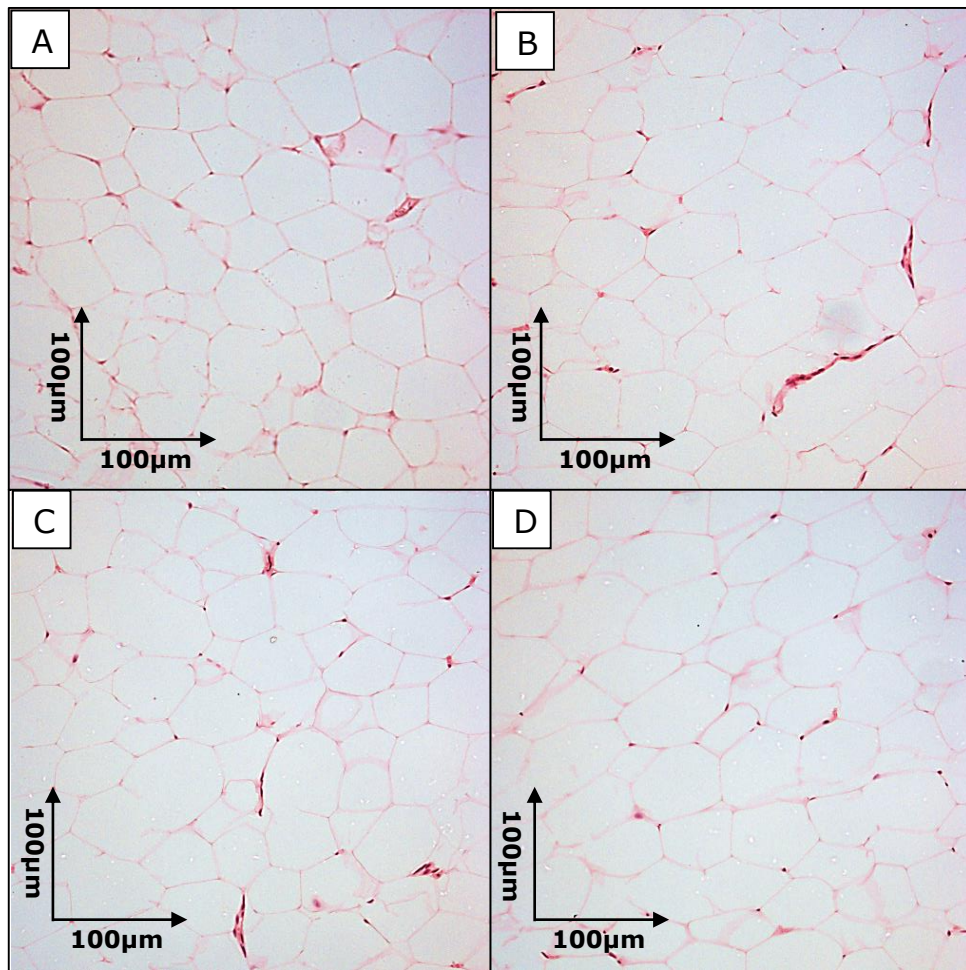


Figure 4.14 Representative H&E stained histological sections of omental adipose tissue from sheep from (A) R-M offspring, (B) R-F offspring, (C) N-M offspring and (D) N-F offspring visualised at 20X magnification.

4.3.5.2 GRP78 and pJNK staining of adipose tissue

As previously demonstrated in Section 3.3.5.2, glucose-regulated protein 78 (GRP78) staining was localised to the cytoplasm whereas phosphorylated c-Jun N-terminal kinase (pJNK) was concentrated in the perinuclear region. There was no difference in the quantified stained area per adipocyte with the experimental interventions (Table 4.15). There was a statistical trend towards increased pJNK staining ($p=0.06$) in omental adipose tissue of nutrient restricted offspring as compared to offspring of sheep fed to requirement.

	Prenatal nutrition	Feeding method		Prenatal Nutrition	Feeding method	Interaction
		Mother fed	Formula fed	p value	p value	p value
GRP78 ($\mu\text{m}^2/\text{cell}$)	R	42.2 \pm 14.7	55.2 \pm 26.0	0.51	0.29	0.46
	N	65.1 \pm 29.5	27.1 \pm 14.4			
pJNK ($\mu\text{m}^2/\text{cell}$)	R	39.4 \pm 15.0	27.5 \pm 9.2	0.06	0.93	0.75
	N	50.1 \pm 8.8	93.6 \pm 54.7			

Table 4.15 Quantitative analysis of GRP78 and pJNK stain expressed as area stained in μm^2 / adipocyte from omental adipose tissue in offspring of ewes fed to requirement during pregnancy randomised to formula feeding (R-F, n=9) or being fed by mother (R-M, n=9) and offspring of ewes nutrient restricted during late gestation randomised to formula feeding (N-F, n=9) or to being fed by mother (N-M, n=9). Data presented as means \pm SEM. Statistical analyses performed using 2-way ANOVA. GRP78, glucose-regulated protein 78; pJNK, phosphorylated c-Jun N-terminal kinase

4.3.6 Omental adipose tissue gene expression analysis

4.3.6.1 Gene expression of regulatory factors of metabolic inflammation

The experimental interventions of late gestation nutrient restriction with, or without, formula feeding did not result in any direct change in the gene expression of CD68, leptin or adiponectin. The statistical analysis demonstrated a significant interaction between prenatal nutrition and feeding choice for the gene expression for TLR4. The simple effects analysis, however, did not reach statistical significance (Table 4.16).

	Prenatal nutrition	Feeding method		Prenatal nutrition	Feeding method	Interaction
		Mother fed	Formula fed	p value	p value	p value
Leptin	R	1.00±0.18	2.07±0.57	0.35	0.62	0.33
	N	1.92±0.50	1.80±0.73			
Adiponectin	R	1.00±0.12	0.80±0.13	0.09	0.75	0.66
	N	1.12±0.18	0.78±0.16			
CD68	R	1.00±0.14	1.48±0.57	0.46	0.48	0.09
	N	1.75±0.51	0.90±0.18			
TLR4	R	1.00±0.09	1.35±0.12	0.98	0.29	0.04
	N	1.24±0.08	1.06±0.10			

Table 4.16 Gene expression analysis of leptin, adiponectin, CD68 and TLR4 in omental adipose tissue from offspring of ewes fed to requirement during pregnancy randomised to formula feeding (R-F, n=9) or being fed by mother (R-M, n=9) and offspring of ewes nutrient restricted during late gestation randomised to formula feeding N-F, n=9) or to being fed by mother (N-M, n=9). Data presented as means ± SEM. Statistical analyses performed using 2-way ANOVA. TLR4, toll like receptor 4; CD95, cluster of differentiation 95; CD68, cluster of differentiation 68.

4.3.6.2 Gene expression of components of UPR in omental adipose tissue

The experimental interventions did not have any consistent impact on relative gene expression of the components of the UPR, namely ATF4, ATF6, GRP78 and EDEM1, in omental adipose tissue (Table 4.17).

Gene	Prenatal nutrition	Feeding method		Prenatal nutrition	Feeding method	Interaction
		Mother fed	Formula fed	p value	p value	p value
ATF4	R	1.00±0.05	0.97±0.04	0.16	0.07	0.18
	N	1.00±0.06	0.83±0.04			
ATF6	R	1.00±0.09	1.05±0.05	0.60	0.77	0.12
	N	1.19±0.11	1.01±0.07			
GRP78	R	1.00±0.09	1.00±0.09	0.71	0.93	0.97
	N	0.96±0.11	0.96±0.11			
EDEM1	R	1.00±0.09	1.35±0.12	0.41	0.83	0.01
	N	1.24±0.08	1.06±0.10			

Table 4.17 Relative gene expression ATF4, ATF6, GRP78 and EDEM1 in omental adipose tissue of in offspring of ewes fed to requirement during pregnancy randomised to formula feeding (R-F, n=9) or being fed by mother (R-M, n=9) and offspring of ewes nutrient restricted during late gestation randomised to formula feeding (N-F, n=9) or to being fed by mother (N-M, n=9). Data presented as means ± SEM. Statistical analyses performed using 2-way ANOVA. ATF4, activating transcription factor-4; ATF6, activating transcription factor-6; EDEM1, ER degradation enhancer, mannosidase alpha-like 1; GRP78, glucose-regulated protein-78.

4.3.6.3 Gene expression of the components of autophagy in the omental adipose tissue

The gene expression for mTOR demonstrated interaction between prenatal nutrition and feeding type during ANOVA testing prompting a simple effects analysis. R-F offspring had increased mTOR gene expression as compared to N-F and R-M offspring. The gene expression for AMPK, ATG12 and BECN1 was not significantly affected by the interventions (Figure 4.15).

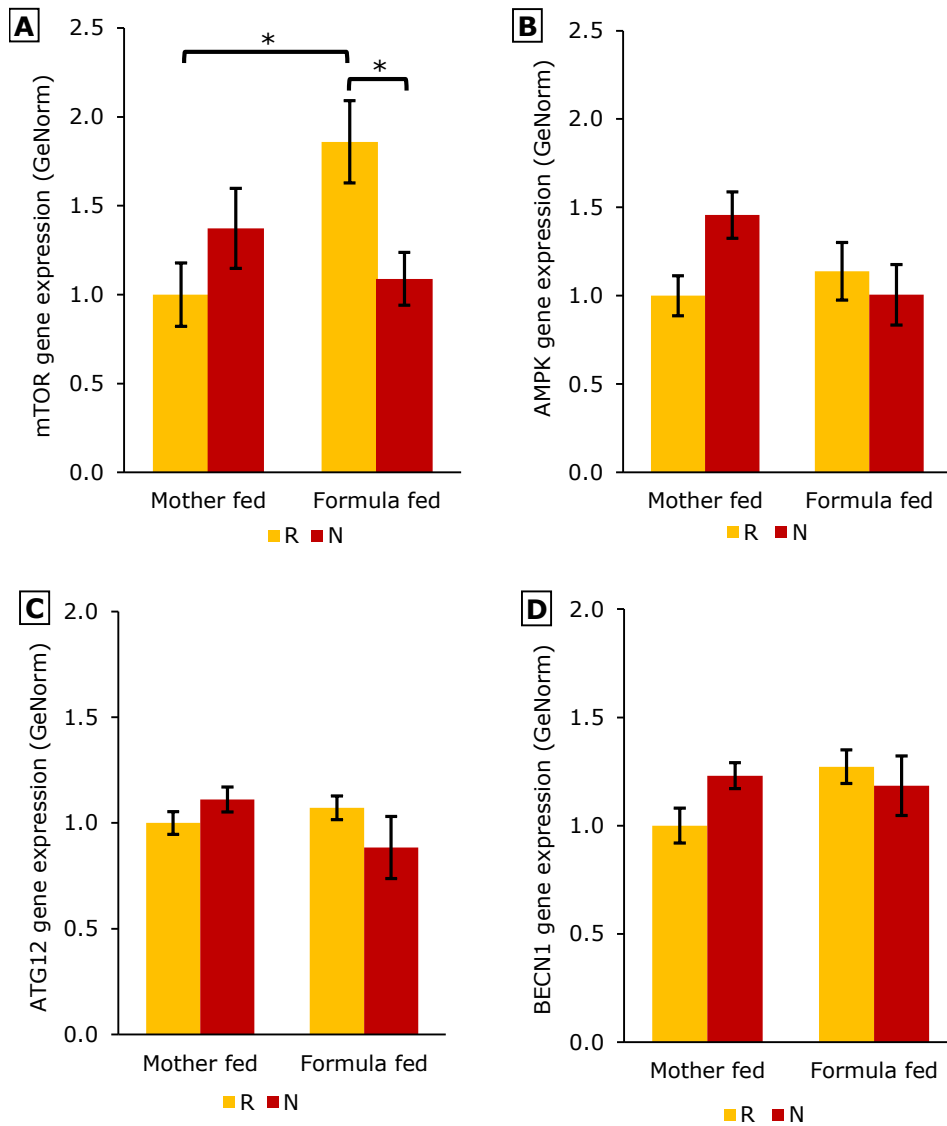


Figure 4.15 Relative gene expression of A, mTOR; B, AMPK; C, ATG12; D, BECN1 in omental adipose tissue of in offspring of ewes fed to requirement during pregnancy randomised to formula feeding (R-F, n=9) or being fed by mother (R-M, n=9) and offspring of ewes nutrient restricted during late gestation randomised to formula feeding N-F, n=9) or to being fed by mother (N-M, n=9). Data presented as means with error bars representing SEM. * $p < 0.05$ for simple effects following a significant 2-way ANOVA. AMPK, 5' adenosine monophosphate-activated protein kinase; mTOR, mammalian target of rapamycin; ATG12, autophagy related gene 12; BECN1, gene encoding Beclin1.

4.4 Discussion

The experiments described in this chapter aimed to examine the potential effects of formula feeding with, or without, prenatal undernutrition upon the liver and adipose tissue in a sheep model of juvenile onset obesity. Following intrauterine growth restriction mediated by maternal nutrient restriction, mother fed offspring gained weight faster than formula fed offspring. When physical activity was quantified during the pre-weaning stage at 45 days of age, formula feeding was associated with decreased activity, a finding which was not present when the physical activity was again measured at 15 months of age. There were no significant differences in metabolic parameters and GTT results in tests performed at 7 and 16 months of age respectively.

In keeping with findings described in Chapter 3, prenatal undernutrition was not associated with histological features of hepatic steatohepatitis nor with increases in the expression of components of inflammation and cell stress response. Furthermore, the add-on intervention of formula feeding during infancy was not associated with exacerbation of the above outcome parameter in liver.

Adipocyte size and mediators of inflammation in omental adipose tissue were not consistently increased with prenatal nutrient restriction with, or without, formula feeding. There was no consistent difference in gene expression for components of UPR and autophagy with the experimental interventions. The above findings are discussed in the following sections.

4.4.1 Maternal and offspring metabolic profiles

4.4.1.1 Maternal weight gain, plasma metabolic profile and offspring birth weight and weight gain during the suckling period.

The twin bearing sheep restricted to a diet providing 60% of ME demonstrated relatively decreased weight gain, had lower plasma glucose concentrations, higher NEFA concentrations and delivered offspring that were significantly lighter at birth. The above results confirm the findings of maternal weight gain and metabolic profile of the twin bearing sheep undergoing late gestation NR described in Chapter 3. All these parameters confirm the development of a sheep model of relative macronutrient insufficiency during late gestation. Such an animal model, with a control group of offspring of sheep fed to requirements, therefore, is well suited for the study of fetal programming.

At birth, the weight of the N offspring was 23% lower than the birth weight of the R offspring. During the 90 days suckling period, the N-F offspring remained significantly lighter than R-F offspring whereas, the N-M offspring gained weight relatively faster and their body weight measurements were similar to the R-M offspring after 38 days. Such a weight gain profile of N-F offspring was different from the rapid growth described in formula fed human infants [483]. However, in sheep, such relatively slower weight gain following formula feeding has previously been described [484]. The sheep formula used in the study was a commercially available formula which differs in relative micronutrient composition from the known composition of sheep mother's milk (Table 4.18). Overall, the sheep formula contains 20% less fat and 14% less carbohydrates as compared to the sheep mother's milk. Such differences in the relative composition and overall lower calorific value may not make this equivalent

to human formula milk, which is designed to closely replicate the macronutrient composition of milk consumed by breastfed infants.

	Sheep milk [#]	Formula milk [*]
Protein (%)	~5	4.8
Fat (%)	~6	4.8
Carbohydrate (%)	~4.8	4.1
Energetic value (MJ/kg)	4.5	4.1

Table 4.18 Macronutrient and calorific content in sheep milk and formula milk used in the study.

#As reported by Park et. al. and Dove et. al. [327, 328]; *as reported in information sheet provided by the manufacturer (Volac International, Royston, UK).

Appetite may be another factor contributing to the variation in growth identified in formula fed lambs compared with those reared by their mother using a shared feeding system. One contributory factor is that rearing the lamb away from the mother clearly removes any interaction between them. In humans, maternal deprivation during early infancy has been known to affect neuroendocrine function and behaviour in infants with the potential to affect offspring appetite and growth [485, 486]. In sheep, maternal deprivation during early life has also been shown to be associated with changes to neuroendocrine axis with potential effects on hypothalamic nuclei important for appetite regulation [487, 488]. In order to differentiate the independent impact of maternal deprivation or type of feed on the offspring, a much larger study would be required with independent arms of a maternally deprived lamb who is fed on age appropriate sheep milk with a bottle or feeder as appropriate. At the onset of the study design, the impact of maternal deprivation was not the primary focus of our study. Furthermore, the addition of such an arm would have significant financial and logistical implications on an already elaborate large animal study design. The results described in this study demonstrate the need for independent scrutiny of relative impact of

maternal deprivation and type of milk feed on offspring growth and physiology in future studies.

In addition to the variation in the macronutrient composition of the sheep formula milk as compared to the sheep mothers' milk, it has also been proposed that formula milk lacks hormonal and growth factors present in sheep mother's milk [484], all of which could account for the relatively slower weight gain in formula fed sheep offspring. Late gestation undernutrition is known to affect the composition of sheep milk [489]. It is plausible that the resultant milk composition either affects offspring appetite, metabolism or macronutrient intake during the suckling period enabling the N-M offspring to achieve a much faster growth rate. Further investigation of this aspect would require a study of monitoring of milk intake and composition in all groups and was not in the scope of these experiments.

When analysed as fold change of birth weight (Figure 4.6, Section 4.3.1.2), it becomes apparent that, whilst the N-M offspring experience a rapid weight gain enabling them to 'catch up' with the R-M, N-F offspring gain weight at a rate comparable to the R-F offspring. The resulting absence of 'catch-up' growth ensures that they remain lighter in body weight as compared to R-F offspring. In human terms, this may be similar to a small for gestational age (SGA) infant who maintain their weight gain along the birth percentiles. Rapid weight gain following a SGA birth, by itself, has been proposed to be a factor increasing the likelihood of later cardiovascular and metabolic morbidity [286, 293]. However, the absence of such rapid early growth in the N-F subgroup, whilst inadvertent, eliminates this potentially important contributory factor's impact on the outcome.

4.4.1.2 Decreased physical activity in formula fed offspring at age 45 days correlates with physical activity phenotype in young adolescence.

Physical activity, by itself, has been investigated as a target of nutritional programming [490]. Offspring of undernourished rats (fed 30% of ad libitum intake) were permanently less physically active than offspring of ad libitum fed rats [490]. Furthermore, analysis of the Dutch famine birth cohort found that individuals who were prenatally exposed to famine were less physically active as adults according to a physical activity questionnaire and self-rating scale [491]. A previous sheep study has reported that physical activity level varies amongst individual animals and persists from early life to adulthood [492]. Persistence of a phenotype of decreased physical activity confirms the presence of a proposed centrally regulated physical activity phenotype [490] which is amenable to programming.

During the accelerometer recordings of physical activity performed over 24 hour period at 45 days of age, the formula fed offspring were significantly less active as compared to the lambs reared with their mothers, a result which was consistent in offspring of N and R sheep and was also not affected by the diurnal variation in physical activity. When the same measurements were made at 15 months of age, prenatal nutrient restriction or postnatal feeding type was not associated with any statistically significant difference in physical activity. However, a significant correlation was present between the recordings at 45 days and at 15 months of age for the mean physical activity measurements during the 24 hour study period. This suggests that a physical activity phenotype is set in response to environmental measures such as rearing or feeding method and persists during later life. It is plausible that the increased physical activity of the mother fed offspring at 45 days of age was a reflection of their environmental factors such as proximity to their mother and they

were following the movements of the mother. However, programming of a physical activity phenotype was not a primary objective for this study. It is plausible that the identified correlation of physical activity phenotype in this study did not reflect into a statistically significant difference in the 15 months measurements due to the large variance in the outcome measures. A retrospective sample size calculation identified that to demonstrate a mean difference of 10%, a sample size of 156 would be required in each group. A definitive determination of presence or absence of a physical activity phenotype determined by early life factors would therefore require a study powered and specifically designed to investigate this in a systematic fashion.

4.4.1.3 Formula feeding did not exacerbate obesity, adiposity or markers of metabolic derangement.

Post weaning, the measurements for body weight including the final adult weight and the size of adipose tissue depots did not differ between the experimental groups. The absence of a change in final body weight as a result of prenatal nutrient restriction conforms to the results described in Chapter 3 and other sheep studies of NR-LG [264]. For this study, it was hypothesised that that formula feeding would lead to exacerbation in obesity which would present as increased body weight and increase in size of adipose depots. However, the study findings do not conform these hypotheses. Similarly, formula feeding did not lead to the predicted worsening of markers of metabolic profile (including GTT, plasma triglycerides, NEFA, cortisol and leptin) at the age of 7 months and at 16 months.

After the first 90 days, all the study animals were kept in a restricted environment designed to encourage obesity. As described in Chapter 3, sheep reared in obesogenic environment, when compared to lean animals,

demonstrate GTT results consistent with insulin resistance at 16 months of age.

It is possible that the effects of obesogenic environment on the development of adiposity and insulin resistance is proportionately much larger so that a relatively smaller effect of formula feeding is masked as a result. Such a phenomenon is called effect modification [493].

Identification of a relatively small effect size would require a much larger study and this should include lean comparison groups and a large sample size. However, on basis of the presented results, it can be concluded that even if such an independent effect was present, it would likely be of relatively small effect size.

As described previously, the rate of weight gain during formula feeding is another factor which is significantly different between our study model and the human epidemiological data. Human infants fed on formula milk have a much higher growth rate in comparison to breast fed infants [483], a factor that has been considered significant enough to prompt changes in the WHO growth charts [292]. Such early weight gain is strongly associated with the development of later obesity [289, 494] and adverse metabolic outcomes [495], whereas a relatively slower growth rate has been proposed to have a protective effect [496]. The N-F animals in this study had a relatively decreased growth rate which is in contrast to the rapid early growth of formula fed infants. It is plausible that the obesogenic effect and adverse metabolic outcomes known to be associated with formula feeding is a consequence of the programming influence of rapid weight gain and, in absence of the latter, the impact was not apparent in this study. Such an independent effect of growth rate is the focus of investigation in the study described in Chapter 5.

4.4.2 Hepatic fat deposition and cell stress response in formula feeding with, or without, pre-existing NR-LG.

The measurements for liver weight and triglyceride deposition were comparable to the results described in Chapter 3 and in previously published studies [279, 315, 446]. In the formula fed offspring, the liver weight was positively correlated with the measured liver triglyceride concentrations and TBARS, whereas no such correlation was evident in offspring fed on mother's milk. However, features of NAFLD including intrahepatocyte lipid droplets, cellular infiltrate or quantification for periportal fibrosis were not increased with formula feeding.

Currently, very little research has been performed to investigate the effect of type of feed on development of steatohepatitis. Nobili *et al.* reported decreased odds (OR 0.04, 95% CI 0.01 to 0.10) for developing steatohepatitis at a median age of 12 years in individuals who were breast fed as compared to formula fed during infancy [309]. Such a difference was, however, not evident when investigated during early infancy (age 6-12 weeks) [310]. In the study described in this chapter, there was a trend towards increasing liver triglyceride concentrations with formula feeding ($p=0.058$). Furthermore, similar to the results described in Section 3.3.2, there was a positive correlation between liver weight and hepatic triglyceride concentrations, specifically in formula fed animals. It is plausible that formula feeding during early life brings about alteration in mechanisms of hepatic lipid deposition and disposal which, over time, present as hepatic steatosis as indicated by the trend towards increased hepatic triglycerides in formula fed offspring in this study. Inflammation and the cell stress response associated with such hepatic fat deposition have been proposed as factors in development of the metabolic syndrome (discussed in Section 1.5.3.2). However, formula feeding with, or without, a background of prenatal nutrient restriction was not associated with any

change in gene expression for components of metabolic inflammation, UPR and autophagy. The current study model, therefore, does not confirm the hypothesised increase in metabolic inflammation and cell stress response in formula fed offspring.

This is the first such study in a large animal model of formula feeding and provides baseline data for future investigations, including data which can be used to inform sample size calculations for well powered studies. The absence of the predicted inflammation and cell stress response could be an outcome of the characteristics of the study model. Formula fed offspring demonstrated a slower rate of weight gain, which is potentially protective effect against development of insulin resistance [286] and obesity associated metabolic complications [495]. It is also plausible that the relatively modest effect of formula feeding are masked by effects of obesity as described in Chapter 3. For example, if obesity led to substantial changes in the gene expression of pathways of cell stress response in all obese animals, any modulation of these pathways, of relatively smaller quantity, brought about by formula feeding would be masked and its demonstration would require a very large sample size or a lean comparison group with interventions of formula feeding.

The age of offspring at the study endpoint (17 months age) is equivalent to young adulthood in human counterparts. Studies of the association of hepatosteatitis with formula feeding have demonstrated that, whilst there is no difference at young ages [310], such an association is present when tested in older children (median age 12 years, range 3-18 years).

Increasing age is a known independent risk factor for development of both NAFLD [497] and the metabolic syndrome [498] even in the paediatric population. It is plausible that, with age, the demonstrated trend towards increased hepatic triglycerides in formula fed offspring, would continue to increase eventually reaching a significant level, not just in statistical terms

but also in terms of affecting metabolic inflammation at a later age. Any future studies of the impact of formula feeding would ideally include testing at different endpoints to identify progressive stages in natural developmental process of metabolic syndrome. Another option would be to perform biopsies (similar to needle biopsy) of liver tissue in individual animals at different ages paired with a select combination of plasma biomarkers such as alanine aminotransferase. Research in hepatic biomarkers is rapidly advancing with report of 1500 new publications within a 6 month period [499]. The choice of biomarkers studied should therefore be made depending upon the latest data and availability of a reliable assay in sheep population at the time such study is performed.

4.4.3 Omental adipose tissue characteristics and cell stress response in formula feeding with or without pre-existing NR-LG

4.4.3.1 Formula feeding was not associated with adipocyte characteristics or gene expression for inflammation

The mean area of omental adipocytes measured in histological sections from sheep, all reared in obesogenic environment, was similar to measured adipocyte area of the obese offspring described in Chapter 3 ($\sim 4000 \mu\text{m}^2$). In keeping with lack of any change to the weight of omental adipose depot, formula feeding or prenatal nutrient restriction did not affect the adipocyte size. Immunohistological and gene expression studies did not demonstrate the predicted increase in inflammation and UPR. The gene expression for the components of autophagy were also not increased with formula feeding or prenatal nutrient restriction. However, the gene expression for mTOR demonstrated a significant interaction with R-F offspring demonstrating maximal gene expression, significantly increased in comparison to N-F and R-M offspring respectively. mTOR is a nodal regulator for multiple cellular functions including autophagy, adipogenesis, mitochondrial metabolism and cell survival. As a component of cellular

energy sensing mechanism, a change in gene expression for mTOR has the potential for affecting downstream cellular homeostasis and survival. However, in absence of any evidence for a significant difference in adipose tissue structure, inflammation or related gene expression, the isolated finding of mTOR gene expression change cannot be interpreted.

4.5 Conclusion

The experiments described in this chapter had set out to establish a sheep model of formula feeding in a background of prenatal undernutrition with respective control groups. A standard restricted postweaning environment promoting development of obesity was established with the intention to amplify any programming effect of the experimental interventions.

Unlike human equivalents, formula fed offspring of nutrient restricted sheep did not demonstrate a rapid weight gain during the entire period before they were weaned. Such a deviation from the observed pattern in human studies has the potential to make this sheep model not representative of the mechanisms underlying increased predisposition to obesity and adverse metabolic outcomes witnessed in human studies.

When tested at age of 45 days, the formula fed offspring were less active than the offspring fed by their mother. Furthermore, a significant correlation was evident between the physical activity measurements at age 45 days and 15 months indicating presence of an environmentally programmable physical activity phenotype as previously proposed [490, 492] which persists until young adult age. Further investigation of this aspect would require targeted experimental studies to confirm and describe the possibility of such a programmable physical activity phenotype.

Formula feeding was not associated with exacerbation of obesity, insulin resistance or hepatic and adipose tissue metabolic inflammation.

The liver of formula fed offspring demonstrated a positive correlation between liver weight and measured triglyceride and TBARS assay. It is plausible that at the age of 17 months, when the sheep were euthanased, hepatic triglyceride accumulation and associated oxidative stress was at an early stage and would have become evident at a later age. However, in absence of any features of metabolic inflammation, or modification of cell stress response, such a proposition remains speculative. Formula feeding with, and without, a background of late gestation nutrient restriction in the obese sheep model did not lead to a consistent pattern of increase in metabolic inflammation or altered cell stress response.

The results described in this chapter also underline the need for further studies to explore the potential impact on interaction between maternal deprivation on offspring growth and physiology and also to explore the potential setting of physical activity phenotype in response to early life environmental factors such as formula feeding.

5 Effect of prenatal nutrient restriction followed by accelerated postnatal growth on the cell stress response and metabolic inflammation in liver and adipose tissue.

5.1 Introduction and hypothesis

The studies described in Chapter 4 investigated the longer term impact of formula feeding during the early postnatal period which brings about qualitative changes to nutrition. However, quantitative nutrient availability during early life with its effect on rate of early postnatal growth has been a subject of investigation for its association with glucose tolerance and obesity in later life [280]. The growth acceleration hypothesis [281], formulated in 2004, proposed that the increased risk of adult metabolic and cardiovascular morbidity associated with being born small for gestational age (SGA) is a consequence of accelerated early growth. A meta-analysis [289] of 10 cohort studies (n=47661) investigating obesity as an outcome of rapid early growth during infancy, demonstrated that for each unit increase in weight SD scores of an infant between 0 and 1 year age, the adjusted risk for childhood obesity increased two fold and the adjusted risk for adult obesity increased by 23%. However, such results have been contradicted by other more recent studies [290] and remain a subject of further investigation [293].

A prospective birth cohort study of 851 children investigated insulin sensitivity as an outcome measure [285] and demonstrated that greater weight gain between birth to 3 years of age predicted lower insulin sensitivity. In another randomised controlled trial of preterm infants [286], children randomised to receiving lower nutrition had lower fasting plasma

split proinsulin as compared to those children receiving a nutrient enriched diet.

Animal experiments using rodent models have demonstrated that rapid early growth results in adult offspring with increased adiposity, raised systolic blood pressure, hyperinsulinaemia [296] and alteration of adipose tissue insulin signalling [136]. Whilst these experiments showed increased adiposity and modulation of insulin sensitivity due to early postnatal growth, it is well recognised that rodent development differs significantly from that of large animals and humans including substantial differences in fetal organ growth rate and metabolic rate [297] and maturity of the hypothalamic pituitary adrenal axis [298]. There is, therefore, a need for experiments in a large animal model which explore the later metabolic consequences of accelerated early growth.

Infant nutrition, especially during the first 30 days after birth, is the primary determinant of growth [283] along with genetic, environmental and endocrine factors [282, 283]. Manipulation of macronutrient availability during early life as a means of modulating early growth is, therefore, a potential target of controlled experiments in a large animal model. The outcome of such nutritional management of early growth may be significant to public health and has the potential to influence longer term health. This is particularly relevant in children born with intrauterine growth restriction (IUGR) who experience rapid early growth during the early postnatal period. As described in previous chapters, the pathways of the cell stress response and metabolic inflammation in the liver and adipose tissue, with their influence on metabolic health, are important targets of such investigations. The experiments described in this chapter, therefore, attempt to build upon the epidemiological and rodent studies which have indicated that modulation of adiposity and insulin sensitivity occur in response to early accelerated postnatal growth. In light of the

limited evidence described above, and the need for such a study in a large animal model, the experiments in the study described in this chapter investigate the following experimental hypotheses:

1. IUGR, generated as an outcome of late gestational nutrient restriction followed by relative acceleration of early postnatal growth in twin offspring reared as singletons on their mother's milk in comparison to offspring reared as twins, will lead to development of adult obesity.
2. Such accelerated early growth in offspring following IUGR will be associated with decreased insulin sensitivity and increased expression of components of metabolic inflammation and altered cell stress response in liver and omental adipose tissue.

5.2 Methods

The design of the study, animal interventions and all experimental methods used to establish the results described in this chapter are described in detail in the Chapter 2. Briefly, after confirmation of twin gestation by ultrasound scanning, twin bearing ewes were fed with a diet meeting 60% of metabolic requirements from gestational day 110 until term (145 ± 2 days). After birth, the offspring were randomised to achieve two growth rates during suckling period (birth to 90 days). The offspring randomised to achieve standard growth (St) for a twin offspring were both kept with, and were fed by, their mother. In the comparison group, one twin offspring was fed on its mother's milk without competition from its sibling in order to achieve relatively accelerated (Ac) growth, whilst the other twin was not part of this comparison and was removed to be raised and fed separately on formula milk. Post-weaning, all the offspring included in this study were raised in a barn with a stocking rate of 6 sheep per 19m^2 . In line with the principles of the reduction of the use of animals in experimental paradigms [500], for maximal utilisation of resources and standardisation of experimental conditions, there is overlap in animals used in the study described in this chapter and the previous chapters (Figure 5.1). The Ac offspring described in this chapter are the same as mother fed (M) offspring described in Chapter 4 and the St offspring in this study were one of the experimental groups described in Chapter 3.

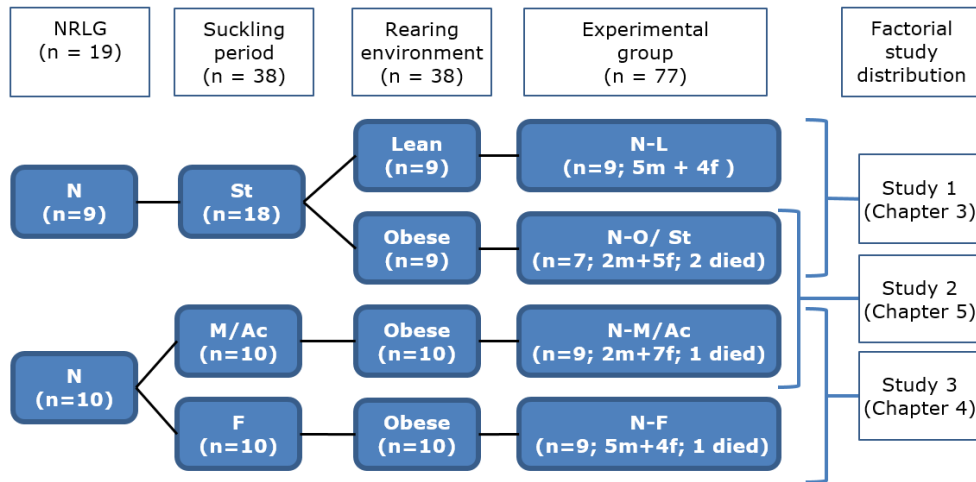


Figure 5.1 Schematic diagram depicting the overlap between studies described in Chapters 3, 4 and 5 achieved for maximal utilisation of resources and standardisation of experimental conditions.

In Study 2, twin offspring of ewes restricted to 60% nutrient restriction (N) during late gestation (NR-LG) were either separated and only one offspring fed to mother's milk without competition achieving an accelerated rate of growth (Ac) or were both fed by the ewes achieving a standard rate of growth for a twin (St). All offspring were raised in obesogenic environment of restricted activity. The offspring randomised to lean experimental group (N-L) and formula feeding (N-F) were included in studies described in Chapters 3 and 4 respectively.

During pregnancy, blood sampling was performed from the ewe at 130 days gestational age and plasma was analysed for concentrations of glucose, insulin, non-esterified fatty acids (NEFA) and for triglyceride content. Following delivery of the lambs, birth weight and regular body weight measurements were recorded; physical activity was measured using accelerometers when offspring were aged 1.5 months and 15 months; glucose tolerance tests and blood sampling was performed at age 7 months and 16 months respectively; body composition analysis was performed by dual X-ray absorptiometry (DXA) scanning at 16 months of age. The randomisation and investigations are summarised in Figure 5.2. The animal experiments were performed at the joint animal breeding unit, Sutton Bonington Campus of the University of Nottingham (Nottingham, UK), by Dr S. Sebert under supervision of Professor M.E. Symonds and Dr D. Gardner.

The statistical analyses are described in detail in Chapter 2. Briefly, between-group differences were analysed using independent sample t-tests. If required, non-parametric testing was performed by Mann Whitney test. Outcome for GTT and body weight measurements produced data of repeated measures in same animal over time. Analyses for such data with repeated measures were performed with two way mixed ANOVA and time was included as within-subject factor to assess for interaction between time and feeding method. For sake of uniformity of presentation and in keeping with standard practice, data have been expressed as mean and standard error of the mean for all the experimental output irrespective of the type of distribution of the data.

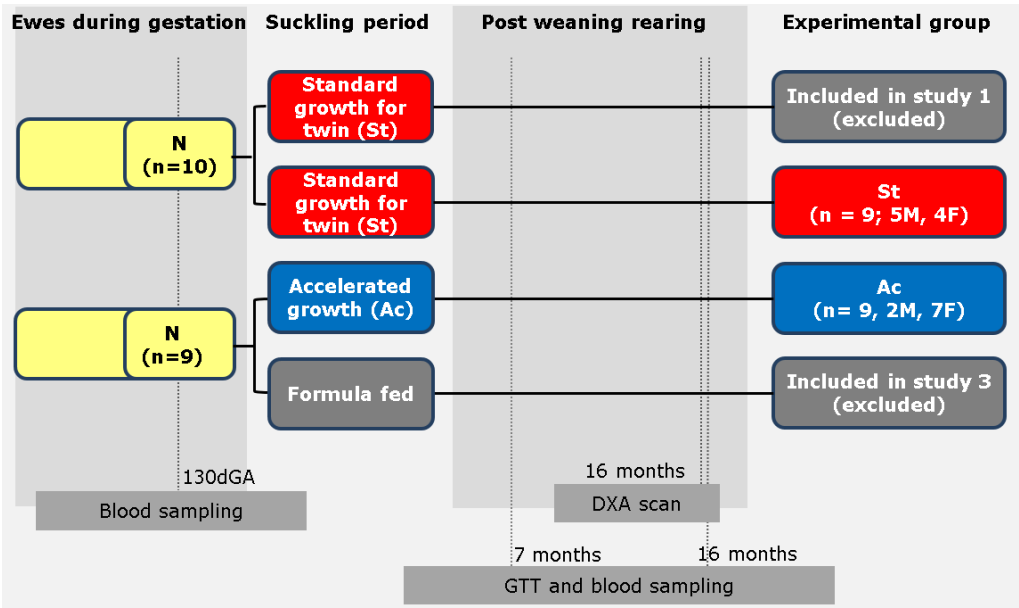


Figure 5.2 Schematic diagram demonstrating the randomisation and timing of blood sampling and DXA scan investigations in the experimental study.

Offspring of twin bearing sheep fed to 60% of metabolic requirements were randomised to be fed by their mother as twins, achieving standard growth for a twin offspring (St) or, after removal of one offspring, to be the remaining offspring fed by mother without competition for milk and achieving accelerated (Ac) growth for a twin offspring. Blood sampling were performed from the twin bearing sheep at 130 days gestational age (dGA) and offspring had glucose tolerance test (GTT) and blood sampling performed at age 7 and 16 months. Dual X ray absorptiometry (DXA) analysis was performed in the offspring at age 16 months.

5.3 Results

5.3.1 Maternal and offspring metabolic and endocrine profile

5.3.1.1 Effect of rearing as a singleton or twin on the weight gain of the offspring

The birth weight of offspring randomised to the Ac (mean±SEM; 3.76±0.18 kg, n=9) and St (4.07±0.14 kg, n=9) groups was comparable (p=0.116). The serial weight measurements from birth to the end of the suckling period at 90 days was analysed using a two-way mixed ANOVA to account repeated measures of weight at different timepoints. The analysis was significant for interaction between experimental groups and time (p=0.017). During the suckling period (birth to 90 days), the St offspring were significantly lighter than the Ac offspring in all the bodyweight measurements between age of 21 days until the age of 90 days (Figure 5.3).

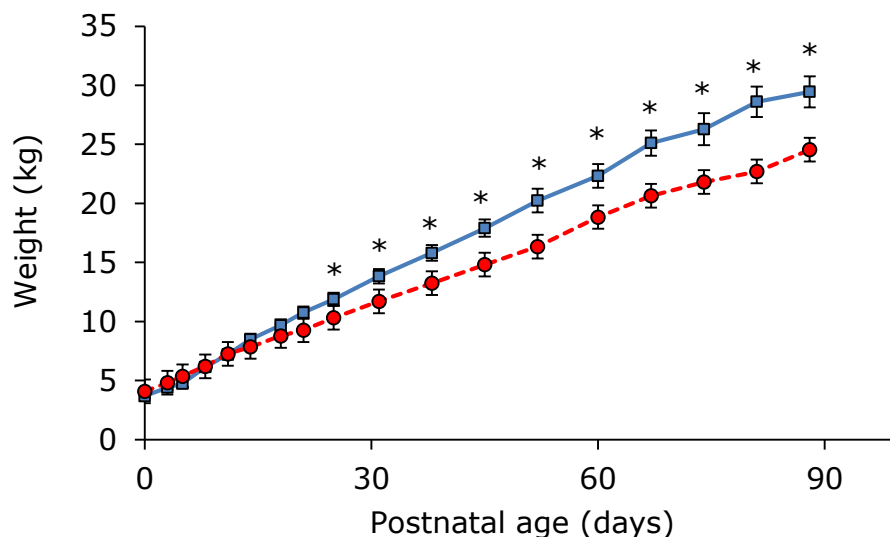


Figure 5.3 Offspring weight gain from birth to age of 90 days for lambs randomized to rearing as described to achieve a standard growth rate for a twin (St, red circle, dotted line, n=9) or to accelerated rate of growth (Ac, blue squares, solid line, n=9) during the suckling period. Two-way mixed ANOVA to account repeated measures of weight at different timepoints was significant for interaction between experimental groups and time (p=0.017). Data points depict mean with error bars depicting SEM. * p<0.05 for Ac versus St simple main effects comparison.

Accelerated early growth did not lead to any difference in the final body weight of the offspring as measured at 17 months of age. In addition, measurements of physical activity using an accelerometer performed during the suckling period (i.e. at 45 days of age) and at age 15 months did not differ between the two groups (Table 5.1).

	St	Ac
Body weight at 17 months (kg)	69.6±5	68.0±3.1
Mean physical activity at age 45 days (counts)	158.6±21.6	157.7±14.1
Duration mobile in 24 hours at age 45 days (minutes)	916±95	1048±55
Mean physical activity at age 15 months (counts)	74±33	149±22
Duration mobile in 24 hours at age 15 months (minutes)	541±199	892±79

Table 5.1 Body weight and physical activity parameters at the age of 45 days and 15 months for lambs randomized to rearing as described to achieve a standard growth rate for a twin (St, n=6) or to accelerated rate of growth (Ac, n=9) during the suckling period. Data presented as means ± SEM. Statistical analysis performed with independent sample t test.

5.3.1.2 Effect of accelerated early growth on the body composition and liver weight at 17 months of age

The total body and relative fat mass measurements obtained from DXA scan and from weighing of adipose depots at dissection did not demonstrate any difference in overall adiposity between the two groups (Table 5.2). The absolute weight of the omental adipose tissue was not different between the two groups. However, relative omental adipose tissue weight (percentage of total body fat mass) of Ac offspring was significantly less than the St offspring. The absolute and relative weights of other adipose depots and the liver were not different between the two groups.

	St	Ac
Total fat mass from DXA (%)	14.4±1.0	17.1±2.8
Total fat mass from DXA (kg)	9.9±0.6	11.7±2.1
Omental fat mass at dissection (kg)	1.66±0.15	1.56±0.38
Omentum, relative to total fat mass (%)	16.8±1.1 ^a	12.7±1.5 ^b
Pericardial fat mass at dissection (kg)	0.12±0.01	0.96±0.07
Pericardial fat, relative to total fat mass (%)	0.14±0.01	0.17±0.02
Perirenal fat mass at dissection (kg)	1.01±0.10	1.07±0.25
Perirenal fat, relative to total fat mass (%)	1.48±0.16	1.57±0.34
Total visceral fat depots at dissection (kg)	2.78±0.26	2.73±0.62
Visceral fat depots, relative to total fat (%)	28.1±1.8	22.7±2.3
Liver weight at dissection (kg)	0.76±0.06	0.67±0.04
Liver, relative to total body weight (%)	1.08±0.04	0.96±0.02

Table 5.2 Body composition and organ weight of the offspring for lambs randomized to rearing as described to achieve a standard growth rate for a twin (St, n=9) or to accelerated rate of growth (Ac, n=9) during the sucking period. Data are presented as mean±SEM. a versus b, p=0.03 (independent sample t-test). DXA, dual X-ray absorptiometry

5.3.1.3 Effect of accelerated early growth on plasma metabolic and endocrine profile.

Analyses of the plasma glucose and insulin samples from the GTT (Figure 5.4) were performed using two-way mixed ANOVA to account for repeated measurements.

For GTT at 7 months age, the statistical test was significant for interaction between early growth and time ($p=0.02$). Univariate analysis at individual time points did not demonstrate a statistically significant difference except for the marginal difference in measurement at 120 minutes ($p=0.048$). Statistical analysis of the plasma insulin concentrations at 7 months age did not demonstrate a significant interaction between early growth and time ($p=0.37$) or for the main effect of early growth ($p=0.16$)

At 16 months of age, the glucose concentrations did not show a significant two-way interaction between early growth and time ($p=0.36$) or for the main effects of early growth ($p=0.63$). The plasma insulin concentrations did not demonstrate a significant interaction between early growth and time ($p=0.88$) or for the main effects of early growth ($p=0.37$).

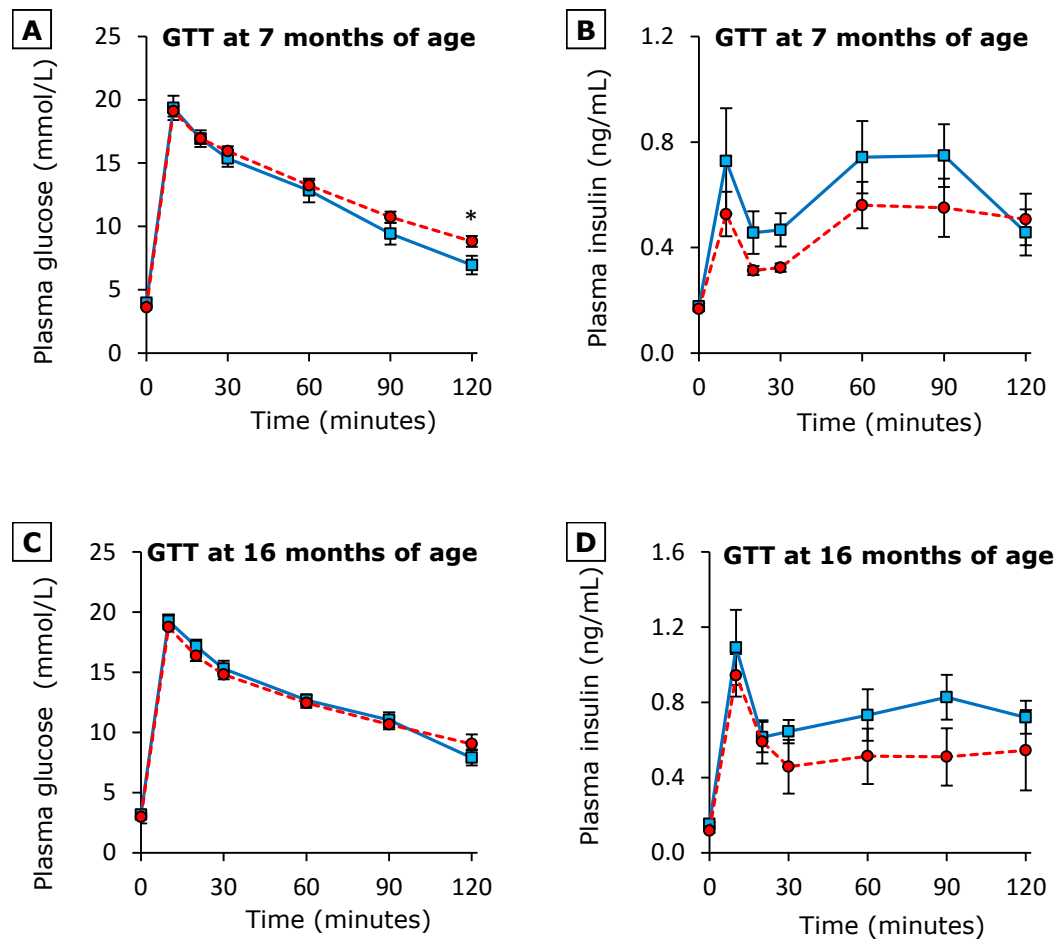


Figure 5.4 Plasma glucose and insulin measurements during glucose tolerance test performed at 7 months (A and B respectively) and 16 months (C and D respectively) for lambs randomized to rearing as described to achieve a standard growth rate for a twin (St, n=6) or to accelerated rate of growth (Ac, n=9) during the sucking period. Statistical analysis performed using two-way mixed ANOVA. * $p < 0.05$ for simple main effects analysis. Data are displayed as mean with error bars depicting SEM.

The measurements of glucose and insulin concentrations during the GTT were used to calculate the AUC. The calculated AUC values did not differ between the experimental groups for glucose and insulin measured at 7 and 16 months respectively. The absence of differences in insulin sensitivity was confirmed on calculation of the HOMA-IR for sheep. Plasma cortisol, triglyceride and NEFA measurements also did not differ between the two groups (Table 5.3). Although they were similar at the age of 7 months, plasma leptin measurements at 16 months were increased in the Ac as compared to the St growth group.

	Age (months)	St	Ac
AUC glucose (mmol/L)	7	1549±44	1462±90
	16	1491±69	1504±64
AUC insulin (ng/ml)	7	55.4±9.6	36±7.6
	16	49.8±14.5	71.9±11.6
HOMA-IR	7	0.60±0.04	0.75±0.06
	16	0.36±0.03	0.47±0.04
Plasma leptin (ng/mL)	7	2.31±0.45	2.45±0.45
	16	3.81±0.52 ^a	6.16±0.94 ^b
Plasma cortisol (nmol/L)	7	55.1±7.8	60.5±14.2
	16	41.9±11.6	56.1±13.9
Plasma triglycerides (mg/dL)	7	0.14±0.02	0.16±0.01
	16	0.12±0.02	0.13±0.03
Plasma NEFA (mmol/L)	7	1.18±0.13	1.11±0.08
	16	0.54±0.07	0.43±0.09

Table 5.3 Plasma metabolic and endocrine profile of offspring at age 7 and 16 months for lambs randomized to rearing as described to achieve a standard growth rate for a twin (St, n=9) or to accelerated rate of growth (Ac, n=9) during the sucking period. Data presented as means ± SEM. Statistical analysis performed with independent sample t test. A versus b <0.05. HOMA-IR, homeostatic model assessment – insulin resistance. NEFA, Non-esterified fatty acids.

5.3.2 Liver weight, triglyceride deposition and oxidative stress.

Liver weight, triglyceride concentrations and malondialdehyde (MDA) concentrations (as a marker for thiobarbituric acid reactive substances (TBARS)) did not differ between the experimental groups (Table 5.4).

	St	Ac
Liver weight (g)	755±59	660±39
Liver triglyceride (mg/g liver)	48.3±7.8	30.8±1.5
Total liver triglyceride (g)	27.8±4.5	20.4±1.6
Liver TBARS (MDA μM/protein μg/μl)	0.98±0.09	0.90±0.08

Table 5.4 Liver organ weight, triglyceride content and TBARS measurements for lambs randomized to rearing as described to achieve a standard growth rate for a twin (St, n=9) or to accelerated rate of growth (Ac, n=9) during the sucking period. Data presented as means \pm SEM. Statistical analysis performed with independent sample t test . TBARS, Thiobarbituric acid reactive substances.

5.3.3 Liver histology

Histological images could not be quantified for appearance of steatosis and steatohepatitis (Figure 5.5). There was no difference in appearances of macrovesicular steatosis or cellular infiltration with experimental intervention which was similar to findings described in Section 3.3.3.

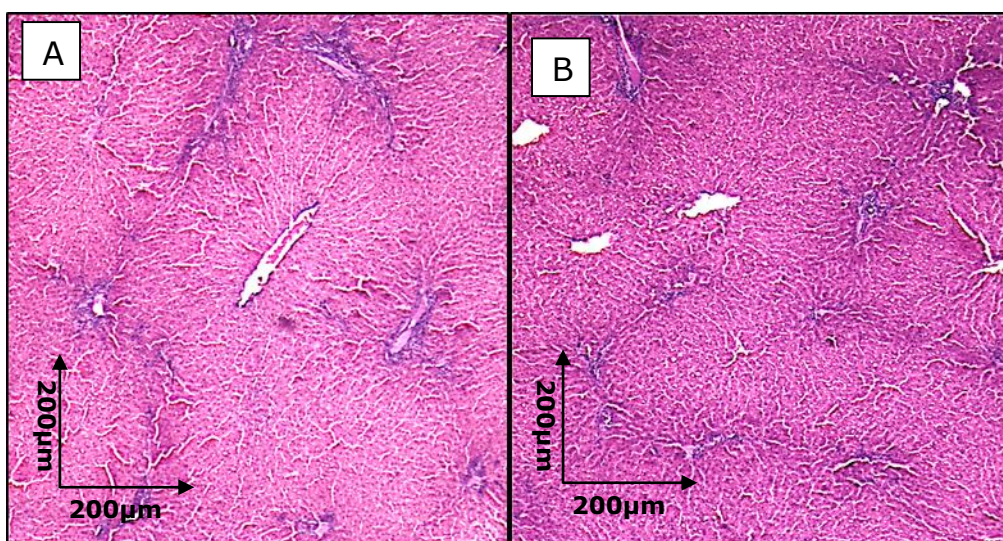


Figure 5.5 Representative images of histological sections of liver from (A) St and (B) Ac offspring stained with Masson's Trichrome demonstrating components of hepatic lobules at 10x magnification.

5.3.4 Hepatic gene expression

5.3.4.1 Gene expression for modulators and effectors of metabolic inflammation in liver

The gene expression for leptin receptor and TLR4 were significantly increased in the Ac group as compared to the St group (Figure 5.6).

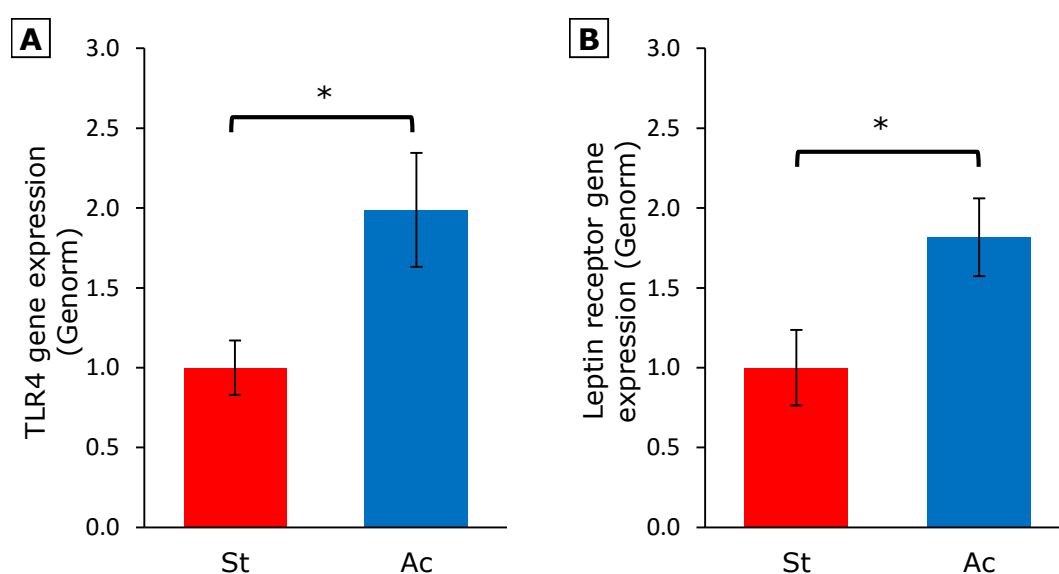


Figure 5.6 Gene expression for liver TLR4 (A) and leptin receptor (B) for lambs randomized to rearing as described to achieve a standard growth rate for a twin (St, n=7) or to accelerated rate of growth (Ac, n=9) during the sucking period. Data presented as means with error bars depicting SEM. *p<0.05 (independent sample t test). CD95, cluster of differentiation 95; TLR4, toll-like receptor 4.

There was no difference in the gene expression for hepatic cluster of differentiation 95 (CD95), cluster of differentiation 68 (CD68), glucocorticoid receptor and 11 β -hydroxysteroid dehydrogenase isoform 1 (11 β HSD1) (Table 5.5).

	St	Ac
CD68	1.00 \pm 0.09	1.00 \pm 0.10
CD95	1.00 \pm 0.03	0.99 \pm 0.10
11βHSD1	1.00 \pm 0.06	1.01 \pm 0.07

Table 5.5 Relative gene expression of liver CD68, CD95 and 11 β HSD1 for lambs randomized to rearing as described to achieve a standard growth rate for a twin (St, n=7) or to accelerated rate of growth (Ac, n=9) during the sucking period. Data presented as means \pm SEM. Statistical analysis performed with independent sample t test. CD68, cluster of differentiation 68; CD95, cluster of differentiation 95, 11 β HSD1, 11 β -hydroxysteroid dehydrogenase isoform 1.

5.3.4.2 Gene expression for the components of the unfolded protein response in the liver

Analysis of the components of unfolded protein response by comparing the gene expression for ATF4, ATF6, EDEM1 and GRP78 did not demonstrate any modification by the experimental intervention (Table 5.6).

	St	Ac
ATF4	1.00±0.09	0.88±0.06
ATF6	1.00±0.02	1.02±0.09
EDEM1	1.00±0.04	1.02±0.05
GRP78	1.00±0.12	0.99±0.11

Table 5.6 Relative gene expression for the components of the UPR (ATF4, ATF6, EDEM1 and GRP78) for lambs randomized to rearing as described to achieve a standard growth rate for a twin (St, n=7) or to accelerated rate of growth (Ac, n=9) during the sucking period. Data presented as means ± SEM. Statistical analysis performed with independent sample t test. ATF4, Activating transcription factor 4; ATF6, Activating transcription factor 6; ER degradation-enhancing alpha-mannosidase-like 1; GRP78, glucose-regulated protein 78.

5.3.4.3 Gene expression for the components of the autophagy in the liver.

The gene expression for mTOR was significantly increased in Ac group as compared to the St group. However, this was not associated with any changes in the gene expression of AMPK (Figure 5.7) or ATG12 Ac (1.00 ± 0.03 , $n=9$) and St (1.05 ± 0.04 , $n=7$).

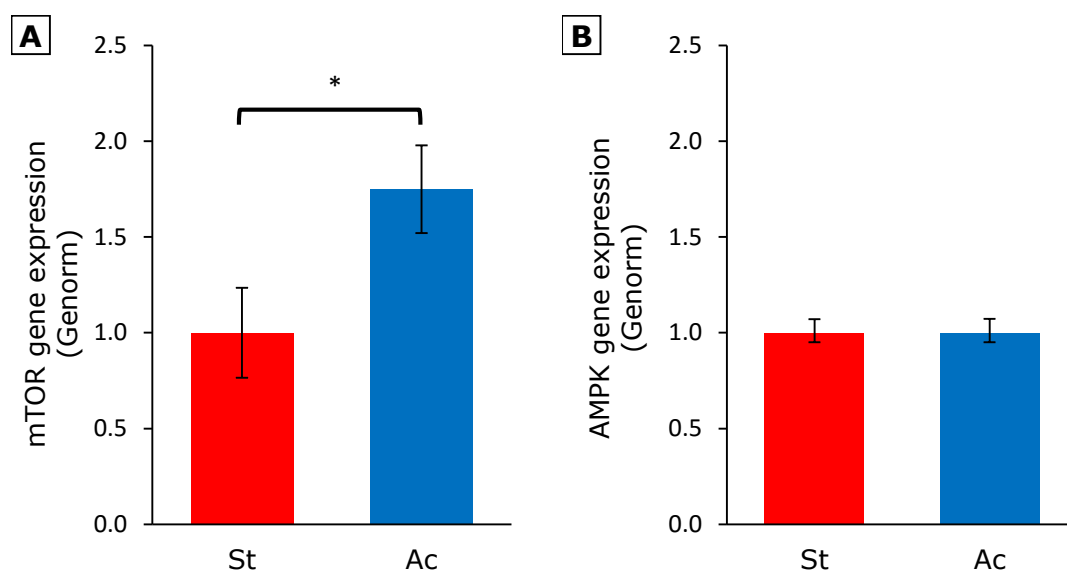


Figure 5.7 Relative gene expression in liver for mTOR (A) and AMPK (B) for lambs randomized to rearing as described to achieve a standard growth rate for a twin (St, $n=7$) or to accelerated rate of growth (Ac, $n=9$) during the sucking period. Data presented as means \pm SEM. Statistical analysis performed with independent sample t test. mTOR, mammalian target of rapamycin; AMPK, 5' adenosine monophosphate-activated protein kinase.

5.3.5 Omental adipose tissue histological characteristics

5.3.5.1 Cell size, GRP78 and pJNK staining in omental adipose tissue

There was no difference in the measured area of omental adipocytes and the microscopic characteristics of the adipose tissue were consistent with the description of omental adipose tissue from obese offspring given in Chapters 3 and 4 including unilocular lipid droplets, scant stromal connective tissue and non-homogenously dispersed clusters of IBA1 positive macrophages present within crown like structures and milky spots.

There was no difference in measured quantities of GRP78 staining which was localised to the cytoplasmic content or of the phosphorylated c-Jun N-terminal kinase (pJNK) staining concentrated in the perinuclear region (Table 5.7 and Figure 5.8).

	St	Ac
Adipocyte area (μm^2)	4429 \pm 445	4116 \pm 545
GRP78 ($\mu\text{m}^2/\text{cell}$)	70 \pm 21	65 \pm 29
pJNK ($\mu\text{m}^2/\text{cell}$)	44 \pm 13	50 \pm 9

Table 5.7 Mean adipocyte area in μm^2 and quantification of GRP78 and pJNK calculated from the histological sections of omental adipose tissue of 17 month old lambs randomized during the sucking period to rearing as described to achieve a standard growth rate for a twin (St, n=7) or to accelerated rate of growth (Ac, n=9). Data presented as means \pm SEM. Statistical analysis performed with independent sample t test. GRP78 Glucose regulated protein-78; pJNK, phosphorylated c-Jun N-terminal kinase

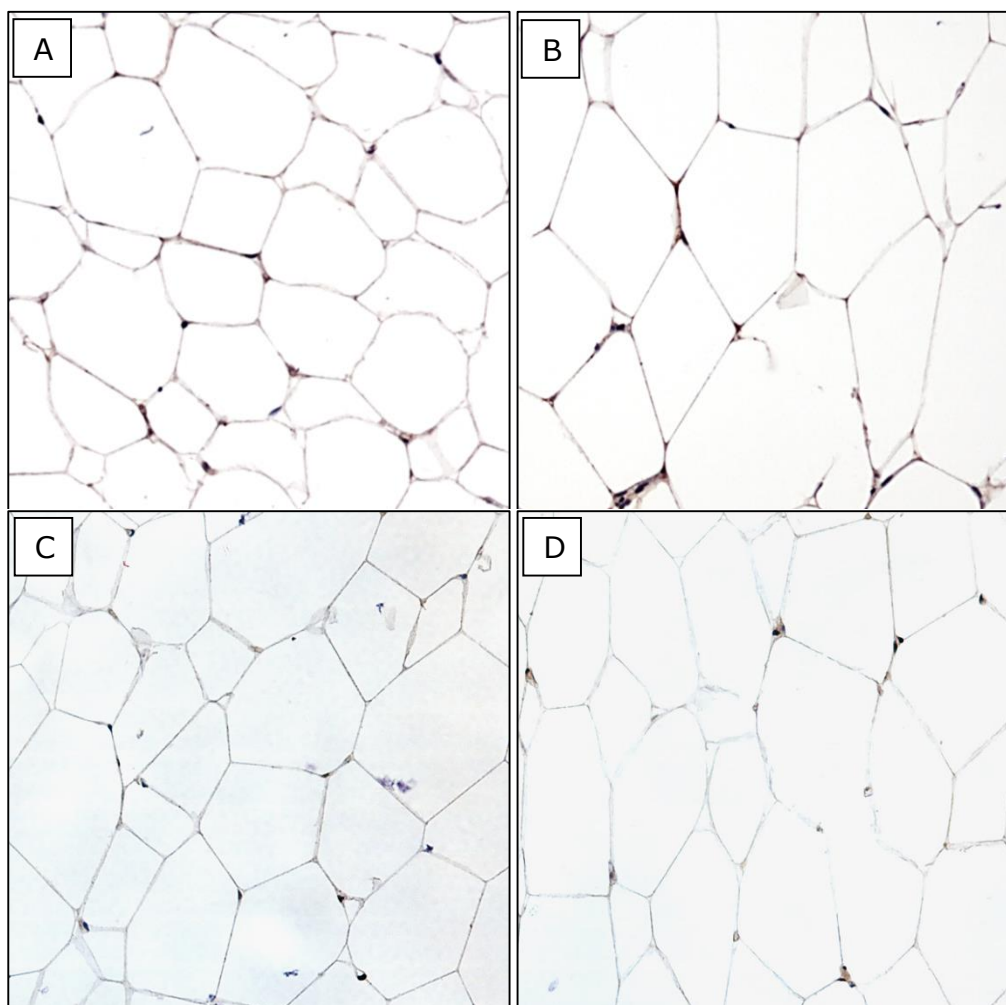


Figure 5.8 Representative images demonstrating distribution of staining in omental adipose tissue for GRP in (A) St and (B) Ac offspring and staining for Iba1 in (C) St and (D) Ac offspring, Location of GRP and pJNK staining can be identified by brown DAB staining

5.3.6 Omental adipose tissue gene expression analysis

5.3.6.1 Gene expression of regulatory factors of metabolic inflammation and components of UPR.

There was no difference in the gene expression of omental adipose tissue leptin, adiponectin, CD68, TLR4 and 11 β HSD1 (Table 5.8).

	St	Ac
Leptin	1.00 \pm 0.27	1.01 \pm 0.28
Adiponectin	1.00 \pm 0.15	1.17 \pm 0.10
CD68	1.00 \pm 0.52	0.78 \pm 0.23
TLR4	1.00 \pm 0.06	1.05 \pm 0.11
11βHSD1	1.00 \pm 0.11	0.88 \pm 0.14

Table 5.8 Gene expression for leptin, adiponectin, CD68, TLR4 and 11 β HSD1 in the omental adipose tissue of lambs randomized as described during the sucking period to achieve a standard growth rate for a twin (St, n=7) or to accelerated rate of growth (Ac, n=9). Data presented as means \pm SEM. Statistical analysis performed with independent sample t test. Data are presented as mean \pm SEM. CD68, cluster of differentiation 68; 11 β HSD1, 11 β -hydroxysteroid dehydrogenase isoform 1; TLR4, toll-like receptor 4.

5.3.6.2 Gene expression of components of UPR in omental adipose tissue.

The experimental intervention did not lead to any change in the gene expression of the UPR genes, ATF4, ATF6, GRP78 and EDEM1 (Table 5.9).

	St	Ac
ATF4	1.00±0.08	0.95±0.06
ATF6	1.00±0.07	1.03±0.09
EDEM1	1.00±0.05	1.03±0.07
GRP78	1.00±0.11	0.98±0.12

Table 5.9 Expression of genes responsible for UPR in the omental adipose tissue of lambs randomized as described during the sucking period to achieve a standard growth rate for a twin (St, n=7) or to accelerated rate of growth (Ac, n=9). Data presented as means ± SEM. Statistical analysis performed with independent sample t test. ATF4, activating transcription factor 4; ATF6, activating transcription factor 6; ER degradation-enhancing alpha-mannosidase-like 1; GRP78, glucose-regulated protein 78.

5.3.6.3 Gene expression of the components of autophagy in the omental adipose issue.

The gene expression for regulators and components of autophagy, AMPK, mTOR, ATG12 and BECN1 did not differ between the experimental groups (Table 5.10).

	St	Ac
AMPK	1.00±0.14	1.09±0.10
mTOR	1.00±0.24	0.96±0.16
ATG	1.00±0.06	1.04±0.06
BECN1	1.00±0.08	0.99±0.05

Table 5.10 Gene expression of regulators and components of autophagy in omental adipose tissue of randomized as described during the sucking period to achieve a standard growth rate for a twin (St, n=7) or to accelerated rate of growth (Ac, n=9). Data presented as means ± SEM. Statistical analysis performed with independent sample t test. mTOR, mammalian target of rapamycin; AMPK, 5' adenosine monophosphate-activated protein kinase; Autophagy-related protein 12; BECN1, gene encoding Beclin1.

5.4 Discussion

Nutritional intake during early life is known to be the primary determinant of infant growth. The experiments described in this chapter were designed to investigate the impact of accelerated early postnatal growth rate in IUGR animals upon development of later obesity, insulin resistance or on metabolic inflammation and cell stress response. Sheep offspring fed by their mother as a singleton grew at a faster rate as compared to the twin offspring, both feeding on their mother's milk. This was not associated with any difference in final adult weight or adiposity. Testing for GTT, plasma triglycerides, NEFA or plasma cortisol did not identify any differences in the carbohydrate or lipid metabolism of the offspring. Offspring in the accelerated early growth rate group had significantly higher plasma leptin levels as compared to the offspring experiencing standard growth for a twin.

Hepatic weight, triglyceride content and TBARS as a marker of oxidative stress were comparable between the two groups. Ac offspring demonstrated increased gene expression for hepatic TLR4 and leptin receptors. However, this was not associated with any change in gene expression of hepatic inflammatory markers, components of UPR or autophagy.

Ac offspring had increased circulating leptin at 16 months of age, however this was not associated with differential adipose tissue deposition, change in adipocyte size or with a consistent pattern of change to gene expression of metabolic inflammation and adipocyte cell stress response.

5.4.1 Accelerated early growth in sheep is not associated with development of adult obesity, insulin resistance or altered cell stress response.

Offspring of nutrient restricted twin bearing sheep demonstrated increased growth rate when one of the twins was removed from feeding from their mother's milk as compared to the offspring which were both fed on their mother's milk. As early growth rate is primarily determined by food intake, offspring's milk intake, although not measured in this study, can be assumed to be higher in the Ac offspring as compared to the St offspring. However, when reared in similar postweaning environment, the adult Ac offspring were not heavier than the St offspring, indicating the increased nutritional intake and the rapid early weight gain during early life did not predispose the Ac offspring to increased obesity or adipose tissue deposition.

The stimulus for research of the programming potential of nutritional intake during early life [501, 502] arises from evidence from early epidemiological [289] and rodent animal studies [269] indicating potential deleterious effect of rapid early growth. This is particularly important as many infants born SGA subsequently experience rapid postnatal growth in early infancy.

Whilst the associations between early weight gain and adult obesity and adiposity identified in epidemiological studies have been contradicted in more recent studies [289, 290], rodent studies of nutritionally mediated rapid early postnatal growth have demonstrated its association with obesity in adulthood [296]. Rodent organ development, maturity of endocrine axis, milk composition are some of the potentially significant factors which differ from large mammals such as sheep [247]. The inability to replicate the increased obesity in response to rapid early postnatal growth in this study as predicted from the rodent studies could be due to

relatively underdeveloped rodent endocrine axes [298] or differences in the characteristics of adipocyte depots [503] during early postnatal life. It is plausible that such factors make early postnatal life in rodents a critical window of development susceptible to programming through nutrition intake and rapid growth whereas sheep, with relatively mature endocrine and differing adipocyte profile are relatively resistant to such programming.

Metabolic syndrome and insulin resistance can occur independent of obesity [7] and, therefore, it was important to investigate if the offspring were predisposed to these potentially deleterious phenomena irrespective of a difference in final adult weight or adiposity. However, in conjunction with no change in predisposition to obesity, insulin sensitivity measured using GTT and metabolic parameters, NEFA and plasma triglyceride concentrations did not differ between Ac and St offspring. The circulating leptin concentrations at 16 months of age were higher in Ac than in Sc despite similar body fat mass indicating that the adipose tissue in the Ac animals may have a different phenotype and inflammatory profile. However, leptin gene expression in omental adipose tissue was not significantly increased in the Ac sheep. Hyperleptinaemia has been associated with development of insulin resistance, suggesting a role in the metabolic syndrome [504]. It is plausible that the increased baseline plasma leptin concentration is an outcome of production from another adipose depot such as perirenal or subcutaneous adipose tissue or an outcome of selective post translational modifications of the product. It is thought that the chronic exposure of higher leptin levels observed in obese subjects leads to leptin desensitisation and development of leptin resistance. The raised plasma leptin concentrations in the Ac offspring could also indicate a compensatory response to a leptin resistance at tissue level. The gene expression for leptin receptors in the adipose tissue

was below the detectable limits of the PCR assay and the gene expression for hepatic leptin receptor was increased in the Ac offspring. This was not associated with a consistent increase in gene expression of any markers of inflammation apart from increase in hepatic TLR4 receptor gene expression in the AC offspring. The effect of such isolated gene expression changes is difficult to interpret and would be speculative at best.

Circulating leptin is known to be associated with modulation of the immune system [505]. However, the adipocyte size, structure and immunohistochemistry for components of GRP78 and pJNK did not identify any such difference. Omental adipose tissue gene expression of inflammatory markers and cell stress response also was not increased with accelerated postnatal growth. Along with modulator of metabolic inflammation, leptin is known to have an effect on appetite regulation. Such possibility of leptin action and leptin resistance in this setting of early postnatal nutritional programming is already being investigated [506].

The results from the experiments do not confirm the predictions of the study hypotheses. As with any scientific experimental study, the interpretations of results are restricted to the limitations of the scientific model being used. Notably, this model is not able to determine if the relatively faster rate of growth in the Ac offspring as compared to the St offspring is a reflection of overnutrition in the Ac group or relative undernutrition in the St group. The study was designed to bring about a nutritionally mediated alteration in the rate of early growth following IUGR. The nutritional intake and growth rate of the twin offspring in the St group would match the naturally occurring parameters of this population of twin offspring. Therefore the St offspring were designated as the control group and Ac offspring represent the experimental intervention.

The experiments investigated whether IUGR offspring followed by relatively accelerated postnatal growth would exacerbate obesity induced insulin resistance and worsen hepatic and adipose tissue inflammation and cell stress response. Whilst, there is no definition of sheep IUGR, the offspring of sheep undergoing nutrient restriction with the z-score of sample mean of -3 as compared to the entire population indicates a significant difference from the population mean (Chapter 3). This was interpreted as an indicator of significant IUGR. It is plausible that nutrient restriction mediated IUGR developed in this sheep model is not entirely representative of the IUGR in humans which is an outcome of the multiple mutually interacting maternal and fetal factors such as placental health, intrauterine infections, maternal micronutrient intake and genetic factors [423, 507]. Such differing intrauterine mechanisms could still differentially regulate the predisposition of a growth restricted offspring to the programming effect of postnatal growth. It is also plausible that a more severe maternal nutrient restriction with, or without, a relatively faster postnatal growth would have demonstrated development of severe metabolic outcome. However, such an extreme nutrient restriction during pregnancy or forced acceleration of postnatal growth during early postnatal life is unlikely to reflect human equivalence or to have a public health implication. Future efforts of research into metabolic impact of the interaction of IUGR and postnatal growth should instead focus on a different model of sheep IUGR [507] followed by postnatal accelerated growth. The data presented in this thesis can serve to be a reference measure and for power calculations while designing any such study.

5.5 Conclusion

Accelerated postnatal growth following development of IUGR brought about by maternal nutrient restriction in a sheep model did not predispose the offspring to worsening of adult adiposity, insulin resistance, metabolic inflammation or altered hepatic and adipose tissue cell stress response. Whilst the circulating plasma leptin is increased in adult sheep who experienced accelerated postnatal growth, this did not lead to a difference in the metabolic inflammatory profile or in the cell stress response of the offspring in adulthood. The data presented in this unique study lay a background and reference point for future investigations in this topic which has potentially significant public health implications.

6 Conclusions

6.1 Aims

The studies described in this thesis investigate the developmental programming effects of nutrition during early life on the obesity associated hepatic and omental adipose tissue cell stress response. Obesity is known to be associated with a state of chronic metabolic inflammation [508] and cell stress response pathways [112] in organs such as liver and adipose tissue. The ability of the organ cell stress response to alleviate the adverse effects of such inflammation determines, in part, the cellular and organ dysfunction of the derangements associated with metabolic syndrome [459]. The state of metabolic health in this study was described using the parameters of body weight, adiposity, glucose tolerance, plasma metabolite concentrations, endocrine parameters, hepatic oxidative stress and histological characteristics of adipose and hepatic tissue. Gene expression and immunohistochemistry studies were performed to describe the hepatic and omental adipose tissue cell stress response in adult sheep.

Three different studies were performed to analyse combinations of early life nutrition influences on the outcome measures. The first study (Chapter 3) established the baseline metabolic and cell stress characteristics in obese and lean sheep and compared them to obese and lean sheep that had experienced intrauterine growth restriction (IUGR) secondary to maternal nutrient restriction during late gestation (NR-LG). The study described in Chapter 5 investigated the effect of accelerated early postnatal growth in IUGR lambs fed by mother on the same outcome measures in adult sheep. Formula feeding as a programming mechanism was investigated in Chapter 4 which described the outcome measures in offspring of sheep undergoing NR-LG or of sheep fed to requirements who

had been randomised to formula feeding or to being fed on their mother's milk.

6.2 Summary of findings

Table 6.1 summarises the findings of the studies described in this thesis which are described in the following subsections.


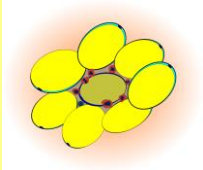
Experimental intervention	Obesity	Prenatal nutrient restriction + Obesity	Prenatal nutrient restriction + Formula Feeding + Obesity	Prenatal nutrient restriction + Accelerated early growth + Obesity
Physiological characteristics of offspring	<ul style="list-style-type: none"> 1.35 fold increased adult weight Weight gain apparent after 12 months Raised insulin on 16 month GTT Increased plasma leptin 	<ul style="list-style-type: none"> Birth weight z-score -3 No effect on adult body weight or endocrine parameters 	<ul style="list-style-type: none"> Relatively slow early growth (0-90 days) in IUGR formula fed offspring. Decreased physical activity No difference in adult body weight or endocrine parameters 	<ul style="list-style-type: none"> Singleton rearing of twin offspring resulted in increased weight gain during suckling (0-90 days) No difference in adult body weight. Increased plasma leptin
	<ul style="list-style-type: none"> Increased liver weight Increased hepatic triglyceride 	<ul style="list-style-type: none"> Increased relative liver weight Further increase in hepatic triglycerides 	<ul style="list-style-type: none"> No exacerbation of lipid deposition. 	<ul style="list-style-type: none"> No exacerbation of lipid deposition.
	<ul style="list-style-type: none"> Increased hepatic UPR gene expression 	<ul style="list-style-type: none"> Increased autophagy gene (BECN1) 	<ul style="list-style-type: none"> No change in hepatic gene expression of inflammation or cell stress response 	<ul style="list-style-type: none"> Increased hepatic TLR4 and leptin gene expression. No change to UPR gene expression
	<ul style="list-style-type: none"> Preferential deposition to visceral adipose depots Adipocyte hypertrophy Increased macrophages, crown-like structures and milky spots 	<ul style="list-style-type: none"> No change 	<ul style="list-style-type: none"> No change in adiposity or histological characteristics. 	<ul style="list-style-type: none"> No change in adiposity or histological characteristics.
	<ul style="list-style-type: none"> Increased gene expression for leptin, TLR4 and CD68 Increased autophagy gene expression (ATG12 and Beclin1) 	<ul style="list-style-type: none"> Increased omental UPR response gene expression (ATF6, GRP78 and EDEM1) 	<ul style="list-style-type: none"> No change in omental adipose gene expression for inflammation or cell stress 	<ul style="list-style-type: none"> No change in omental adipose gene expression for inflammation or cell stress

Table 6.1 Summary of the findings of studies described in this thesis listed in a tabular format.

UPR, unfolded protein response; GTT, glucose tolerance test, TLR4, toll like receptors-4; CD68, cluster of differentiation 68; ATG12, autophagy related protein-12; ATF, activating transcription factor 6; EDEM1, ER stress degradation enhancer molecule-1; BECN1, gene encoding Beclin1.

6.2.1 Effects of obesity in young adult sheep

Sheep reared in a restricted environment of decreased physical activity demonstrated a 1.35 fold weight gain compared to controls. This is modest in contrast to other studies with a 1.5 fold [264] or 2 fold [223, 436] weight gain induced in the obese sheep compared to the control animals.

Rearing in an obesogenic environment was associated with development of peripheral insulin resistance. As hypothesised, obesity was associated with increased gene expression of unfolded protein response (UPR) components which is in consensus with observational human studies [105] and small animal experiments [99]. In addition, upregulated gene expression of hepatic autophagy components, increased hepatic triglyceride deposition without increase in plasma triglyceride concentrations indicate defective autophagy contributing further to hepatic cell stress. Upregulated gene expression of hepatic autophagy, by itself, is insufficient to conclusively reveal the state of hepatic autophagic flux [237] since upregulation of the gene expression can be a reflection of either increased, or defective, autophagy. Ongoing studies of the relationship between hepatic autophagy and development of NAFLD [235] are important for improving the knowledge of the pathogenesis of metabolic syndrome. However, the focus of this component of the studies was to establish the baseline state of the gene expression. In the interest of time and resources, further efforts were not made to perform further analysis of the autophagic flux.

6.2.2 Effects of maternal nutrient restriction followed by obesity in offspring

Maternal NR-LG during late pregnancy to 60% of maternal nutrient requirements caused maternal hypoglycaemia, higher plasma non-esterified fatty acids (NEFA) concentrations and gave birth to IUGR offspring of nutrient restricted sheep (N) had sample mean birth weight z-score of -3 as compared to the offspring of the

sheep fed to appetite (A). In concurrence with other studies of sheep nutrition during late gestation, [264] nutrient restriction did not predispose the offspring to increased obesity or adiposity. However, the relative liver weight and hepatic triglyceride concentration of the N-O offspring was significantly increased as compared to obese offspring of sheep fed to appetite (A-O) which is similar to the outcome of a sheep study applying a 50% nutrient restriction in mid-gestation paired with increased expression of PPAR γ and PGC1 α suggesting a decrease in beta-oxidation [279]. The increased hepatic triglyceride in N-O animals was associated with increased hepatic autophagy gene expression for BECN1. It has been proposed that a defective autophagy in nutritionally mediated IUGR predisposes to hepatic triglyceride accumulation. Confirmation of such a mechanism will require study of markers of autophagy function and should form part of any future investigation of this mechanism.

In the omental adipose tissue, NR-LG did not exacerbate obesity related changes in adipose depots, adipocyte size, macrophage infiltration or gene expression for adipokines. Gene expression for UPR components demonstrated obesity related increased expression limited to N-O versus N-L. Enhanced UPR with prenatal nutrient restriction, targeted between early-to-mid gestation, has previously been shown in perirenal adipose tissue of sheep at 1 year of age [68].

Late gestation in sheep coincides with rapid expansion of the fetal omental serosa [69] which contains adipocyte precursors. A state of energy deficit, as seen during the late gestation undernutrition, is known to cause ER stress and activate UPR [477, 478]. Preadipocytes are vulnerable to external stress [509, 510], and will survive to develop into mature adipocytes in this scenario if they have effective ER stress response. The selective survival of such adipocytes, would potentially prepare the organ to a postnatal environment of undernourishment. The contrasting nutrient replete state of obesity, which is also known to induce ER stress in adipocytes [91], would lead to sustained

activation of UPR. After the initial pro-survival actions, prolonged UPR in these offspring would initiate inflammation and cell death pathways [25].

Another possible explanation for the exaggerated UPR in the nutrient restricted offspring could be through resetting of total adipocyte number in the depot. It has been shown that the maximal adipocyte number in adipose depots of an adult is set in early life and does not further increase with adult obesity [34]. However, the timing of such determination of preadipocyte destination has not yet been precisely established [511]. If the late gestational undernutrition programmes the developing organism to possess fewer adipocytes, lipid storage with obesity during later life would require a greater degree of hypertrophy. The ensuing cell stress would potentially activate a greater degree of UPR [36] in response to hypertrophy as compared to cells in adipose depots with more abundant adipocytes which would undergo a relatively less degree of hypertrophy while accommodating the excess lipid.

The selective increase in gene expression of UPR components was not supported by immunohistochemistry for GRP78 which was consistently increased with obesity irrespective of prenatal intervention. Moreover, the study did not confirm the hypothesised predisposition to insulin resistance and metabolic syndrome due to prenatal undernutrition as compared to offspring of sheep fed to appetite. The age of 17 months in sheep is considered equivalent to young adulthood and it is plausible that, by this age, the programming mechanisms of NR-LG may not yet have contributed significantly to the progression of insulin resistance. Previous sheep studies of NR-LG either employed a more severe nutritional challenge (50%) [274] or studied the glucose-insulin axis at older age [264]. Additional work is necessary to determine if the upregulated UPR gene expression in obese offspring of sheep undergoing NR-LG would contribute to a worse metabolic outcome at either a later age or following a more severe in utero nutritional challenge.

6.2.3 Interaction of prenatal nutrient restriction and formula feeding during the suckling period.

During the 90 day suckling period, the IUGR formula fed offspring of NR-LG sheep (N-F) remained significantly lighter than formula fed offspring of sheep fed to requirement (R-F). This is in contrast to the pattern of increased growth described in some formula fed human infants [483]. This could reflect better proximity of human formula micronutrient composition to breast milk or could be the outcome of maternal deprivation [485, 486], which is known to result in growth failure [512]. In addition, in this study, the formula fed offspring were noted to be significantly less active as compared to offspring of mother fed sheep at 45 days of age. The physical activity counts at the age of 45 days correlated with physical activity measurements performed at 15 months indicating that early environmental influences lead to establishment of a physical activity phenotype which persists during adolescence.

There was a trend towards increasing liver triglyceride concentrations with formula feeding ($p=0.058$). However, this was not associated with the studied histological features characteristic of NAFLD. Formula feeding with, or without, a background of prenatal nutrient restriction was not associated with any change in gene expression for components of metabolic inflammation, UPR or autophagy. The current study model, therefore, does not confirm the hypothesised increase in the cell stress response and metabolic inflammation in formula fed offspring. It is plausible that, with age, the demonstrated trend towards increased hepatic triglycerides in formula fed offspring would reach a level consistent with hepatic steatosis and contribute to development of the metabolic inflammation. Future studies would ideally include testing at different endpoints using hepatic biomarkers or liver biopsies to identify progressive stages in natural history of the disease with a final endpoint at a much older age.

mTOR, a component of cellular energy sensing mechanism, was significantly increased in R-F offspring as compared to both N-F and R-M groups respectively. In the absence of evidence for a significant difference in adipose tissue structure, inflammation or cell stress response gene expression, the relevance of an isolated finding of mTOR gene expression change cannot be fully interpreted.

The results described in this study, therefore, do not support the hypothesised interaction between formula feeding and prenatal undernutrition leading to development of a phenotype with insulin resistance and exaggerated cell stress response. This is the first large animal model experimental study that has attempted to describe the potential interaction of formula feeding and prenatal undernutrition. The failure to support the hypothesised outcome measures are applicable to the study model and there is a need for further studies in large and small animal models to identify the potential mechanisms of adverse metabolic outcomes witnessed in formula fed infants.

6.2.4 Effects of rate of weight gain during suckling period following nutrient restriction in a twin pregnancy.

Offspring of twin bearing sheep who had undergone NR-LG demonstrated increased growth (Ac - accelerated growth) when one of the twins was removed from the mother as compared to the group of twin offspring which were both fed on their mother's milk (St – standard growth for a twin offspring). The rapid weight gain in the former is a reflection of increased nutritional intake, the primary determinant of postnatal growth. Such rapid early weight gain did not lead to an increase in final adult weight or adiposity. Early human epidemiological data exploring the relationship between early weight gain and risk for obesity had used BMI as outcome measure whereas recent studies evaluating the former's association with adiposity demonstrated lack of an association (Table 6.2). Rodent experimental studies [269, 296], in contrast, have demonstrated hyperphagia and increased adiposity as an outcome of rapid early growth. However, the significant differences in intrauterine and postnatal organ development between rodents and a large animals and in their maturity of endocrine axis at birth and milk composition are all potentially significant factors influencing the plasticity of a developing organism, highlighting the need for experimental studies in the latter.

Study	Method	Outcome
Druet <i>et al.</i> 2005[289]	<ul style="list-style-type: none"> • Meta analysis; n=47661 • SD scores of body weight at birth and age 1 year. • Outcome measure: Risk of adult obesity (BMI>30) 	<ul style="list-style-type: none"> • 1 unit increase in SD score of weight from birth to 1 year increases risk of obesity as adult OR 1.23 (1.16,1.30)
Bann <i>et al.</i> 2014[290]	<ul style="list-style-type: none"> • Cohort study; n=1558 • SD scores of body weight at birth and regular measurements until 20y. • Outcome measure: Lean mass and fat mass from DXA scans at mean age 63y. 	<ul style="list-style-type: none"> • Increased weight gain from birth to 2 years associated with increased lean mass. • Increased weight gain from 2-20 years associated with increased fat and lean mass.
Wells <i>et al.</i> 2012 [513]	<ul style="list-style-type: none"> • Cohort study; n=425 • Weight gain from birth to 2y. • Outcome measure: Body composition at age 14 y. 	<ul style="list-style-type: none"> • Rapid weight gain associated with larger size and lean mass but not with adiposity.
Stettler <i>et al.</i> 2005[287]	<ul style="list-style-type: none"> • Cohort study; n=653 • Weight gain during the first week after birth • Outcome measure: Risk for adult overweight (BMI>25) 	<ul style="list-style-type: none"> • For each 100 g increase in weight gain from birth to age 8d OR for adult overweight 1.28 (1.08,1.52)

Table 6.2 Summary of methodology and relevant outcomes of major epidemiological studies investigating association between early postnatal growth with obesity and adiposity.

B.M.I, body mass index; y, years; g, gram; OR, odds ratio; DXA, dual-energy x-ray absorptiometry; SD, standard deviation.

No differences were apparent in the insulin sensitivity or metabolic profiles of the two groups at 6 and 16 months of age. The Ac animals had increased plasma leptin at 16 months of age as compared to St offspring. This was not associated with a consistent increase in gene expression of any markers of inflammation apart from increase in hepatic TLR4 receptor gene expression in the Ac offspring. The effect of such isolated gene expression change is difficult to interpret and would be speculative, at best. Along with modulation of metabolic inflammation, leptin is known to regulate appetite and is the subject of ongoing investigations [506].

It was hypothesised that rapid early weight gain in nutritionally mediated IUGR would predispose the offspring to a greater adverse outcome of obesity manifesting as decreased insulin sensitivity and metabolic inflammation. The results do not support this hypothesis. Maternal nutrition is just one of many mutually interacting mechanisms which determine the development of IUGR. Different models of sheep IUGR obtained secondary to methods such as carunclectomy, hyperthermia, embolisation and single umbilical artery ligation of adolescent overfeeding have differing intrauterine physiological profiles [514]. Fetal hypoxia, hypoglycaemia and acidemia, amongst other endocrine and physiological changes, are all known to be present in human IUGR, which has not been replicated in its entirety by any of the known sheep models [514]. It is plausible that the nutritionally mediated sheep IUGR, in an otherwise healthy animal, was a relatively insignificant stimulus in comparison to the multiple mutually interacting causative factors of IUGR. It is, however, important to systematically elucidate the impact of individual components of the aetiology of IUGR as a programming stimulus. The outcomes of this study demonstrate the absence of exaggerated metabolic inflammation or metabolic outcome secondary to accelerated postnatal growth following nutritionally mediated IUGR.

6.3 Limitations of the model

6.3.1 The sheep as a model of obesity and metabolic syndrome

Distinct differences between the sheep model and human physiology have the potential to confound the programming effect of early life environmental influences. As discussed, ruminants have a distinctly different digestive system and dietary requirements from humans. This model, however, was an investigation into intrauterine undernutrition, postnatal growth rate and physical inactivity induced obesity on the later metabolic health. Developmental programming in both liver and adipose tissue in association with predisposition of obesity and insulin resistance has previously been demonstrated in other sheep studies of nutrition during early life and decreased physical activity [68,

264, 279] with experimental interventions performed at varying timings and of differing magnitude.

There has not been any large animal model which has manifested all the components of metabolic syndrome secondary to obesity. Age, an independent risk factor for development of metabolic syndrome, is an important aspect precluding development of such a model in a research setting. A large animal study which permits the experimental intervention to last through the longer lifespan of a large animal would be logistically and financially very difficult to organise. The focus of this study was to identify the presence of alterations of metabolic inflammation preceding the development of metabolic derangement of metabolic syndrome. The timing of the end point of this study was, therefore, not expected to demonstrate the full complement of metabolic derangements. In addition, there are no defined criterion for sheep metabolic syndrome or insulin resistance. The outcome of endocrine and metabolic parameters were, therefore, studied with comparison to a control group.

6.3.2 The sheep as a model of IUGR secondary to maternal undernutrition.

IUGR is an outcome of multiple factors intrinsic and extrinsic to the mother and fetus such as umbilical blood flow, placental function, adverse maternal and fetal endocrine profiles and pathogen exposure along with maternal nutrition. The results of this study would be applicable to individuals with low birth weight secondary to late gestation undernutrition. An alternative approach could be to divide offspring at birth to cohorts of low birth weight and normal weight.

However, such an approach would have some limitations including an inability to differentiate healthy small for gestation age (SGA) individuals from those who genuinely suffer from IUGR. Furthermore, in order to elucidate the mammalian processes behind any pathogenesis would require an extremely large cohort to

account for all the confounding factors potentially contributing to the development of IUGR. In contrast, the interventions described in this thesis were performed systematically in a randomly selected population with the experimental groups differing only in the amount of macronutrient availability during the late gestation, enabling a focussed study of this specific model.

There is no standard for sheep birth weight which makes it difficult to determine if a certain birth weight qualifies a birth weight value to meet SGA or IUGR criterion. A birth weight z-score of -2 in human studies is conventionally used to represent IUGR [515]. The z-score for offspring in the NR-LG group was >3 below the values for the control animals and, in the absence of any other differences in experimental conditions, this outcome was deemed to be secondary to IUGR. It is plausible that, despite a large difference in birth weight in comparison to the control group, the nutrient restriction to 60% during late gestation was not a severe enough stimulus. Furthermore, twin pregnancies in sheep are known to be inherently different from singleton in terms of fetal growth, postnatal growth and offspring adiposity [516]. It has been proposed that the relatively lower birth weight in twin sheep as compared to singleton are a reflection of IUGR in twin pregnancies [517]. The nature of hypothalamic pituitary adrenal axis in twins has also been shown to be different as compared to singletons. In twin fetal sheep, basal cortisol and ACTH concentrations are lower than in singletons [518] and differences persist even in young adult sheep [519]. Ideally a study of offspring of twin pregnancy as subject would have a singleton control group. This may, therefore, not be a directly transferrable model of IUGR in which the fetuses experience hypoinsulinaemia with the potential to programme later insulin sensitivity. However, the phenotype displayed by the offspring is consistent with findings in human cohorts of nutrient restriction during late gestation.

6.3.3 The sheep as a model for formula feeding.

The study of long term metabolic effects of formula feeding aimed to replicate the growth patterns of human IUGR offspring fed with formula milk. However, these formula fed IUGR offspring grew at a slower rate from the comparison groups and the IUGR offspring fed by their mother. This did not replicate the pattern of enhanced postnatal growth in formula fed IUGR human infants [483]. It is plausible that this could be the outcome of one or more factors such as isolation from the mother and the difference in milk nutrient composition. The impact of maternal deprivation on offspring growth and health was not the primary focus of this study and would require an independent study for such investigation. The absence of excessive postnatal growth in formula fed IUGR offspring in this study provides an opportunity to investigate the independent effect of formula feeding independent of rapid postnatal growth which was the subject of investigation in the study described in Chapter 5.

6.3.4 The sheep model of rapid postnatal growth

The unique model of using offspring of twin bearing sheep to alter the postnatal growth provides an excellent opportunity to study the programming effect of growth and nutrition in early postnatal life. Offspring of twin pregnancies in sheep are known to be inherently different from singleton in terms of fetal growth, postnatal growth and adiposity [516]. It is not possible to ascertain whether similar alterations of postnatal growth rates would lead to identical outcomes in singleton offspring.

6.3.5 Effect of gender

The impact of gender on differential programming of adult health has not been addressed in the study described in this thesis. Where possible, efforts were made to maintain a homogenous distribution of animals of both sexes in each group. However, due to unbalanced gender distribution of offspring birth and death, an even distribution of males and females in all groups was not achieved. Developmental programming is a phenomenon known to occur in both males and females. Nevertheless, gender may have an influence in modulating an individual's risk of developing adverse health outcomes (reviewed in [520]). Notably, in the Dutch famine follow up study, the association of maternal undernutrition during the first trimester with higher BMI and waist circumference was demonstrated in 50 year old women and not in men. Male offspring of sheep fed low methionine and vitamin B diet in periconceptual period demonstrate a more marked hypertensive effect as compared to female ovine offspring [521]. The studies described in this thesis are unable to measure gender specific effects due to lack of adequate statistical power to address this question. It would have been desirable to have a greater number of animals in each group so that an independent effect of gender of such programming could be analysed.

6.3.6 Technical challenges

Commercial assays for sheep are not readily available owing to infrequent use of the species for experimental research. A wider availability of reliable biomarkers and antibodies would have permitted a wider and more robust examination of the phenotype and underlying mechanisms. For example, TLR4 protein expression, to corroborate the gene expression findings or quantification of plasma cytokines, was attempted but was not reliably reproducible. Similarly, the absence of fully described sheep genome at the time of these experiments limited the number of genes which could be analysed. For example, attempts to design primers for important ER stress response components X-box binding

protein 1(XBP1) and homocysteine-inducible endoplasmic reticulum stress protein1 (HERP1) using cow (Bos Taurus) genome were not successful.

The absence of a standardised criterion for NAFLD definitions in sheep means some aspects of NAFLD could not be fully identified. In addition, the clusters of immune system cells consistent with crown-like structures and milky spots in the omental adipose tissue were non-homogenously distributed which prevented reliable quantification of the distribution. The analysis was, therefore, limited to assessments of the tissue performed by observers blinded to experimental group allocation.

6.4 Future work

The research described in this thesis could be further elucidated by modified study models and advanced analysis of the model described.

6.4.1 Elucidation of metabolic inflammation in obesity, its effects on organism and developmental programming.

As demonstrated, the gene expression of UPR and autophagy was pliable to obesity and to NR-LG in both hepatic and omental adipose tissue. Advance lipidomic analysis of hepatic and adipose tissue in this model could provide valuable information regarding the impact of such modified gene expression on the organ. As more antibodies with reliable action become available, further elucidation of the state of autophagy could also facilitate in defining the role played by autophagy in pathogenesis of metabolic derangements. This would ideally be done by quantification of the protein contents if the components of autophagy.

Glucose tolerance test was performed in the studies to describe the state of insulin resistance. At the tissue level, future work may focus on insulin signalling pathways with a focus on describing the expression of insulin receptors, insulin sensing mechanisms, the state of phosphorylation of insulin receptor and the expression of insulin mediated glucose transporters. Insulin receptor and glucose

transporters have been shown to be amenable to developmental programming [522] and description of the state of tissue insulin sensitivity would help describe the phenotype in more detail.

The international sheep genome consortium [523] is actively working to describe the full genome. Newer technologies, such as, transcriptome analysis [524], followed by gene cluster mapping [525] with focus upon the cell stress response, has the potential of demonstrating a robust confirmation of the results described in the thesis. In absence of a fully described sheep genome, whole transcriptome analysis was performed using SOLiD™ sequencing technique available at the University of Nottingham with *bos taurus* as reference genome on mRNA from a small number of representative animals. However, the results from such modified analysis were not replicated in gene expression of specific genes using polymerase chain reaction when all animals were subsequently analysed. With the availability of the complete sheep genome in the future, and further development of sequencing methodologies and data processing, such an analysis should be revisited.

Epigenetic modification of the gene expression has also been proposed as a potential mechanism of developmental programming [526] and has been the focus of ongoing investigations [527]. However, as the technology matures, the current concerns regarding inconsistencies [528] will need to be addressed before it can be reliably applied for analysis.

The important question of sexual dimorphism in pathogenesis of metabolic syndrome and specifically in metabolic inflammation needs to be addressed using focused models of larger studies of animals [364] designed to identify and

describe such a dimorphism and relate it to endocrine and phenotypic differences in males and females.

6.5 Final remarks

As the first large animal model to demonstrate characteristics of obesity associated metabolic inflammation and the cell stress response in liver and omental adipose tissue, this study provides an important baseline for investigation of programming of these cellular processes. Investigations into mutual interaction of three different programming influences, maternal undernutrition during late gestation, formula feeding and postnatal growth rate identified that the prenatal intervention exacerbated the gene expression of the UPR in the omental adipose tissue and autophagy in liver. Formula feeding and accelerated postnatal growth did not programme the hepatic and adipose tissue cell stress response.

Bibliography

1. Alberti, K.G.M.M., R.H. Eckel, S.M. Grundy, P.Z. Zimmet, J.I. Cleeman, K.A. Donato, J.-C. Fruchart, W.P.T. James, C.M. Loria, and S.C. Smith, *Harmonizing the Metabolic Syndrome: A Joint Interim Statement of the International Diabetes Federation Task Force on Epidemiology and Prevention; National Heart, Lung, and Blood Institute; American Heart Association; World Heart Federation; International Atherosclerosis Society; and International Association for the Study of Obesity*. *Circulation*, 2009. 120(16): p. 1640-1645.
2. Gami, A.S., B.J. Witt, D.E. Howard, P.J. Erwin, L.A. Gami, V.K. Somers, and V.M. Montori, *Metabolic syndrome and risk of incident cardiovascular events and death: a systematic review and meta-analysis of longitudinal studies*. *Journal of the American College of Cardiology*, 2007. 49(4): p. 403-14.
3. Lorenzo, C., K. Williams, K.J. Hunt, and S.M. Haffner, *The National Cholesterol Education Program - Adult Treatment Panel III, International Diabetes Federation, and World Health Organization definitions of the metabolic syndrome as predictors of incident cardiovascular disease and diabetes*. *Diabetes Care*, 2007. 30(1): p. 8-13.
4. Beltran-Sanchez, H., M.O. Harhay, M.M. Harhay, and S. McElligott, *Prevalence and trends of metabolic syndrome in the adult U.S. population, 1999-2010*. *Journal of the American College of Cardiology*, 2013. 62(8): p. 697-703.
5. Grundy, S.M., *Metabolic Syndrome Pandemic*. *Arteriosclerosis, Thrombosis, and Vascular Biology*, 2008. 28(4): p. 629-636.
6. Seidell, J.C., *Obesity, insulin resistance and diabetes — a worldwide epidemic*. *British Journal of Nutrition*, 2000. 83: p. S5-S8.
7. Symonds, M.E., S.P. Sebert, M.A. Hyatt, and H. Budge, *Nutritional programming of the metabolic syndrome*. *Nature Reviews Endocrinology*, 2009. 5(11): p. 604-610.
8. Steinberger, J. and S.R. Daniels, *Obesity, Insulin Resistance, Diabetes, and Cardiovascular Risk in Children: An American Heart Association Scientific Statement From the Atherosclerosis, Hypertension, and Obesity in the Young Committee (Council on Cardiovascular Disease in the Young) and the Diabetes Committee (Council on Nutrition, Physical Activity, and Metabolism)*. *Circulation*, 2003. 107(10): p. 1448-1453.
9. Bonadonna, R.C., L. Groop, N. Kraemer, E. Ferrannini, S. Del Prato, and R.A. DeFronzo, *Obesity and insulin resistance in humans: a dose-response study*. *Metabolism*, 1990. 39(5): p. 452-9.

10. Caprio, S., M. Bronson, R.S. Sherwin, F. Rife, and W.V. Tamborlane, *Co-existence of severe insulin resistance and hyperinsulinaemia in pre-adolescent obese children*. *Diabetologia*, 1996. 39(12): p. 1489-97.
11. Kissebah, A.H. and G.R. Krakower, *Regional adiposity and morbidity*. *Physiological Reviews*, 1994. 74(4): p. 761-811.
12. Su, H.Y., W.H. Sheu, H.M. Chin, C.Y. Jeng, Y.D. Chen, and G.M. Reaven, *Effect of weight loss on blood pressure and insulin resistance in normotensive and hypertensive obese individuals*. *American Journal of Hypertension*, 1995. 8(11): p. 1067-71.
13. Egan, B.M., E.L. Greene, and T.L. Goodfriend, *Insulin resistance and cardiovascular disease*. *American Journal of Hypertension*, 2001. 14(S3): p. 116S-125S.
14. USCB, *United States Census Bureau data available at <http://www.census.gov/ipc/www/popclockworld.html>*. 2010.
15. WHO, *World Health Organisation (WHO) fact sheet Feb 2011*. 2011.
16. Hossain, P., B. Kavar, and M. El Nahas, *Obesity and Diabetes in the Developing World - A Growing Challenge*. *New England Journal of Medicine*, 2007. 356(3): p. 213-215.
17. Ogden, C.L., M.D. Carroll, L.R. Curtin, M.M. Lamb, and K.M. Flegal, *Prevalence of High Body Mass Index in US Children and Adolescents, 2007-2008*. *JAMA: The Journal of the American Medical Association*. 303(3): p. 242-249.
18. Lebovitz, H.E. and M.A. Banerji, *Point: Visceral Adiposity Is Causally Related to Insulin Resistance*. *Diabetes Care*, 2005. 28(9): p. 2322-2325.
19. Nettleton, J.A., L.M. Steffen, H. Ni, K. Liu, and D.R. Jacobs, *Dietary Patterns and Risk of Incident Type 2 Diabetes in the Multi-Ethnic Study of Atherosclerosis (MESA)*. *Diabetes Care*, 2008. 31(9): p. 1777-1782.
20. Mujahid, M.S., A.V.D. Roux, M. Shen, D. Gowda, B. Sánchez, S. Shea, D.R. Jacobs, and S.A. Jackson, *Relation between Neighborhood Environments and Obesity in the Multi-Ethnic Study of Atherosclerosis*. *American Journal of Epidemiology*, 2008. 167(11): p. 1349-1357.
21. Xu, H., G.T. Barnes, Q. Yang, G. Tan, D. Yang, C.J. Chou, J. Sole, A. Nichols, J.S. Ross, L.A. Tartaglia, and H. Chen, *Chronic inflammation in fat plays a crucial role in the development of obesity-related insulin resistance*. *Journal of Clinical Investigation*, 2003. 112(12): p. 1821-1830.
22. Bahtiyar, G., J. Shin, A. Aytaman, J. Sowers, and S. McFarlane, *Association of diabetes and hepatitis C infection: Epidemiologic evidence and pathophysiologic insights*. *Current Diabetes Reports*, 2004. 4(3): p. 194-198.

23. Pao, V., G. Lee, and C. Grunfeld, *HIV therapy, metabolic syndrome, and cardiovascular risk*. Current Atherosclerosis Reports, 2008. 10(1): p. 61-70.
24. Sidiropoulos, P., S. Karvounaris, and D. Boumpas, *Metabolic syndrome in rheumatic diseases: epidemiology, pathophysiology, and clinical implications*. Arthritis Research & Therapy, 2008. 10(3): p. 207.
25. Fulda, S., A.M. Gorman, O. Hori, and A. Samali, *Cellular Stress Responses: Cell Survival and Cell Death*. International Journal of Cell Biology, 2010. 2010.
26. Schroder, M. and R.J. Kaufman, *The mammalian unfolded protein response*. Annual Review of Biochemistry, 2005. 74(1): p. 739-789.
27. Puscheck, E.E., A.O. Awonuga, Y. Yang, Z. Jiang, and D.A. Rappolee, *Molecular biology of the stress response in the early embryo and its stem cells*. Adv Exp Med Biol, 2015. 843: p. 77-128.
28. Bradshaw, R.A. and E.A. Dennis, *Regulation of Organelle and Cell Compartment Signaling: Cell Signaling Collection*. 2011: Elsevier Science.
29. Montague, C.T. and S. O'Rahilly, *The perils of portliness: causes and consequences of visceral adiposity*. Diabetes, 2000. 49(6): p. 883-888.
30. Kern, P.A., S. Ranganathan, C. Li, L. Wood, and G. Ranganathan, *Adipose tissue tumor necrosis factor and interleukin-6 expression in human obesity and insulin resistance*. American Journal of Physiology - Endocrinology And Metabolism, 2001. 280(5): p. E745-E751.
31. Cypess, A.M., S. Lehman, G. Williams, I. Tal, D. Rodman, A.B. Goldfine, F.C. Kuo, E.L. Palmer, Y.H. Tseng, A. Doria, G.M. Kolodny, and C.R. Kahn, *Identification and importance of brown adipose tissue in adult humans*. New England Journal of Medicine, 2009. 360(15): p. 1509-17.
32. Virtanen, K.A., M.E. Lidell, J. Orava, M. Heglind, R. Westergren, T. Niemi, M. Taittonen, J. Laine, N.J. Savisto, S. Enerback, and P. Nuutila, *Functional brown adipose tissue in healthy adults*. New England Journal of Medicine, 2009. 360(15): p. 1518-25.
33. Gregoire, F.M., *Adipocyte differentiation: from fibroblast to endocrine cell*. Experimental biology and medicine, 2001. 226(11): p. 997-1002.
34. Spalding, K.L., E. Arner, P.O. Westermark, S. Bernard, B.A. Buchholz, O. Bergmann, L. Blomqvist, J. Hoffstedt, E. Naslund, T. Britton, H. Concha, M. Hassan, M. Ryden, J. Frisen, and P. Arner, *Dynamics of fat cell turnover in humans*. Nature, 2008. 453(7196): p. 783-7.
35. Skurk, T., C. Alberti-Huber, C. Herder, and H. Hauner, *Relationship between adipocyte size and adipokine expression and secretion*. Journal of clinical endocrinology and metabolism, 2007. 92(3): p. 1023-33.

36. Lionetti, L., M.P. Mollica, A. Lombardi, G. Cavaliere, G. Gifuni, and A. Barletta, *From chronic overnutrition to insulin resistance: The role of fat-storing capacity and inflammation*. Nutrition, Metabolism and Cardiovascular Diseases, 2009. 19(2): p. 146-152.
37. Luft, V.C., M.I. Schmidt, J.S. Pankow, D. Couper, C.M. Ballantyne, J.H. Young, and B.B. Duncan, *Chronic inflammation role in the obesity-diabetes association: a case-cohort study*. Diabetology & Metabolic Syndrome, 2013. 5.
38. Devaraj, S., N. Glaser, S. Griffen, J. Wang-Polagruto, E. Miguelino, and I. Jialal, *Increased Monocytic Activity and Biomarkers of Inflammation in Patients With Type 1 Diabetes*. Diabetes, 2006. 55(3): p. 774-779.
39. Gregor, M.F. and G.S. Hotamisligil, *Inflammatory Mechanisms in Obesity*. Annual Review of Immunology, 2011. 29(1): p. 415-445.
40. Hotamisligil, G.S., N.S. Shargill, and B.M. Spiegelman, *Adipose expression of tumor necrosis factor-alpha: direct role in obesity-linked insulin resistance*. Science, 1993. 259(5091): p. 87-91.
41. Hotamisligil, G.S., P. Arner, J.F. Caro, R.L. Atkinson, and B.M. Spiegelman, *Increased adipose tissue expression of tumor necrosis factor-alpha in human obesity and insulin resistance*. Journal of Clinical Investigation, 1995. 95(5): p. 2409-2415.
42. Uysal, K.T., S.M. Wiesbrock, M.W. Marino, and G.S. Hotamisligil, *Protection from obesity-induced insulin resistance in mice lacking TNF-[alpha] function*. Nature, 1997. 389(6651): p. 610-614.
43. Zhang, Y., R. Proenca, M. Maffei, M. Barone, L. Leopold, and J.M. Friedman, *Positional cloning of the mouse obese gene and its human homologue*. Nature, 1994. 372(6505): p. 425-32.
44. Corica, F., A. Allegra, A. Corsonello, M. Buemi, G. Calapai, A. Ruello, V. Nicita Mauro, and D. Ceruso, *Relationship between plasma leptin levels and the tumor necrosis factor-alpha system in obese subjects*. International journal of obesity and related metabolic disorders, 1999. 23(4): p. 355-60.
45. Ahima, R.S., C.B. Saper, J.S. Flier, and J.K. Elmquist, *Leptin regulation of neuroendocrine systems*. Frontiers in neuroendocrinology, 2000. 21(3): p. 263-307.
46. Farooqi, I.S., G. Matarese, G.M. Lord, J.M. Keogh, E. Lawrence, C. Agwu, V. Sanna, S.A. Jebb, F. Perna, S. Fontana, R.I. Lechler, A.M. DePaoli, and S. O'Rahilly, *Beneficial effects of leptin on obesity, T cell hyporesponsiveness, and neuroendocrine/metabolic dysfunction of human congenital leptin deficiency*. Journal of Clinical Investigation, 2002. 110(8): p. 1093-103.

47. Margetic, S., C. Gazzola, G.G. Pegg, and R.A. Hill, *Leptin: a review of its peripheral actions and interactions*. International journal of obesity and related metabolic disorders, 2002. 26(11): p. 1407-33.
48. Lord, G.M., G. Matarese, J.K. Howard, R.J. Baker, S.R. Bloom, and R.I. Lechler, *Leptin modulates the T-cell immune response and reverses starvation-induced immunosuppression*. Nature, 1998. 394(6696): p. 897-901.
49. La Cava, A. and G. Matarese, *The weight of leptin in immunity*. Nature reviews. Immunology, 2004. 4(5): p. 371-9.
50. Paz-Filho, G., M.L. Wong, and J. Licinio, *Ten years of leptin replacement therapy*. Obesity reviews, 2011. 12(5): p. e315-23.
51. Bjorbaek, C. and B.B. Kahn, *Leptin signaling in the central nervous system and the periphery*. Recent progress in hormone research, 2004. 59: p. 305-31.
52. Qatanani, M. and M.A. Lazar, *Mechanisms of obesity-associated insulin resistance: many choices on the menu*. Genes & Development, 2007. 21(12): p. 1443-1455.
53. Ouchi, N., J.L. Parker, J.J. Lugus, and K. Walsh, *Adipokines in inflammation and metabolic disease*. Nature reviews. Immunology, 2011. 11(2): p. 85-97.
54. Tilg, H. and A.R. Moschen, *Adipocytokines: mediators linking adipose tissue, inflammation and immunity*. Nature reviews. Immunology, 2006. 6(10): p. 772-83.
55. Bjorntorp, P., H. Bergman, and E. Varnauskas, *Plasma free fatty acid turnover rate in obesity*. Acta medica Scandinavica, 1969. 185(4): p. 351-6.
56. Boden, G., *Obesity and free fatty acids*. Endocrinology and metabolism clinics of North America, 2008. 37(3): p. 635-46, viii-ix.
57. Doyle, S.L. and L.A. O'Neill, *Toll-like receptors: from the discovery of NFkappaB to new insights into transcriptional regulations in innate immunity*. Biochemical Pharmacology, 2006. 72(9): p. 1102-13.
58. Shi, H., M.V. Kokoeva, K. Inouye, I. Tzamelis, H. Yin, and J.S. Flier, *TLR4 links innate immunity and fatty acid-induced insulin resistance*. Journal of Clinical Investigation, 2006. 116(11): p. 3015-3025.
59. Tsukumo, D.M.L., M.A. Carvalho-Filho, J.B.C. Carvalheira, P.O. Prada, S.M. Hirabara, A.A. Schenka, E.P. Araújo, J. Vassallo, R. Curi, L.A. Velloso, and M.J.A. Saad, *Loss-of-Function Mutation in Toll-Like Receptor 4 Prevents Diet-Induced Obesity and Insulin Resistance*. Diabetes, 2007. 56(8): p. 1986-1998.

60. Saberi, M., N.-B. Woods, C. de Luca, S. Schenk, J.C. Lu, G. Bandyopadhyay, I.M. Verma, and J.M. Olefsky, *Hematopoietic Cell-Specific Deletion of Toll-like Receptor 4 Ameliorates Hepatic and Adipose Tissue Insulin Resistance in High-Fat-Fed Mice*. *Cell Metabolism*, 2009. 10(5): p. 419-429.
61. Martinon, F., X. Chen, A.H. Lee, and L.H. Glimcher, *TLR activation of the transcription factor XBP1 regulates innate immune responses in macrophages*. *Nature Immunology*, 2010. 11(5): p. 411-8.
62. Williams, B.R., *PKR; a sentinel kinase for cellular stress*. *Oncogene*, 1999. 18(45): p. 6112-20.
63. Nakamura, T., M. Furuhashi, P. Li, H. Cao, G. Tuncman, N. Sonenberg, C.Z. Gorgun, and G.S. Hotamisligil, *Double-Stranded RNA-Dependent Protein Kinase Links Pathogen Sensing with Stress and Metabolic Homeostasis*. *Cell*, 2010. 140(3): p. 338-348.
64. Nakamura, T., A. Arduini, B. Baccaro, M. Furuhashi, and G.S. Hotamisligil, *Small-molecule inhibitors of PKR improve glucose homeostasis in obese diabetic mice*. *Diabetes*, 2014. 63(2): p. 526-534.
65. Weisberg, S.P., D. McCann, M. Desai, M. Rosenbaum, R.L. Leibel, and A.W. Ferrante, *Obesity is associated with macrophage accumulation in adipose tissue*. *Journal of Clinical Investigation*, 2003. 112(12): p. 1796-1808.
66. Cinti, S., G. Mitchell, G. Barbatelli, I. Murano, E. Ceresi, E. Faloia, S. Wang, M. Fortier, A.S. Greenberg, and M.S. Obin, *Adipocyte death defines macrophage localization and function in adipose tissue of obese mice and humans*. *Journal of Lipid Research*, 2005. 46(11): p. 2347-2355.
67. Cencello, R., C. Henegar, N. Viguerie, S. Taleb, C. Poitou, C. Rouault, M. Coupaye, V. Pelloux, D. Hugol, J.-L. Bouillot, A. Bouloumié, G. Barbatelli, S. Cinti, P.-A. Svensson, G.S. Barsh, J.-D. Zucker, A. Basdevant, D. Langin, and K. Clément, *Reduction of Macrophage Infiltration and Chemoattractant Gene Expression Changes in White Adipose Tissue of Morbidly Obese Subjects After Surgery-Induced Weight Loss*. *Diabetes*, 2005. 54(8): p. 2277-2286.
68. Sharkey, D., D.S. Gardner, H.P. Fainberg, S. Sébert, P. Bos, V. Wilson, R. Bell, M.E. Symonds, and H. Budge, *Maternal nutrient restriction during pregnancy differentially alters the unfolded protein response in adipose and renal tissue of obese juvenile offspring*. *FASEB Journal*, 2009. 23(5): p. 1314-1324.
69. Shimotsuma, M., M.W. Simpson-Morgan, T. Takahashi, and A. Hagiwara, *Ontogeny of milky spots in the fetal lamb omentum*. *Archives of Histology and Cytology*, 1994. 57(3): p. 291-9.
70. Mebius, R.E., *Lymphoid organs for peritoneal cavity immune response: milky spots*. *Immunity*, 2009. 30(5): p. 670-2.

71. Rangel-Moreno, J., J.E. Moyron-Quiroz, D.M. Carragher, K. Kusser, L. Hartson, A. Moquin, and T.D. Randall, *Omental milky spots develop in the absence of lymphoid tissue-inducer cells and support B and T cell responses to peritoneal antigens*. *Immunity*, 2009. 30(5): p. 731-43.
72. Cupedo, T., N.K. Crellin, N. Papazian, E.J. Rombouts, K. Weijer, J.L. Grogan, W.E. Fibbe, J.J. Cornelissen, and H. Spits, *Human fetal lymphoid tissue-inducer cells are interleukin 17-producing precursors to RORC+ CD127+ natural killer-like cells*. *Nature Immunology*, 2009. 10(1): p. 66-74.
73. Mantovani, A., A. Sica, S. Sozzani, P. Allavena, A. Vecchi, and M. Locati, *The chemokine system in diverse forms of macrophage activation and polarization*. *Trends in Immunology*, 2004. 25(12): p. 677-686.
74. Zeyda, M., D. Farmer, J. Todoric, O. Aszmann, M. Speiser, G. Gyori, G.J. Zlabinger, and T.M. Stulnig, *Human adipose tissue macrophages are of an anti-inflammatory phenotype but capable of excessive pro-inflammatory mediator production*. *International Journal of Obesity*, 2007. 31(9): p. 1420-1428.
75. Aron-Wisnewsky, J., J. Tordjman, C. Poitou, F. Darakhshan, D. Hugol, A. Basdevant, A. Aissat, M.I. Guerre-Millo, and K. Cl  ment, *Human Adipose Tissue Macrophages: M1 and M2 Cell Surface Markers in Subcutaneous and Omental Depots and after Weight Loss*. *Journal of Clinical Endocrinology & Metabolism*, 2009. 94(11): p. 4619-4623.
76. Lee, M.-J. and S.K. Fried, *Integration of hormonal and nutrient signals that regulate leptin synthesis and secretion*. *American Journal of Physiology - Endocrinology and Metabolism*, 2009. 296(6): p. E1230-E1238.
77. Bruun, J.M., A.S. Lihn, A.K. Madan, S.B. Pedersen, K.M. Schiott, J.N. Fain, and B. Richelsen, *Higher production of IL-8 in visceral vs. subcutaneous adipose tissue. Implication of nonadipose cells in adipose tissue*. *American Journal of Physiology - Endocrinology and Metabolism*, 2004. 286(1): p. E8-13.
78. Fried, S.K., D.A. Bunkin, and A.S. Greenberg, *Omental and subcutaneous adipose tissues of obese subjects release interleukin-6: depot difference and regulation by glucocorticoid*. *Journal of clinical endocrinology and metabolism*, 1998. 83(3): p. 847-50.
79. Lundgren, M., J. Bur  n, T. Ruge, T. Myrn  s, and J.W. Eriksson, *Glucocorticoids Down-Regulate Glucose Uptake Capacity and Insulin-Signaling Proteins in Omental But Not Subcutaneous Human Adipocytes*. *Journal of clinical endocrinology and metabolism*, 2004. 89(6): p. 2989-2997.
80. Lee, M.J., P. Pramyothin, K. Karastergiou, and S.K. Fried, *Deconstructing the roles of glucocorticoids in adipose tissue biology and the development of central obesity*. *Biochimica et Biophysica Acta (BBA) - Molecular and Cell Biology of Lipids*, 2014. 1842(3): p. 473-81.

81. Rask, E., B.R. Walker, S. Soderberg, D.E. Livingstone, M. Eliasson, O. Johnson, R. Andrew, and T. Olsson, *Tissue-specific changes in peripheral cortisol metabolism in obese women: increased adipose 11 β -hydroxysteroid dehydrogenase type 1 activity*. J Clin Endocrinol Metab, 2002. 87(7): p. 3330-6.
82. Rask, E., T. Olsson, S. Soderberg, R. Andrew, D.E. Livingstone, O. Johnson, and B.R. Walker, *Tissue-specific dysregulation of cortisol metabolism in human obesity*. J Clin Endocrinol Metab, 2001. 86(3): p. 1418-21.
83. Patsouris, D., J.G. Neels, W. Fan, P.P. Li, M.T. Nguyen, and J.M. Olefsky, *Glucocorticoids and thiazolidinediones interfere with adipocyte-mediated macrophage chemotaxis and recruitment*. Journal of Biological Chemistry, 2009. 284(45): p. 31223-35.
84. Webster, J.C., R.H. Oakley, C.M. Jewell, and J.A. Cidlowski, *Proinflammatory cytokines regulate human glucocorticoid receptor gene expression and lead to the accumulation of the dominant negative beta isoform: a mechanism for the generation of glucocorticoid resistance*. Proceedings of the National Academy of Sciences, 2001. 98(12): p. 6865-70.
85. Brogan, I.J., I.A. Murray, G. Cerillo, M. Needham, A. White, and J.R.E. Davis, *Interaction of glucocorticoid receptor isoforms with transcription factors AP-1 and NF- κ B: lack of effect of glucocorticoid receptor β* . Molecular and Cellular Endocrinology, 1999. 157(1-2): p. 95-104.
86. Dobson, C.M., A. Šali, and M. Karplus, *Protein Folding: A Perspective from Theory and Experiment*. Angewandte Chemie International Edition, 1998. 37(7): p. 868-893.
87. Yoshida, H., T. Matsui, N. Hosokawa, R.J. Kaufman, K. Nagata, and K. Mori, *A Time-Dependent Phase Shift in the Mammalian Unfolded Protein Response*. Developmental Cell, 2003. 4(2): p. 265-271.
88. Gething, M.J., *Role and regulation of the ER chaperone BiP*. Semin Cell Dev Biol, 1999. 10(5): p. 465-72.
89. Sousa, M.C., M.A. Ferrero-Garcia, and A.J. Parodi, *Recognition of the oligosaccharide and protein moieties of glycoproteins by the UDP-Glc:glycoprotein glucosyltransferase*. Biochemistry, 1992. 31(1): p. 97-105.
90. Han, J., S.H. Back, J. Hur, Y.H. Lin, R. Gildersleeve, J. Shan, C.L. Yuan, D. Krokowski, S. Wang, M. Hatzoglou, M.S. Kilberg, M.A. Sartor, and R.J. Kaufman, *ER-stress-induced transcriptional regulation increases protein synthesis leading to cell death*. Nature Cell Biology, 2013. 15(5): p. 481-90.
91. Zha, B.S. and H. Zhou, *ER stress and lipid metabolism in adipocytes*. Biochemistry Research International, 2012.

92. Qin, L., Z. Wang, L. Tao, and Y. Wang, *ER stress negatively regulates AKT/TSC/mTOR pathway to enhance autophagy*. *Autophagy*, 2010. 6(2): p. 239-47.
93. Calfon, M., H. Zeng, F. Urano, J.H. Till, S.R. Hubbard, H.P. Harding, S.G. Clark, and D. Ron, *IRE1 couples endoplasmic reticulum load to secretory capacity by processing the XBP-1 mRNA*. *Nature*, 2002. 415(6867): p. 92-6.
94. Hai, T.W., F. Liu, W.J. Coukos, and M.R. Green, *Transcription factor ATF cDNA clones: an extensive family of leucine zipper proteins able to selectively form DNA-binding heterodimers*. *Genes & Development*, 1989. 3(12B): p. 2083-90.
95. B'Chir, W., A.C. Maurin, V. Carraro, J. Averous, C. Jousse, Y. Muranishi, L. Parry, G. Stepien, P. Fafournoux, and A. Bruhat, *The eIF2 α /ATF4 pathway is essential for stress-induced autophagy gene expression*. *Nucleic acids research*, 2013. 41(16): p. 7683-7699.
96. Du, K., S. Herzig, R.N. Kulkarni, and M. Montminy, *TRB3: a tribbles homolog that inhibits Akt/PKB activation by insulin in liver*. *Science*, 2003. 300(5625): p. 1574-7.
97. Ohoka, N., S. Yoshii, T. Hattori, K. Onozaki, and H. Hayashi, *TRB3, a novel ER stress-inducible gene, is induced via ATF4-CHOP pathway and is involved in cell death*. *The EMBO journal*, 2005. 24(6): p. 1243-55.
98. Oyadomari, S., H.P. Harding, Y. Zhang, M. Oyadomari, and D. Ron, *Dephosphorylation of translation initiation factor 2 α enhances glucose tolerance and attenuates hepatosteatosis in mice*. *Cell metabolism*, 2008. 7(6): p. 520-32.
99. Ozcan, U., Q. Cao, E. Yilmaz, A.H. Lee, N.N. Iwakoshi, E. Ozdelen, G. Tuncman, C. Gorgun, L.H. Glimcher, and G.S. Hotamisligil, *Endoplasmic reticulum stress links obesity, insulin action, and type 2 diabetes*. *Science*, 2004. 306(5695): p. 457-461.
100. Nakatani, Y., H. Kaneto, D. Kawamori, K. Yoshiuchi, M. Hatazaki, T.A. Matsuoka, K. Ozawa, S. Ogawa, M. Hori, Y. Yamasaki, and M. Matsuhisa, *Involvement of endoplasmic reticulum stress in insulin resistance and diabetes*. *Journal of Biological Chemistry*, 2005. 280(1): p. 847-851.
101. Kammoun, H.L., H. Chabanon, I. Hainault, S. Luquet, C. Magnan, T. Koike, P. Ferré, and F. Foufelle, *GRP78 expression inhibits insulin and ER stress-induced SREBP-1c activation and reduces hepatic steatosis in mice*. *Journal of Clinical Investigation*, 2009. 119(5): p. 1201-1215.
102. Latreille, M., M.-K. Laberge, G. Bourret, L. Yamani, and L. Larose, *Deletion of Nck1 attenuates hepatic ER stress signaling and improves glucose tolerance and insulin signaling in liver of obese mice*. *American Journal of Physiology - Endocrinology And Metabolism*, 2011. 300(3): p. E423-E434.

103. Boden, G. and S. Merali, *Measurement of the increase in endoplasmic reticulum stress-related proteins and genes in adipose tissue of obese, insulin-resistant individuals*. Methods in Enzymology, 2011. 489: p. 67-82.
104. Alhusaini, S., K. McGee, B. Schisano, A. Harte, P. McTernan, S. Kumar, and G. Tripathi, *Lipopolysaccharide, high glucose and saturated fatty acids induce endoplasmic reticulum stress in cultured primary human adipocytes: Salicylate alleviates this stress*. Biochemical and Biophysical Research Communications, 2010. 397(3): p. 472-8.
105. Gregor, M.F., L. Yang, E. Fabbrini, B.S. Mohammed, J.C. Eagon, G.S. Hotamisligil, and S. Klein, *Endoplasmic reticulum stress is reduced in tissues of obese subjects after weight loss*. Diabetes, 2009. 58(3): p. 693-700.
106. Nunez, C.E., V.S. Rodrigues, F.S. Gomes, R.F. Moura, S.C. Victorio, B. Bombassaro, E.A. Chaim, J.C. Pareja, B. Geloneze, L.A. Velloso, and E.P. Araujo, *Defective regulation of adipose tissue autophagy in obesity*. International Journal of Obesity, 2013. 37(11): p. 1473-80.
107. Maixner, N., J. Kovsky, I. Harman-Boehm, M. Blüher, N. Bashan, and A. Rudich, *Autophagy in adipose tissue*. Obesity Facts, 2012. 5(5): p. 710-721.
108. Malhi, H. and R.J. Kaufman, *Endoplasmic reticulum stress in liver disease*. Journal of hepatology, 2011. 54(4): p. 795-809.
109. Strissel, K.J., Z. Stancheva, H. Miyoshi, J.W. Perfield, J. DeFuria, Z. Jick, A.S. Greenberg, and M.S. Obin, *Adipocyte Death, Adipose Tissue Remodeling, and Obesity Complications*. Diabetes, 2007. 56(12): p. 2910-2918.
110. Kroemer, G., L. Galluzzi, P. Vandenabeele, J. Abrams, E.S. Alnemri, E.H. Baehrecke, M.V. Blagosklonny, W.S. El-Deiry, P. Golstein, D.R. Green, M. Hengartner, R.A. Knight, S. Kumar, S.A. Lipton, W. Malorni, G. Nunez, M.E. Peter, J. Tschopp, J. Yuan, M. Piacentini, B. Zhivotovsky, and G. Melino, *Classification of cell death: recommendations of the Nomenclature Committee on Cell Death 2009*. Cell Death and Differentiation, 2009. 16(1): p. 3-11.
111. Gozuacik, D. and A. Kimchi, *Autophagy and Cell Death*. 2007. p. 217-245.
112. Cnop, M., F. Foufelle, and L.A. Velloso, *Endoplasmic reticulum stress, obesity and diabetes*. Trends in Molecular Medicine, 2012. 18(1): p. 59-68.
113. Lavallard, V.J., A.J. Meijer, P. Codogno, and P. Gual, *Autophagy, signaling and obesity*. Pharmacological research, 2012. 66(6): p. 513-25.
114. Ohsumi, Y., *Molecular dissection of autophagy: two ubiquitin-like systems*. Nature Reviews Molecular Cell Biology, 2001. 2(3): p. 211-6.

115. Wullschlegel, S., R. Loewith, and M.N. Hall, *TOR signaling in growth and metabolism*. Cell, 2006. 124(3): p. 471-84.
116. Inoki, K., Y. Li, T. Xu, and K.L. Guan, *Rheb GTPase is a direct target of TSC2 GAP activity and regulates mTOR signaling*. Genes & Development, 2003. 17(15): p. 1829-34.
117. Arico, S., A. Petiot, C. Bauvy, P.F. Dubbelhuis, A.J. Meijer, P. Codogno, and E. Ogier-Denis, *The Tumor Suppressor PTEN Positively Regulates Macroautophagy by Inhibiting the Phosphatidylinositol 3-Kinase/Protein Kinase B Pathway*. Journal of Biological Chemistry, 2001. 276(38): p. 35243-35246.
118. Kouroku, Y., E. Fujita, I. Tanida, T. Ueno, A. Isoai, H. Kumagai, S. Ogawa, R.J. Kaufman, E. Kominami, and T. Momoi, *ER stress (PERK/eIF2alpha phosphorylation) mediates the polyglutamine-induced LC3 conversion, an essential step for autophagy formation*. Cell Death and Differentiation, 2007. 14(2): p. 230-9.
119. Corradetti, M.N., K. Inoki, N. Bardeesy, R.A. DePinho, and K.-L. Guan, *Regulation of the TSC pathway by LKB1: evidence of a molecular link between tuberous sclerosis complex and Peutz-Jeghers syndrome*. Genes & Development, 2004. 18(13): p. 1533-1538.
120. Gwinn, D.M., D.B. Shackelford, D.F. Egan, M.M. Mihaylova, A. Mery, D.S. Vasquez, B.E. Turk, and R.J. Shaw, *AMPK Phosphorylation of Raptor Mediates a Metabolic Checkpoint*. Molecular Cell, 2008. 30(2): p. 214-226.
121. Egan, D.F., D.B. Shackelford, M.M. Mihaylova, S. Gelino, R.A. Kohnz, W. Mair, D.S. Vasquez, A. Joshi, D.M. Gwinn, R. Taylor, J.M. Asara, J. Fitzpatrick, A. Dillin, B. Viollet, M. Kundu, M. Hansen, and R.J. Shaw, *Phosphorylation of ULK1 (hATG1) by AMP-Activated Protein Kinase Connects Energy Sensing to Mitophagy*. Science, 2011. 331(6016): p. 456-461.
122. Kim, J., M. Kundu, B. Viollet, and K.-L. Guan, *AMPK and mTOR regulate autophagy through direct phosphorylation of Ulk1*. Nature Cell Biology, 2011. 13(2): p. 132-141.
123. Cohen, H.Y., C. Miller, K.J. Bitterman, N.R. Wall, B. Hekking, B. Kessler, K.T. Howitz, M. Gorospe, R. de Cabo, and D.A. Sinclair, *Calorie restriction promotes mammalian cell survival by inducing the SIRT1 deacetylase*. Science, 2004. 305(5682): p. 390-392.
124. Lee, I.H., L. Cao, R. Mostoslavsky, D.B. Lombard, J. Liu, N.E. Bruns, M. Tsokos, F.W. Alt, and T. Finkel, *A role for the NAD-dependent deacetylase Sirt1 in the regulation of autophagy*. Proceedings of the National Academy of Sciences, 2008. 105(9): p. 3374-3379.
125. Kume, S., T. Uzu, K. Horiike, M. Chin-Kanasaki, K. Isshiki, S.-i. Araki, T. Sugimoto, M. Haneda, A. Kashiwagi, and D. Koya, *Calorie restriction enhances cell adaptation to hypoxia through Sirt1-dependent*

- mitochondrial autophagy in mouse aged kidney*. Journal of Clinical Investigation, 2010. 120(4): p. 1043-1055.
126. Mammucari, C., G. Milan, V. Romanello, E. Masiero, R. Rudolf, P. Del Piccolo, S.J. Burden, R. Di Lisi, C. Sandri, J. Zhao, A.L. Goldberg, S. Schiaffino, and M. Sandri, *FoxO3 Controls Autophagy in Skeletal Muscle In Vivo*. Cell Metabolism, 2007. 6(6): p. 458-471.
 127. Christian, P., J. Sacco, and K. Adeli, *Autophagy: Emerging roles in lipid homeostasis and metabolic control*. Biochimica et Biophysica Acta (BBA) - Molecular and Cell Biology of Lipids, 2013. 1831(4): p. 819-824.
 128. Kovsan, J., N. Bashan, A.S. Greenberg, and A. Rudich, *Potential role of autophagy in modulation of lipid metabolism*. American Journal of Physiology - Endocrinology And Metabolism, 2010. 298(1): p. E1-E7.
 129. Shibata, M., K. Yoshimura, N. Furuya, M. Koike, T. Ueno, M. Komatsu, H. Arai, K. Tanaka, E. Kominami, and Y. Uchiyama, *The MAP1-LC3 conjugation system is involved in lipid droplet formation*. Biochemical and Biophysical Research Communications, 2009. 382(2): p. 419-423.
 130. Singh, R., S. Kaushik, Y. Wang, Y. Xiang, I. Novak, M. Komatsu, K. Tanaka, A.M. Cuervo, and M.J. Czaja, *Autophagy regulates lipid metabolism*. Nature, 2009. 458(7242): p. 1131-5.
 131. Singh, R., Y. Xiang, Y. Wang, K. Baikati, A.M. Cuervo, Y.K. Luu, Y. Tang, J.E. Pessin, G.J. Schwartz, and M.J. Czaja, *Autophagy regulates adipose mass and differentiation in mice*. Journal of Clinical Investigation, 2009. 119(11): p. 3329-39.
 132. Zhang, Y., S. Goldman, R. Baerga, Y. Zhao, M. Komatsu, and S. Jin, *Adipose-specific deletion of autophagy-related gene 7 (atg7) in mice reveals a role in adipogenesis*. Proceedings of the National Academy of Sciences, 2009. 106(47): p. 19860-19865.
 133. Baerga, R., Y. Zhang, P.H. Chen, S. Goldman, and S. Jin, *Targeted deletion of autophagy-related 5 (atg5) impairs adipogenesis in a cellular model and in mice*. Autophagy, 2009. 5(8): p. 1118-30.
 134. Kovsan, J., M. Blüher, T. Tarnovskii, N. Klöting, B. Kirshtein, L. Madar, I. Shai, R. Golan, I. Harman-Boehm, M.R. Schön, A.S. Greenberg, Z. Elazar, N. Bashan, and A. Rudich, *Altered Autophagy in Human Adipose Tissues in Obesity*. Journal of clinical endocrinology and metabolism, 2011. 96(2): p. E268-E277.
 135. Ost, A., K. Svensson, I. Ruishalme, C. Brannmark, N. Franck, H. Krook, P. Sandstrom, P. Kjolhede, and P. Stralfors, *Attenuated mTOR signaling and enhanced autophagy in adipocytes from obese patients with type 2 diabetes*. Molecular Medicine, 2010. 16(7-8): p. 235-46.
 136. Rodrigues, A.L., É.P.G. De Souza, S.V. Da Silva, D.S.B. Rodrigues, A.B. Nascimento, C. Barja-Fidalgo, and M.S. De Freitas, *Low expression of*

- insulin signaling molecules impairs glucose uptake in adipocytes after early overnutrition.* Journal of Endocrinology, 2007. 195(3): p. 485-494.
137. Rodríguez, A., J. Gómez-Ambrosi, V. Catalán, F. Rotellar, V. Valentí, C. Silva, C. Mugueta, M.R. Pulido, R. Vázquez, J. Salvador, M.M. Malagón, I. Colina, and G. Frühbeck, *The ghrelin O-Acyltransferase-Ghrelin system reduces TNF- α -Induced apoptosis and autophagy in human visceral adipocytes.* Diabetologia, 2012. 55(11): p. 3038-3050.
 138. Yoshizaki, T., C. Kusunoki, M. Kondo, M. Yasuda, S. Kume, K. Morino, O. Sekine, S. Ugi, T. Uzu, Y. Nishio, A. Kashiwagi, and H. Maegawa, *Autophagy regulates inflammation in adipocytes.* Biochemical and Biophysical Research Communications, 2012. 417(1): p. 352-357.
 139. Kerr J, W.A., Currie A, *Apoptosis: a basic biological phenomenon with wide-ranging implications in tissue kinetics.* British journal of cancer, 1972. 26(4): p. 239-57.
 140. Fribley, A., K. Zhang, and R.J. Kaufman, *Regulation of apoptosis by the unfolded protein response.* Methods in molecular biology, 2009. 559: p. 191-204.
 141. Elmore, S., *Apoptosis: a review of programmed cell death.* Toxicologic pathology, 2007. 35(4): p. 495-516.
 142. Li, J., B. Lee, and A.S. Lee, *Endoplasmic Reticulum Stress-induced Apoptosis: multiple pathways and activation of p-53 upregulated modulator of Apoptosis (PUMA) and NOXA by p53.* Journal of Biological Chemistry, 2006. 281(11): p. 7260-7270.
 143. Nikolettou, V., M. Markaki, K. Palikaras, and N. Tavernarakis, *Crosstalk between apoptosis, necrosis and autophagy.* Biochimica et Biophysica Acta (BBA) - Molecular and Cell Biology of Lipids, 2013. 1833(12): p. 3448-59.
 144. Sun, K., C.M. Kusminski, and P.E. Scherer, *Adipose tissue remodeling and obesity.* Journal of Clinical Investigation, 2011. 121(6): p. 2094-101.
 145. Schattenberg, J.M. and M. Schuchmann, *Diabetes and apoptosis: liver.* Apoptosis, 2009. 14(12): p. 1459-71.
 146. Alkhouri, N., C. Carter-Kent, and A.E. Feldstein, *Apoptosis in nonalcoholic fatty liver disease: diagnostic and therapeutic implications.* Expert Review of Gastroenterology and Hepatology, 2011. 5(2): p. 201-12.
 147. Adams, J.M. and S. Cory, *The Bcl-2 apoptotic switch in cancer development and therapy.* Oncogene, 2007. 26(9): p. 1324-1337.
 148. Zinszner, H., M. Kuroda, X. Wang, N. Batchvarova, R.T. Lightfoot, H. Remotti, J.L. Stevens, and D. Ron, *CHOP is implicated in programmed cell death in response to impaired function of the endoplasmic reticulum.* Genes & Development, 1998. 12(7): p. 982-95.

149. Sabapathy, K., Y. Hu, T. Kallunki, M. Schreiber, J.P. David, W. Jochum, E.F. Wagner, and M. Karin, *JNK2 is required for efficient T-cell activation and apoptosis but not for normal lymphocyte development*. Current biology, 1999. 9(3): p. 116-25.
150. Zou, T., J.N. Rao, X. Guo, L. Liu, H.M. Zhang, E.D. Strauch, B.L. Bass, and J.-Y. Wang, *NF- κ B-mediated IAP expression induces resistance of intestinal epithelial cells to apoptosis after polyamine depletion*. American Journal of Physiology - Cell Physiology, 2004. 286(5): p. C1009-C1018.
151. Berenbom, M., P.I. Chang, H.E. Betz, and R.E. Stowell, *Chemical and Enzymatic Changes Associated with Mouse Liver Necrosis in Vitro*. Cancer Research, 1955. 15(1): p. 1-5.
152. Hitomi, J., D.E. Christofferson, A. Ng, J. Yao, A. Degterev, R.J. Xavier, and J. Yuan, *Identification of a Molecular Signaling Network that Regulates a Cellular Necrotic Cell Death Pathway*. Cell, 2008. 135(7): p. 1311-1323.
153. Ye, J., *Emerging role of adipose tissue hypoxia in obesity and insulin resistance*. International Journal of Obesity, 2009. 33(1): p. 54-66.
154. Liu, Z.G., H. Hsu, D.V. Goeddel, and M. Karin, *Dissection of TNF receptor 1 effector functions: JNK activation is not linked to apoptosis while NF- κ B activation prevents cell death*. Cell, 1996. 87(3): p. 565-76.
155. Zhang, K. and R.J. Kaufman, *From endoplasmic-reticulum stress to the inflammatory response*. Nature, 2008. 454(7203): p. 455-62.
156. Aguirre, V., T. Uchida, L. Yenush, R. Davis, and M.F. White, *The c-Jun NH(2)-terminal kinase promotes insulin resistance during association with insulin receptor substrate-1 and phosphorylation of Ser(307)*. Journal of biological chemistry, 2000. 275(12): p. 9047-54.
157. Hirosumi, J., G. Tuncman, L. Chang, C.Z. Gorgun, K.T. Uysal, K. Maeda, M. Karin, and G.S. Hotamisligil, *A central role for JNK in obesity and insulin resistance*. Nature, 2002. 420(6913): p. 333-336.
158. Sabio, G., M. Das, A. Mora, Z. Zhang, J.Y. Jun, H.J. Ko, T. Barrett, J.K. Kim, and R.J. Davis, *A Stress Signaling Pathway in Adipose Tissue Regulates Hepatic Insulin Resistance*. Science, 2008. 322(5907): p. 1539-1543.
159. Solinas, G., C. Vilcu, J.G. Neels, G.K. Bandyopadhyay, J.-L. Luo, W. Naugler, S. Grivennikov, A. Wynshaw-Boris, M. Scadeng, J.M. Olefsky, and M. Karin, *JNK1 in Hematopoietically Derived Cells Contributes to Diet-Induced Inflammation and Insulin Resistance without Affecting Obesity*. Cell Metabolism, 2007. 6(5): p. 386-397.
160. Yuan, M., N. Konstantopoulos, J. Lee, L. Hansen, Z.-W. Li, M. Karin, and S.E. Shoelson, *Reversal of Obesity- and Diet-Induced Insulin Resistance with Salicylates or Targeted Disruption of Ikk β* . Science, 2001. 293(5535): p. 1673-1677.

161. Gao, Z., D. Hwang, F. Bataille, M. Lefevre, D. York, M.J. Quon, and J. Ye, *Serine phosphorylation of insulin receptor substrate 1 by inhibitor kappa B kinase complex*. Journal of Biological Chemistry, 2002. 277(50): p. 48115-21.
162. Herschkovitz, A., Y.F. Liu, E. Ilan, D. Ronen, S. Boura-Halfon, and Y. Zick, *Common inhibitory serine sites phosphorylated by IRS-1 kinases, triggered by insulin and inducers of insulin resistance*. Journal of biological chemistry, 2007. 282(25): p. 18018-27.
163. Cai, D., M. Yuan, D.F. Frantz, P.A. Melendez, L. Hansen, J. Lee, and S.E. Shoelson, *Local and systemic insulin resistance resulting from hepatic activation of IKK-[beta] and NF-[kappa]B*. Nature Medicine, 2005. 11(2): p. 183-190.
164. Arkan, M.C., A.L. Hevener, F.R. Greten, S. Maeda, Z.-W. Li, J.M. Long, A. Wynshaw-Boris, G. Poli, J. Olefsky, and M. Karin, *IKK-[beta] links inflammation to obesity-induced insulin resistance*. Nature Medicine, 2005. 11(2): p. 191-198.
165. Wajant, H., K. Pfizenmaier, and P. Scheurich, *Non-apoptotic Fas signaling*. Cytokine Growth Factor Rev, 2003. 14(1): p. 53-66.
166. Fischer-Posovszky, P., H. Tornqvist, K.M. Debatin, and M. Wabitsch, *Inhibition of death-receptor mediated apoptosis in human adipocytes by the insulin-like growth factor I (IGF-I)/IGF-I receptor autocrine circuit*. Endocrinology, 2004. 145(4): p. 1849-59.
167. Guicciardi, M.E. and G.J. Gores, *FasL and Fas in Liver Homeostasis and Hepatic Injuries*, in *Fas Signaling*. 2006, Springer US: Boston, MA. p. 103-117.
168. Chan, H., D.P. Bartos, and L.B. Owen-Schaub, *Activation-dependent transcriptional regulation of the human Fas promoter requires NF-kappaB p50-p65 recruitment*. Mol Cell Biol, 1999. 19(3): p. 2098-108.
169. Bluher, M., N. Kloting, S. Wueest, E.J. Schoenle, M.R. Schon, A. Dietrich, M. Fasshauer, M. Stumvoll, and D. Konrad, *Fas and FasL expression in human adipose tissue is related to obesity, insulin resistance, and type 2 diabetes*. J Clin Endocrinol Metab, 2014. 99(1): p. E36-44.
170. Wueest, S., R.A. Rapold, D.M. Schumann, J.M. Rytka, A. Schildknecht, O. Nov, A.V. Chervonsky, A. Rudich, E.J. Schoenle, M.Y. Donath, and D. Konrad, *Deletion of Fas in adipocytes relieves adipose tissue inflammation and hepatic manifestations of obesity in mice*. The Journal of Clinical Investigation, 2010. 120(1): p. 191-202.
171. Malhi, H., F.J. Barreiro, H. Isomoto, S.F. Bronk, and G.J. Gores, *Free fatty acids sensitise hepatocytes to TRAIL mediated cytotoxicity*. Gut, 2007. 56(8): p. 1124-1131.

172. Cave, M., I. Deaciuc, C. Mendez, Z. Song, S. Joshi-Barve, S. Barve, and C. McClain, *Nonalcoholic fatty liver disease: predisposing factors and the role of nutrition*. Journal of Nutritional Biochemistry, 2007. 18(3): p. 184-195.
173. Kotronen, A., J. Westerbacka, R. Bergholm, K.H. Pietilainen, and H. Yki-Jarvinen, *Liver fat in the metabolic syndrome*. Journal of clinical endocrinology and metabolism, 2007. 92(9): p. 3490-7.
174. Ludwig, J., T.R. Viggiano, D.B. McGill, and B.J. Oh, *Nonalcoholic steatohepatitis: Mayo Clinic experiences with a hitherto unnamed disease*. Mayo Clinic Proceedings, 1980. 55(7): p. 434-8.
175. Bellentani, S., F. Scaglioni, M. Marino, and G. Bedogni, *Epidemiology of non-alcoholic fatty liver disease*. Digestive diseases, 2010. 28(1): p. 155-161.
176. Browning, J.D., L.S. Szczepaniak, R. Dobbins, P. Nuremberg, J.D. Horton, J.C. Cohen, S.M. Grundy, and H.H. Hobbs, *Prevalence of hepatic steatosis in an urban population in the United States: Impact of ethnicity*. Hepatology, 2004. 40(6): p. 1387-1395.
177. Bedogni, G., L. Miglioli, F. Masutti, C. Tiribelli, G. Marchesini, and S. Bellentani, *Prevalence of and risk factors for nonalcoholic fatty liver disease: the Dionysos nutrition and liver study*. Hepatology, 2005. 42(1): p. 44-52.
178. Farrell, G.C., D. van Rooyen, L. Gan, and S. Chitturi, *NASH is an Inflammatory Disorder: Pathogenic, Prognostic and Therapeutic Implications*. Gut Liver, 2012. 6(2): p. 149-71.
179. Musso, G., R. Gambino, S. Bo, B. Uberti, G. Biroli, G. Pagano, and M. Cassader, *Should Nonalcoholic Fatty Liver Disease Be Included in the Definition of Metabolic Syndrome?: A cross-sectional comparison with Adult Treatment Panel III criteria in nonobese nondiabetic subjects*. Diabetes Care, 2008. 31(3): p. 562-568.
180. Kotronen, A. and H. Yki-Järvinen, *Fatty Liver: A Novel Component of the Metabolic Syndrome*. Arteriosclerosis, Thrombosis, and Vascular Biology, 2008. 28(1): p. 27-38.
181. Donnelly, K.L., C.I. Smith, S.J. Schwarzenberg, J. Jessurun, M.D. Boldt, and E.J. Parks, *Sources of fatty acids stored in liver and secreted via lipoproteins in patients with nonalcoholic fatty liver disease*. Journal of Clinical Investigation, 2005. 115(5): p. 1343-51.
182. Owen, J.L., Y. Zhang, S.H. Bae, M.S. Farooqi, G. Liang, R.E. Hammer, J.L. Goldstein, and M.S. Brown, *Insulin stimulation of SREBP-1c processing in transgenic rat hepatocytes requires p70 S6-kinase*. Proceedings of the National Academy of Sciences, 2012. 109(40): p. 16184-9.
183. Shimano, H., J.D. Horton, I. Shimomura, R.E. Hammer, M.S. Brown, and J.L. Goldstein, *Isoform 1c of sterol regulatory element binding protein is*

- less active than isoform 1a in livers of transgenic mice and in cultured cells.* Journal of Clinical Investigation, 1997. 99(5): p. 846-54.
184. Yahagi, N., H. Shimano, A.H. Hasty, T. Matsuzaka, T. Ide, T. Yoshikawa, M. Amemiya-Kudo, S. Tomita, H. Okazaki, Y. Tamura, Y. Iizuka, K. Ohashi, J. Osuga, K. Harada, T. Gotoda, R. Nagai, S. Ishibashi, and N. Yamada, *Absence of sterol regulatory element-binding protein-1 (SREBP-1) ameliorates fatty livers but not obesity or insulin resistance in Lep(ob)/Lep(ob) mice.* Journal of biological chemistry, 2002. 277(22): p. 19353-7.
 185. Uyeda, K. and J.J. Repa, *Carbohydrate response element binding protein, ChREBP, a transcription factor coupling hepatic glucose utilization and lipid synthesis.* Cell metabolism, 2006. 4(2): p. 107-10.
 186. Iizuka, K., R.K. Bruick, G. Liang, J.D. Horton, and K. Uyeda, *Deficiency of carbohydrate response element-binding protein (ChREBP) reduces lipogenesis as well as glycolysis.* Proceedings of the National Academy of Sciences, 2004. 101(19): p. 7281-6.
 187. Shimano, H., *SREBPs: physiology and pathophysiology of the SREBP family.* FEBS journal, 2009. 276(3): p. 616-21.
 188. Petersen, K.F., E.A. Oral, S. Dufour, D. Befroy, C. Ariyan, C. Yu, G.W. Cline, A.M. DePaoli, S.I. Taylor, P. Gorden, and G.I. Shulman, *Leptin reverses insulin resistance and hepatic steatosis in patients with severe lipodystrophy.* Journal of Clinical Investigation, 2002. 109(10): p. 1345-50.
 189. Vigano, A., G.V. Zuccotti, C. Cerini, S. Stucchi, M. Puzzovio, V. Giacomet, and S. Mora, *Lipodystrophy, insulin resistance, and adiponectin concentration in HIV-infected children and adolescents.* Current HIV research, 2011. 9(5): p. 321-6.
 190. Puri, P., R.A. Baillie, M.M. Wiest, F. Mirshahi, J. Choudhury, O. Cheung, C. Sargeant, M.J. Contos, and A.J. Sanyal, *A lipidomic analysis of nonalcoholic fatty liver disease.* Hepatology, 2007. 46(4): p. 1081-90.
 191. Kumashiro, N., D.M. Erion, D. Zhang, M. Kahn, S.A. Beddow, X. Chu, C.D. Still, G.S. Gerhard, X. Han, J. Dziura, K.F. Petersen, V.T. Samuel, and G.I. Shulman, *Cellular mechanism of insulin resistance in nonalcoholic fatty liver disease.* Proceedings of the National Academy of Sciences, 2011. 108(39): p. 16381-16385.
 192. Erion, D.M. and G.I. Shulman, *Diacylglycerol-mediated insulin resistance.* Nature Medicine, 2010. 16(4): p. 400-2.
 193. Jornayvaz, F.R. and G.I. Shulman, *Diacylglycerol activation of protein kinase Cepsilon and hepatic insulin resistance.* Cell metabolism, 2012. 15(5): p. 574-84.

194. Schmitz-Peiffer, C. and T.J. Biden, *Protein kinase C function in muscle, liver, and beta-cells and its therapeutic implications for type 2 diabetes*. Diabetes, 2008. 57(7): p. 1774-83.
195. Jornayvaz, F.R., A.L. Birkenfeld, M.J. Jurczak, S. Kanda, B.A. Guigni, D.C. Jiang, D. Zhang, H.-Y. Lee, V.T. Samuel, and G.I. Shulman, *Hepatic insulin resistance in mice with hepatic overexpression of diacylglycerol acyltransferase 2*. Proceedings of the National Academy of Sciences, 2011. 108(14): p. 5748-5752.
196. Cantley, J.L., T. Yoshimura, J.P.G. Camporez, D. Zhang, F.R. Jornayvaz, N. Kumashiro, F. Guebre-Egziabher, M.J. Jurczak, M. Kahn, B.A. Guigni, J. Serr, J. Hankin, R.C. Murphy, G.W. Cline, S. Bhanot, V.P. Manchem, J.M. Brown, V.T. Samuel, and G.I. Shulman, *CGI-58 knockdown sequesters diacylglycerols in lipid droplets/ER-preventing diacylglycerol-mediated hepatic insulin resistance*. Proceedings of the National Academy of Sciences, 2013. 110(5): p. 1869-1874.
197. Kim, J.K., J.J. Fillmore, M.J. Sunshine, B. Albrecht, T. Higashimori, D.W. Kim, Z.X. Liu, T.J. Soos, G.W. Cline, W.R. O'Brien, D.R. Littman, and G.I. Shulman, *PKC- θ knockout mice are protected from fat-induced insulin resistance*. Journal of Clinical Investigation, 2004. 114(6): p. 823-7.
198. Choi, S.S. and A.M. Diehl, *Hepatic triglyceride synthesis and nonalcoholic fatty liver disease*. Current Opinion in Lipidology, 2008. 19(3): p. 295-300.
199. Frangioudakis, G., J. Garrard, K. Raddatz, J.L. Nadler, T.W. Mitchell, and C. Schmitz-Peiffer, *Saturated- and n-6 polyunsaturated-fat diets each induce ceramide accumulation in mouse skeletal muscle: reversal and improvement of glucose tolerance by lipid metabolism inhibitors*. Endocrinology, 2010. 151(9): p. 4187-96.
200. Gault, C.R., L.M. Obeid, and Y.A. Hannun, *An overview of sphingolipid metabolism: from synthesis to breakdown*. Advances in Experimental Medicine and Biology, 2010. 688: p. 1-23.
201. Chang, Z.Q., S.Y. Lee, H.J. Kim, J.R. Kim, S.J. Kim, I.K. Hong, B.C. Oh, C.S. Choi, I.J. Goldberg, and T.S. Park, *Endotoxin activates de novo sphingolipid biosynthesis via nuclear factor kappa B-mediated upregulation of Sptlc2*. Prostaglandins Other Lipid Mediat, 2011. 94(1-2): p. 44-52.
202. Bikman, B.T. and S.A. Summers, *Ceramides as modulators of cellular and whole-body metabolism*. Journal of Clinical Investigation, 2011. 121(11): p. 4222-30.
203. Ribaux, P.G. and P.B. Iynedjian, *Analysis of the role of protein kinase B (cAKT) in insulin-dependent induction of glucokinase and sterol regulatory element-binding protein 1 (SREBP1) mRNAs in hepatocytes*. Biochemical Journal, 2003. 376(Pt 3): p. 697-705.

204. Yang, G., L. Badeanlou, J. Bielawski, A.J. Roberts, Y.A. Hannun, and F. Samad, *Central role of ceramide biosynthesis in body weight regulation, energy metabolism, and the metabolic syndrome*. American Journal of Physiology - Endocrinology and Metabolism, 2009. 297(1): p. E211-24.
205. Holland, W.L. and S.A. Summers, *Sphingolipids, insulin resistance, and metabolic disease: new insights from in vivo manipulation of sphingolipid metabolism*. Endocrine reviews, 2008. 29(4): p. 381-402.
206. Chen, C.L., C.F. Lin, W.T. Chang, W.C. Huang, C.F. Teng, and Y.S. Lin, *Ceramide induces p38 MAPK and JNK activation through a mechanism involving a thioredoxin-interacting protein-mediated pathway*. Blood, 2008. 111(8): p. 4365-74.
207. Holland, W.L., T.A. Knotts, J.A. Chavez, L.P. Wang, K.L. Hoehn, and S.A. Summers, *Lipid mediators of insulin resistance*. Nutrition reviews, 2007. 65(6 Pt 2): p. S39-46.
208. Kleiner, D.E., E.M. Brunt, M. Van Natta, C. Behling, M.J. Contos, O.W. Cummings, L.D. Ferrell, Y.-C. Liu, M.S. Torbenson, A. Unalp-Arida, M. Yeh, A.J. McCullough, and A.J. Sanyal, *Design and validation of a histological scoring system for nonalcoholic fatty liver disease*. Hepatology, 2005. 41(6): p. 1313-1321.
209. Klein, S., D.B. Allison, S.B. Heymsfield, D.E. Kelley, R.L. Leibel, C. Nonas, and R. Kahn, *Waist Circumference and Cardiometabolic Risk: A Consensus Statement from Shaping America's Health: Association for Weight Management and Obesity Prevention; NAASO, The Obesity Society; the American Society for Nutrition; and the American Diabetes Association*. Diabetes Care, 2007. 30(6): p. 1647-1652.
210. Park, B.J., Y.J. Kim, D.H. Kim, W. Kim, Y.J. Jung, J.H. Yoon, C.Y. Kim, Y.M. Cho, S.H. Kim, K.B. Lee, J.J. Jang, and H.S. Lee, *Visceral adipose tissue area is an independent risk factor for hepatic steatosis*. Journal of gastroenterology and hepatology, 2008. 23(6): p. 900-7.
211. Tran, T.T., Y. Yamamoto, S. Gesta, and C.R. Kahn, *Beneficial Effects of Subcutaneous Fat Transplantation on Metabolism*. Cell Metabolism, 2008. 7(5): p. 410-420.
212. Stanton, M.C., S.C. Chen, J.V. Jackson, A. Rojas-Triana, D. Kinsley, L. Cui, J.S. Fine, S. Greenfeder, L.A. Bober, and C.H. Jenh, *Inflammatory Signals shift from adipose to liver during high fat feeding and influence the development of steatohepatitis in mice*. Journal of inflammation, 2011. 8: p. 8.
213. Gauthier, M.S., K. Couturier, J.G. Latour, and J.M. Lavoie, *Concurrent exercise prevents high-fat-diet-induced macrovesicular hepatic steatosis*. Journal of applied physiology, 2003. 94(6): p. 2127-34.
214. Horton, J.D., I. Shimomura, S. Ikemoto, Y. Bashmakov, and R.E. Hammer, *Overexpression of sterol regulatory element-binding protein-1a in mouse adipose tissue produces adipocyte hypertrophy, increased fatty*

- acid secretion, and fatty liver*. Journal of Biological Chemistry, 2003. 278(38): p. 36652-60.
215. Voshol, P.J., G. Haemmerle, D.M. Ouwens, R. Zimmermann, R. Zechner, B. Teusink, J.A. Maassen, L.M. Havekes, and J.A. Romijn, *Increased hepatic insulin sensitivity together with decreased hepatic triglyceride stores in hormone-sensitive lipase-deficient mice*. Endocrinology, 2003. 144(8): p. 3456-62.
 216. Kaplan, M.L. and G.A. Leveille, *Obesity: prediction of preobesity among progeny from crosses of ob+ mice*. Proceedings of the Society for Experimental Biology and Medicine, 1973. 143(4): p. 925-8.
 217. Tartaglia, L.A., M. Dembski, X. Weng, N. Deng, J. Culpepper, R. Devos, G.J. Richards, L.A. Campfield, F.T. Clark, J. Deeds, C. Muir, S. Sanker, A. Moriarty, K.J. Moore, J.S. Smutko, G.G. Mays, E.A. Wool, C.A. Monroe, and R.I. Tepper, *Identification and expression cloning of a leptin receptor, OB-R*. Cell, 1995. 83(7): p. 1263-71.
 218. Danforth, E., Jr., *Failure of adipocyte differentiation causes type II diabetes mellitus?* Nature genetics, 2000. 26(1): p. 13.
 219. Lee, J.H., J.L. Chan, E. Sourlas, V. Raptopoulos, and C.S. Mantzoros, *Recombinant methionyl human leptin therapy in replacement doses improves insulin resistance and metabolic profile in patients with lipoatrophy and metabolic syndrome induced by the highly active antiretroviral therapy*. Journal of clinical endocrinology and metabolism, 2006. 91(7): p. 2605-11.
 220. Uygun, A., A. Kadayifci, Z. Yesilova, A. Erdil, H. Yaman, M. Saka, M.S. Deveci, S. Bagci, M. Gulsen, N. Karaeren, and K. Dagalp, *Serum leptin levels in patients with nonalcoholic steatohepatitis*. American College of Gastroenterology, 2000. 95(12): p. 3584-9.
 221. Chitturi, S., G. Farrell, L. Frost, A. Kriketos, R. Lin, C. Fung, C. Liddle, D. Samarasinghe, and J. George, *Serum leptin in NASH correlates with hepatic steatosis but not fibrosis: a manifestation of lipotoxicity?* Hepatology, 2002. 36(2): p. 403-9.
 222. Angulo, P., L.M. Alba, L.M. Petrovic, L.A. Adams, K.D. Lindor, and M.D. Jensen, *Leptin, insulin resistance, and liver fibrosis in human nonalcoholic fatty liver disease*. Journal of Hepatology, 2004. 41(6): p. 943-9.
 223. Adam, C.L. and P.A. Findlay, *Decreased blood-brain leptin transfer in an ovine model of obesity and weight loss: resolving the cause of leptin resistance*. International journal of obesity, 2010. 34(6): p. 980-8.
 224. Glavas, M.M., M.A. Kirigiti, X.Q. Xiao, P.J. Enriori, S.K. Fisher, A.E. Evans, B.E. Grayson, M.A. Cowley, M.S. Smith, and K.L. Grove, *Early Overnutrition Results in Early-Onset Arcuate Leptin Resistance and Increased Sensitivity to High-Fat Diet*. Endocrinology, 2010. 151(4): p. 1598-1610.

225. Marra, F. and C. Bertolani, *Adipokines in liver diseases*. Hepatology, 2009. 50(3): p. 957-69.
226. Yang, S.Q., H.Z. Lin, M.D. Lane, M. Clemens, and A.M. Diehl, *Obesity increases sensitivity to endotoxin liver injury: implications for the pathogenesis of steatohepatitis*. Proceedings of the National Academy of Sciences, 1997. 94(6): p. 2557-62.
227. Ikejima, K., Y. Takei, H. Honda, M. Hirose, M. Yoshikawa, Y.J. Zhang, T. Lang, T. Fukuda, S. Yamashina, T. Kitamura, and N. Sato, *Leptin receptor-mediated signaling regulates hepatic fibrogenesis and remodeling of extracellular matrix in the rat*. Gastroenterology, 2002. 122(5): p. 1399-410.
228. Dara, L., C. Ji, and N. Kaplowitz, *The contribution of endoplasmic reticulum stress to liver diseases*. Hepatology, 2011. 53(5): p. 1752-63.
229. Engelking, L.J., H. Kuriyama, R.E. Hammer, J.D. Horton, M.S. Brown, J.L. Goldstein, and G. Liang, *Overexpression of Insig-1 in the livers of transgenic mice inhibits SREBP processing and reduces insulin-stimulated lipogenesis*. Journal of Clinical Investigation, 2004. 113(8): p. 1168-75.
230. Joon No, L. and Y. Jin, *Proteolytic activation of sterol regulatory element-binding protein induced by cellular stress through depletion of Insig-1*. Journal of Biological Chemistry, 2004. 279(43): p. 45257-65.
231. Ota, T., C. Gayet, and H.N. Ginsberg, *Inhibition of apolipoprotein B100 secretion by lipid-induced hepatic endoplasmic reticulum stress in rodents*. Journal of Clinical Investigation, 2008. 118(1): p. 316-32.
232. Kammoun, H., xE, xE, L. ne, H. Chabanon, xE, I. Hainault, S. Luquet, C. Magnan, T. Koike, Ferr, xE, Pascal, and F. Foufelle, *GRP78 expression inhibits insulin and ER stress-induced SREBP-1c activation and reduces hepatic steatosis in mice*. Journal of Clinical Investigation, 2009. 119(5): p. 1201-1215.
233. Ozcan, U., E. Yilmaz, L. Ozcan, M. Furuhashi, E. Vaillancourt, R.O. Smith, C.Z. Gorgun, and G.S. Hotamisligil, *Chemical chaperones reduce ER stress and restore glucose homeostasis in a mouse model of type 2 diabetes*. Science, 2006. 313(5790): p. 1137-40.
234. Yang, L., P. Li, S. Fu, E.S. Calay, and G.S. Hotamisligil, *Defective Hepatic Autophagy in Obesity Promotes ER Stress and Causes Insulin Resistance*. Cell Metabolism, 2010. 11(6): p. 467-478.
235. Rautou, P.E., A. Mansouri, D. Lebrech, F. Durand, D. Valla, and R. Moreau, *Autophagy in liver diseases*. Journal of Hepatology, 2010. 53(6): p. 1123-1134.
236. Ding, W.X., M. Li, X. Chen, H.M. Ni, C.W. Lin, W. Gao, B. Lu, D.B. Stolz, D.L. Clemens, and X.M. Yin, *Autophagy reduces acute ethanol-induced hepatotoxicity and steatosis in mice*. Gastroenterology, 2010. 139(5): p. 1740-52.

237. Klionsky, D.J., F.C. Abdalla, H. Abeliovich, R.T. Abraham et. al , *Guidelines for the use and interpretation of assays for monitoring autophagy*. Autophagy, 2012. 8(4): p. 445-544.
238. Fernandez-Millan, E., J. de Toro-Martin, E. Lizarraga-Mollinedo, F. Escriva, and C. Alvarez, *Defective autophagy results in reduced glycogen breakdown in the liver of IUGR newborn Wistar rats. Consequences for glucose homeostasis*, in *European Association for the Study of Diabetes annual meeting 2014*. 2014: Vienna, Austria.
239. Cai Dongsheng, M.Y., Daniel F Frantz, Peter A Melendez, Lone Hansen, Jongsoon Lee & Steven E Shoelson, *Local and systemic insulin resistance resulting from hepatic activation of IKK- beta and NF-kappaB*. Nature Medicine, 2005. 11: p. 183-190.
240. Videla, L.A., R. Rodrigo, M. Orellana, V. Fernandez, G. Tapia, L. Quinones, N. Varela, J. Contreras, R. Lazarte, A. Csendes, J. Rojas, F. Maluenda, P. Burdiles, J.C. Diaz, G. Smok, L. Thielemann, and J. Poniachik, *Oxidative stress-related parameters in the liver of non-alcoholic fatty liver disease patients*. Clinical science, 2004. 106(3): p. 261-8.
241. Seki, S., T. Kitada, T. Yamada, H. Sakaguchi, K. Nakatani, and K. Wakasa, *In situ detection of lipid peroxidation and oxidative DNA damage in non-alcoholic fatty liver diseases*. Journal of Hepatology, 2002. 37(1): p. 56-62.
242. MacDonald, G.A., K.R. Bridle, P.J. Ward, N.I. Walker, K. Houghlum, D.K. George, J.L. Smith, L.W. Powell, D.H. Crawford, and G.A. Ramm, *Lipid peroxidation in hepatic steatosis in humans is associated with hepatic fibrosis and occurs predominately in acinar zone 3*. Journal of gastroenterology and hepatology, 2001. 16(6): p. 599-606.
243. Chalasani, N., J.C. Gorski, M.S. Asghar, A. Asghar, B. Foresman, S.D. Hall, and D.W. Crabb, *Hepatic cytochrome P450 2E1 activity in nondiabetic patients with nonalcoholic steatohepatitis*. Hepatology, 2003. 37(3): p. 544-550.
244. Gornicka, A., G. Morris-Stiff, S. Thapaliya, B.G. Papouchado, M. Berk, and A.E. Feldstein, *Transcriptional profile of genes involved in oxidative stress and antioxidant defense in a dietary murine model of steatohepatitis*. Antioxidants & redox signaling, 2011. 15(2): p. 437-445.
245. Sanyal, A.J., N. Chalasani, K.V. Kowdley, A. McCullough, A.M. Diehl, N.M. Bass, B.A. Neuschwander-Tetri, J.E. Lavine, J. Tonascia, A. Unalp, M. Van Natta, J. Clark, E.M. Brunt, D.E. Kleiner, J.H. Hoofnagle, P.R. Robuck, and null, *Pioglitazone, vitamin E, or placebo for nonalcoholic steatohepatitis*. New England journal of medicine, 2010. 362(18): p. 1675-1685.
246. Neuschwander-Tetri, B.A., *Nontriglyceride hepatic lipotoxicity: the new paradigm for the pathogenesis of NASH*. Current gastroenterology reports, 2010. 12(1): p. 49-56.

247. Symonds, M.E., *Integration of physiological and molecular mechanisms of the developmental origins of adult disease: new concepts and insights*. Proceedings of the Nutrition Society, 2007. 66(3): p. 442-50.
248. Hales, C. and D. Barker, *Type 2 (non-insulin-dependent) diabetes mellitus: the thrifty phenotype hypothesis*. Diabetologia, 1992. 35(7): p. 595-601.
249. Jarvelin, M.-R., U. Sovio, V. King, L. Lauren, B. Xu, M.I. McCarthy, A.-L. Hartikainen, J. Laitinen, P. Zitting, P. Rantakallio, and P. Elliott, *Early Life Factors and Blood Pressure at Age 31 Years in the 1966 Northern Finland Birth Cohort*. Hypertension, 2004. 44(6): p. 838-846.
250. Roseboom, T., S. de Rooij, and R. Painter, *The Dutch famine and its long-term consequences for adult health*. Early Human Development, 2006. 82(8): p. 485-491.
251. Budge, H., S. Sebert, D. Sharkey, and M.E. Symonds, *Session on 'Obesity' Adipose tissue development, nutrition in early life and its impact on later obesity*. Proceedings of the Nutrition Society, 2009. 68(03): p. 321-326.
252. Chan, L.L.Y., S.P. Sébert, M.A. Hyatt, T. Stephenson, H. Budge, M.E. Symonds, and D.S. Gardner, *Effect of maternal nutrient restriction from early to midgestation on cardiac function and metabolism after adolescent-onset obesity*. American Journal of Physiology - Regulatory, Integrative and Comparative Physiology, 2009. 296(5): p. R1455-R1463.
253. Symonds, M.E., Stephenson, T. , Gardner, D. S. ,Budge, H. , *Long-term effects of nutritional programming of the embryo and fetus: mechanisms and critical windows*. Reproduction, Fertility and Development, 2006. 19(1): p. 53-63
254. Lumey, L.H., A.C. Ravelli, L.G. Wiessing, J.G. Koppe, P.E. Treffers, and Z.A. Stein, *The Dutch famine birth cohort study: design, validation of exposure, and selected characteristics of subjects after 43 years follow-up*. Paediatr Perinat Epidemiol, 1993. 7(4): p. 354-67.
255. Lumey, L.H., A.D. Stein, H.S. Kahn, K.M. van der Pal-de Bruin, G.J. Blauw, P.A. Zybert, and E.S. Susser, *Cohort Profile: The Dutch Hunger Winter Families Study*. International Journal of Epidemiology, 2007. 36(6): p. 1196-1204.
256. McCance, D.R., D.J. Pettitt, R.L. Hanson, L.T.H. Jacobsson, W.C. Knowler, and P.H. Bennett, *Birth weight and non-insulin dependent diabetes: thrifty genotype, thrifty phenotype, or surviving small baby genotype?* BMJ, 1994. 308(6934): p. 942-945.
257. Lumey, L.H., *Decreased birthweights in infants after maternal in utero exposure to the Dutch famine of 1944–1945*. Paediatric and Perinatal Epidemiology, 1992. 6(2): p. 240-253.

258. Painter, R.C., T.J. Roseboom, and O.P. Bleker, *Prenatal exposure to the Dutch famine and disease in later life: An overview*. Reproductive Toxicology, 2005. 20(3): p. 345-352.
259. Williamson, C.S., *Nutrition in pregnancy*. Nutrition Bulletin, 2006. 31(1): p. 28-59.
260. DH, *Department of Health Report on Health and Social Subjects No. 41. Dietary Reference Values for Food, Energy and Nutrients for the United Kingdom. Report of the Committee on Medical Aspects of Food Policy.*, in HMSO: London. 1991, Department of Health: London, UK.
261. Ravelli, A.C., J.H. van der Meulen, R.P. Michels, C. Osmond, D.J. Barker, C.N. Hales, and O.P. Bleker, *Glucose tolerance in adults after prenatal exposure to famine*. Lancet, 1998. 351(9097): p. 173-7.
262. Roseboom, T.J., J.H. van der Meulen, C. Osmond, D.J. Barker, A.C. Ravelli, and O.P. Bleker, *Plasma lipid profiles in adults after prenatal exposure to the Dutch famine*. American Journal of Clinical Nutrition, 2000. 72(5): p. 1101-1106.
263. Li, Y., V.W. Jaddoe, L. Qi, Y. He, D. Wang, J. Lai, J. Zhang, P. Fu, X. Yang, and F.B. Hu, *Exposure to the Chinese Famine in Early Life and the Risk of Metabolic Syndrome in Adulthood*. Diabetes Care, 2011. 34(4): p. 1014-1018.
264. Rhodes, P., J. Craigon, C. Gray, S.M. Rhind, P.T. Loughna, and D.S. Gardner, *Adult-Onset Obesity Reveals Prenatal Programming of Glucose-Insulin Sensitivity in Male Sheep Nutrient Restricted during Late Gestation*. PLoS ONE, 2009. 4(10): p. e7393.
265. Kind, K.L., P.M. Clifton, P.A. Grant, P.C. Owens, A. Sohlstrom, C.T. Roberts, J.S. Robinson, and J.A. Owens, *Effect of maternal feed restriction during pregnancy on glucose tolerance in the adult guinea pig*. American Journal of Physiology - Regulatory, Integrative and Comparative Physiology, 2003. 284(1): p. R140-52.
266. Tygesen, M.P., M.O. Nielsen, P. Norgaard, H. Ranvig, A.P. Harrison, and A.H. Tauson, *Late gestational nutrient restriction: effects on ewes' metabolic and homeorhetic adaptation, consequences for lamb birth weight and lactation performance*. Archives of Animal Nutrition, 2008. 62(1): p. 44-59.
267. Sebert, S.P., N.S. Dellschaft, L.L.Y. Chan, H. Street, M. Henry, C. Francois, V. Sharma, H.P. Fainberg, N. Patel, J. Roda, D. Keisler, H. Budge, and M.E. Symonds, *Maternal Nutrient Restriction During Late Gestation and Early Postnatal Growth in Sheep Differentially Reset the Control of Energy Metabolism in the Gastric Mucosa*. Endocrinology, 2011. 152(7): p. 2816-2826.
268. Budge, H., J. Dandrea, A. Mostyn, Y. Evens, R. Watkins, C. Sullivan, P. Ingleton, T. Stephenson, and M.E. Symonds, *Differential effects of fetal number and maternal nutrition in late gestation on prolactin receptor*

abundance and adipose tissue development in the neonatal lamb. Pediatric Research, 2003. 53(2): p. 302-8.

269. Vickers, M.H., B.H. Breier, W.S. Cutfield, P.L. Hofman, and P.D. Gluckman, *Fetal origins of hyperphagia, obesity, and hypertension and postnatal amplification by hypercaloric nutrition.* American Journal of Physiology - Endocrinology and Metabolism, 2000. 279(1): p. E83-7.
270. Ozanne, S.E., R. Lewis, B.J. Jennings, and C.N. Hales, *Early programming of weight gain in mice prevents the induction of obesity by a highly palatable diet.* Clinical science, 2004. 106(2): p. 141-5.
271. Zambrano, E., C.J. Bautista, M. Deás, P.M. Martínez-Samayoa, M. González-Zamorano, H. Ledesma, J. Morales, F. Larrea, and P.W. Nathanielsz, *A low maternal protein diet during pregnancy and lactation has sex- and window of exposure-specific effects on offspring growth and food intake, glucose metabolism and serum leptin in the rat.* Journal of Physiology, 2006. 571(1): p. 221-230.
272. Bispham, J., D.S. Gardner, M.G. Gnanalingham, T. Stephenson, M.E. Symonds, and H. Budge, *Maternal nutritional programming of fetal adipose tissue development: differential effects on messenger ribonucleic acid abundance for uncoupling proteins and peroxisome proliferator-activated and prolactin receptors.* Endocrinology, 2005. 146(9): p. 3943-9.
273. Budge, H., L.J. Edwards, I.C. McMillen, A. Bryce, K. Warnes, S. Pearce, T. Stephenson, and M.E. Symonds, *Nutritional manipulation of fetal adipose tissue deposition and uncoupling protein 1 messenger RNA abundance in the sheep: differential effects of timing and duration.* Biology of reproduction, 2004. 71(1): p. 359-65.
274. Gardner, D.S., K. Tingey, B.W. Van Bon, S.E. Ozanne, V. Wilson, J. Dandrea, D.H. Keisler, T. Stephenson, and M.E. Symonds, *Programming of glucose-insulin metabolism in adult sheep after maternal undernutrition.* American Journal of Physiology - Regulatory, Integrative and Comparative Physiology, 2005. 289(4): p. R947-54.
275. Sharkey, D., M.E. Symonds, and H. Budge, *Adipose Tissue Inflammation: Developmental Ontogeny and Consequences of Gestational Nutrient Restriction in Offspring.* Endocrinology, 2009. 150(8): p. 3913-3920.
276. Latini, G., B. De Mitri, A. Del Vecchio, G. Chitano, C. De Felice, and R. Zetterstrom, *Foetal growth of kidneys, liver and spleen in intrauterine growth restriction: "programming" causing "metabolic syndrome" in adult age.* Acta Paediatrica, 2004. 93(12): p. 1635-9.
277. Fraser, A., S. Ebrahim, G. Davey Smith, and D.A. Lawlor, *The associations between birthweight and adult markers of liver damage and function.* Paediatric and Perinatal Epidemiology, 2008. 22(1): p. 12-21.
278. Burns, S.P., M. Desai, R.D. Cohen, C.N. Hales, R.A. Iles, J.P. Germain, T.C. Going, and R.A. Bailey, *Gluconeogenesis, glucose handling, and*

- structural changes in livers of the adult offspring of rats partially deprived of protein during pregnancy and lactation.* Journal of Clinical Investigation, 1997. 100(7): p. 1768-74.
279. Hyatt, M.A., D.S. Gardner, S. Sebert, V. Wilson, N. Davidson, Y. Nigmatullina, L.L.Y. Chan, H. Budge, and M.E. Symonds, *Suboptimal maternal nutrition, during early fetal liver development, promotes lipid accumulation in the liver of obese offspring.* Reproduction, 2011. 141(1): p. 119-126.
 280. Hales, C.N., D.J. Barker, P.M. Clark, L.J. Cox, C. Fall, C. Osmond, and P.D. Winter, *Fetal and infant growth and impaired glucose tolerance at age 64.* BMJ, 1991. 303(6809): p. 1019-22.
 281. Singhal, A. and A. Lucas, *Early origins of cardiovascular disease: is there a unifying hypothesis?* Lancet, 2004. 363(9421): p. 1642-1645.
 282. Hui, L.L., G.M. Leung, B.J. Cowling, T.H. Lam, and C.M. Schooling, *Determinants of Infant Growth: Evidence from Hong Kong's "Children of 1997" Birth Cohort.* Annals of Epidemiology, 2010. 20(11): p. 827-835.
 283. Touwslager, R.N., M. Gielen, A.L. Mulder, W.J. Gerver, L.J. Zimmermann, T. Fowler, A.J. Houben, C.D. Stehouwer, C. Derom, R. Vlietinck, R.J.F. Loos, and M.P. Zeegers, *Changes in genetic and environmental effects on growth during infancy.* American Journal of Clinical Nutrition, 2011. 94(6): p. 1568-1574.
 284. Eid, E.E., *Follow-up study of physical growth of children who had excessive weight gain in first six months of life.* BMJ, 1970. 2(5701): p. 74-6.
 285. Ong, K., C. Petry, P. Emmett, M. Sandhu, W. Kiess, C. Hales, A. Ness, t.A.s. team, and D. Dunger, *Insulin sensitivity and secretion in normal children related to size at birth, postnatal growth, and plasma insulin-like growth factor-I levels.* Diabetologia, 2004. 47(6): p. 1064-1070.
 286. Singhal, A., M. Fewtrell, T.J. Cole, and A. Lucas, *Low nutrient intake and early growth for later insulin resistance in adolescents born preterm.* Lancet, 2003. 361(9363): p. 1089-1097.
 287. Stettler, N., V.A. Stallings, A.B. Troxel, J. Zhao, R. Schinnar, S.E. Nelson, E.E. Ziegler, and B.L. Strom, *Weight Gain in the First Week of Life and Overweight in Adulthood.* Circulation, 2005. 111(15): p. 1897-1903.
 288. Stettler, N., B.S. Zemel, S. Kumanyika, and V.A. Stallings, *Infant Weight Gain and Childhood Overweight Status in a Multicenter, Cohort Study.* Pediatrics, 2002. 109(2): p. 194-199.
 289. Druet, C., N. Stettler, S. Sharp, R.K. Simmons, C. Cooper, G. Davey Smith, U. Ekelund, C. Lévy-Marchal, M.-R. Jarvelin, D. Kuh, and K.K. Ong, *Prediction of childhood obesity by infancy weight gain: an individual-level meta-analysis.* Paediatric and Perinatal Epidemiology, 2012. 26(1): p. 19-26.

290. Bann, D., A. Wills, R. Cooper, R. Hardy, A. Aihie Sayer, J. Adams, and D. Kuh, *Birth weight and growth from infancy to late adolescence in relation to fat and lean mass in early old age: findings from the MRC National Survey of Health and Development*. International Journal of Obesity, 2014. 38(1): p. 69-75.
291. Kramer, M.S., T. Guo, R.W. Platt, I. Vanilovich, Z. Sevkovskaya, I. Dzikovich, K.F. Michaelsen, K. Dewey, and I. Promotion Breastfeeding, *Feeding effects on growth during infancy*. Journal of Pediatrics, 2004. 145(5): p. 600-605.
292. WHO, *Multicentre Growth Reference Study Group. WHO Child Growth Standards based on length/height, weight and age*. Acta Paediatrica, 2006. Suppl 450: p. 76-85.
293. Singhal, A., K. Kennedy, J. Lanigan, M. Fewtrell, T.J. Cole, T. Stephenson, A. Elias-Jones, L.T. Weaver, S. Ibhanesebhor, P.D. MacDonald, J. Bindels, and A. Lucas, *Nutrition in infancy and long-term risk of obesity: evidence from 2 randomized controlled trials*. American Journal of Clinical Nutrition, 2010. 92(5): p. 1133-44.
294. Khan, I.Y., V. Dekou, G. Douglas, R. Jensen, M.A. Hanson, L. Poston, and P.D. Taylor, *A high-fat diet during rat pregnancy or suckling induces cardiovascular dysfunction in adult offspring*. American Journal of Physiology - Regulatory, Integrative and Comparative Physiology, 2005. 288(1): p. R127-33.
295. Schmidt I, F.A., Schölch C, Schneider D, Simon E and Plagemann A, *The effect of leptin treatment on the development of obesity in overfed suckling Wistar rats*. 2001. 25(8): p. 1168-1174.
296. Plagemann, A., I. Heidrich, F. Gotz, W. Rohde, and G. Dorner, *Obesity and enhanced diabetes and cardiovascular risk in adult rats due to early postnatal overfeeding*. Experimental and Clinical Endocrinology, 1992. 99(3): p. 154-158.
297. Widdowson, E.M., *Chemical Composition of Newly Born Mammals*. Nature, 1950. 166(4224): p. 626-628.
298. Fowden, A.L., J. Li, and A.J. Forhead, *Glucocorticoids and the preparation for life after birth: are there long-term consequences of the life insurance?* Proceedings of the Nutrition Society, 1998. 57(1): p. 113-22.
299. Owen, C.G., R.M. Martin, P.H. Whincup, G.D. Smith, and D.G. Cook, *Effect of Infant Feeding on the Risk of Obesity Across the Life Course: A Quantitative Review of Published Evidence*. Pediatrics, 2005. 115(5): p. 1367-1377.
300. Arenz, S., R. Ruckerl, B. Koletzko, and R. von Kries, *Breast-feeding and childhood obesity - a systematic review*. International Journal of Obesity, 2004. 28(10): p. 1247-1256.

301. Le Huërou-Luron, I., S. Blat, and G. Boudry, *Breast- v. formula-feeding: impacts on the digestive tract and immediate and long-term health effects*. Nutrition Research Reviews, 2010. 23(01): p. 23-36.
302. Harder, T., R. Bergmann, G. Kallischnigg, and A. Plagemann, *Duration of breastfeeding and risk of overweight: a meta-analysis*. American Journal of Epidemiology, 2005. 162(5): p. 397-403.
303. Horta, B.L. and W.H. Organization, *Evidence on the long-term effects of breastfeeding*. 2007: WHO Geneva.
304. Owen, C.G., P.H. Whincup, K. Odoki, J.A. Gilg, and D.G. Cook, *Infant Feeding and Blood Cholesterol: A Study in Adolescents and a Systematic Review*. Pediatrics, 2002. 110(3): p. 597-608.
305. Owen, C.G., R.M. Martin, P.H. Whincup, G.D. Smith, and D.G. Cook, *Does breastfeeding influence risk of type 2 diabetes in later life? A quantitative analysis of published evidence*. American Journal of Clinical Nutrition, 2006. 84(5): p. 1043-54.
306. Lawlor, D.A., C.J. Riddoch, A.S. Page, L.B. Andersen, N. Wedderkopp, M. Harro, D. Stansbie, and G. Davey Smith, *Infant feeding and components of the metabolic syndrome: findings from the European Youth Heart Study*. Archives of Disease in Childhood, 2005. 90(6): p. 582-588.
307. Koletzko, B., C. Agostoni, S.E. Carlson, T. Clandinin, G. Hornstra, M. Neuringer, R. Uauy, Y. Yamashiro, and P. Willatts, *Long chain polyunsaturated fatty acids (LC-PUFA) and perinatal development*. Acta Paediatrica, 2001. 90(4): p. 460-464.
308. Savino, F., S. Liguori, M. Fissore, and R. Oggero, *Breast Milk Hormones and Their Protective Effect on Obesity*. International Journal of Pediatric Endocrinology, 2009. 2009(1): p. 327505.
309. Nobili, V., G. Bedogni, A. Alisi, A. Pietro Battista, A. Alterio, C. Tiribelli, and C. Agostoni, *A protective effect of breastfeeding on the progression of non-alcoholic fatty liver disease*. Archives of Disease in Childhood, 2009. 94(10): p. 801-805.
310. Gale, C., E.L. Thomas, S. Jeffries, G. Durighel, K.M. Logan, J.R. Parkinson, S. Uthaya, S. Santhakumaran, J.D. Bell, and N. Modi, *Adiposity and hepatic lipid in healthy full-term, breastfed, and formula-fed human infants: a prospective short-term longitudinal cohort study*. American Journal of Clinical Nutrition, 2014. 99(5): p. 1034-40.
311. Mouralidarane, A., J. Soeda, C. Visconti-Pugmire, A.M. Samuelsson, J. Pombo, X. Maragkoudaki, A. Butt, R. Saraswati, M. Novelli, G. Fusai, L. Poston, P.D. Taylor, and J.A. Oben, *Maternal obesity programs offspring nonalcoholic fatty liver disease by innate immune dysfunction in mice*. Hepatology, 2013. 58(1): p. 128-38.
312. Symonds, M.E., M. Pope, D. Sharkey, and H. Budge, *Adipose tissue and fetal programming*. Diabetologia, 2012.

313. Hyatt, M.A., H. Budge, D. Walker, T. Stephenson, and M.E. Symonds, *Effects of maternal parity and late gestational nutrition on mRNA abundance for growth factors in the liver of postnatal sheep*. American Journal of Physiology - Regulatory, Integrative and Comparative Physiology, 2007. 292(5): p. R1934-R1942.
314. Bryden, M.M., H. Evans, and W. Binns, *Embryology of the sheep. III. The respiratory system, mesenteries and celom in the fourteen to thirty-four day embryo*. The Anatomical Record, 1973. 175(4): p. 725-735.
315. Gardner, D.S., K. Tingey, B.W.M. Van Bon, S.E. Ozanne, V. Wilson, J. Dandrea, D.H. Keisler, T. Stephenson, and M.E. Symonds, *Programming of glucose-insulin metabolism in adult sheep after maternal undernutrition*. American Journal of Physiology - Regulatory, Integrative and Comparative Physiology, 2005. 289(4): p. R947-R954.
316. Gopalakrishnan, G.S., D.S. Gardner, J. Dandrea, S.C. Langley-Evans, S. Pearce, L.O. Kurlak, R.M. Walker, I.W. Seetho, D.H. Keisler, M.M. Ramsay, T. Stephenson, and M.E. Symonds, *Influence of maternal pre-pregnancy body composition and diet during early-mid pregnancy on cardiovascular function and nephron number in juvenile sheep*. British Journal of Nutrition, 2005. 94(06): p. 938-947.
317. Veilleux, A., M. Caron-Jobin, S. Noel, P.Y. Laberge, and A. Tchernof, *Visceral adipocyte hypertrophy is associated with dyslipidemia independent of body composition and fat distribution in women*. Diabetes, 2011. 60(5): p. 1504-11.
318. Canello, R., J. Tordjman, C. Poitou, G. Guilhem, J.L. Bouillot, D. Hugol, C. Coussieu, A. Basdevant, A. Bar Hen, P. Bedossa, M. Guerre-Millo, and K. Clement, *Increased infiltration of macrophages in omental adipose tissue is associated with marked hepatic lesions in morbid human obesity*. Diabetes, 2006. 55(6): p. 1554-61.
319. Kolak, M., J. Westerbacka, V.R. Velagapudi, D. Wagsater, L. Yetukuri, J. Makkonen, A. Rissanen, A.M. Hakkinen, M. Lindell, R. Bergholm, A. Hamsten, P. Eriksson, R.M. Fisher, M. Oresic, and H. Yki-Jarvinen, *Adipose tissue inflammation and increased ceramide content characterize subjects with high liver fat content independent of obesity*. Diabetes, 2007. 56(8): p. 1960-8.
320. Apovian, C.M., S. Bigornia, M. Mott, M.R. Meyers, J. Ulloor, M. Gagua, M. McDonnell, D. Hess, L. Joseph, and N. Gokce, *Adipose macrophage infiltration is associated with insulin resistance and vascular endothelial dysfunction in obese subjects*. Arterioscler Thromb Vasc Biol, 2008. 28(9): p. 1654-9.
321. Bruun, J.M., A.S. Lihn, S.B. Pedersen, and B. Richelsen, *Monocyte chemoattractant protein-1 release is higher in visceral than subcutaneous human adipose tissue (AT): implication of macrophages resident in the AT*. J Clin Endocrinol Metab, 2005. 90(4): p. 2282-9.

322. Bryden, M.M., H.E. Evans, and W. Binns, *Embryology of the Sheep 2: The alimentary tract and associated glands*. Journal of Morphology, 1972. 138: p. 187-206.
323. Davies, G., M. Birtwistle, M. Pope, V. Perry, H. Sacks, H. Budge, and M. Symonds, *The developmental transition of epicardial, paracardial and omental adipose tissue during early life in the sheep (1160.7)*, in *Unpublished results*. 2014.
324. Si-Tayeb, K., F.P. Lemaigre, and S.A. Duncan, *Organogenesis and Development of the Liver*. Developmental Cell, 2010. 18(2): p. 175-189.
325. Archie, J.G., J.S. Collins, and R.R. Lebel, *Quantitative Standards for Fetal and Neonatal Autopsy*. American Journal of Clinical Pathology, 2006. 126(2): p. 256-265.
326. Consortium, M.P., *The Early Nutrition Programming Project available at <http://www.metabolic-programming.org>*. 2005.
327. Park, Y., M. Juárez, M. Ramos, and G. Haenlein, *Physico-chemical characteristics of goat and sheep milk*. Small ruminant research, 2007. 68(1): p. 88-113.
328. Dove, H. and M. Freer, *Sheep Nutrition*. 2002: CABI.
329. Berger, Y.M., *Lamb mortality and causes – A nine year summary at the Spooner Agricultural Research Station*. (http://www.ansci.wisc.edu/extensionnew%20copy/sheep/Publications_and_Proceedings/Pdf/Nutrition%20and%20Health/Lamb%20mortality%20and%20causes.pdf), in *Proceedings of the 45th Annual Spooner Sheep Day*. 1997: Dept. of Animal Sciences, UW-Madison. p. 33-40.
330. Dwyer, C.M., *Genetic and physiological determinants of maternal behavior and lamb survival: implications for low-input sheep management*. Journal of Animal Science 2008. 86(14 Suppl): p. E246-58.
331. Borai, A., C. Livingstone, I. Kaddam, and G. Ferns, *Selection of the appropriate method for the assessment of insulin resistance*. BMC Med Res Methodol, 2011. 11: p. 158.
332. Echouffo-Tcheugui, J.B., M.K. Ali, S.J. Griffin, and K.M.V. Narayan, *Screening for Type 2 Diabetes and Dysglycemia*. Epidemiologic Reviews, 2011. 33(1): p. 63-87.
333. Stumvoll, M., A. Mitrakou, W. Pimenta, T. Jenssen, H. Yki-Jarvinen, T. Van Haften, W. Renn, and J. Gerich, *Use of the oral glucose tolerance test to assess insulin release and insulin sensitivity*. Diabetes Care, 2000. 23(3): p. 295-301.
334. Radziuk, J., *Insulin Sensitivity and Its Measurement: Structural Commonalities among the Methods*. Journal of Clinical Endocrinology & Metabolism, 2000. 85(12): p. 4426-4433.

335. Delavaud, C., F. Bocquier, Y. Chilliard, D.H. Keisler, A. Gertler, and G. Kann, *Plasma leptin determination in ruminants: effect of nutritional status and body fatness on plasma leptin concentration assessed by a specific RIA in sheep*. Journal of endocrinology, 2000. 165(2): p. 519-26.
336. Westerterp, K.R., *Physical activity assessment with accelerometers*. International Journal of Obesity & Related Metabolic Disorders: Journal of the International Association for the Study of Obesity, 1999. 23 Suppl 3: p. S45-9.
337. Caspersen, C.J., K.E. Powell, and G.M. Christenson, *Physical activity, exercise, and physical fitness: definitions and distinctions for health-related research*. Public Health Reports, 1985. 100(2): p. 126-31.
338. Folch, J., M. Lees, and G.H. Sloane Stanley, *A simple method for the isolation and purification of total lipides from animal tissues*. Journal of Biological Chemistry, 1957. 226(1): p. 497-509.
339. Pryor, W.A., *The antioxidant nutrients and disease prevention--what do we know and what do we need to find out?* American Journal of Clinical Nutrition, 1991. 53(1 Suppl): p. 391S-393S.
340. Kosugi, H., T. Kato, and K. Kikugawa, *Formation of yellow, orange, and red pigments in the reaction of alk-2-enals with 2-thiobarbituric acid*. Analytical Biochemistry, 1987. 165(2): p. 456-64.
341. Armstrong, D. and R. Browne, *The analysis of free radicals, lipid peroxides, antioxidant enzymes and compounds related to oxidative stress as applied to the clinical chemistry laboratory*. Advances in Experimental Medicine and Biology, 1994. 366: p. 43-58.
342. Depboylu, B., M. Giris, V. Olgac, S. Dogru-Abbasoglu, and M. Uysal, *Response of liver to lipopolysaccharide treatment in male and female rats*. Experimental and Toxicologic Pathology, 2012.
343. Salamone, F., F. Galvano, F. Cappello, A. Mangiameli, I. Barbagallo, and G. Li Volti, *Silibinin modulates lipid homeostasis and inhibits nuclear factor kappa B activation in experimental nonalcoholic steatohepatitis*. Translational Research, 2012. 159(6): p. 477-86.
344. Plagemann, A., T. Harder, K. Schellong, S. Schulz, and J.H. Stupin, *Early postnatal life as a critical time window for determination of long-term metabolic health*. Best practice & research. Clinical endocrinology & metabolism, 2012. 26(5): p. 641-53.
345. Smith, P.K., R.I. Krohn, G.T. Hermanson, A.K. Mallia, F.H. Gartner, M.D. Provenzano, E.K. Fujimoto, N.M. Goeke, B.J. Olson, and D.C. Klenk, *Measurement of protein using bicinchoninic acid*. Analytical Biochemistry, 1985. 150(1): p. 76-85.
346. Chomczynski, P. and N. Sacchi, *Single-step method of RNA isolation by acid guanidinium thiocyanate-phenol-chloroform extraction*. Analytical Biochemistry, 1987. 162(1): p. 156-159.

347. Chomczynski, P., *A reagent for the single-step simultaneous isolation of RNA, DNA and proteins from cell and tissue samples*. BioTechniques, 1993. 15(3): p. 532-4.
348. Rio, D.C., M. Ares, Jr., G.J. Hannon, and T.W. Nilsen, *Polyacrylamide gel electrophoresis of RNA*. Cold Spring Harbor Protocols, 2010. 2010(6): p. pdb prot5444.
349. Rio, D.C., M. Ares, Jr., G.J. Hannon, and T.W. Nilsen, *Nondenaturing agarose gel electrophoresis of RNA*. Cold Spring Harbor Protocols, 2010. 2010(6): p. pdb prot5445.
350. Desjardins, P. and D. Conklin, *NanoDrop microvolume quantitation of nucleic acids*. Journal of Visualized Experiments, 2010(45).
351. Schroeder, A., O. Mueller, S. Stocker, R. Salowsky, M. Leiber, M. Gassmann, S. Lightfoot, W. Menzel, M. Granzow, and T. Ragg, *The RIN: an RNA integrity number for assigning integrity values to RNA measurements*. BMC Molecular Biology, 2006. 7: p. 3.
352. Masek, T., V. Vopalensky, P. Suchomelova, and M. Pospisek, *Denaturing RNA electrophoresis in TAE agarose gels*. Analytical Biochemistry, 2005. 336(1): p. 46-50.
353. Beer, *Bestimmung der Absorption des rothen Lichts in farbigen Flüssigkeiten (Determination of the absorption of red light in colored liquids)*. Annalen der Physik und Chemie, 1852. 86: p. 78-88.
354. Lambert, J.H., *Photometria sive de mensura et gradibus luminis, colorum et umbrae [Photometry, or, On the measure and gradations of light, colors, and shade]*. 1760, Germany: Eberhardt Klett.
355. Wilfinger, W.W., K. Mackey, and P. Chomczynski, *Effect of pH and ionic strength on the spectrophotometric assessment of nucleic acid purity*. BioTechniques, 1997. 22(3).
356. Opitz, L., G. Salinas-Riester, M. Grade, K. Jung, P. Jo, G. Emons, B.M. Ghadimi, T. Beissbarth, and J. Gaedcke, *Impact of RNA degradation on gene expression profiling*. BMC Med Genomics, 2010. 3: p. 36.
357. Imbeaud, S., E. Graudens, V. Boulanger, X. Barlet, P. Zaborski, E. Eveno, O. Mueller, A. Schroeder, and C. Auffray, *Towards standardization of RNA quality assessment using user-independent classifiers of microcapillary electrophoresis traces*. Nucleic Acids Res, 2005. 33(6): p. e56.
358. Copois, V., F. Bibeau, C. Bascoul-Mollevi, N. Salvétat, P. Chalbos, C. Bareil, L. Candeil, C. Fraslon, E. Conseiller, V. Granci, P. Maziere, A. Kramar, M. Ychou, B. Pau, P. Martineau, F. Molina, and M. Del Rio, *Impact of RNA degradation on gene expression profiles: assessment of different methods to reliably determine RNA quality*. Journal of Biotechnology, 2007. 127(4): p. 549-59.

359. Russell, S.a., *Molecular Cloning: A Laboratory Manual* . . Cold Spring Harbor Laboratory Press, 2001. 3rd ed.
360. Robinson, T.L., I.A. Sutherland, and J. Sutherland, *Validation of candidate bovine reference genes for use with real-time PCR*. Veterinary Immunology and Immunopathology 2007. 115(1-2): p. 160-5.
361. Garcia-Crespo, D., R.A. Juste, and A. Hurtado, *Selection of ovine housekeeping genes for normalisation by real-time RT-PCR; analysis of PrP gene expression and genetic susceptibility to scrapie*. BMC veterinary research, 2005. 1: p. 3.
362. Muhlhausler, B.S., J.A. Duffield, and I.C. McMillen, *Increased maternal nutrition stimulates peroxisome proliferator activated receptor-gamma, adiponectin, and leptin messenger ribonucleic acid expression in adipose tissue before birth*. Endocrinology, 2007. 148(2): p. 878-85.
363. Sharkey, D., H.P. Fainberg, V. Wilson, E. Harvey, D.S. Gardner, M.E. Symonds, and H. Budge, *Impact of early onset obesity and hypertension on the unfolded protein response in renal tissues of juvenile sheep*. Hypertension, 2009. 53(6): p. 925-31.
364. Bloor, I.D. and M.E. Symonds, *Sexual dimorphism in white and brown adipose tissue with obesity and inflammation*. Hormones and behavior, 2014. 66(1): p. 95-103.
365. Williams, P.J., L.O. Kurlak, A.C. Perkins, H. Budge, T. Stephenson, D. Keisler, M.E. Symonds, and D.S. Gardner, *Hypertension and impaired renal function accompany juvenile obesity: the effect of prenatal diet*. Kidney international, 2007. 72(3): p. 279-89.
366. Saiki, R., D. Gelfand, S. Stoffel, S. Scharf, R. Higuchi, G. Horn, K. Mullis, and H. Erlich, *Primer-directed enzymatic amplification of DNA with a thermostable DNA polymerase*. Science, 1988. 239(4839): p. 487-491.
367. Longo, M.C., M.S. Berninger, and J.L. Hartley, *Use of uracil DNA glycosylase to control carry-over contamination in polymerase chain reactions*. Gene, 1990. 93(1): p. 125-8.
368. Pfaffl, M.W., *A new mathematical model for relative quantification in real-time RT-PCR*. Nucleic Acids Research, 2001. 29(9): p. e45.
369. Spanakis, E., *Problems related to the interpretation of autoradiographic data on gene expression using common constitutive transcripts as controls*. Nucleic Acids Research, 1993. 21(16): p. 3809-3819.
370. Vandesompele, J., K. De Preter, F. Pattyn, B. Poppe, N. Van Roy, A. De Paepe, and F. Speleman, *Accurate normalization of real-time quantitative RT-PCR data by geometric averaging of multiple internal control genes*. Genome Biology, 2002. 3(7): p. research0034.1 - research0034.11.
371. Tricarico, C., P. Pinzani, S. Bianchi, M. Paglierani, V. Distante, M. Pazzagli, S.A. Bustin, and C. Orlando, *Quantitative real-time reverse transcription*

- polymerase chain reaction: normalization to rRNA or single housekeeping genes is inappropriate for human tissue biopsies*. Analytical Biochemistry, 2002. 309(2): p. 293-300.
372. Hellemans, J., G. Mortier, A. De Paepe, F. Speleman, and J. Vandesompele, *qBase relative quantification framework and software for management and automated analysis of real-time quantitative PCR data*. Genome Biology, 2007. 8(2): p. R19.
 373. Lisowski, P., M. Pierzchala, J. Goscik, C.S. Pareek, and L. Zwierzchowski, *Evaluation of reference genes for studies of gene expression in the bovine liver, kidney, pituitary, and thyroid*. Journal of Applied Genetics, 2008. 49(4): p. 367-72.
 374. Bancroft J D, G.M., ed. *Theory and Practice of Histological Techniques*. 6 ed. 2007, Churchill livingstone Elsevier.
 375. Eltoun, I., J. Fredenburgh, R.B. Myers, and W.E. Grizzle, *Introduction to the Theory and Practice of Fixation of Tissues*. Journal of Histotechnology, 2001. 24(3): p. 173-190.
 376. Kiernan, J.A., ed. *Histological and histochemical methods : theory and practice*. 2002, Arnold.
 377. Brunt, E.M., C.G. Janney, A.M. Di Bisceglie, B.A. Neuschwander-Tetri, and B.R. Bacon, *Nonalcoholic steatohepatitis: a proposal for grading and staging the histological lesions*. American College of Gastroenterology, 1999. 94(9): p. 2467-2474.
 378. Puchtler, H. and S.N. Meloan, *On the chemistry of formaldehyde fixation and its effects on immunohistochemical reactions*. Histochemistry, 1985. 82(3): p. 201-4.
 379. Shi, S.-R., R.J. Cote, and C.R. Taylor, *Antigen Retrieval Immunohistochemistry: Past, Present, and Future*. Journal of Histochemistry & Cytochemistry, 1997. 45(3): p. 327-343.
 380. Lowe, S.A., *Human Histology*. : . Third edition. ed. 2005, London: Elseveir Mosby.
 381. Kubota, N., Y. Terauchi, H. Miki, H. Tamemoto, T. Yamauchi, K. Komeda, S. Satoh, R. Nakano, C. Ishii, T. Sugiyama, K. Eto, Y. Tsubamoto, A. Okuno, K. Murakami, H. Sekihara, G. Hasegawa, M. Naito, Y. Toyoshima, S. Tanaka, K. Shiota, T. Kitamura, T. Fujita, O. Ezaki, S. Aizawa, T. Kadowaki, and et al., *PPAR gamma mediates high-fat diet-induced adipocyte hypertrophy and insulin resistance*. Molecular Cell, 1999. 4(4): p. 597-609.
 382. Sjostrom, L., P. Bjorntorp, and J. Vrana, *Microscopic fat cellsize measurements on frozen-cut adipose tissue in comparison with automatic determinations of osmium-fixed fat cells*. Journal of Lipid Research, 1971. 12(5): p. 521-530.

383. Fakler, T., E. O'Brian Smith, R.L. McNeel, and H.J. Mersmann, *Evaluation of alternative methods to prepare porcine adipocytes for measurement with an electronic particle number and size determination apparatus*. Journal of Animal Science 1996. 74(10): p. 2385-93.
384. Hirsch, J. and E. Gallian, *Methods for the determination of adipose cell size in man and animals*. Journal of Lipid Research, 1968. 9(1): p. 110-119.
385. Ashwell, M., P. Priest, M. Bondoux, C. Sowter, and C.K. McPherson, *Human fat cell sizing--a quick, simple method*. Journal of Lipid Research, 1976. 17(2): p. 190-2.
386. Chen, H.C. and R.V. Farese, Jr., *Determination of adipocyte size by computer image analysis*. Journal of Lipid Research, 2002. 43(6): p. 986-9.
387. Spencer, M., A. Yao-Borengasser, R. Unal, N. Rasouli, C.M. Gurley, B. Zhu, C.A. Peterson, and P.A. Kern, *Adipose tissue macrophages in insulin-resistant subjects are associated with collagen VI and fibrosis and demonstrate alternative activation*. American Journal of Physiology - Endocrinology And Metabolism, 2010. 299(6): p. E1016-E1027.
388. Collins, T.J., *ImageJ for microscopy*. BioTechniques, 2007. 43(1 Suppl): p. 25-30.
389. Schneider, C.A., W.S. Rasband, and K.W. Eliceiri, *NIH Image to ImageJ: 25 years of image analysis*. Nature Methods, 2012. 9(7): p. 671-675.
390. Brey, E.M., Z. Lalani, C. Johnston, M. Wong, L.V. McIntire, P.J. Duke, and C.W. Patrick, *Automated Selection of DAB-labeled Tissue for Immunohistochemical Quantification*. Journal of Histochemistry & Cytochemistry, 2003. 51(5): p. 575-584.
391. Auffret, J., S. Viengchareun, N. Carre, R.G. Denis, C. Magnan, P.Y. Marie, A. Muscat, B. Feve, M. Lombes, and N. Binart, *Beige differentiation of adipose depots in mice lacking prolactin receptor protects against high-fat-diet-induced obesity*. FASEB Journal, 2012. 26(9): p. 3728-37.
392. Galic, S., M.D. Fullerton, J.D. Schertzer, S. Sikkema, K. Marcinko, C.R. Walkley, D. Izon, J. Honeyman, Z.-P. Chen, B.J. van Denderen, B.E. Kemp, and G.R. Steinberg, *Hematopoietic AMPK β 1 reduces mouse adipose tissue macrophage inflammation and insulin resistance in obesity*. Journal of Clinical Investigation, 2011. 121(12): p. 4903-4915.
393. Rasband, W.S., *Calculator_Plus.java available from <http://rsb.info.nih.gov/ij/plugins/calculator-plus.html>* . Date accessed 18 October 2012. 2004.
394. Landini, G. *Colour Deconvolution available at <http://www.dentistry.bham.ac.uk/landinig/software/cdeconv/cdeconv.html>* . Date accessed 18 October 2012. 2004-12.

395. Landini, G., *Auto_threshold.jar v 1.14* available from http://fiji.sc/Auto_Threshold and http://www.dentistry.bham.ac.uk/landinig/software/auto_threshold.jar Last accessed 18 October 2012. 2011.
396. Millership, S., N. Ninkina, I.A. Guschina, J. Norton, R. Brambilla, P.J. Oort, S.H. Adams, R.J. Dennis, P.J. Voshol, J.J. Rochford, and V.L. Buchman, *Increased lipolysis and altered lipid homeostasis protect γ -synuclein-null mutant mice from diet-induced obesity*. Proceedings of the National Academy of Sciences, 2012. 109(51): p. 20943-20948.
397. Dias, P., B. Chen, B. Dilday, H. Palmer, H. Hosoi, S. Singh, C. Wu, X. Li, J. Thompson, D. Parham, S. Qualman, and P. Houghton, *Strong Immunostaining for Myogenin in Rhabdomyosarcoma Is Significantly Associated with Tumors of the Alveolar Subclass*. American Journal of Pathology, 2000. 156(2): p. 399-408.
398. Aasmundstad, T.A., O.A. Haugen, E. Johannesen, A.L. Høe, and S. Kvinnsland, *Oestrogen receptor analysis: correlation between enzyme immunoassay and immunohistochemical methods*. Journal of Clinical Pathology, 1992. 45(2): p. 125-129.
399. Diaz, L.K. and N. Sneige, *Estrogen receptor analysis for breast cancer: current issues and keys to increasing testing accuracy*. Advances in Anatomic Pathology, 2005. 12(1): p. 10-9.
400. Umemura, S., J. Itoh, H. Itoh, A. Serizawa, Y. Saito, Y. Suzuki, Y. Tokuda, T. Tajima, and R.Y. Osamura, *Immunohistochemical evaluation of hormone receptors in breast cancer: which scoring system is suitable for highly sensitive procedures?* Applied Immunohistochemistry and Molecular Morphology, 2004. 12(1): p. 8-13.
401. Cross, S.S., *Observer accuracy in estimating proportions in images: implications for the semiquantitative assessment of staining reactions and a proposal for a new system*. Journal of Clinical Pathology, 2001. 54(5): p. 385-90.
402. Landini, G. *How to correct background illumination in brightfield microscopy*. Available at http://imagejdocu.tudor.lu/doku.php?id=howto:working:how_to_correct_background_illumination_in_brightfield_microscopy. 2006-2012.
403. Ruifrok, A.C., R.L. Katz, and D.A. Johnston, *Comparison of quantification of histochemical staining by hue-saturation-intensity (HSI) transformation and color-deconvolution*. Applied Immunohistochemistry and Molecular Morphology, 2003. 11(1): p. 85-91.
404. Ruifrok, A.C. and D.A. Johnston, *Quantification of histochemical staining by color deconvolution*. Analytical and Quantitative Cytology and Histology, 2001. 23(4): p. 291-9.
405. Leventhal, L., *Statistical power calculations: Comment*. Journal of Animal Science, 2009. 87(6): p. 1854-1855.

406. Lenth, R., *Statistical power calculations*. Journal of animal science, 2007. 85(13_suppl): p. E24-E29.
407. Dell, R.B., S. Holleran, and R. Ramakrishnan, *Sample size determination*. The ILAR Journal, 2002. 43(4): p. 207-13.
408. Snedecor, G.W. and W.G. Cochran, *Statistical methods*. 8th ed. 1989, Ames: Iowa state press.
409. Cohen, J., *Cohen, J. 1988. Statistical Power Analysis for the Behavioral Sciences*. 2nd ed. 1988: Lawrence Erlbaum Associates.
410. McGough, J.J. and S.V. Faraone, *Estimating the size of treatment effects: moving beyond p values*. Psychiatry, 2009. 6(10): p. 21-9.
411. Hoenig, J.M. and D.M. Heisey, *The Abuse of Power: The Pervasive Fallacy of Power Calculations for Data Analysis*. The American Statistician, 2001. 55(1): p. 19-24.
412. Olejnik, S., J. Li, S. Supattathum, and C.J. Huberty, *Multiple Testing and Statistical Power With Modified Bonferroni Procedures*. Journal of Educational and Behavioral Statistics, 1997. 22(4): p. 389-406.
413. Field, A., *Discovering Statistics Using SPSS*. third edition ed. 2009, UK: SAGE Publications Ltd
414. Schmider, E., M. ZIEGLER, E. DANAY, L. BEYER, and M. BÜHNER, *Is It Really Robust?* Methodology, 2010. 6: p. 147-151.
415. LaerdStatistics. *Three-way mixed ANOVA (with one within-subjects and two between-subjects factors) using SPSS Statistics. Statistical tutorials and software guides*. 2015 [cited 2017 6/30/2017]; Available from: <https://statistics.laerd.com/>.
416. Baffy, G., *Kupffer cells in non-alcoholic fatty liver disease: The emerging view*. Journal of Hepatology, 2009. 51(1): p. 212-223.
417. de Rooij, S.R., R.C. Painter, T.J. Roseboom, D.I. Phillips, C. Osmond, D.J. Barker, M.W. Tanck, R.P. Michels, P.M. Bossuyt, and O.P. Bleker, *Glucose tolerance at age 58 and the decline of glucose tolerance in comparison with age 50 in people prenatally exposed to the Dutch famine*. Diabetologia, 2006. 49(4): p. 637-43.
418. de Rooij, S.R., R.C. Painter, F. Holleman, P.M. Bossuyt, and T.J. Roseboom, *The metabolic syndrome in adults prenatally exposed to the Dutch famine*. American Journal of Clinical Nutrition, 2007. 86(4): p. 1219-1224.
419. Finn, P.F. and J.F. Dice, *Proteolytic and lipolytic responses to starvation*. Nutrition, 2006. 22(7-8): p. 830-844.
420. Casper, R.C., *Carbohydrate metabolism and its regulatory hormones in anorexia nervosa*. Psychiatry Research, 1996. 62(1): p. 85-96.

421. Johnston, D.G., A. Pernet, A. McCulloch, G. Blesa-Malpica, J.M. Burrin, and K.G. Alberti, *Some hormonal influences on glucose and ketone body metabolism in normal human subjects*. Ciba Foundation Symposium 87 - Metabolic Acidosis (eds R. Porter and G. Lawrenson), 1982. 87: p. 168-91.
422. Hay, W.W., Jr., *Energy and substrate requirements of the placenta and fetus*. Proceedings of the Nutrition Society, 1991. 50(2): p. 321-36.
423. Gootwine, E., *Meta-analysis of morphometric parameters of late-gestation fetal sheep developed under natural and artificial constraints*. Journal of Animal Science, 2012.
424. Aldoretta, P.W., T.D. Carver, and W.W. Hay Jr, *Maturation of Glucose-Stimulated Insulin Secretion in Fetal Sheep*. Neonatology, 1998. 73(6): p. 375-386.
425. Van Assche, F.A., F.D. Prins, L. Aerts, and M. Verjans, *The endocrine pancreas in small for date infants*. BJOG: An International Journal of Obstetrics & Gynaecology, 1977. 84(10): p. 751-753.
426. Bazaes, R.A., T.E. Salazar, E. Pittaluga, V. Pena, A. Alegria, G. Iniguez, K.K. Ong, D.B. Dunger, and M.V. Mericq, *Glucose and lipid metabolism in small for gestational age infants at 48 hours of age*. Pediatrics, 2003. 111(4 Pt 1): p. 804-9.
427. Fowden, A.L., A.J. Forhead, P.M. Coan, and G.J. Burton, *The placenta and intrauterine programming*. Journal of Neuroendocrinology, 2008. 20(4): p. 439-50.
428. Regnault, T.R., J.E. Friedman, R.B. Wilkening, R.V. Anthony, and W.W. Hay, Jr., *Fetoplacental transport and utilization of amino acids in IUGR--a review*. Placenta, 2005. 26 Suppl A: p. S52-62.
429. Reynolds, L.P., P.P. Borowicz, K.A. Vonnahme, M.L. Johnson, A.T. Grazul-Bilska, D.A. Redmer, and J.S. Caton, *Placental angiogenesis in sheep models of compromised pregnancy*. Journal of Physiology, 2005. 565(1): p. 43-58.
430. Brown, J.E. and M. Carlson, *Nutrition and Multifetal Pregnancy*. Journal of the American Dietetic Association, 2000. 100(3): p. 343-348.
431. Smith, J.P. and P.J. Harvey, *Chronic disease and infant nutrition: Is it significant to public health?* Public Health Nutrition, 2011. 14(2): p. 279-289.
432. Graham, N., T. Searle, and D. Griffiths, *Basal metabolic rate in lambs and young sheep*. Australian Journal of Agricultural Research, 1974. 25(6): p. 957-971.
433. Wang, Z., T.P. O'Connor, S. Heshka, and S.B. Heymsfield, *The reconstruction of Kleiber's law at the organ-tissue level*. Journal of Nutrition, 2001. 131(11): p. 2967-70.

434. Goliomytis, M., S. Orfanos, E. Panopoulou, and E. Rogdakis, *Growth curves for body weight and carcass components, and carcass composition of the Karagouniko sheep, from birth to 720 days of age*. Small Ruminant Research, 2006. 66(1-3): p. 222-229.
435. Yambayamba, E.S., M.A. Price, and G.R. Foxcroft, *Hormonal status, metabolic changes, and resting metabolic rate in beef heifers undergoing compensatory growth*. Journal of Animal Science 1996. 74(1): p. 57-69.
436. McCann, J.P., E.N. Bergman, and D.H. Beermann, *Dynamic and static phases of severe dietary obesity in sheep: food intakes, endocrinology and carcass and organ chemical composition*. Journal of Nutrition, 1992. 122(3): p. 496-505.
437. Ravelli, G.P., Z.A. Stein, and M.W. Susser, *Obesity in young men after famine exposure in utero and early infancy*. New England Journal of Medicine, 1976. 295(7): p. 349-53.
438. Ravelli, A.C., J.H. van der Meulen, C. Osmond, D.J. Barker, and O.P. Bleker, *Obesity at the age of 50 y in men and women exposed to famine prenatally*. American Journal of Clinical Nutrition, 1999. 70(5): p. 811-816.
439. Ivy, J.L., *Role of exercise training in the prevention and treatment of insulin resistance and non-insulin-dependent diabetes mellitus*. Sports medicine, 1997. 24(5): p. 321-336.
440. Hollenbeck, C.B., W. Haskell, M. Rosenthal, and G.M. Reaven, *Effect of habitual physical activity on regulation of insulin-stimulated glucose disposal in older males*. Journal of the American Geriatrics Society, 1985. 33(4): p. 273-7.
441. Bergen, W.G. and H.J. Mersmann, *Comparative Aspects of Lipid Metabolism: Impact on Contemporary Research and Use of Animal Models*. Journal of Nutrition, 2005. 135(11): p. 2499-2502.
442. Nafikov, R.A. and D.C. Beitz, *Carbohydrate and Lipid Metabolism in Farm Animals*. Journal of Nutrition, 2007. 137(3): p. 702-705.
443. Vernon, R.G., *Lipid metabolism in the adipose tissue of ruminant animals*. Progress in Lipid Research, 1980. 19(1-2): p. 23-106.
444. Hanson, R.W. and F.J. Ballard, *The relative significance of acetate and glucose as precursors for lipid synthesis in liver and adipose tissue from ruminants*. Biochemical Journal, 1967. 105(2): p. 529-36.
445. Smith, S.B. and J.D. Crouse, *Relative contributions of acetate, lactate and glucose to lipogenesis in bovine intramuscular and subcutaneous adipose tissue*. Journal of Nutrition, 1984. 114(4): p. 792-800.
446. Boxenbaum, H., *Interspecies variation in liver weight, hepatic blood flow, and antipyrine intrinsic clearance: Extrapolation of data to*

- benzodiazepines and phenytoin*. Journal of Pharmacokinetics and Biopharmaceutics, 1980. 8(2): p. 165-176.
447. Szczepaniak, L.S., P. Nurenberg, D. Leonard, J.D. Browning, J.S. Reingold, S. Grundy, H.H. Hobbs, and R.L. Dobbins, *Magnetic resonance spectroscopy to measure hepatic triglyceride content: prevalence of hepatic steatosis in the general population*. American Journal of Physiology - Endocrinology And Metabolism, 2005. 288(2): p. E462-E468.
 448. Vanni, E., E. Bugianesi, A. Kotronen, S. De Minicis, H. Yki-Järvinen, and G. Svegliati-Baroni, *From the metabolic syndrome to NAFLD or vice versa?* Digestive and Liver Disease, 2010. 42(5): p. 320-330.
 449. Lake, A.D., P. Novak, R.N. Hardwick, B. Flores-Keown, F. Zhao, W.T. Klimecki, and N.J. Cherrington, *The adaptive endoplasmic reticulum stress response to lipotoxicity in progressive human nonalcoholic fatty liver disease*. Toxicological sciences, 2014. 137(1): p. 26-35.
 450. González-Rodríguez, Á., R. Mayoral, N. Agra, M. Valdecantos, V. Pardo, M. Miquilena-Colina, J. Vargas-Castrillon, O.L. Iacono, M. Corazzari, and G. Fimia, *Impaired autophagic flux is associated with increased endoplasmic reticulum stress during the development of NAFLD*. Cell death & disease, 2014. 5(4): p. e1179.
 451. Amir, M. and M.J. Czaja, *Autophagy in nonalcoholic steatohepatitis*. Expert Review of Gastroenterology and Hepatology, 2011. 5(2): p. 159-166.
 452. Greer, E.L., P.R. Oskoui, M.R. Banko, J.M. Maniar, M.P. Gygi, S.P. Gygi, and A. Brunet, *The energy sensor AMP-activated protein kinase directly regulates the mammalian FOXO3 transcription factor*. Journal of Biological Chemistry, 2007. 282(41): p. 30107-19.
 453. Greer, E.L., D. Dowlathshahi, M.R. Banko, J. Villen, K. Hoang, D. Blanchard, S.P. Gygi, and A. Brunet, *An AMPK-FOXO pathway mediates longevity induced by a novel method of dietary restriction in C. elegans*. Current biology, 2007. 17(19): p. 1646-56.
 454. Nobili, V., M. Marcellini, G. Marchesini, E. Vanni, M. Manco, A. Villani, and E. Bugianesi, *Intrauterine Growth Retardation, Insulin Resistance, and Nonalcoholic Fatty Liver Disease in Children*. Diabetes Care, 2007. 30(10): p. 2638-2640.
 455. Thorn, S.R., T.R. Regnault, L.D. Brown, P.J. Rozance, J. Keng, M. Roper, R.B. Wilkening, W.W. Hay, Jr., and J.E. Friedman, *Intrauterine growth restriction increases fetal hepatic gluconeogenic capacity and reduces messenger ribonucleic acid translation initiation and nutrient sensing in fetal liver and skeletal muscle*. Endocrinology, 2009. 150(7): p. 3021-30.
 456. Thorn, S.R., L.D. Brown, P.J. Rozance, W.W. Hay, and J.E. Friedman, *Increased Hepatic Glucose Production in Fetal Sheep With Intrauterine Growth Restriction Is Not Suppressed by Insulin*. Diabetes, 2013. 62(1): p. 65-73.

457. Huang, H., X. Hua, N. Liu, X. Li, S. Liu, X. Chen, C. Zhao, X. Lan, C. Yang, Q.P. Dou, and J. Liu, *Anacardic acid induces cell apoptosis associated with induction of ATF4-dependent endoplasmic reticulum stress*. Toxicology letters, 2014. 228(3): p. 170-8.
458. Hyvonen, M.T. and K.L. Spalding, *Maintenance of white adipose tissue in man*. International Journal of Biochemistry and Cell Biology, 2014. 56: p. 123-32.
459. Gregor, M.F. and G.S. Hotamisligil, *Thematic review series: Adipocyte Biology. Adipocyte stress: the endoplasmic reticulum and metabolic disease*. Journal of Lipid Research, 2007. 48(9): p. 1905-1914.
460. Patel, N., *Nutrition manipulation during development and its impact of metabolic homeostasis in the adult offspring. PhD thesis, University of Nottingham.*, in School of Medicine. 2014, University of Nottingham.
461. Litbarg, N., K. Gudehithlu, P. Sethupathi, J.L. Arruda, G. Dunea, and A. Singh, *Activated omentum becomes rich in factors that promote healing and tissue regeneration*. Cell and Tissue Research, 2007. 328(3): p. 487-497.
462. Gainsford, T., T.A. Willson, D. Metcalf, E. Handman, C. McFarlane, A. Ng, N.A. Nicola, W.S. Alexander, and D.J. Hilton, *Leptin can induce proliferation, differentiation, and functional activation of hemopoietic cells*. Proceedings of the National Academy of Sciences, 1996. 93(25): p. 14564-8.
463. Alexander, G., *Quantitative development of adipose tissue in foetal sheep*. Australian Journal of Biological Sciences, 1978. 31(5): p. 489-503.
464. Hotamisligil, G.S., *Endoplasmic Reticulum Stress and the Inflammatory Basis of Metabolic Disease*. Cell, 2010. 140(6): p. 900-917.
465. Kuballa, P., W.M. Nolte, A.B. Castoreno, and R.J. Xavier, *Autophagy and the immune system*. Annual Review of Immunology, 2012. 30: p. 611-46.
466. Zhou, L., J. Zhang, Q. Fang, M. Liu, X. Liu, W. Jia, L.Q. Dong, and F. Liu, *Autophagy-mediated insulin receptor down-regulation contributes to endoplasmic reticulum stress-induced insulin resistance*. Molecular Pharmacology, 2009. 76(3): p. 596-603.
467. Zhang, K. and R.J. Kaufman, *Signaling the Unfolded Protein Response from the Endoplasmic Reticulum*. Journal of Biological Chemistry, 2004. 279(25): p. 25935-25938.
468. Wolins, N.E., D.L. Brasaemle, and P.E. Bickel, *A proposed model of fat packaging by exchangeable lipid droplet proteins*. FEBS Letters, 2006. 580(23): p. 5484-91.
469. Wang, C., Z. Huang, Y. Du, Y. Cheng, S. Chen, and F. Guo, *ATF4 regulates lipid metabolism and thermogenesis*. Cell Res, 2010. 20(2): p. 174-84.

470. Chau, Y.Y., R. Bandiera, A. Serrels, O.M. Martinez-Estrada, W. Qing, M. Lee, J. Slight, A. Thornburn, R. Berry, S. McHaffie, R.H. Stimson, B.R. Walker, R.M. Chapuli, A. Schedl, and N. Hastie, *Visceral and subcutaneous fat have different origins and evidence supports a mesothelial source*. *Nature Cell Biology*, 2014. 16(4): p. 367-75.
471. Erguler, K., M. Pieri, and C. Deltas, *A mathematical model of the unfolded protein stress response reveals the decision mechanism for recovery, adaptation and apoptosis*. *BMC Syst Biol*, 2013. 7: p. 16.
472. Hetz, C., *The unfolded protein response: controlling cell fate decisions under ER stress and beyond*. *Nat Rev Mol Cell Biol*, 2012. 13(2): p. 89-102.
473. Tirosh, B., N.N. Iwakoshi, L.H. Glimcher, and H.L. Ploegh, *Rapid turnover of unspliced Xbp-1 as a factor that modulates the unfolded protein response*. *J Biol Chem*, 2006. 281(9): p. 5852-60.
474. Scheuner, D., B. Song, E. McEwen, C. Liu, R. Laybutt, P. Gillespie, T. Saunders, S. Bonner-Weir, and R.J. Kaufman, *Translational control is required for the unfolded protein response and in vivo glucose homeostasis*. *Molecular Cell*, 2001. 7(6): p. 1165-76.
475. Kaufman, R.J., D. Scheuner, M. Schroder, X. Shen, K. Lee, C.Y. Liu, and S.M. Arnold, *The unfolded protein response in nutrient sensing and differentiation*. *Nature Reviews Molecular Cell Biology*, 2002. 3(6): p. 411-21.
476. Lee, A.S., *Discovery of molecular chaperone GRP78 and GRP94 Inducible by Endoplasmic stress*, in *Protein Discovery Technologies*, W. Arap and R. Pasqualini, Editors. 2009, CRC Press. p. 129-139.
477. Park, H.-R., A. Tomida, S. Sato, Y. Tsukumo, J. Yun, T. Yamori, Y. Hayakawa, T. Tsuruo, and K. Shin-ya, *Effect on Tumor Cells of Blocking Survival Response to Glucose Deprivation*. *Journal of the National Cancer Institute*, 2004. 96(17): p. 1300-1310.
478. Yacoub Wasef, S.Z., K.A. Robinson, M.N. Berkaw, and M.G. Buse, *Glucose, dexamethasone, and the unfolded protein response regulate TRB3 mRNA expression in 3T3-L1 adipocytes and L6 myotubes*. *American Journal of Physiology - Endocrinology And Metabolism*, 2006. 291(6): p. E1274-E1280.
479. Symonds, M., A. Mostyn, S. Pearce, H. Budge, and T. Stephenson, *Endocrine and nutritional regulation of fetal adipose tissue development*. *Journal of Endocrinology*, 2003. 179(3): p. 293-299.
480. Bateson, P., P.P.G. Bateson, and P.R. Martin, *Design for a life: How behaviour develops*. 1999: Vintage.
481. Walsh, C.T., *Posttranslational Modification of Proteins: Expanding Nature's Inventory*. . Vol. 1. 2006: Roberts and Company Publishers.

482. Plagemann, A. and T. Harder, *Breast feeding and the risk of obesity and related metabolic diseases in the child*. Metabolic Syndrome and Related Disorders, 2005. 3(3): p. 222-32.
483. Dewey, K.G., *Growth characteristics of breast-fed compared to formula-fed infants*. Biology of the neonate, 1998. 74(2): p. 94-105.
484. Bos, P., *Regional Differences in adipose tissue development: Effects of nutritional challenges on genes involved in insulin, insulin like growth factor and glucocorticoid signalling*, in *School of Clinical Sciences*. 2009, University of Nottingham: Nottingham, UK. p. 313.
485. Schanberg, S.M., G. Evoniuk, and C.M. Kuhn, *Tactile and nutritional aspects of maternal care: specific regulators of neuroendocrine function and cellular development*. Proceedings of the Society for Experimental Biology and Medicine, 1984. 175(2): p. 135-46.
486. Curley, J.P. and F.A. Champagne, *Influence of Maternal Care on the Developing Brain: Mechanisms, Temporal Dynamics and Sensitive Periods*. Frontiers in Neuroendocrinology.
487. Wankowska, M. and J. Polkowska, *Effect of maternal deprivation on the gonadotrophin-releasing hormone (GnRH) and GnRH-associated peptide neurobiology in lambs during the transition from infancy to prepuberty*. Folia histochemica et cytobiologica / Polish Academy of Sciences, Polish Histochemical and Cytochemical Society, 2010. 48(1): p. 12-8.
488. Polkowska, J. and M. Wankowska, *Effects of maternal deprivation on the somatotrophic axis and neuropeptide Y in the hypothalamus and pituitary in female lambs. The histomorphometric study*. Folia histochemica et cytobiologica / Polish Academy of Sciences, Polish Histochemical and Cytochemical Society, 2010. 48(2): p. 299-305.
489. Chadio, S., A. Katsafadou, B. Kotsampasi, G. Michailidis, K.C. Mountzouris, D. Kalogiannis, and V. Christodoulou, *Effects of maternal undernutrition during late gestation and/or lactation on colostrum synthesis and immunological parameters in the offspring*. Reproduction, Fertility and Development, 2014: p. -.
490. Wilkin, T.J., K.M. Mallam, B.S. Metcalf, A.N. Jeffery, and L.D. Voss, *Variation in physical activity lies with the child, not his environment: evidence for an 'activitystat' in young children*. International Journal of Obesity, 2006. 30(7): p. 1050-1055.
491. Lussana, F., R.C. Painter, M.C. Ocke, H.R. Buller, P.M. Bossuyt, and T.J. Roseboom, *Prenatal exposure to the Dutch famine is associated with a preference for fatty foods and a more atherogenic lipid profile*. American Journal of Clinical Nutrition, 2008. 88(6): p. 1648-52.
492. Gardner, D.S. and P. Rhodes, *Developmental origins of obesity: programming of food intake or physical activity?* Advances in Experimental Medicine and Biology, 2009. 646: p. 83-93.

493. VanderWeele, T.J., *On the distinction between interaction and effect modification*. Epidemiology, 2009. 20(6): p. 863-71.
494. Yanovski, J.A., *Rapid weight gain during infancy as a predictor of adult obesity*. American Journal of Clinical Nutrition, 2003. 77(6): p. 1350-1351.
495. Ekelund, U., K.K. Ong, Y. Linne, M. Neovius, S. Brage, D.B. Dunger, N.J. Wareham, and S. Rossner, *Association of weight gain in infancy and early childhood with metabolic risk in young adults*. Journal of clinical endocrinology and metabolism, 2007. 92(1): p. 98-103.
496. Singhal, A., T.J. Cole, M. Fewtrell, J. Deanfield, and A. Lucas, *Is Slower Early Growth Beneficial for Long-Term Cardiovascular Health?* Circulation, 2004. 109(9): p. 1108-1113.
497. Nobili, V., A. Alisi, A. Vania, C. Tiribelli, A. Pietrobbattista, and G. Bedogni, *The pediatric NAFLD fibrosis index: a predictor of liver fibrosis in children with non-alcoholic fatty liver disease*. BMC Medicine, 2009. 7: p. 21.
498. Friend, A., L. Craig, and S. Turner, *The prevalence of metabolic syndrome in children: a systematic review of the literature*. Metabolic Syndrome and Related Disorders, 2013. 11(2): p. 71-80.
499. Wichro, E., T. Macheiner, J. Schmid, B. Kavsek, and K. Sargsyan, *The Wide and Complex Field of NAFLD Biomarker Research: Trends*. ISRN Hepatology, 2014. 2014: p. 12.
500. Russell, W.M.S., R.L. Burch, and C.W. Hume, *The principles of humane experimental technique*. 1959.
501. Kucharski, R., J. Maleszka, S. Foret, and R. Maleszka, *Nutritional control of reproductive status in honeybees via DNA methylation*. Science, 2008. 319(5871): p. 1827-30.
502. Wolff, G.L., R.L. Kodell, S.R. Moore, and C.A. Cooney, *Maternal epigenetics and methyl supplements affect agouti gene expression in Avy/a mice*. FASEB Journal, 1998. 12(11): p. 949-57.
503. Scarpace, P.J., M. Matheny, B.H. Pollock, and N. Tumer, *Leptin increases uncoupling protein expression and energy expenditure*. American Journal of Physiology, 1997. 273(1 Pt 1): p. E226-30.
504. Kennedy, A., T.W. Gettys, P. Watson, P. Wallace, E. Ganaway, Q. Pan, and W.T. Garvey, *The metabolic significance of leptin in humans: gender-based differences in relationship to adiposity, insulin sensitivity, and energy expenditure*. J Clin Endocrinol Metab, 1997. 82(4): p. 1293-300.
505. Bjorbaek, C. and B.B. Kahn, *Leptin signaling in the central nervous system and the periphery*. Recent Prog Horm Res, 2004. 59: p. 305-31.
506. Dellschaft, N.S., M.C. Alexandre-Gouabau, D.S. Gardner, J.P. Antignac, D.H. Keisler, H. Budge, M.E. Symonds, and S.P. Sebert, *Effect of pre- and*

- postnatal growth and post-weaning activity on glucose metabolism in the offspring.* Journal of endocrinology, 2015. 224(2): p. 171-82.
507. Anthony, R.V., A.N. Scheaffer, C.D. Wright, and T.R. Regnault, *Ruminant models of prenatal growth restriction.* Reproduction supplement, 2003. 61: p. 183-94.
 508. Shoelson, S.E., J. Lee, and A.B. Goldfine, *Inflammation and insulin resistance.* Journal of Clinical Investigation, 2006. 116(7): p. 1793-1801.
 509. Sorisky, A., A.S.D. Molgat, and A. Gagnon, *Macrophage-Induced Adipose Tissue Dysfunction and the Preadipocyte: Should I Stay (and Differentiate) or Should I Go?* Advances in Nutrition: An International Review Journal, 2013. 4(1): p. 67-75.
 510. Doan-Xuan, Q.M., A.K. Sarvari, P. Fischer-Posovszky, M. Wabitsch, Z. Balajthy, L. Fesus, and Z. Bacso, *High content analysis of differentiation and cell death in human adipocytes.* Cytometry. Part A : the journal of the International Society for Analytical Cytology, 2013. 83(10): p. 933-43.
 511. Berry, R., E. Jeffery, and Matthew S. Rodeheffer, *Weighing in on Adipocyte Precursors.* Cell Metabolism, 2014. 19(1): p. 8-20.
 512. Johnson, D.E., D. Guthrie, A.T. Smyke, S.F. Koga, N.A. Fox, C.H. Zeanah, and C.A. Nelson, 3rd, *Growth and associations between auxology, caregiving environment, and cognition in socially deprived Romanian children randomized to foster vs ongoing institutional care.* Archives of Pediatrics & Adolescent Medicine, 2010. 164(6): p. 507-16.
 513. Wells, J.C., S.C. Dumith, U. Ekelund, F.F. Reichert, A.M. Menezes, C.G. Victora, and P.C. Hallal, *Associations of intrauterine and postnatal weight and length gains with adolescent body composition: prospective birth cohort study from Brazil.* Journal of Adolescent Health, 2012. 51(6): p. S58-S64.
 514. Morrison, J.L., *Sheep models of intrauterine growth restriction: fetal adaptations and consequences.* Clinical and experimental pharmacology & physiology, 2008. 35(7): p. 730-43.
 515. Chakraborty, S., D.V. Joseph, M.J.G. Bankart, S.A. Petersen, and M.P. Wailoo, *Fetal growth restriction: relation to growth and obesity at the age of 9 years.* Archives of Disease in Childhood. Fetal and Neonatal Edition, 2007. 92(6): p. F479-F483.
 516. Hancock, S.N., M.H. Oliver, C. McLean, A.L. Jaquiery, and F.H. Bloomfield, *Size at birth and adult fat mass in twin sheep are determined in early gestation.* Journal of physiology, 2012. 590(Pt 5): p. 1273-85.
 517. Muhlhausler, B.S., S.N. Hancock, F.H. Bloomfield, and R. Harding, *Are Twins Growth Restricted?* Pediatr Res, 2011. 70(2): p. 117-122.
 518. Rumball, C.W., J.E. Harding, M.H. Oliver, and F.H. Bloomfield, *Effects of twin pregnancy and periconceptional undernutrition on maternal*

- metabolism, fetal growth and glucose-insulin axis function in ovine pregnancy.* J Physiol, 2008. 586(5): p. 1399-411.
519. Bloomfield, F.H., M.H. Oliver, and J.E. Harding, *Effects of twinning, birth size, and postnatal growth on glucose tolerance and hypothalamic-pituitary-adrenal function in postpubertal sheep.* Am J Physiol Endocrinol Metab, 2007. 292(1): p. E231-7.
 520. Aiken, C.E. and S.E. Ozanne, *Sex differences in developmental programming models.* Reproduction, 2013. 145(1): p. R1-R13.
 521. Sinclair, K.D., C. Allegrucci, R. Singh, D.S. Gardner, S. Sebastian, J. Bispham, A. Thurston, J.F. Huntley, W.D. Rees, C.A. Maloney, R.G. Lea, J. Craigon, T.G. McEvoy, and L.E. Young, *DNA methylation, insulin resistance, and blood pressure in offspring determined by maternal periconceptional B vitamin and methionine status.* Proc Natl Acad Sci U S A, 2007. 104(49): p. 19351-6.
 522. Gardner, D.S., K. Tingey, B.W. Van Bon, S.E. Ozanne, V. Wilson, J. Dandrea, D.H. Keisler, T. Stephenson, and M.E. Symonds, *Programming of glucose-insulin metabolism in adult sheep after maternal undernutrition.* Am J Physiol Regul Integr Comp Physiol, 2005. 289(4): p. R947-54.
 523. Jiang, Y., M. Xie, W. Chen, R. Talbot, J.F. Maddox, T. Faraut, C. Wu, D.M. Muzny, Y. Li, W. Zhang, J.-A. Stanton, R. et al, *The sheep genome illuminates biology of the rumen and lipid metabolism.* Science, 2014. 344(6188): p. 1168-1173.
 524. Morozova, O., M. Hirst, and M.A. Marra, *Applications of new sequencing technologies for transcriptome analysis.* Annual review of genomics and human genetics, 2009. 10: p. 135-51.
 525. D'Haeseleer, P., *How does gene expression clustering work?* Nature Biotechnology, 2005. 23(12): p. 1499-501.
 526. Sebert, S., D. Sharkey, H. Budge, and M.E. Symonds, *The early programming of metabolic health: is epigenetic setting the missing link?* American Journal of Clinical Nutrition, 2011. 94(6 Suppl): p. 1953S-1958S.
 527. Martino, J., R.D. Emes, L. Garcia-Valdes, M.T. Segura, I. Rusanova, M.D.C. Padilla, H. Budge, M.E. Symonds, and C. Campoy, *DNA Methylation in the human placenta and its association with high maternal body mass index.*, in *46th Annual Meeting of European Society for Paediatric Gastroenterology Hepatology and Nutrition (ESPGHAN).* 2013, Wolters Kluwer: London. p. 473.
 528. Mao, S., A. Lima Souza, R.J. Goodrich, and S.A. Krawetz, *Identification of artifactual microarray probe signals constantly present in multiple sample types.* BioTechniques, 2012. 53(2): p. 91.